Characterization of a BMP co-Receptor

Inaugural-Dissertation
to obtain the academic degree
Doctor rerum naturalium (Dr. rer. nat.)

submitted to the Department of Biology, Chemistry and Pharmacy
of Freie Universität Berlin

by

Christina Sieber

from Frankfurt am Main, Germany

February 2009

This thesis was prepared under the supervision of Prof. Dr. Petra Knaus at the Institute for Chemistry and Biochemsitry from July 2004 to February 2009.

1st Reviewer: Prof. Dr. Petra Knaus

2nd Reviewer: Prof. Dr. Stefan Mundlos

date of defence: 27.04.2009

Science is always wrong.
It never solves a problem without creating ten more.
~George Bernard Shaw

Main Index

The days are long but the years are short.

Index of Figures

Index of Tables

1 Introduction

1.1 BMP signaling

Bone Morphogenetic Proteins (BMPs) belong to the Transforming Growth Factor β (TGFβ) superfamily. They include the growth factors (ligands) BMP2 and Growth and Differentiation Factor 5 (GDF5), among many others. A receptor complex formed by BMP receptor type II (BRII), BMP receptor type Ia (BRIa) and BMP receptor type Ib (BRIb) translates signals from the outside to the inside of the cell in response to binding of the ligand. In the cytoplasm stimuli are received by signal transducer molecules, which in turn relate the information to the nucleus, where target genes are activated or repressed. This process passes through many stages and checkpoints, which are depicted in the following paragraphs.

1.1.1 BMP ligands

BMPs are secreted ligands. They are expressed as large precursor proteins, containing an N-terminal signal peptide, a prodomain and a C-terminal peptide from which the mature protein evolves. The monomers typically form covalent homo- or heterodimers in the endoplasmatic reticulum (ER) [1, 2]. The mature protein is released from the proprotein following cleavage by a serine endoprotease within cellular membranes, such as the ER or Golgi. For example furin, a protease predominantly localized in the Golgi membrane, was shown to cleave off the prodomain of BMP4 [2]. GDF2 (BMP9) and GDF8 (myostatin) are exceptions: the proregion remains associated with the mature protein after cleavage and even after secretion. Outside the cell the noncovalently attached proregion may inhibit binding of the ligand to its receptor. However, little is known about the regulation or physiological relevance and activity of these complexes [1].

Mature BMP and GDF ligands are highly homologous. Particularly, a set of seven cysteine residues is highly conserved. Dimers are covalently linked by a single intermolecular disulfide bridge, mediated through one of the conserved cysteines in each monomer [3]. While the cysteine bridge is believed to be critical for dimerization and biological activity for most members of the BMP family [4], it appears to be dispensable for some, such as GDF9 [5], GDF9B (BMP15) [6], and GDF3 [5]. These proteins are biologically active and were shown to form noncovalent homo- and heterodimers in vivo. Moreover, we characterized a point mutation of the critical cysteine residue in GDF5, which resulted in monomeric protein. We could show that monomeric GDF5 has equal biological activity as its dimeric counterpart, possibly due to formation of noncovalent dimers [7]. Interestingly, heterodimers of BMP2/5,

BMP2/6, BMP2/7 and BMP4/7 form naturally *in vivo* and *in vitro* when co-expressed and show enhanced activity compared to the corresponding homodimers [8].

Six of the conserved cysteine residues serve to stabilize the monomers [3], forming a structure known as cystine knot. In BMP2 two intramolecular disulfide bonds (Cys43/Cys111 and Cys47/Cys113) shape a ring-like topology wide enough for the third cysteine bridge (Cys14/Cys79) to pass through [9]. The crystal structures of BMP2 [9], BMP7 [10, 11], BMP9 [12], and GDF5 [13] revealed great similarities between these and other members of the TGFβ superfamily ligands. The typical TGFβ fold is often described as a double left-hand, with each monomer containing a wrist epitope, four fingers, and a knuckle epitope. The wrist epitope (concave) comprises residues from both monomers. One part is located on a long alpha helix, from which two antiparallel beta sheets, the fingers, poject away like butterfly wings. The second part of the wrist epitope is made up of residues on the inner side of the beta sheets. The knuckle epitope (convex) is located on the outer slope of the beta strands (Figure 1.3) [14].

Figure 1.1 Folding topology of the native BMP2 dimer [9]

BMP2 is a dimer formed from two identical monomers, color-coded here in blue and orange. The cystine knot motif which connects the two monomers is shown here as green sticks.

1.1.1.1 BMP ligands and disease

Due to the central role of BMPs in development, naturally occurring mutations in all proteins along the BMP pathway have severe effects. In humans, mutations in GDF5 give rise to various **skeletal defects** such as abnormally short and deformed limbs (**acrosomelic dysplasia**), joint fusions (**symphalangism**), shortened phalanges in fingers and toes (**Brachydactyly type C and type A2**) or a combination of these and other defects (**multiple synostosis syndrome**) [15-18]. Several naturally occurring mutations in the receptor binding site of GDF5 were described, that alter affinity of GDF5 to its type I receptors. One mutation prevents binding of GDF5 to its high affinity receptor BRIb and results in **Mohr-Wriedt Brachydactyly type A2**, a condition typically ascribed to mutations in the receptor itself [16].

Furthermore, a different mutation was found to enhance affinity of GDF5 to BRIa leading to **symphalangism**, a phenotype previously described for mutations in the GDF5 antagonist Noggin [18].

1.1.1.2 BMP knockouts

In mice several *bmp* knockouts are described that give insight into the functions of BMPs in tissue development. For example mice carrying homozygous *bmp2* deletions exhibit amnion/chorion abnormalities as well as cardiac defects. The knockout is lethal between embryonic stages E7.5 and E9.0 [19]. Likewise, a null mutation of the bmp4 gene is lethal between 6.5 and 9.5 days post coitum and reveals that BMP4 is required for gastrulation and mesoderm formation [20]. Mice deficient in *bmp7* on the other hand survive until shortly after birth and die due to insufficient kidney development. Furthermore, the lack of BMP7 causes defects in eye and skeletal development [21, 22].

1.1.2 BMP antagonists

The activity of the BMP ligands can be regulated through the presence of extracellular antagonists. These secreted peptides typically bind to distinct ligands and prevent interaction of the ligand with the receptor by blocking its receptor binding sites. The extracellular BMP antagonists contain a cysteine-rich domain that allows formation of the cystine knot motif and determines protein-protein interaction. Based on their characteristic cysteine ring structure, BMP antagonists are distinguished and classified into several subgroups: the Noggin/chordin family, twisted gastrulation, and the Dan/Cerberus family [23, 24]. Noggin will be described in more detail.

1.1.2.1 BMP antagonist Noggin

Noggin is secreted as a covalently linked homodimer and exhibits a high affinity for BMP2 and GDF5 amongh other ligands of the BMP family. Structurally, Noggin contains an acidic aminoterminal region and the previously mentioned cystine knot at its C-terminus [25]. The structure of BMP7 in complex with Noggin demonstrates that Noggin specifically blocks both type I and type II receptor binding interfaces on the ligand (Figure 1.2) [26].

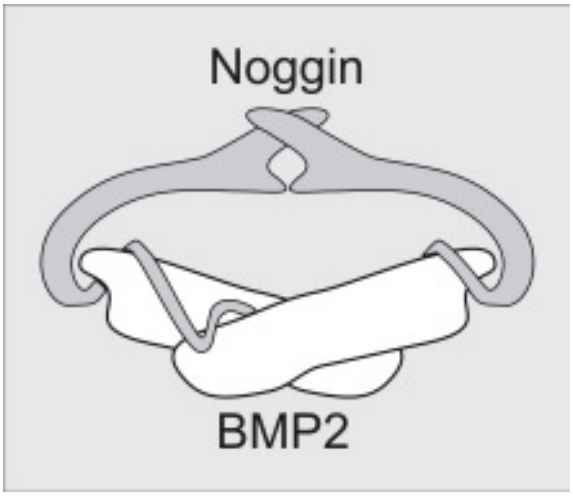

Figure 1.2 Model of Noggin in complex with BMP2 [27]

Noggin prevents binding of type I and type II receptors to their ligands by blocking the receptor binding epitopes on the ligand in a clamp-like fashion (ligand trap).

Secretion of Noggin during embryogenesis induces formation of neural tissue and dorsalisation of mesoderm cells by antagonizing BMP signaling [28-30]. Noggin continues to play crucial roles in controlling BMP signaling in the adult organism [31-33].

1.1.2.2 Noggin and disease

In humans mutations in *noggin* were identified in cases of **proximal symphalangism** and **multiple synostoses syndrome 1** [34, 35]. Interestingly, missense mutations in *noggin* were identified as the cause of a subtype of **Brachydactyly Tpye B** (BDB) [36]. BDB had previously been described to be caused by mutations in the tyrosine kinase receptor Ror2, a protein which will be discussed in more detail in chapter 1.2 [37].

Several studies in mice revealed its critical role in proper embryonic development. Homozygous *noggin* null mutations cause failure of neural tube formation, defects of the axial skeleton and joint lesions. The knockout is lethal at birth due to multiple malformations, including bony fusion of the appendicular skeleton [33, 38]. Targeted overexpression of Noggin in osteoblast cells in vivo results in spontaneous fractures and leads to a significant decrease in osteoblast activity and subsequent loss of bone volume [39].

1.1.3 BMP receptors

BMPs signal through two types of transmembrane serine/threonine kinase receptors (BRI and BRII). Both receptors carry an extracellular ligand binding domain, followed by a transmembrane domain and an intracellular serine/threonine kinase domain. Additionally, BRI contains two distinct motives that are important for receptor activation and signal

transduction. First, a glycine/serine (SGSGSG) rich region, the so called GS-box, is located at the juxtramembrane region preceding the kinase. Phosphorylation of the GS-box by the constitutively active type II receptor activates type I receptor kinase activity [1]. Secondly, within the kinase domain, a short region of eight amino acids termed L45 loop, determines isoform specific activation of Smads, the intracellular signal transducer molecules of Smad-dependent BMP signaling [40]. Receptor specificity of Smads is conferred by their L3 loop, a 17 amino acid region which protrudes from the C-terminal domain of Smads [41].

Three type I receptors serve the BMP pathway: BMP receptor type Ia (BRIa or activin-like kinase 3 (Alk3)) [42], BMP receptor type Ib (BRIb or Alk6) [43] and Activin receptor type Ia (ActRIa or Alk2) [44]. They are highly homologous, yet have very specific preferences for their respective ligands. Both BRIa and BRIb can bind BMP2, but BRIa binds BMP2 with higher affinity, while BRIb is the high affinity receptor for GDF5. Both receptors form heteromeric complexes with BMP receptor type II (BRII) or Activin receptor type II (ActRII) and both can initiate Smad-dependent as well as Smad-independent pathways [1]. Nevertheless, they play different roles during embryogenesis and in the adult organism. While BRIb is essential for differentiation of osteoblasts from mesenchymal precursor cells, BRIa triggers adipogenic differentiation in the same cell line [40].

BRII exists in two alternative splice variants, referred to as short form (SF) and long form (LF) [45-48]. The human BRII gene consists of 13 exons, with exon 12 coding for the so called BRII-tail, an extension at the C-terminal end of the receptor. BRII SF resembles the typical type II receptor of the TGFβ superfamily. The BRII LF tail region has been postulated to serve as a binding site for multiple adaptor proteins to modulate BMP signaling specificity, complexity and intensity. This was demonstrated with proteomics based approaches applying different cytoplasmic domains of BRII as GST fusion proteins [49].

1.1.3.1 BMP receptors and disease

Studies performed on chick limb development revealed that BRIb is required for the initial steps of mesenchyme condensation and cartilage formation, as well as regulating programmed cell death, necessary to form separate digits and joints. BRIa however controls the later stages of chondrocyte differentiation [50]. Mutations in BRIa cause **juvenile polyposis syndrome** (JPS). JPS predisposes to hamartomatous juvenile polyps in the gastrointestinal tract, which may undergo malignant transformation and result in cancer [51]. The BRIa mutations causing JPS are located outside the ligand binding epitope of the BRIa ectodomain and lead to inactivation of the receptor. A recent study revealed that the promiscuous binding of BMP2 to its two type I receptors is possible because the ligand-

receptor interface is very flexible. Apparently, the JPS mutations disturb the ability of BRIa to fold correctly and hence lead to its inactivation [52]. Besides BRIa, also mutations in Smad4, the common mediator Smad (co-Smad), can cause JPS [53]. As mentioned, **Brachydactyly type A2** was described to involve mutations in GDF5 and other cases have revealed mutations in BRIb [16, 17]. **Fibrodysplasia ossificans progressiva** (FOP) is a rare autosomal dominant disorder of connective tissue, characterized by congenital malformation of the great toes and progressive heterotopic ossification of tendons, ligaments, fasciae, and striated muscles [54]. The genetic locus was mapped to the gene of ActRIa. The mutation affects the GS domain of ActRIa and possibly leads to constitutive activation of the receptor [55, 56]. Overexpression of BMP4 was observed in FOP patients in accordance with the fact that constitutive activation of ActRIa upregulates BMP4, downregulates BMP antagonist expression and induces ectopic chondrogenesis as well as joint fusions [55].

Pulmonary arterial hypertension (PAH), a disease characterized by remodeling of small pulmonary arteries, is caused in part by mutations in BRII [57], which lead to reduced expression of the BMP target gene *inhibitor of DNA binding 1* (*Id1*) [58]. The phenotype reveals severe mucosal hemorrhage, incomplete cell coverage on vessel walls, and gastrointestinal hyperplasia. Interestingly, the BRII tail is postulated as interaction site for LIMK1, a crucial regulator of actin dynamics. Studies revealed that the interaction of BRII with LIMK1 inhibited LIMK1-mediated phosporylation of the actin depolymerizing factor cofilin. These data suggest that a disruption in the regulation of actin dynamics may contribute to PAH [59]. Liu et al. described silencing of BRII expression in mice using a BRII-specific short hairpin RNA transgene [60]. Repressed BRII expression and subsequent disruption of BRII signaling causes increased activation of protein kinase B (PKB, also known as AKT). AKT in turn suppresses canonical Wnt signaling in response to BMP signaling through BRIa. BRII also controls expression of endothelial guidance molecules that promote vascular remodeling. The effects are dosage-dependent in that the phenotype becomes more severe when BRII expression is constitutively attenuated by two copies of the shRNA transgene [60]. RACK1 (Receptor for Activated C-Kinase 1) was identified as a BRII interaction partner, negatively regulating pulmonary arterial smooth muscle cell proliferation and downregulated in a PAH rat model. BRII mutants that cause PAH, show reduced interaction with RACK1, suggesting a role for RACK1 in the pathogenesis of PAH [61].

1.1.4 Structural insights on ligand and ligand/receptor complex

Resolution of crystal structures of ligands and receptor domains has been a major achievement in determining important sites for protein-protein interactions. The crystal structure of BMP2 in complex with the extracellular domain (ECD) of BRIa confirmed binding

of the high affinity type I receptor to the wrist epitope (Figure 1.3), where it interacts with both BMP2 monomers [62, 63]. The ternary signaling complex, consisting of the ECDs of BRIa and ActRII and BMP2 was solved almost simultaneously by two groups [64, 65]. While the structure of the binary complex (ligand bound to its high affinity receptor) gave important hints on binding specificity, the ternary complex revealed, that BMP2 does not undergo significant conformational changes upon binding to its receptors [64]. The ActRII-ECD adopts a threefinger (six β-strands) toxin fold which creates the complementary binding surface for attaching to the concave face (knuckle epitope) of one BMP2 monomer. This mostly hydrophobic interface consists of 12 residues from BMP2 and 10 residues from ActRII. Three of these residues from ActRII are indispensable for ligand binding, forming a hydrophobic core contacting five residues at the BMP2 knuckle epitope [66]. Even though the five amino acids involved in shaping this core are identical in BMP2, BMP6 and BMP7, with the exception of one residue in BMP7, ActRII does not have the same affinity to all three ligands. It is thus speculated that nonconserved residues outside the hydrophobic core account for ligand specificity and affinity. Confirmation comes from studies performed on BMP2, in which a silent H-bond was activated through mutation of one or two amino acids to transform BMP2 into a high affinity ligand for ActRIIB [65]. In contrast to ActRII, BRIa interacts with both monomers in the wrist epitope. For the greatest part, the convex face of one BMP2 monomer contributes to the BRIa binding interface, while the second monomer provides mostly hydrophobic contacts between its concave side and the receptor ECD (Figure 1.3). The interface of BMP2 with BRIa-ECD was described as “knob-into-hole” motif, typical for all type I receptor binding sites [62]. Recent studies demonstrated that both the ligand BMP and its high affinity receptor BRIa undergo significant conformational changes within the binding epitope for the respective interaction partner. This mutual flexibility of both BMP2 and BRIa possibly accounts for the promiscuous ligand-receptor interaction within the BMP superfamily [67].

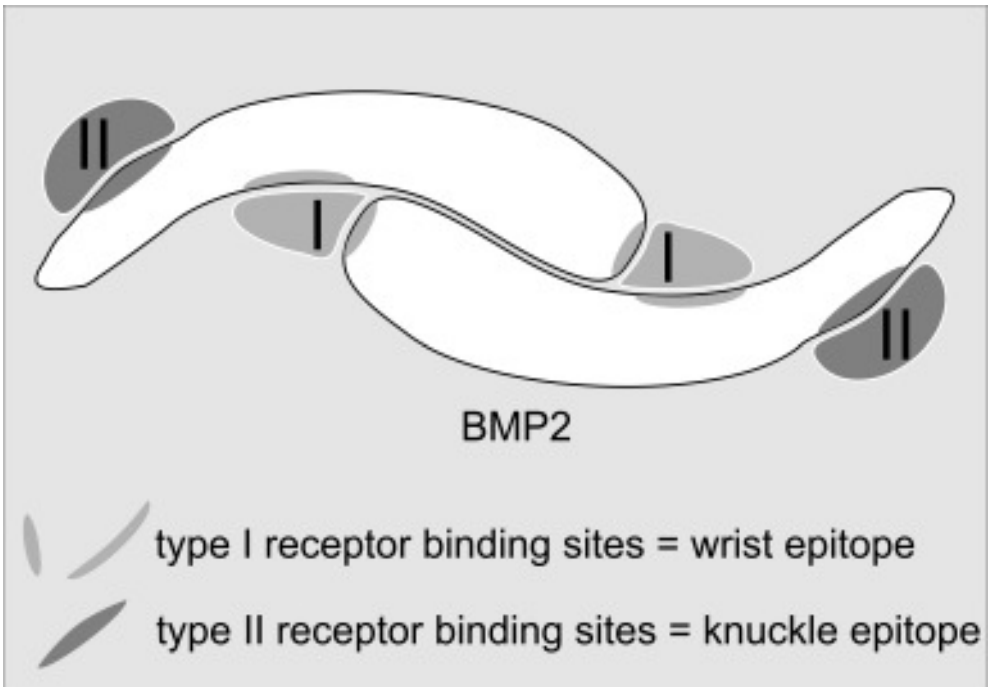

Figure 1.3 BMP ligand receptor complex [27]

BMP monomers assume a left-hand shape, forming a double left-hand structure in the dimeric ligand. Binding sites for the receptors are located on the concave and convex sides of the protein. The type I receptor binds to the wrist epitope (concave) where it is in contact with both monomers. The type II receptor on the other hand interacts with the knuckle epitope (convex), making contact with only one monomer.

Analysis of BMP2 heteromeric muteins, in which the binding epitope for either type I or type II receptor were depleted on one monomer, demonstrated that two functional type II receptors are required for biological activity, while depletion of a single type I receptor only affects Smad-independent signaling. Complete loss of biological activity is achieved in homomeric muteins missing the wrist epitope on both monomers [68].

1.1.5 BMP receptor oligomerization

TGFβ and BMP signaling, even though both pathways use their respective type I and type II receptors, follow a very distinct and different mode of receptor activation. TGFβ signaling is initiated by binding of the ligand to its high affinity type II receptor, whereupon the type I receptor is recruited into the complex. The activated complex eventually translocates to clathrin-coated pits (CCPs) from where it proceeds to early endosomes and initiates signal transduction. This internalization route was also proposed to result in recycling or degradation of the receptors [69]. If, however, the complex is not sequestered from detergent resistant membrane regions (DRMs), it will shuttle into caveolae, resulting in endocytosis to caveosomes and subsequent degradation [70].

As for BMPs, the binding mode of the ligand to its receptors can trigger Smad-dependent or Smad-independent signaling [71-73]. BMP2 first binds to its high affinity receptor (BRI) upon

which the low affinity receptor (BRII) is recruited into a ternary complex. This binding mode leads to formation of the BMP induced signaling complex (BISC) and was shown to initiate Smad-independent signaling. BRI receptors are predominantly localized in DRMs, whereas BRII is found in all membrane domains. When BMP2 binds to BRI, BRII is recruited into BISC, which moves to caveolae and internalizes into caveosomes. This pathway initiates Smad-independent signaling (Figure 1.4). In contrast to TGFβ, BMP was shown to bind preformed complexes (PFC) of type I and type II receptors, leading to activation of Smad-dependent signaling. Smad1/5/8 is associated with BRI in PFCs at the plasma membrane. Following stimulation with BMP2, Smad1/5/8 is phosphorylated before the complex internalizes from CCPs to early endosomes. Dissociation of activated Smads from BRI occurs after endocytosis (Figure 1.4) [73]. A recent study shows that interaction of BRII with caveolin1 is required for BRII plasma membrane localization, interaction with BRIa, subsequent Smad phosphorylation and downstream activation of target genes. Hence caveolin1 may be required for targeting BRII to the plasma membrane [74].

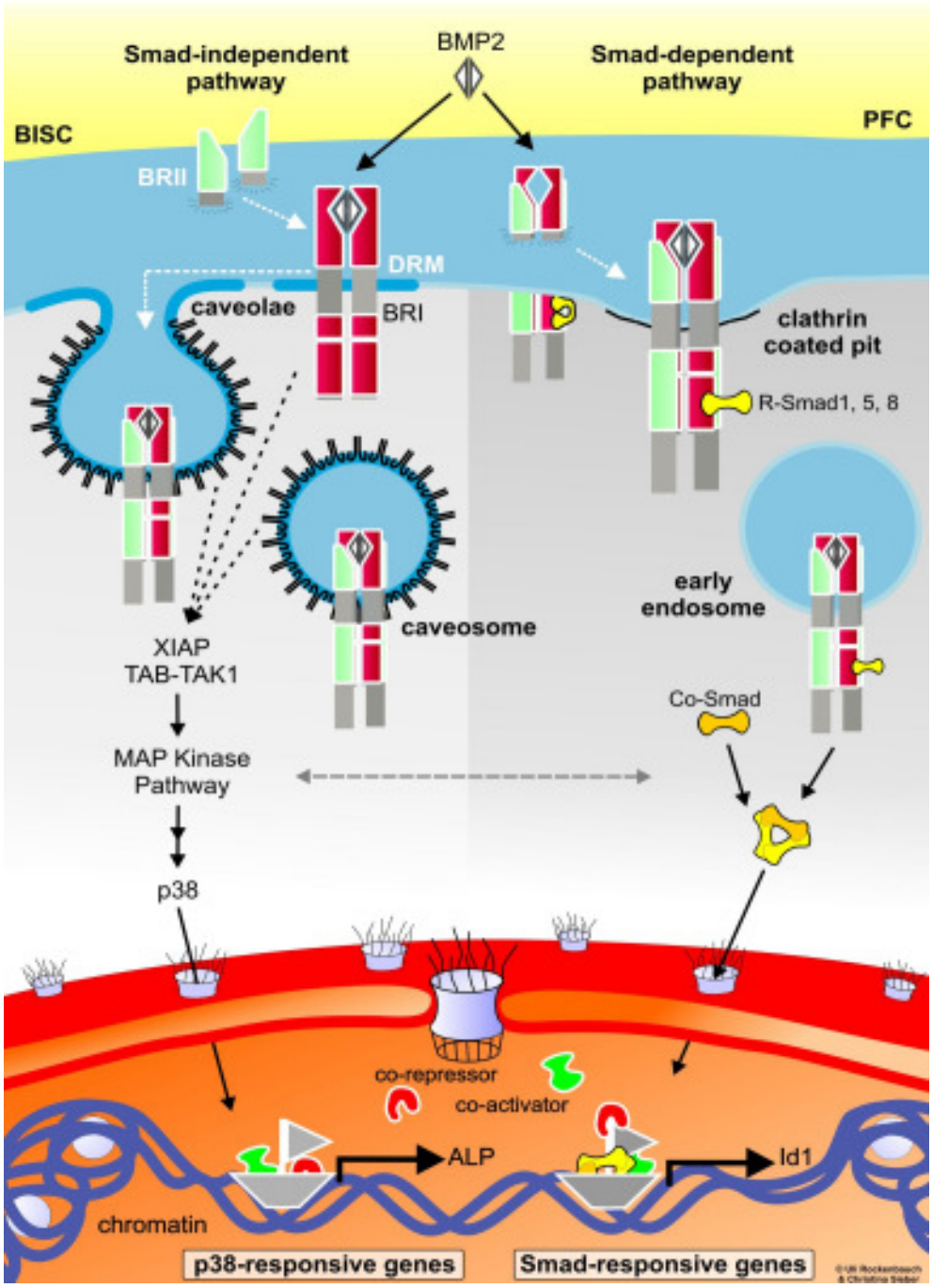

Figure 1.4 BMP signaling routes from cell surface to the nucleus [27]

BMP2 can bind to its receptors in two different modes. It can either induce a signaling complex (BISC) by first binding its high affinity type I receptor (BRI) upon which the type two receptor (BRII) is recruited or it can attach to preformed complexes (PFC) consisting of type I and type II receptors. Depending on the binding mode different pathways are switched on.
BRI predominantly resides in detergent resistant membranes (DRM). Binding of the ligand to DRM-located BRI followed by recruiting of BRII will result in transfer of the complex into caveolae and caveosomes. Subsequently, Smad-independent pathways are initiated, here resembled by the MAP kinase pathway resulting in expression of p38-responsive genes like *Alkaline Phosphatase* (*ALP*). The Smad-dependent pathway is targeted when BMP2 binds to a PFC. After ligand binding R-Smads are phosphorylated by BRI at the cell surface, indicated by structural change of the Smad protein. The complex moves into clathrin-coated pits and is internalized into early endosomes. Here phosphorylated R-Smads detach from BRI to form complexes with Co-Smads, which then translocate into the nucleus to trigger expression of Smad-responsive genes, such as Id1. Gene expression can be further regulated by presence of co-repressors or co-activators.

1.1.6 Smad-dependent BMP pathway

As mentioned previously, the Smad-dependent BMP pathway is initiated when the ligand binds to a preformed complex of type I and type II receptors. This will activate the receptors and lead to phosphorylation of Smads.

In regards to their function, three different categories of Smad proteins have been described. The receptor-associated Smads (R-Smads) interact with and are phosphorylated by type I receptors. R-Smads Smad1/5/8 respond to BMP signaling, while Smad2/3 are TGFβ-specific. The common mediator Smad (Co-Smad) Smad4 forms a complex with phosphorylated R-Smads, which can then translocate into the nucleus to regulate expression of target genes. The inhibitory Smads (I-Smads) prevent binding of R-Smads to the receptor by blocking the Smad binding site on the receptor. Additionally, I-Smads prevent complex formation between phosphorylated R-Smads and Co-Smad. Smad6 and Smad7 were identified as I-Smads and preferentially inhibit BMP signaling or both TGFβ and BMP signaling, respectively [75].

1.1.6.1 Structural basis

Structurally, R-Smads are characterized by two distinct and highly conserved domains termed Mad homology 1 (MH1; N-terminal) and MH2 (C-terminal) (Figure 1.5). The two domains are connected by an intermediate linker region which contains sites for phosphorylation and protein interaction [75].

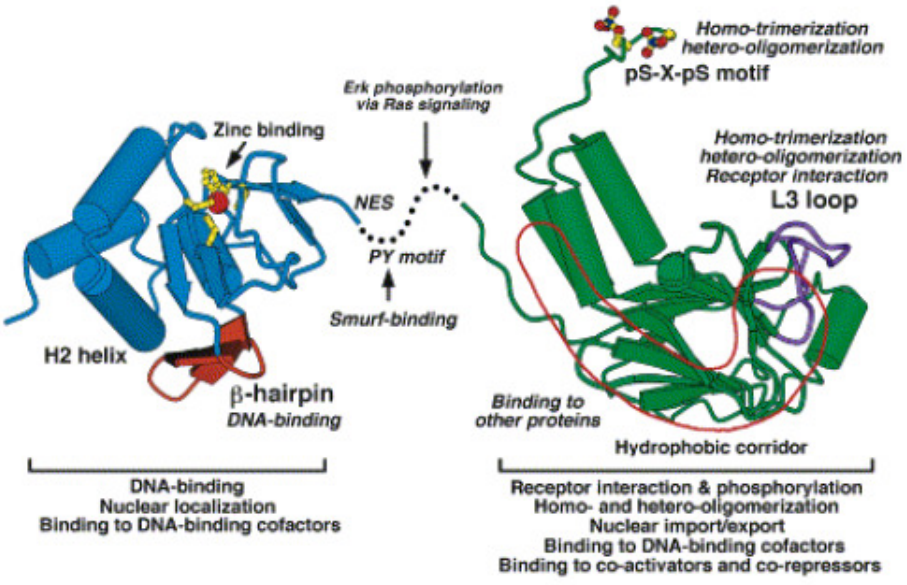

Figure 1.5 Structure of the Smad protein [76]

The MH domains are shown in blue (MH1) and in green (MH2). The linker region connecting the two domains is shown as a dotted line. Structural features are depicted or additionally coloured (red, DNA binding site; magenta, L3 loop; yellow, zinc binding motif and SSXS motif; red encircled, hydrophobic corridor).

The MH1 domain mediates nuclear localization and DNA binding specificity of Smad proteins. Additionally, it serves as interaction site for DNA-binding co-factors. As mentioned previously, R-Smads achieve specific receptor interaction through the L3 loop, a 17 amino acid region, which protrudes from their C-terminal MH2 domain. The type I receptor phosphorylation site on R-Smads lies within the MH2 domain's SSXS motif (pS-X-pS motif in Figure 1.5), a characteristic sequence of two Serines, a Valine or Methionine and a terminal Serine [41, 75, 76].

1.1.6.2 Regulation of R-Smads

Downstream Smad signaling is a tightly regulated process, not only at the plasma membrane, but also within the cytoplasm and the nucleus.

1.1.6.2.1 Endofin

Endofin, a member of the FYVE domain protein family, was first identified as membrane anchor protein for the R-Smad Smad1. Endofin preferentially binds unphosphorylated Smads, recruits them to their type I receptors and thereby facilitates BMP signaling. R-Smads detach from Endofin as they become phosphorylated, and Endofin subsequently binds to and recruits protein phosphatase 1 c (PP1c), which dephosphorylates type I receptors and shuts down BMP signaling. Endofin localizes to early endosomes, which confirms our data that phosphorylated Smads remain associated with type I receptors at the plasma membrane and can dissociate and translocate to the nucleus only after the receptor complex has undergone endocytosis into early endosomes [73, 77]. A different study suggests that endofin specifically intereacts with Smad4, recruits Smad4 to the TGFβ receptor complex to enhance Smad2/3-Smad4 complex formation, and that knockdown of endofin has no impact on BMP or Wnt1-mediated reporter gene expression [78]. Since the assays for these two seemingly contradictory publications were carried out in different cell lines, they may give an insight into how different cell types or tissues maintain differential constitutions, for example in regard to their membrane architecture or protein expression profile. These cell type specific characteristics may greatly influence signaling outcomes because highly differentiated cells are typically prepared to read and conduct only a limited amount of signals in a precisely predefined manner. Hence, both publications greatly contribute to our understanding of TGFβ and BMP signaling [79].

1.1.6.2.2 I-Smads

I-Smads Smad6 and Smad7 were shown to inhibit phosphorylation of R-Smads by competing with R-Smads for binding to activated type I receptos. Furthermore, I-Smads interact with phosphorylated R-Smads to disrupt complex formation of R-Smads with Co-Smad. Moreover, I-Smads are also found in the nucleus, where they inhibit transcription of certain genes [75].

1.1.6.2.3 Smurfs

Initially, Smad ubiquitin regulatory factor 1 (Smurf1) was shown to interact with Smad1 and decrease Smad1 and Smad5 protein levels, independent of BMP stimulation or presence of BRIb [80]. However, in the presence of Smurf1 levels of activated BRIb were decreased. Moreover, Smurf1 significantly accelerated ubiquitin- and proteasome-dependent Smad1 turnover. The interaction site was mapped to the PY motif of Smad1 and the WW domains of Smurf1. The studies further revealed that Smurf1 antagonizes BMP signaling in the Xenopus embryo. It also sensitizes cells for the TGFβ/Smad2 pathway, possibly by an indirect increase of the pool of unbound Smad4, which all R-Smads compete for [80, 81]. Also Smurf2 was shown to interact with Smad1 and lead to its degradation. In contrast to Smurf1, Smurf2 also interacts weakly with Smad2 and Smad3 and was found to slightly decrease Smad2, but not Smad3 protein levels [82].

Later, Smurf1 and Smurf2 were shown to interact with I-Smads, Smad6 and Smad7 and trigger nuclear export of Smad7 as well as its degradation. Smurfs were also found to interact with and induce degradation of the TGFβ receptor complex [83, 84]. Apparently, Smurf1 enhances interaction of Smad7 with the TGFβ receptor complex by targeting Smad7 to the plasma membrane, where it can compete for the type I receptor binding site with R-Smads [85]. Another study demonstrates that Smurf1 cooperates with I-Smads in inhibiting BMP signaling and targeting both R-Smads and BMP type I receptors for degradation. Interestingly, binding of Smurf1 to Smad1/5 was enhanced by Smad6/7 [86]. More recently, inhibitory Smad1 linker phosphorylation through mitogen-activated protein kinases (MAPKs) was shown to promote recognition of Smad1 by Smurf1. Moreover, binding of Smurf1 prevents interaction of Smad1 with the nuclear translocation factor Nup214 [87].

The above described findings were confirmed on the physiological level by studies that explored the roles of Smurf1 in myogenic differentiation and osteoblast differentiation. Ying et al. demonstrated that Smurf1 promotes myogenic differentiation by targeting Smad5 for degradation, while Zhao et al. could show that it inhibits osteoblast differentiation by causing the degradation of the osteoblast-specific transcription factor Runx2/Cbfa1. Later, Smad6 was shown to act in concert with Smurf1 to mediate degradation of Runx2 [88-91]. A study from Yamashita et al., based on Smurf1-deficient mice, finds that loss of Smurf1 does not

influence Smad-dependent BMP signaling. According to this group, the effect of Smurf1 on osteoblast activity is due to its interaction with MEKK2. Interaction with Smurf1 leads to ubiquitination and degradation of MEKK2, negatively affecting downstream JNK signaling [92]. Data from a recent study on tumor necrosis factor (TNF) transgenic mice and transgenig *smurf1*(-/-) mice indicate that Smurf1 causes increased degradation of Smad1. The study concludes that systemic bone loss in chronic inflammatory disorders, which exhibit increased levels of TNF, is a result of TNF-mediated Smurf1 expression [93]. Besides osteoblast differentiation, also cartilage formation is affected and delayed by a concerted overexpression of Smad6 and Smurf1 [94].

Notably, Smurf1 was also shown to target RhoA for degradation, a protein that plays a critical role in regulating cell polarity and protrusion formation. As this pathway appears to be required for the transformed nature of tumor cells, Smurf1 was discussed as a link between cell polarity and ubiquitination [95, 96].

Smad4 was also described to be degradaded by several E3 ubiquitin ligases, including Smurfs, in a complex mediated by Smad2 or Smad6/7. In this complex, Smad4 was poly-ubiquitinated by Smurfs, although it normally binds to neither Smurf1 nor Smurf2 [97].

Interestingly, Smurf1 was shown to be degraded in response to BMP stimulation. Mediator of this event is Tribbles-like protein 3 (Trb3), a BRII tail-interacting protein that dissociates from the BRII tail domain upon BMP stimulation and triggers degradation of Smurf1 [98].

Other than Smurf1 and Smurf2, several other E3 ligases inhibit TGFβ and BMP signaling, among them are Jab1, CHIP, SCFβ-TrCP1, Sumo-1/Ubc9, and WWP1 [97, 99-104].

1.1.6.2.4 R-Smad linker phosphorylation

As discussed previously, R-Smads are activated by type I receptor phosphorylation on their C-terminus. This phosphorylation triggers a conformational change, leading to an unfolding and presentation of the MH1 and MH2 domains. In the unphosphorylated state R-Smads are autoinhibited through an intramolecular interaction of MH1 and MH2 domains [105].

However, R-Smads also carry phosphorylation sites within the linker region. Smad1 was shown to be phosphorylated within the linker region on a PXSP motif, a consensus site for mitogen-activated protein kinases (MAPK). Smad1 contains four repeats of this PXSP motif. The phosphorylation of these MAPK sites was triggered by ligands signaling through receptor tyrosine kinases like EGF and HGF. These pathways activate Erk MAP kinases through Raf and MEK1. Specific inhibition of MEK1 strongly suppressed Smad1 linker phosphorylation, indicating that Smad1 is a target of Erk. The linker phosphorylation apparently prevents nuclear accumulation of Smad1 and thus has an inhibitory effect on BMP signaling [106]. Furthermore, FGF and IGF mediated MAPK signaling was also shown to induce phosphorylation of Smad1 linker, thereby promoting neurogenesis [107]. Another

study showed that inhibition of BMP signaling via receptor tyrosine kinases and Erk is not solely dependent on direct Smad1 linker phosphorylation as expression of *smad6*, an early response gene of BMP2, was also repressed when Smad1 mutants lacking the Erk phosphorylation sites mediated BMP signaling. These data propose that other Erk-dependent transcription factors have an impact on BMP signaling and regulating differentiation of osteoblasts [108]. Interestingly, Smad1 linker phosphorylation on MAPK sites is a prerequisite for interaction of Smad1 with Smurf1 and Smad1 subsequently becomes polyubiquitinated and targeted for proteasome-dependent degradation. Binding of Smurf1 to Smad1 also prevents interaction of Smad1 with the nuclear translocation factor Nup214, leading to cytoplasmic retention of Smad1 [87].

Smad1 was also found to be phosphorylated by Glycogen Synthase Kinase 3 (GSK3). The linker region of Smad1 contains four GSK3 sites upstream of the MAPK sites. Typically, GSK3 requires a phosphorylated substrate. Hence, linker phosphorylation of Smad1 via GSK3 depends on phosphorylated MAPK sites and enhances Smurf1-mediated proteasomal degradation of Smad1. The study further suggests, that canoncial Wnt signaling enhances BMP signaling, as it leads to the inactivation of GSK3 [109].

1.1.6.2.5 R-Smad dephosphorylation

After C-terminal and linker phosphorylation of Smads were established, Smad1 was described to be dephosphorylated by several phosphatases. Pyruvate dehydrogenase phosphatase (PDP) specifically dephosphorylates Smad1 in mammals and the Drosophila ortholog Mothers against Decapentaplegic (MAD) [110]. The protein serine/threonine phosphatase PPM1A dephosphorylates nuclear Smad1 on its SSXS motif, which leads to inhibition of downstream BMP signaling [111]. The small C-terminal domain phosphatases (SCPs) on the other hand were shown to dephosphoylate Smad1 at both its C-terminus and linker region. The linker region is dephosphorylated, regardless of whether the phosphorylation was initiated by the previously described MAPK pathway or BMP itself, and promotes BMP signaling, while C-terminal dephosphorylation has an inhibitory effect [112, 113]. Another phosphatase shown to stimulate BMP signaling is the serine/threonine protein phosphatase 2A (PP2A). The Bβ subunit of PP2A interacts with BMP type I and type II receptors and dephosphorylate the Smad1 linker region within the cytoplasm. This event enhances BMP signaling by promoting translocation of Smads into the nucleus [114].

1.1.6.3 Smad nuclear translocation and shuttling

C-terminal phosphorylation of Smads typically triggers complex formation of two R-Smads with Smad4 through MH2 domains and subsequent nuclear translocation of the R-Smad/Co-Smad complex. The main insight into shuttling of Smads came from studies performed on

TGFβ Smads and these data have not yet been confirmed for BMP Smads. Thus the situation as it was described for TGFβ Smad2/3 will be discussed briefly.

R-Smads undergo a constant cycle of shuttling into and out of the nucleus. However, in the absence of ligand the rate of nuclear export prevails over nuclear import, which is why the majority of R-Smads resides in the cytoplasm. Upon stimulation, R-Smad phosphorylation and subsequent complex formation with Smad4, the R-Smad/Co-Smad complex translocates into the nucleus. Once the complex has reached the nucleus it is trapped because the nuclear export signal within Smad4 is masked when Smad4 is in a complex with R-Smads. Dephosphorylation of R-Smads releases the complex and leads to nuclear export of all components [115-117].

1.1.6.4 Smad-dependent gene regulation

Not only do Smads translate signals initiated at the cell membrane and cytoplasm to the nucleus, they are also involved in the regulation of target genes. Again, many insights into how Smads regulate gene transcription came from studies on TGFβ Smads. Hence, both data from TGFβ and BMP signalling will be summarized collectively.

Through their MH1 domain Smads can directly bind to specific DNA sequences [118]. The first specific sequence to be identified was the Smad Binding Element (SBE) within the promoter of the *JunB* gene [119]. *JunB* is a target gene of both the TGFβ and BMP pathway [120]. Later a BMP specific Smad binding element, termed BMP response element (BRE), was identified within the *Id1* promoter [121].

Besides binding to DNA itself, Smads can also interact with other DNA-binding proteins. Runt-related transcription factor 2 (Runx2) for example was shown to interact with R-Smads to induce osteoblast-specific gene expression in C2C12 cells, both in response to TGFβ and BMP stimulation [122, 123].

Furthermore, Smads can recruit co-activators and co-repressors of transcription. An example of a transcriptional co-activators interacting with R-Smads are p300 and CBP (CREB binding protein). Interaction of p300/CBP with Smad1 was shown to promote transcription of Smad target genes [124]. Interestingly, BMP2 stimulates acetylation of Runx2, thereby preventing Smurf-dependent ubiquitination and degradation of Runx2 [125]. The same mechanism was observed previously for Runx3 in response to stimulation with TGFβ [126].

Smad2 and Smad3 were reported to interact with transcriptional co-repressors c-Ski and SnoN, which leads to repression of TGFβ target genes [127]. c-Ski was shown to repress BMP signaling by interacting with BMP-specific Smad complexes [128]. Later this was suggested to be mediated through the interaction of c-Ski with Smad4 [129].

1.1.7 Smad-independent BMP pathways

The Smad-independent BMP pathways are activated, when the ligand binds to its high affinity type I receptor and then recruits the type II receptor into the complex. Several distinct pathways are activated via this receptor oligomerization. The most prominent pathways will be briefly summarized in the following.

1.1.7.1 MAP kinase pathways

The X-chromosome-linked inhibitor of apoptosis (XIAP) was identified as a link between the BMP and the MAP kinase pathway. XIAP mediates interaction of the TGFβ-activated kinase (Tak1; MAPKKK) with BRI [130]. Tak1 can induce activation of MKK3/6 (MAPKK) which results in the activation of the p38 MAPK pathway [131, 132]. Alternatively, Tak1 can activate c-Jun-N-terminal kinase (JNK) through MKK4 [133]. Both p38 and JNK can translocate to the nucleus, where they activate the transcription factors ATF2 and c-Fos/c-Jun that regulate specific BMP target genes [134, 135]. Notably, the inhibitory Smad6 inhibits the Tak1-dependent p38 pathway, while Smad7 promotes it [136, 137].
BMP4 was shown to signal through the Ras/Raf pathway, which in turn signals through MEK1/2 (MAPKK) and Erk (MAPK), leading to the activation of the transcription factors AP1 and GATA2 [138, 139]. Later, BMP2 was described to activate Erk, which induces osteoblast differentiation in C2C12 cells [140]. Furthermore, a crosstalk between Ras/MEK and Smad1 in intestinal epithelial cells was described to promote phosphorylation of Smad1 in response to TGFβ stimulation [141].

1.1.8 Co-Receptors

Co-receptors can adopt several roles that lead to either inhibition or promotion of the given pathway. The membrane-anchored proteoglycan Betaglycan for example acts as a type III receptor in the TGFβ signaling pathway. It associates with and presents TGFβ isoforms to the TGFβ type II receptor (TRII), thereby enhancing TGFβ signaling [142].
Several transmembrane and membrane attached proteins were shown to interact with BMP receptors and modulate their signaling outcome.

1.1.8.1 BAMBI

One of the first co-receptors to be identified was the pseudoreceptor BMP and activin membrane-bound protein (BAMBI). BAMBI is a transmembrane protein with a similar extracellular domain structure as the TGFβ superfamily type I receptors, but it is lacking an intracellular kinase domain. BAMBI can bind to type II receptors of the TGFβ superfamily, where it subsequently interferes with receptor heterodimerziation and activation of type I

receptors. More specifically, BAMBI was shown to antagonize dorso-anterior structures promoted by activin and BMP4 during embryogenesis. This negative regulation of TGFβ family signaling is achieved through ligand-independent association of BAMBI with BRIa and BRIb [143].

1.1.8.2 RGM family

Several members of the glycosylphosphatidylinositol-anchored repulsive guidance molecule (RGM) family were described as BMP co-receptors [144]. Dragon (RGMb) is expressed in the developing nervous system, where it mediates homophilic and heterophilic adhesion of neurons. It binds to BMP2 and BMP4, as well as to BRI and BRII and enhances BMP signaling [144, 145]. Like Dragon, RGMa is expressed in the central nervous system where it mediates repulsive axonal guidance and neural tube closure [146]. RGMa interacts with BMP2, BMP4 and BRI and was shown to enhance BMP-mediated Smad signaling [147]. Likewise, hemojuvelin (RGMc) binds to BMP2 and BMP4 and to BRIb (in the presence of BMP2) to enhance Smad signaling [148]. Hemojuvelin is mainly expressed in liver, heart, and skeletal muscle. *HAMP* and *HFE2*, the genes encoding for hepcidin and hemojuvelin respectively, are loci for mutations causing juvenile hemochromatosis, a disorder of iron overload. Hepcidin was described as soluble mediator of iron homeostasis, however little is known about the role of Hemojuvelin in iron metabolism. Recent findings suggest that Hemojuvelin as well as BMP2 promote expression of Hepcidin. Presence of Hemojuvelin as co-receptor for BMP2 is crucial in this respect. The model is further supported by liver-specific conditional Smad4 knockouts in mice, which demonstrate reduced Hepcidin expression and iron overload [148, 149]. Knockdown of RGMa, Dragon or Hemojuvelin in the mouse myoblast cell line C2C12 results in significant reduction of Smad-dependent and Smad-independent BMP signaling. In conclusion, every single RGM BMP co-receptor is required for solid BMP signaling and members of the family can not compensate for one another [150].

The presence of these co-receptors sensitizes cells to the ligand, which may lead to a greater or more rapid response. Furthermore, these co-receptors may enable cells to respond to lower ligand concentrations.

1.1.8.3 c-kit

The tyrosine kinase stem cell factor receptor (c-kit) is a proto-oncogene, associated with several forms of highly malignant human cancers. In healthy cells c-kit mediates survival and development of hematopietic stem cells and was also found to be expressed in osteoblasts, epithelial, endothelial, and mast cells [151, 152]. Interestingly, transcription of c-kit is significantly reduced following removal of the leukaemia inhibitory factor (LIF) when mouse

embryonic stem cells migrate from the pluripotent to a differentiated stage. The study suggests that expression of c-kit reappears in later stages of differentiation [153]. The c-kit ligand stem cell factor (SCF) induces homodimerization and subsequent activation of c-kit [154]. Activation is accompanied by autophosphorylation of c-kit on tyrosine residues, which then serve as interface for proteins containing SH2 and phosphotyrosine-binding domains, such as Src family kinases, the adaptor protein Grb2, phosphatidyl-inositol 3-kinase, and phospholipase Cγ [155].

In a proteomics-based approach c-kit was isolated as a BRII tail associated protein. Effective complex formation requires presence of either BMP2 or BMP2 and SCF, suggesting that the interaction site only becomes available in activated BRII. Treatment of C2C12 cells with SCF had no effect on Smad phosphorylation. However, Smad phosphorylation was enhanced upon simultanous treatment with BMP2 and SCF, as compared to stimulation with BMP2 alone. Compared to BMP2 stimuatlion, phosphorylation of Erk occurred with a delay in response to treatment with both BMP2 and SCF and the overall dynamics were changed [156]. Interestingly, kit ligand stimulates expression of BMP15 and mutations in kit ligand and c-kit both cause infertility in female mice [1].

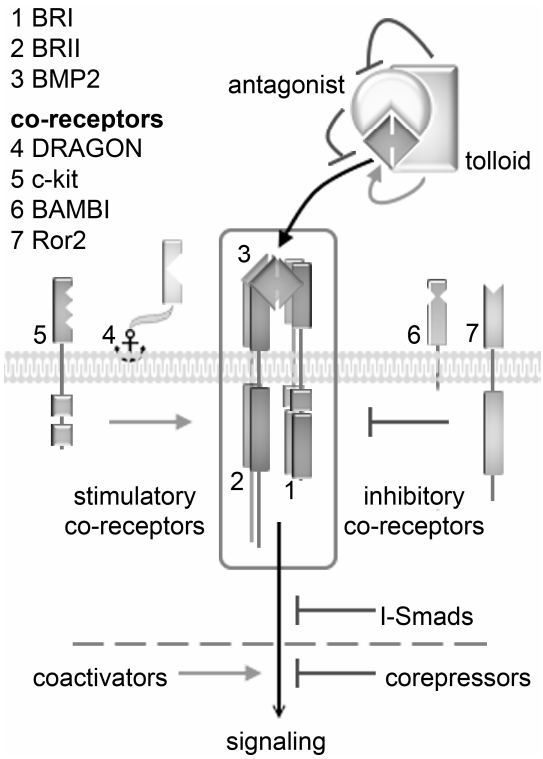

Figure 1.6 Regulation of BMP signaling on different levels [157]

BMP signaling events can be altered at different sites along the pathway. First antagonists such as chordin can bind to the ligand and decrease its receptor affinity. The chordin-BMP2 complex is recognized by tolloid, a metalloprotease which is able to cleave chordin. It thereby suspends the inhibitory effect on BMP2 and at the same time stimulates its activity. Further down the pathway co-receptors can both enhance and attenuate receptor activity. DRAGON and c-kit are both stimulatory co-receptors while BAMBI and Ror2 were found to inhibit BMP signaling. I-Smads achieve their inhibitory effect by competing with R-Smads for the binding site on the type I receptoe. Once the signal has reached the nucleus its effect depends on the interplay with several factors including nuclear coactivators or corepressors.

1.2 Ror2

The Regeneron orphan receptor Ror2, which is no longer orphan, is a transmembrane receptor that belongs to the Ror subfamily of cell surface receptors, which consist of Ror1 and Ror2, two proteins that share 58% overall amino acid identity [158]. Ror2 is most closely related to the tyrosine protein kinase (Trk) family of receptor tyrosine kinases which has been highly conserved throughout evolution. Initially Ror2 was found to be involved in neuronal development. Later Ror2 was also described to be involved in many other developmental processes, mainly cartilage and growth plate development [159].

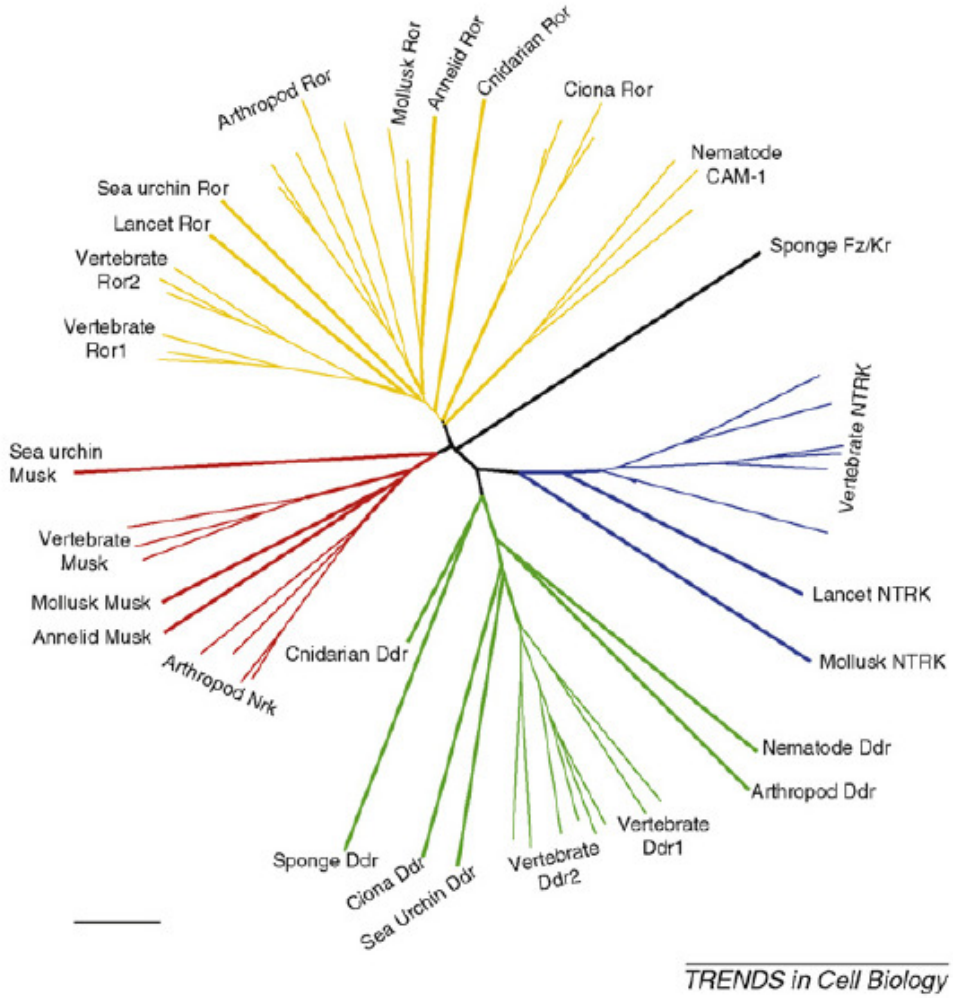

Figure 1.7 NTRK superfamily of receptor tyrosine kinases [160]

The tree, which has no root, represents an approximation of the evolutionary divergence, because different domains within the proteins have evolved at different rates in different species and have experienced independent introductions of the Ig domain. Highlighted are the NTRK (blue), Ddr (green), MuSK and Nrk (red) and Ror (yellow) families; each line represents a single protein from a species in the labelled clade (i.e. the three lines for nematode CAM-1 represent CAM-1 of C. elegans, Brugia malayi and Pristionchus pacificus). The sponge Frizzled Kringle protein (black) does not fit into any family.

1.2.1 Structure

On the extracellular side Ror2 contains an N-terminal immunoglobulin-like domain (Ig), followed by a cysteine-rich frizzled-like domain (CRD), a kringle domain and the

transmembrane domain. Intracellularly, Ror2 carries a tyrosine kinase domain and the C-terminal tail region is composed of serine/threonine- and proline-rich microdomains (Figure 1.8) [158].

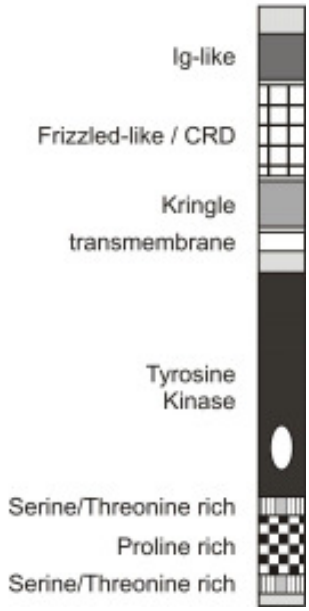

Figure 1.8 Ror2 domain structure, according to [158]

Ror2 possesses an extracellular immunoglobulin-like (Ig) domain, frizzled-like cysteine-rich (CRD) domain, and a kringe domain. On the intracellular side the tyrosine kinase domain is followed by two serine/threonine rich regions, separated by a praline-rich region.

Immunoglobulin (Ig) domains are involved in protein recognition and interaction as well as cell adhesion. The muscle specific kinase (MuSK) for example, a tyrosine kinase receptor related to Ror2, is required for the formation of the neuromuscular junction (NMJ). The NMJ is a peripheral cholinergic synapse that transduces signals from the motor neurons to the muscle cells. It appears that MuSK interacts with the surface of the muscle through two of its three Ig domains. This interaction is a prerequisite for clustering of the acetylcholine receptor complex at the postsynapse [161].
In Ror2 this domain was not yet described to have specific functions.

The **frizzled cysteine-rich domain (CRD)** is found mainly in frizzled receptors, where it acts as ligand interaction domain for Wnts. Frizzled receptors are seven-pass transmembrane receptors. Upon binding of the ligand they dimerize which, in concert with the LDL-receptor related protein 5 or 6 (LRP5 or LRP6) and the intracellular signal transducer Disheveled (Dvl), leads to activation of the Wnt/β-catenin pathway [162, 163].
The frizzled-like domain of Ror2 was identified as interaction platform for several proteins, among them Wnt ligands, the Frizzled receptor 2 (rFzd2) and BRIb [164, 165]. Additionally, point mutations causing Robinow Syndrome were found within the CRD domain of Ror2 [166, 167].

Kringle domains (Kg) are rich in Cyteines with a heavily folded structure stabilized via disulfide bonds. Kringle domains are protein-protein interaction sites and were suggested to play a role in blood clotting and inhibition of angiogenesis [168].
Other than Ror2 only the Torpedo family of recetor tyrosine kinases contains a Kringle domain. Moreover, no specific function of the Kringle domain in Ror2 has been suggested to date. However, several point mutations causing Robinow Syndrome are located within the Kringle domain of Ror2 [167, 166, 169].

Within its extracellular region, Ror2 contains three **potential N-glycosylation sites**. N80 is located just prior to the Ig domain, N188 lies within the CRD domain and N308 within the Kg domain [158].

The **tyrosine kinase domain** of Ror2 is homologous to growth factor receptors like the Trk family or the muscle-specific kinase (MuSK) [158].

The **serine/threonine- (ST)** and **proline-rich (P) microdomains** within the C-terminal tail have been shown to serve as phosphorylation and interaction site for various proteins [170, 171]. The P microdomain was described to contain potential SH3 domain binding sites [172]. Indeed it has been found that the Ror2 tail region is required to recruit the cytosolic tyrosine kinase Src. Moreover, Ror2 is phosphorylated and activated in the presence of Src [173].

1.2.2 Animal models

The *Drosophila* ortholog of Ror2, *Drosophila* neurospecific receptor kinase (Dnrk), was described to be expressed exclusively in the developing nervous system during embryogenesis [174].

Expression of Ror2 in mice was originally characterized for the developing nervous system where Ror1 and Ror2 are widely, but differentially expressed. Expression of Ror2 declines after birth, while Ror1 was also found expressed in non-neuronal tissue in the adult organism [172]. In a subsequent study heterozygous and homozygous Ror2 knockout mice were created. Ror2 -/+ mice appeared healthy and fertile, while the homozygous Ror2 knockout was lethal. Ror2 -/- mice exhibited dwarfism with short limbs and tails as well as facial malformations. Further characteristics were forced respiration and severe cyanosis which was shown to be due to malformations of the heart and lung. Studies of wildtype animals revealed that in embryonic developmental stage E9.5 Ror2 was highly expressed in the branchial arches, tailbud region, forebrain, and midbrain. In E12.5 expression was detected in the nervous system, specifically in the midbrain, cerebral neocortex and spinal cord.

Analysis of the long bones and vertebrae in mutant mice showed that Ror2 is required for proper chondrocyte functioning [159]. These findings were confirmed by another group which also published that Ror2 is expressed in chondrocytes of bones that undergo endochondral ossification, as well as in the heart and the dermis. Post-natally Ror2 is expressed in articular cartilage, perichondrium and periosteum, and a specific subset of growth plate chondrocytes that serve as reserve or have a function in proliferation [175]. Mice deficient in Ror1 do not exhibit skeletal or cardiac abnormalties. Nevertheless, they die post-natally due to respiratory dysfunction. Mice mutant for both Ror1 and Ror2 show more severe skeletal defects than Ror2-mutant mice [176].

1.2.3 Wnt excursus

Since Ror2 has emerged as a critical player in Wnt signaling during recent years, which will be outlined in the paragraphs below, Wnt signaling will be introduced briefly.

Canonical Wnt signaling mediates the stabilization of β-catenin. In the inactivated state, axin binds both β-catenin and Gsk3β. In this complex, Gsk3β can phosphorylate β-catenin which subsequently targets β-catenin for ubiquitination and proteasome-dependent degradation. When Wnt binds to its receptors Frizzled (Fz) and lipoprotein receptor-related protein (LRP), Dishevelled (Dvl) can interact with Fz and recruit the axin/β-catenin/Gsk3β complex to the membrane. Here Gsk3β and CKIγ phosphorylate LRP, which opens up interaction sites for axin. When axin interacts with LRP, β-catenin is released from the destruction complex and can translocate to the nucleus, where it may interact with transcription factors and other proteins to regulate gene transcription (Figure 1.9). Wnts that activate this pathway include Wnt1, Wnt3a and Wnt8 [177].

Essentially, two different noncanonical Wnt signaling pathways are known: the Wnt/Ca^{2+} pathway and the planar cell polarity (PCP) pathway. Although Wnt still binds to Fz and activates Dvl, downstream signaling events in both pathways involve neither β-catenin, nor Gsk3β [178, 179]. The Wnt/ Ca^{2+} signaling cascade was the first noncanonical pathway identified and leads to activation of the calcium/calmodulin-dependent kinase and protein kinase C, as well as activation of heterotrimeric G proteins that in turn activate phosphodiesterase and phospholipase C. These events are accompanied by and depend on an increase of intracellular calcium levels. Overall this pathway plays a critical role in cell adhesion and cell movements during gastrulation [180].
In the PCP pathway, Wnt leads to activation of the small GTPases Rho and Rac and the C-Jun N-terminal kinase (JNK) through Dvl. These signaling cascades mediate asymmetric cytoskeletal organisation and polarization of cells through reorganization of the actin and

microtubuli cytoskeletion. Wnt5a and Wnt11 have been described to activate noncanonical Wnt signaling [180].

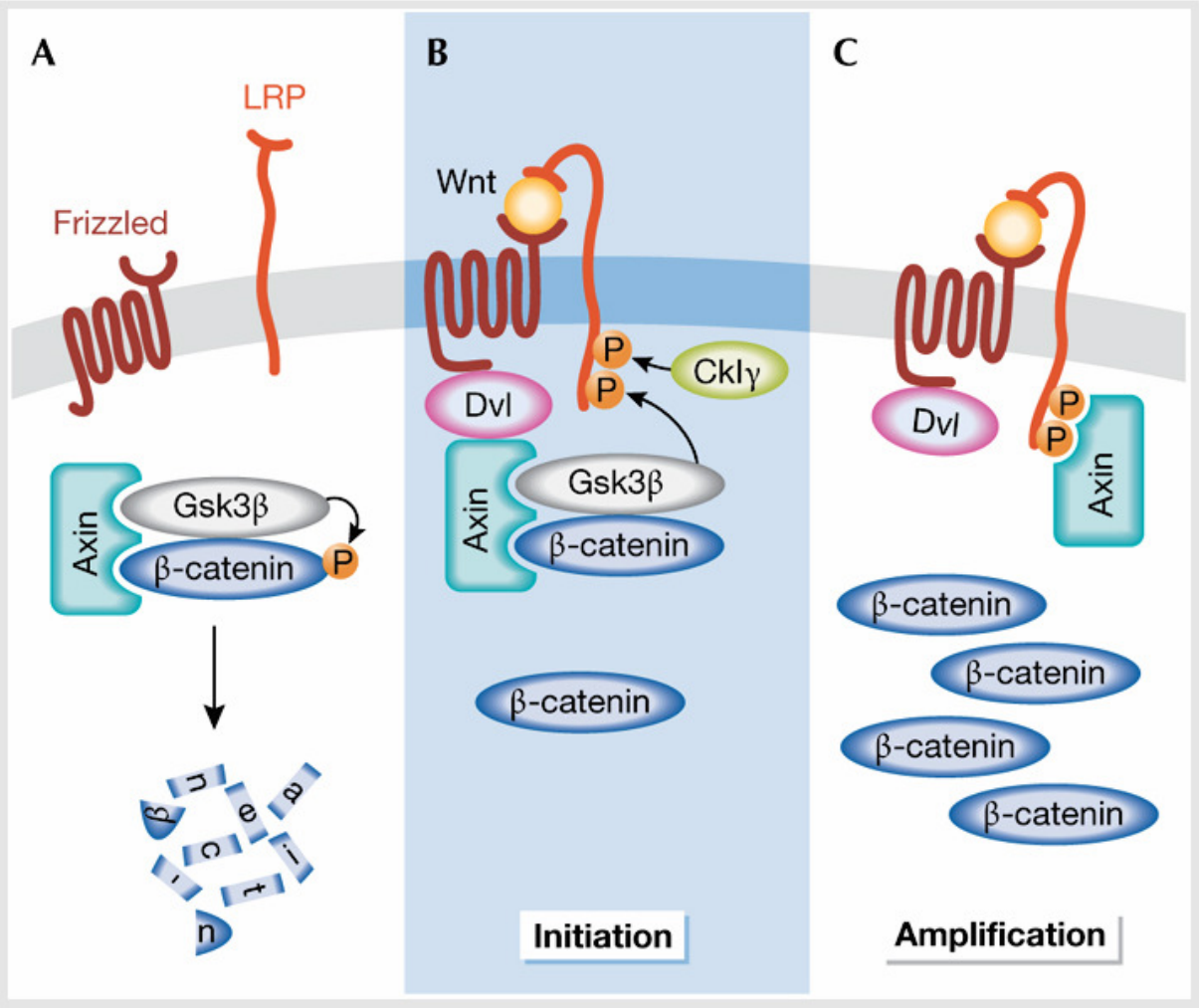

Figure 1.9 Model for the activation of the canonical Wnt/β-catenin pathway [177]

(A) In the absence of a Wnt signal, β-catenin is phosphorylated and targeted for proteasome-mediated degradation by a destruction complex that contains axin and Gsk3β among other proteins.
(B) On binding of Wnt to the receptors Fz and LRP, Dvl binds to Fz and recruits the destruction complex through interaction with axin. Subsequently, Gsk3β phosphorylates critical sites on LRP, which, together with residues phosphorylated by CkIγ, act as docking sites for axin.
(C) Binding of axin to LRP leads to inhibition of the destruction complex and stabilization of β-catenin. CkIγ, casein kinase Iγ; Dvl, dishevelled; Fz, Frizzled; Gsk3β, glycogen synthase kinase 3β.

1.2.4 Ror2 and Wnt signaling

Ror2 was described to promote osteoblast differentiation and enhance ex vivo bone formation [181]. Liu et al. found that expression of Ror2 increases during differentiation of pluripotent stem cells to osteoblasts and declines as cells progress to osteocytes. Later they demonstrated that homodimerization of Ror2 induces the phosphorylation of the scaffold protein 14-3-3β in U2OS osteosarcoma cells [182]. In a follow-up study the group shows that Ror2 homodimerization and its tyrosine kinase activity are induced by Wnt5a. Wnt5a also potentiates Ror2-dependent phosphorylation of 14-3-3β [183]. Another group showed that

constitutive homodimerization of Ror2 induces its tyrosine kinase activity and leads to recruitment and activation of the cytoplasmic tyrosine kinase Src. Inhibition of Src kinase activity blocks and stimulation with Wnt5a induces native Ror2 phosphorylation. These events depend on the presence of the Ror2 C-terminal microdomains, which are deleted in both Brachydactyly Tpye B (BDB) and Robinow Syndrome [173].

Ror2 possesses an extracellular cysteine-rich domain (CRD) that resembles the Wnt-binding site of Frizzled proteins [184]. Several studies propose an interaction of Ror2 with members of the Wnt family [164, 185, 186]. In one publication Ror2 was described to modulate canonical Wnt signaling in cells of the osteoblastic lineage. Wnt signaling promotes survival and differentiation of osteoblastic cells by mediating the stabilization of β-catenin. Ror2 was shown to interact with both Wnt1 and Wnt3, leading to inhibition of Wnt3 on the one hand and potentiation of Wnt1 downstream signaling on the other [186]. Recently, a study could show that Ror2 also positively modulates Wnt3a-mediated canonical Wnt signaling. In lung epithelial cells, the Wnt3a-activated pathway was shown to depend on the interaction of Ror2 with Frizzled receptor 2 (Fzd2). This requires the CRD domain of Ror2, while the C-terminal microdomains are dispensable. The positive effect of Ror2 on canconical Wnt signaling as observed in this study is inhibited by the Wnt antagonists Dickkopf homolog 1 (Dkk1) and Kremen1 (Krm1) [187].

One of the first studies showing that Ror2 is also involved in noncanonical Wnt signaling found that *ror2-/-* and *wnt5a-/-* mice exhibited similar phenotypes. Further experiments revealed that Ror2 and Wn5a interact, leading to activation of the Wnt5a/JNK (c-Jun N-terminal kinase) pathway and inhibition of convergent extension movements in Xenopus [164]. Shortly thereafter the same group published that Ror2 interacts with the downstream Wnt regulator casein kinase Iε (CKIε) and that CKIε phosphorylates Ror2 on its C-terminal serine/threonine-rich microdomain. This leads to autophosphorylation of Ror2 on tyrosine residues and subsequent tyrosine phosphorylation of G protein-coupled receptor kinase 2 [185]. Later this group postulated that Wnt5a-induced phosphorylation of Ror2 is mediated through glycogen synthase kinase-3 (GSK-3) [188]. Nishita et al. could show that Ror2 mediates Filopodia formation and is required for Wnt5a-induced cell migration. While the kinase activity of Ror2 was not required for initiating cell migration, mutants lacking either the extracellular CRD domain or C-terminal regions containing the proline-rich microdomain could not induce cell migraton after stimulation with Wnt5a [189]. Furthermore, Wnt5a-regulated directional cell migration and cell proliferation in mammalian palate development is mediated by Ror2 [190]. A study on wound healing demonstrated that Wnt5a-stimulated activation of JNK at the wound edge is dependent on Ror2. Moreover, Ror2 associates with the actin-binding protein filamin A. Inhibition of JNK activity or the protein kinase Cζ (PKC ζ)

or disruption of the Ror2/filamin A interaction terminate Wnt5a-induced lamellopodia formation and reorientation of the microtubule-organizing center (MTOC), events that are required for directed cell migration and subsequent wound healing [191]. In Xenopus XRor2 was shown to regulate expression of the paraxial protocadherin (XPAPC) through an alternative noncanonical pathway mediated by XWnt5a. During gastrulation of the embryo this pathway is required to regulate convergent extension movements [192]. Mikels et al. found that Wnt5a synergizes with Ror2 to inhibit Wnt3a-mediated reporter activation. The CRD domain of Ror2 is required in mediating this inhibitory effect [193].

Winkel et al. found that Ror2 interacts with Bprp, a basic proline rich protein which was shown to be highly expressed in bone, brain and heart. In several cell types its expression is dependent on cell adhesion. Overexpression of Bprp has a stimulating effect on canonical Wnt signaling. Besides, Bprp interacts with Ror2 and increases its Tak1 dependent phosphorylation. Thus it is speculated that Bprp acts as an adaptor protein which mediates the functional interaction of Ror2 and Tak1. In the presence of Tak1, Ror2 is phosphorylated on a p38-typical T*GY* motif, which was first recognized on phospho-p38 Western blots. Ror2 does indeed possess a TGY motif in its C-terminal domain [171].

1.2.5 Ror2 and BMP signaling

We have shown that Ror2 interacts with the Bone Morphogenetic Protein (BMP) Receptor type Ib (BRIb). This interaction depends on the CRD domain of Ror2 and leads to the inhibition of BRIb-induced Smad signaling. Prechondrogenic ATDC5 cells overexpressing either Ror2 or BRIb were shown to enter chondrogenesis when stimulated with GDF5. However, co-expression of both proteins did not induce chondrogenesis [165].

In our most recent publication we describe that Ror2 is selectively associated with and transphosphorylated by BRIb, independent of Ror2 kinase activity. Furthermore, formation of the Ror2/BRIb complex is independent of post-translational modifications or disulfide bonds. The complex is also stable under high ionic conditions. However, it is sensitive to low concentrations of SDS. Additionally, Ror2 and BRIb co-fractionate in detergent-resistant membrane regions (DRMs), suggesting that the formation of the Ror2/BRIb complex occurs in these membrane microdomains [194].

1.2.6 Ror2 in skeletal disorders

Although Ror2 has been shown to play crucial roles in developmental morphogenesis in different tissues, as well as survival and differentiation of cells, we are only beginning to understand how Ror2 mediates these signaling events in detail.
Many initial insights came from mutant mice [159, 175]. Mutations of Ror2 were also found to be responsible for two skeletal disorders in humans, Brachydactyly type B and Robinow Syndrome [37, 184].

1.2.6.1 Brachydactyly Type B

The word "Brachydactyly" has evolved from the Greek *brachys* for short and *daktylos* for finger. The Brachydactylies are inherited in an autosomal dominant manner and are characterized by excessively shortened tubular bones in hands and feet, which result from the premature closing of epiphyses in growing bones. Symptoms can be extra carpals, short phalanges, short thumbs, short metacarpals, symphalangism of the fingers and 2nd and 3rd toes, short femurs and sometimes absent phalanges. So far several forms of Brachydactyly have been characterized. Brachydactyly type A2 (BDA2) is caused by mutations in BRIb and mutations in GDF5 result in BDC [195].
BDB is caused by mutations in Ror2 and is the most severe form of Brachydactyly [37]. BDB mutations in Ror2 typically occur in two hotspots and truncate the receptor. One hotspot is located just before the kinase domain (proximal) the other just after the kinase domain (distal) (Figure 1.10). It appears that the distal truncations are less viable and cause a more severe phenotype than the proximal truncations of the receptor [196].

1.2.6.2 Robinow Syndrome

Mutations in Ror2 also cause Robinow Syndrome, which shares similarities with the Brachydactyly. It has been described as a dwarfism syndrome with mesomelic limb shortening, hemivertebrae, genital hypoplasia and characteristic facial appearance that were termed "fetal facies" by Robinow. The syndrome was described to be inherited in both autosomal recessive and autosomal dominant manners [184].
Robinow mutations occur both in extracellular and in intracellular domains of the receptor. These mutations can cause single amino acid exchanges as well as receptor truncations (Figure 1.10) [196].
Bioinformatic screening of disease-associated genes revealed that Ror2 point mutations resulting in Robinow Syndrome may be degraded within the Endoplasmatic Reticulum (ER), hence will never reach the cell surface. In fact, subsequent experiments confirmed that ER retention of mutant Ror2 is indeed the mechanism underlying Robinow Syndrome [197].

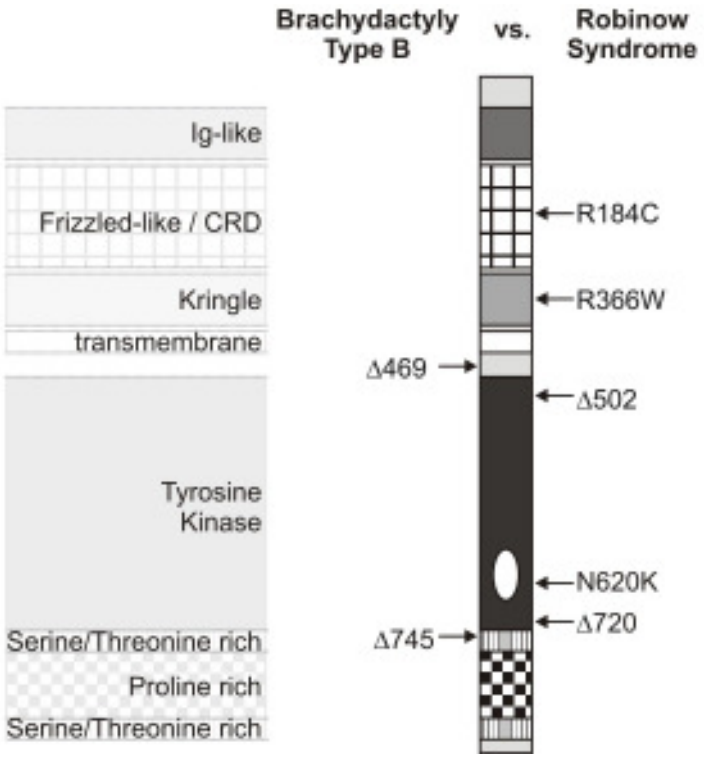

Figure 1.10 Brachydactyly and Robinow mutations in Ror2, according to [196]

The mutations shown in this figure are representative for a collection of mutations that have been described. Point mutations in the extracellular region of Ror2, such as R184C in the cysteine rich (CRD) domain or R366W in the Kringle domain, were described to cause single amino acid exchanges and Robinow Syndrome in humans. Point mutations in the intracellular region just before (Δ469) or after (Δ745) the kinase domain, result in a truncation of the receptor and cause Brachydactyly type B (BDB). Mutations within the kinase domain however, whether they are resulting in a receptor truncation (Δ502 and Δ720) or in a single amino acid exchange (N620K), cause Robinow Syndrome.

1.3 Ubiquitin-depenent protein degradation

Protein synthesis, recycling and degradation are key processes in maintaining cell integrity. These processes enable cells to rapidly adapt to an ever changing extracellular and intracellular environment, especially during development. There are many ways to shut down or fine tune signal transduction within the cell, the major one being protein internalization and/or degradation initiated by ubiquitination.

The total daily protein turnover within the adult human body constitutes approximately 2% of body weight. Based on this theoretical number, the adult body is internally overhauled and renewed roughly every three months. Thus unsurprisingly, the significance of protein degradation via ubiquitination becomes evident in the face of human diseases. The neurodegenerative Alzheimer's disease (AD) for example is, among other things, characterized by an accumulation and aggregation of missfolded proteins. Evidently, a certain step within the quality control mechanism failed to recognize these proteins and direct them to degradation. Furthermore, the amyloid plaques and intraneuronal neurofibrillary tangles were both described to contain an accumulation of ubiquitin protein, possibly containing a mutant form of ubiquitin that was shown to block proteolysis in neuronal cells. Several more data hint to an impairment of the ubiquitin system in AD and underline the importance of the ubiquitin proteasome system for proper cell maintenance [198, 199].

1.3.1 Ubiquitination

Ubiquitin is a highly conserved protein that can be covalently attached to lysine residues on other proteins and as such conveys several functions. First and foremost it can serve as a degradation signal for the protein it was attached to. But also progression of some signaling pathways depends on receptor ubiquitination, and here ubiquitination is not primarily associated with degradation. The attachment of a ubiquitin moiety to a protein can remodel the protein's surface and thereby affect its properties including activity, stability, interaction with other proteins or its subcellular localization [200].

The covalent modification of proteins with ubiquitin on lysine residues is mediated by three types of enzymes. E1, the ubiquitin-activating enzyme, hydrolyzes ATP and forms a complex with ubiquitin; E2, the ubiquitin-conjugating enzyme, accepts ubiquitin from E1 and also forms a complex with ubiquitin; finally E3, the ubiquitin ligase, binds both E2 and the protein substrate, and transfers the ubiquitin to the substrate. In subsequent rounds ubiquitin itsself is the substrate and the initial protein substrate is polyubiquitinated (Figure 1.11) [201].

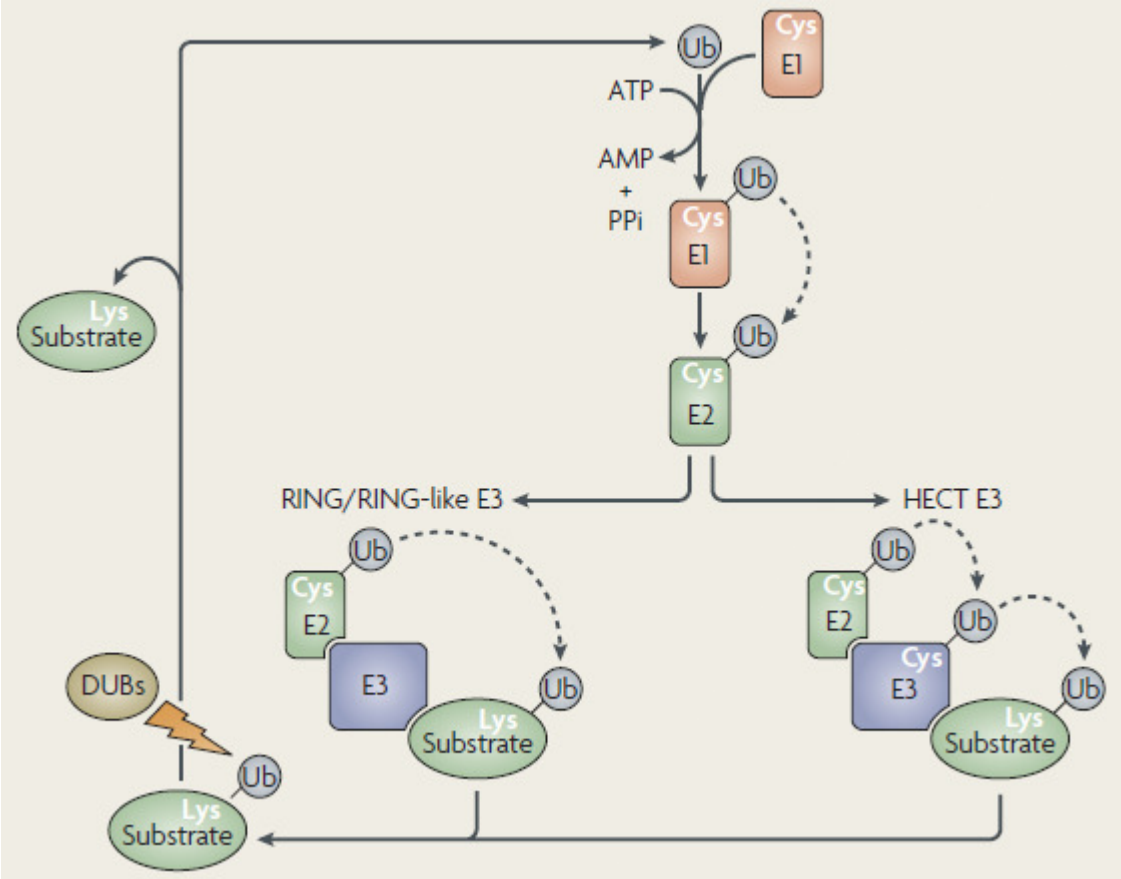

Figure 1.11 The ubiquitin-conjugating machinery [201]

Substrate proteins, destined for elimination, are initially attached to polymers of the highly conserved ubiquitin (Ub) protein. This covalent modification of the substrate targets the conjugated protein to a multicatalytic protease complex, the 26S proteasome5. The Ub attachment site in substrate proteins is commonly a Lys side chain. A well-defined series of enzymes orchestrates the attachment of mono- and polyubiquitin to proteins (see figure). Ub is first activated in an ATP-consuming reaction by an E1 Ub-activating enzyme, to which it becomes attached by a high-energy thioester bond. Subsequently, the activated Ub is transferred to the active site Cys of a second protein, an E2 ubiquitin-conjugating enzyme. With the aid of a third enzyme, called E3 or ubiquitin-protein ligase, E2 catalyses the transfer of (poly)ubiquitin onto the protein that is destined for degradation. E3 is the most important enzyme in determining the specificity of substrate ubiquitylation. There are two major classes of mechanistically distinct E3 enzymes, characterized by the RING (or RING-like) and HECT domains. Both types of E3 enzymes are alike in their ability to establish selective substrate binding. The RING finger uses Cys and His residues to coordinate a pair of zinc ions in a characteristic arrangement (not shown). A smaller set of E3 enzymes contain a domain called the U box, which is a degenerate version of the RING-finger that achieves the same general fold without coordinating any metal ions143. RING and RING-like E3 enzymes bind to both the E2 enzyme and the substrate, and catalyse the transfer of Ub directly from the E2 enzyme to the substrate. Unlike RING and U-box E3 enzymes, the HECT E3 enzymes have a more direct catalytic role in substrate ubiquitylation. The activated Ub of the Ub–E2 enzyme thioester is transferred to a conserved Cys residue in the HECT domain of the E3 before finally being transferred to a substrate. Ubiquitylation is reversed by de-ubiquitylating enzymes (DUBs) that remove ubiquitin from proteins and disassemble polyubiquitin chains. DUBs provide additional regulatory control before protein degradation, and they are also fundamental for maintaining a sufficient pool of free ubiquitin molecules in the cell.

Similar to most signaling pathways, the ubiquitin system follows a strictly hierarchical system. A single E1 enzyme is responsible for activating ubiquitin molecules and transferring them to the over 20 different E2 enzymes. Each E2 enzyme in turn can transfer ubiquitin to one or several of the approximately one thousand E3 enzymes. Two major families of E3 ligases have been characterized: the HECT (homologous to E6-AP C-terminus) domain-containing

and the RING finger domain-containing families of E3 ligases. The latter doesn't recognize and bind ubiquitin directly, but rather serves as a scaffold protein to which both the E2 enzyme and the substrate bind, and through which the transfer of the activated ubiquitin moiety from the E2 onto the substrate is mediated (Figure 1.11) [198].

A polyubiquitin chain consisting of at least four ubiquitin moieties targets the protein substrate to the 26S proteasome. Alternatively, only a single Ubiquitin can be added to one (monoubiquitination) or several (multiubiquitination) lysines on a protein. This typically targets the protein for a different route of internalization, either resulting in recycling back to the plasma membrane or degradation via the lysosome-dependent pathway [200].
Each ubiquitin molecule contains seven lysines which can serve as docking site of the ubiquitin molecule to its substrate or to another ubiquitin molecule within a polyubiquitin chain. Linkage of polyubiquitin chains through Lysine 48 (UbK48) is predominantly used for targeting the substrate to the proteasome. UbK63-linked mono- multi- or linear polyubiquitination has been implicated in DNA damage tolerance, inflammatory response, ribosomal protein synthesis, and the lysosome-dependent (endocytic) pathway [200]. Most recently however, polyubiquitin chains linked through K63 were suggested to serve as a targeting signal for the 26S proteasome [202].

1.3.2 Lysosome-dependent degradation

Lysosomes are organelles with an acidic lumen that readily fuse with endosomes. Thus they are key players in the degradation process of endocytosed substances [203]. Ubiquitinated cargo is delivered to lysosomal compartments from the trans-Golgi network, the cell surface and from late endosome lumenal vesicles, which accumulate to form multivesicular bodies (MVBs).

Both TGFß and BMP receptors have been shown to depend on clathrin-mediated endocytosis for progression of signaling and for the BMP pathway this was described in detail in chapter 1.1.5. Internalization via clathrin-coated pits appears to be the major internalization route for further downstream signaling, but is also a path that leads to receptor degradation. It was suggested that clathrin-coated pits serve as sites where active TGFß receptor complexes are sequestered. Furthermore, the Smad2-anchor for receptor activation (SARA) was found to interact with TGFß receptors in the clathrin pathway where it mediates the interaction of the type I receptor with Smad2, thus promoting downstream TGFß Smad signaling [70, 73].

Translocation of receptor complexes into early endosomes and subsequent initiation of downstream signaling may be followed by either recycling of the receptors back to the plasma membrane or receptor degradation in late endosomes. Late endosomes fuse with lysosomes and can form multivesicular bodies (MVBs) required for the degradation of transmembrane proteins. Multiubiquitination is a key signal for sorting receptors into intralumenal vesicles through the endosomal sorting complex required for transport (ESCRT) machinery. An accumulation of intralumenal vesicles constitutes multivesicular bodies [204].

1.3.3 Proteasome-dependent degradation

Polyubiquitination typically marks proteins for degradation via the 26S proteasome, but also ubiquitin-independent degradation of proteins through the 20S proteasome has been observed [205].

Additionally to what was described above, TGFß receptors also internalize via caveolae-positive or detergent-resistant membrane microdomain (DRM) internalization routes. Caveolin-positive membrane sites were described to contain Smad7-Smurf2 complexes which cause inhibition of TGFß Smad signaling. Smurf2 polyubiquitinates the receptors and thereby targets them to a rapid internalization via DRMs and subsequent proteasome-dependent degradation [70, 206].

Generally, internalization via DRMs is seen as a pathway that rapidly delivers receptors to the proteasome for degradation and down-regulation of surface expression. In the case of TGFß and the epidermal growth factor receptor, this route of internalization has not yet been associated with downstream signaling. This appears to be different for receptors of the BMP family, which was described in chapter 1.1.5.

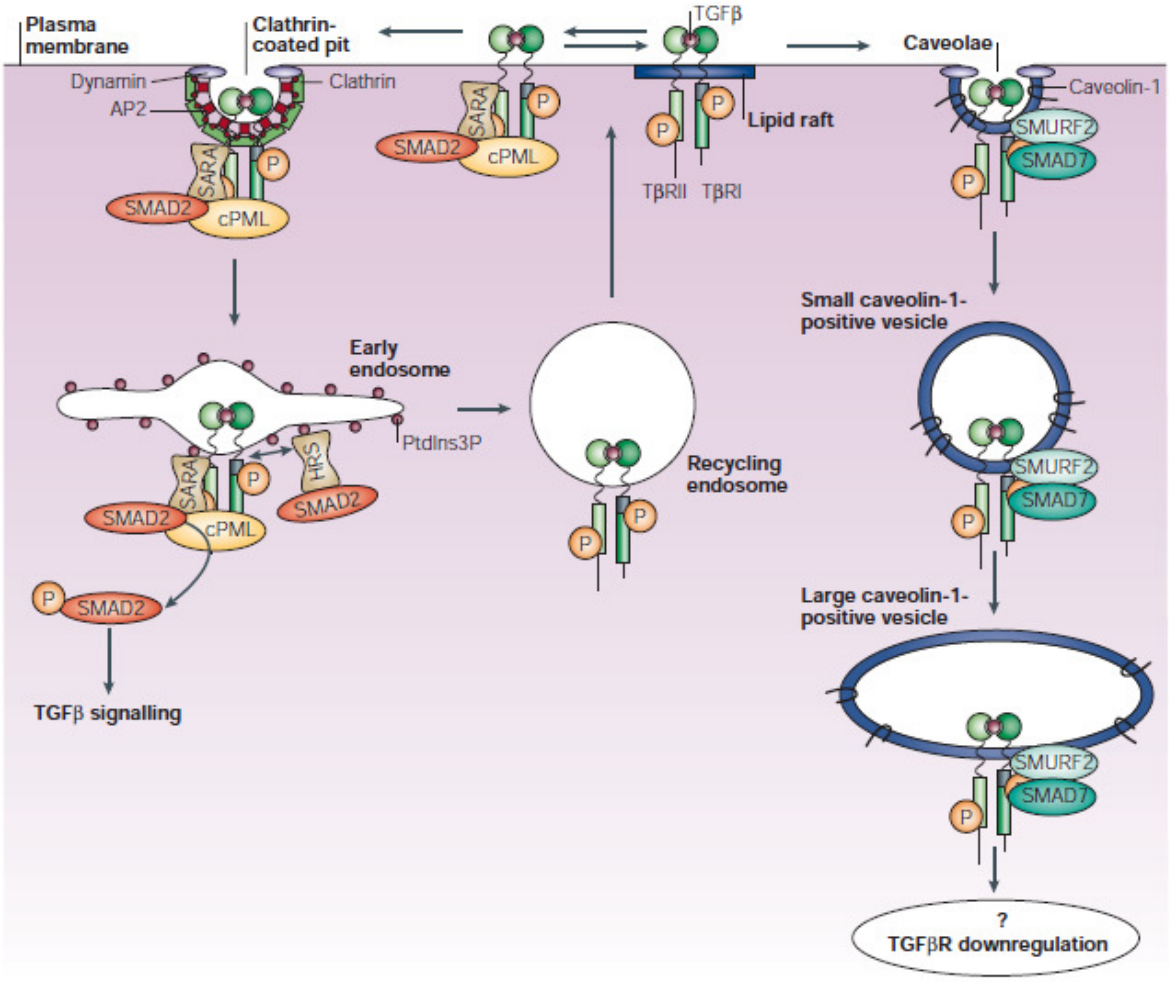

Figure 1.12 Transforming-growth-factor-β-receptor internalization by clathrin- and lipid-raft-mediated endocytosis [204]

At the plasma membrane, the tetrameric transforming-growth-factor-β-receptor (TGFβR) complex is internalized by two distinct endocytic pathways. The TGFβR complex is composed of two type-I TGFβRs (TβRIs) and two type-II TGFβRs (TβRIIs), and in this complex, constitutively active TβRII transphosphorylates TβRI. For simplicity, this tetrameric complex is represented by a dimeric TβRII–TβRI complex in this figure. In the clathrin-mediated endocytic route, receptors are directed towards the early endosomes, which are enriched in phosphatidylinositol-3-phosphate (PtdIns3P). Here, the receptors interact with two 'Fab1, YOTB, Vac1, EEA1' (FYVE)- domain-containing proteins — SMAD anchor for receptor activation (SARA) and hepatocyte-growth-factor-regulated tyrosine-kinase substrate (HRS) — that are associated with SMAD2. The cytoplasmic promyelocytic leukaemia protein (cPML) that interacts with TGFβRs, SARA and SMADs, is required for the early endosomal localization of these TGFβ signalling components. Of note, SARA, SMAD2 and cPML probably also interact with TGFβ–TGFβR complexes at the plasma membrane. From the early endosomes, TGFβRs are able to signal (through SMAD2 phosphorylation) and are recycled back to the cell surface. In the lipid-raft/caveolaemediated endocytic pathway, TGFβRs associate with SMAD7–SMURF2 and are internalized into caveolin1-positive vesicles. This leads to the ubiquitin-dependent degradation of the receptors (SMURF2 is a HECT-domain-containing E3 ubiquitin ligase). The exact compartment in which the receptors are degraded has not been characterized. AP2, adaptor protein-2; P, phosphate.

1.3.4 Endoplasmatic reticulum-associated degradation

Transmembrane proteins are shuttled to the plasma membrane via the endoplasmatic reticulum (ER). Within the ER, proteins achieve their final fold and receive posttranslational modifications. Finally, proteins pass through the ER quality control. When a protein is recognized that has not folded properly, it may either undergo additional folding cycles or it

may be targeted for ER-associated degreadation (ERAD). ERAD substrates are typically marked by ubiquitination and are subsequently degraded via the proteasome. Extraction of polyubiquitinated protein from the ER into the cytoplasm, where it can be degraded in a proteasome-dependent manner, is mediated by a retrotranslocation machinery (retrotranslocan) and the cytoplasmic protein complex cell-division cycle-48 (Cdc48) [207].

1.3.5 Internalization of receptor tyrosine kinases

The epidermal growth factor (EGF) receptor remains the best characterized receptor tyrosine kinase (RTK) with regards to internalization in response to ligand stimulation. The EGF pathway thus constitutes a prototypic model on the basis of which other RTKs are studied and discussed.

Originally, the EGF receptor was found to reside in caveolae and rapidly translocate into clathrin-coated pits upon ligand binding and receptor activation. Overexpression of caveolin-1 was described to inhibit activation of the EGF receptor which is why the current idea is that only inactive receptors occupy caveolin-rich membrane domains [208].

Furthermore, the route of EGF receptor internalization may depend on the amount of ligand available to the receptor. Low doses of ligand induce internalization via clathrin-coated pits which was proposed to be independent of receptor ubiquitination. High amounts of EGF however were suggested to trigger a ubiquitin- and lipid raft-dependent route of internalization [209]. Another study from this group suggests that the EGF receptor is internalized via clathrin-coated pits that form from non-caveolar lipid rafts [210]. These findings were opposed by a study that examined dose- and clathrin-dependent internalization of the EGF receptor. Kazazic et al. could not confirm the involvement of caveolae in endocytosis of ligand activated EGF receptor, neither at high nor low EGF concentrations [211]. These contradictory observations underscore that internalization greatly depends on the constitution of individual cell types and may even differ between subclones of the same cell line [212].

Since little more is known about a caveolae- or lipid raft-dependent internalization of the EGF receptor, its internalization via clathrin-coated pits will be discussed in more detail. Endocytosis of the EGF receptor from the plasma membrane is initiated by binding of the ligand, receptor dimerization, subsequent activation and tyrosine autophosphorylation of the receptor's C-terminal domain. Mutants lacking EGF receptor kinase activity display reduced internalization rates. Moreover, the EGF receptor is recruited to clathrin-coated pits and internalized via this pathway in a Grb2-dependent manner, as was shown by siRNA-mediated depletion of Grb2. Grb2 is a SH2 and SH3 domain-containing protein that binds to

the EGF receptor on phosphorylated tyrosine residues. While Grb2 is associated with the EGF receptor through its SH2 domain, it mediates interaction between proteins attached to its SH3 domain with the EGF receptor. This Grb2-mediated interaction was observed for the RING finger containing E3 ubiquitin ligase Cbl which has been shown to cause ubiquitination of the EGF receptor. Cbl also contains a tyrosine kinase binding motif through which it can directly interact with the EGF receptor. The mode of interaction may again depend on cell type and cell constitution [212].

Nevertheless, Cbl-mediated monoubiquitination of the EGF receptor does not seem to play an exclusive role in its internalization as a mutant lacking the tyrosine interaction site for Cbl displays weak ubiquitination but is still internalized normally. Six lysine residues located in the kinase domain of the EGF receptor were shown to be sites of ubiquitination upon ligand stimulation. But also a mutation of these sites did not have an effect on receptor internalization [212].

Taken together, the EGF receptor resides in caveolin-positive membrane domains. Upon stimulation with EGF the receptor dimerizes, autoactivates and transfers into clathrin-coated pits. Downstream signaling requires internalization, which is promoted by, but not solely dependent on multiubiquitination [212].

Finally, a most recent study demonstrates that proteasome inhibition negatively affects EGF receptor phosphorylation, ubiquitination, internalization and degradation in response to ligand stimulation [213].

1.4 Aim

Initially, mutations in Ror2 were identified as the cause of Brachydactyly type B in humans (BDB) [37]. BDB shows striking phenotypic similarities to Brachydactylies type A2 (BDA2) and type C (BDC). BDA2 is caused by mutations in the BMP type Ib receptor (BRIb), while mutations in its high affinity ligand, GDF5, result in BDC [16, 214].

These findings had suggested a role for Ror2 in limb development and an involvement in BMP signaling. Ror2 was subsequently found to interact with BRIb independent of GDF5. Although GDF5 induces chondrogenic differentiation through Ror2 independent of the Smad signaling cascade, Ror2 inhibits GDF5-stimulated Smad-dependent signaling and chondrogenic differentiation in the presence of BRIb. Apparently, co-expression of both receptors leads to shutdown of pro-chondrogenic signaling [165].

Around the same time several studies proposed that Ror2 may be involved in Wnt signaling and Wnt-regulated bone formation. However, little evidence was available regarding the intracellular events through which Ror2 signaling is mediated [164, 185, 186, 215]. In the meantime it is clear that Ror2 has a role in canonical and noncanonical Wnt signaling and that it is involved in osteoblast differentiation and cell migration [182, 189-191, 216].

Based on the foundation that Ror2 interacts with BRIb and inhibits signaling through the Smad cascade, the aim of this thesis was to characterize Ror2 as a co-receptor of BRIb and to elucidate how Ror2 achieves inhibition of Smad-dependent signaling.

2 Materials and Reagents

2.1 Commercial Products

product type	manufacturer
antibodies	BD Biosciences (Franklin Lakes, NJ, USA) Cell Signaling Technology Incorporation (Danvers, MA, USA) Dianova GmbH (Hamburg, Germany) Millipore Corporation (Billerica, MA, USA) Roche Diagnostics GmbH (Mannheim, Germany) Promega Corporation (Madison, WI, USA) Santa Cruz Biotechnology Incorporation (Santa Cruz, CA, USA)
bacterial growth media	Carl Roth GmbH & Co. KG (Karlsruhe, Germany)
bacterial strains	Stratagene Corporation (San Diego, CA, USA) Invitrogen Corporation (Carlsbad, CA, USA)
cell culture, media and reagents	Biochrom AG (Berlin, Germany) Invitrogen Corporation (Carlsbad, CA, USA) Minerva Biolabs (Berlin, Germany) PAA Laboratories GmbH (Pasching, Austria) Polyplus-transfection Incorporation (New York, NY, USA) Roche Diagnistics GmbH (Mannheim, Germany)
cell culture, sterile products	Greiner Bio-One International AG (Kremsmünster, Austria) Hartenstein Laborbedarf (Würzburg, Germany) Nunc GmbH & Co. KG (Wiesbaden, Germany) Schleicher & Schuell GmbH (Dassel, Germany)
cells	LGC Standards GmbH (Wesel, Germany) PromoCell GmbH (Heidelberg, Germany)
chemicals, highest purity	Carl Roth GmbH & Co. KG (Karlsruhe, Germany) Fluka Chemie AG (Buchs, Switzerland) Merck KGaA (Darmstadt, Germany) Pierce Biotechnology Incorporation (Rockland, IL, USA) Serva Electrophoresis GmbH (Heidelberg, Germany) Sigma-Aldrich GmbH (Hannover, Germany)
consumables, non-sterile	Carl Roth GmbH & Co. KG (Karlsruhe, Germany) Eppendorf AG (Hamburg, Germany) Greiner Bio-One International AG (Kremsmünster, Austria)
consumables, sterile	Bio-Rad Laboratories (Hercules, CA, USA)
enzymes and substrates	Fermentas GmbH (St. Leon-Rot, Germany) New England Biolabs (Ipswich, MA, USA) Qbiogene Incorporation (Morgan Irvine, CA, USA) Roche Diagnistics GmbH (Mannheim, Germany) Sigma-Aldrich GmbH (Hannover, Germany)
growth factors (ligands)	Biolog GmbH (Bremen, Germany) Biopharm GmbH (Heidelberg, Germany) R&D Systems (Minneapolis, MN, USA)
kits	Ambion Incorporation (Foster City, CA, USA) Peqlab Biotechnologie GmbH (Erlangen, Germany) Promega Corporation (Madison, WI, USA) Qiagen GmbH (Hilden, Germany)
radiochemicals	Hartmann Analytic GmbH (Braunschweig, Germany)
standards	Bio-Rad Laboratories (Hercules, CA, USA) Fermentas GmbH (St. Leon-Rot, Germany) Sigma-Aldrich GmbH (Hannover, Germany)
technical gases and liquids	Linde AG (Munich, Germany)
vectors, plasmids and sequencing	addgene Incorporated (Cambridge, MA, USA) Clontech Laboratories Incorporation (Mountain View, CA, USA) GATC Biotech AG (Konstranz, Germany) GE Healthcare Biosciences Corporation (Piscataway, NJ, USA) Invitrogen Corporation (Carlsbad, CA, USA) LGC Standards GmbH (Wesel, Germany) Promega Corporation (Madison, WI, USA)

Table 2.1 Commercial products

2.2 Technical Devices

device	type	manufacturer
agarose gelelectrophoresis	Sub Cell GT Mini Sub Cell GT	Bio-Rad Laboratories (Hercules, CA, USA)
autoclave	5075 ELV	Systec GmbH (Wettenberg, Germany)
balances	XB4200C Precisa SBA33	PESA Waagen AG (Pfäffikon, Switzerland) Scaltec Instruments GmbH (Göttingen, Germany)
centrifuge (speed vac)	speed vac concentrator	Bachofer GmbH (Reutlingen, Germany)
centrifuge (table)	5417C 5804	Eppendorf AG (Hamburg, Germany)
centrifuge (table, refridgerated)	5417R	Eppendorf AG (Hamburg, Germany)
centrifuge (refridgerated)	Sorvall RC6	Thermo Fisher Scientific GmbH (Schwerte, Germany)
centrifuge (ultra)	L-60	Beckman (Palo Alto, CA, USA)
clean bench	HeraSafe	Heraeus GmbH (Hanau, Germany)
deionization system	Milli-Q	Millipore Corporation (Billerica, MA, USA)
developing machine	Optimax Typ TR	MS Laborgeräte GmbH (Wiesloch, Germany)
electrophoresis power supply	Consort E831 PowerPac HC	Consort nv (Turnhout, Belgium) Bio-Rad Laboratories (Hercules, CA, USA)
facs	Epics XL·MCL	Beckman (Fullerton, CA, USA)
incubator (cell culture)	HeraCell 240	Heraeus GmbH (Hanau, Germany)
incubator (shaking)	Duomax 1030	Heidolph Instruments GmbH & Co. KG (Schwabach, Germany)
luminometer (plate)	Mithras LB 940	Berthold Detection Systems (Pforzheim, Germany)
luminometer (tube)	FB12	Berthold Detection Systems (Pforzheim, Germany)
MALDI mass spectrometry	UltraflexII TOF/TOF	Bruker Daltonics (Bremen, Germany)
microplate reader	Sunrise	Tecan AG (Zürich, Switzerland)
microscope (cell culture)	IMT-2 Axiovert 40CFL	Olympus GmbH (Hamburg, Germany) Carl Zeiss AG (Jena, Germany)
microscope (fluorescence)	Axiovert 200M	Carl Zeiss AG (Jena, Germany)
pH meter	761 calimatic	Knick Elektronische Messgeräte GmbH & Co. KG (Berlin, Germany)
phosphor-imager	FLA-5000	Fujifilm Corporation (Stamford, CT, USA)
pipets	research	Eppendorf AG (Hamburg, Germany)
potter	Potter S	Sartorius AG (Göttingen, Germany)
protein blotting	Mini-V 8.10	Bio-Rad Laboratories (Hercules, CA, USA)
protein gel electrophoresis	Mini-Protean III system	Bio-Rad Laboratories (Hercules, CA, USA)
rocking table	Polymax 1040	Heidolph Instruments GmbH & Co. KG (Schwabach, Germany)
rotator	Rotator 211175	Neolab (Heidelberg, Germany)
scanner	CanoScan LiDE 100 Perfection 2480 photo	Canon Deutschland GmbH (Krefeld, Germany) Epson Deutschland GmbH (Böblingen, Germany)
scintillation counter	Wallac 1209Rackbeta Liquid Scintillation Counter	PerkinElmer LAS (Monza, Italy)
shaker (heated)	Thermomixer 5437	Eppendorf AG (Hamburg, Germany)
spectrophotometer	Nanodrop ND-1000 UV 1202	Peqlab Biotechnologie GmbH (Erlangen, Germany) Shimadzu Europa GmbH (Duisburg, Germany)
thermocycler	Mastercycler gradient	Eppendorf AG (Hamburg, Germany)
vortexer	n.a.	Heidolph Instruments GmbH & Co. KG (Schwabach, Germany)
water bath	n.a.	Memmert GmbH & Co. KG (Schwabach, Germany)

Table 2.2 Technical devices

Solutions and media were prepared using double-distilled water (ddH_2O) of Millipore quality.

2.3 Kits

kit	manufacturer
Dual-Luciferase™ Reporter Assay	Promega Corporation (Madison, WI, USA)
Qiagen Plasmid Kits	Qiagen GmbH (Hilden, Germany)
TnT® Quick Coupled Translation Systems	Promega Corporation (Madison, WI, USA)
Zeba™ Desalt Spin Columns	Pierce Biotechnology Incorporation (Rockland, IL, USA)

Table 2.3 Kits

2.4 Protein Standards

name	sizes	manufacturer
SDS7B Molecular Weight Standard Mixture, prestained	26.6kD – 36.5kD – 48.5kD – 58kD – 84kD – 116kD – 180kD	Sigma-Aldrich GmbH (Hannover, Germany)
Precision Plus Protein all blue Standard	10kD – 15kD – 20kD – 25kD – 37kD – 50kD – 75kD – 100kD – 150kD – 250kD (25kD, 50kD and 75kD reference bands appeared more intensive)	Bio-Rad Laboratories (Hercules, CA, USA)
PAGE Ruler Prestained Protein Ladder Plus	10kD – 15kD – 27kD – 35kD – 55kD – 70kD – 100kD – 130kD – 250kD (27kD and 70kD reference bands were prestained in red)	Fermentas GmbH (St. Leon-Rot, Germany)

Table 2.4 Protein standards

2.5 Eukaryotic Expression Vectors

name	description	source
pcAGGS	mammalian expression vector with AG/CMV-IE/lac promoter, carries Amp resistancy	addgene Incorporated (Cambridge, MA, USA) [217]
pcDNA1	suppression of amber mutations causes sensitivity to tetracycline and ampicillin	Invitrogen Corporation (Carlsbad, CA, USA)
pcDNA3	codes for ampicillin and neomycin resistance	Invitrogen Corporation (Carlsbad, CA, USA)
pCMV5	carries gene for ampicilin resistance	[218]
pGFP	mammalian expression vector for green fluorescent protein (GFP), used for expression controls	Clontech Laboratories Incorporation (Mountain View, CA, USA)
pGL3basic	expression vector for luciferase from the firefly *Photinus pyralis*, used in reporter gene assays	Promega Corporation (Madison, WI, USA)
RL-TK	mammalian expression vector for luciferase from the sea pansy *Renilla reniformis*, used as reference plasmid in dual reporter gene assays	Promega Corporation (Madison, WI, USA)
pRGSHis	with ampicillin resistance and RGS6xHis tag	Qiagen GmbH (Hilden, Germany)

Table 2.5 Eukaryotic expression vectors

2.6 Eukaryotic Expression Constructs

name	insert	vector	tag	source / donor
BRIb	mouse	pcDNA3	HA, N-terminal	[73]
BRIb	mouse	pcDNA3	myc, N-terminal	[73]
BRIILF	human	pcDNA1	HA, N-terminal	[219]
βGal	β-Galactosidase	pcDNA1	none	S. Souchelnytski, Karolinska Institute (Stockholm, Sweden)
GFP	GFP from *Aequorea victoria*	pGFP	none	Clontech Laboratories Incorporation (Mountain View, CA, USA)
RL-TK	luciferase from *Renilla reniformis* expressed via constitutive active thymidine kinase promoter	RL-TK	none	Promega Corporation (Madison, WI, USA)
SBE-luc	*Photinus pyralis*	pGL3basic	none	A. Moustakas, LICR (Uppsala, Sweden)
BRE_2-luc	*Photinus pyralis*	pGL3basic	none	P. ten Dijke, University of Leiden (Leiden, Netherlands)
Ror2	mouse	pcDNA3	Flag, C-terminal	Stefan Mundlos, MPI for Molecular Genetics (Berlin, Germany)
Ror2	mouse	pcDNA3	HA, C-terminal	Stefan Mundlos, MPI for Molecular Genetics (Berlin, Germany)
Ror2 Δ469	mouse; lacking almost entire cytoplasmic region	pcDNA3	Flag, C-terminal	Stefan Mundlos, MPI for Molecular Genetics (Berlin, Germany)
Ror2 Δ502	mouse, lacking greatest part of kinase domain and C-terminal tail region	pcDNA3	Flag, C-terminal	Stefan Mundlos, MPI for Molecular Genetics (Berlin, Germany)
Ror2 Δ720	mouse; lacking small part of kinase domain and C-terminal tail region	pcDNA3	Flag, C-terminal	Stefan Mundlos, MPI for Molecular Genetics (Berlin, Germany)
Ror2 Δ745	mouse; lacking C-terminal tail region	pcDNA3	Flag, C-terminal	Stefan Mundlos, MPI for Molecular Genetics (Berlin, Germany)
Ror2 ΔCRD	mouse; lacking extracellular CRD domain	pcDNA3	Flag, C-terminal	Stefan Mundlos, MPI for Molecular Genetics (Berlin, Germany)
Ror2 KR	mouse; K507A mutation	pcDNA3	Flag, C-terminal	Stefan Mundlos, MPI for Molecular Genetics (Berlin, Germany)
Ubiquitin	human	pRGSHis-Ub	RGS6xHis, N-terminal	Qiagen GmbH (Hilden, Germany)
Ubiquitin K7	human; all seven lysines mutated to arginine	pcAGGS	Flag, N-terminal	Julia Mössinger and Michael Krauss, AG Haucke (Berlin, Germany)
Smurf1 WT	human	pCMV5B	Flag, N-terminal	addgene Incorporated (Cambridge, MA, USA)
Smurf1 DN	human; C699A mutation	pCMV5B	Flag, N-terminal	addgene Incorporated (Cambridge, MA, USA)
Tak1dn	human; K63W mutation	pcDNA3	Flag, C-terminal	Andrea Hoffman, AG Gross (Braunschweig, Germany)
Tak1ca	human; lacking 22 N-terminal amino acids	pcDNA3	Flag, C-terminal	Andrea Hoffman, AG Gross (Braunschweig, Germany)

Table 2.6 Eukaryotic expression constructs

2.7 Bacterial Strains

name	source
E. coli DH5α	[220]
E. coli C600	[221]
E. coli MC1061	Invitrogen Corporation (Carlsbad, CA, USA)
E. coli BL21 (DE)	[222]

Table 2.7 Baterial strains

2.8 Cell Lines

name	description	source
Cos7	African green monkey kidney fibroblast-like cell line	LGC Standards GmbH (Wesel, Germany)
C2C12	Murine muscle myoblast line, described to differentiate to myotubes under serum starvation and to osteoblasts under bMP treatment	LGC Standards GmbH (Wesel, Germany)
C2C12-BRIb	C2C12 cells stably expression Bone Morphogenetic Protein Receptor type Ib (BRIb). These cells were created using retroviral transfection.	[223]

Table 2.8 Cell lines

2.9 Cell Culture Media and Reagents

name	comment	source
Dulbecco's modified eagle medium (DMEM)	prepared based on manufacturer's instructions	Invitrogen Corporation (Carlsbad, CA, USA) Biochrom AG (Berlin, Germany)
Fetal calf serum (FCS)	heat-inactivated at 56°C for 30 minutes before use	Invitrogen Corporation (Carlsbad, CA, USA) Biochrom AG (Berlin, Germany)
G418	used for selection of neomycin resistant cells; added to growth medium of C2C12-BRIb cells in final concentration of 0.5mg/ml	PAA Laboratories GmbH (Pasching, Austria)
L-glutamine	final concentration 2mM	Biochrom AG (Berlin, Germany)
Penicillin G	final concentration 100U/ml	Biochrom AG (Berlin, Germany)
Streptomycinsulfate	final concentration 100U/ml	Biochrom AG (Berlin, Germany)
Trypan blue	staining for live cell counting	Biochrom AG (Berlin, Germany)
Trypsin	used in a 2x concentration to detach adhering cells	Biochrom AG (Berlin, Germany)

Table 2.9 Cell culture media and reagents

2.10 Growth Factors

name	comment	source
BMP2 (recombinant)	gift	Prof. Dr. Walter Sebald, Würzburg
GDF5 (recombinant)	gift	Biopharm AG (Heidelberg, Germany)
GDF5 L441P (recombinant)	gift	Biopharm AG (Heidelberg, Germany)
TGFβ2 (recombinant)		R&D Systems (Minneapolis, MN, USA)

Table 2.10 Growth factors

2.11 Inhibitors

name	comment	source
Chloroquine	lysosome inhibitor	Sigma-Aldrich GmbH (Hannover, Germany)
Chlorpromazine	clathrin-coated pit inhibitor	Sigma-Aldrich GmbH (Hannover, Germany)
MG132	proteasome inhibitor	Merck KGaA (Darmstadt, Germany)
MβCD	cholesterol sequestering agent (DRM inhibitor)	Sigma-Aldrich GmbH (Hannover, Germany)
Noggin	BMP family ligand antagonist	R&D Systems (Minneapolis, MN, USA)

Table 2.11 Inhibitors

2.12 Primary Antibodies

Primary Antibody	Western blot	Blocking	IP	Type / Origin	Epitope / Recognition
Flag M2 (Sigma-Aldrich)	1:2500 in $TBST_{0,1\%}$	5% milk in $TBST_{0,1\%}$	1µg	mouse monoclonal, IgG_1	binding is not Ca^{2+}-dependent
HA (home made)	1:500 in $TBST_{0,1\%}$	3% BSA in $TBST_{0,1\%}$	2.5µg	mouse monoclonal, prepared by Peter Kreuzahler (Freie Universität Berlin) according to standard protocols	12CA5 from the hemagglutinin (HA) protein YPYDVPDYA known as HA-tag hybridoma cell line from BAbCO
HA (Roche Diagnostics)	1:1000 in $TBST_{0,1\%}$	5% BSA in $TBST_{0,1\%}$	1µg/IP	mouse monoclonal, $IgG_{2b}\kappa$	12CA5 from the hemagglutinin protein YPYDVPDYA
HA7-coupled agarose beads (Sigma-Aldrich)	-	-	25µl	mouse monoclonal	synthetic peptide corresponding to amino acid residues 98-106 (YPYDVPDYA) of human Influenza virus hemagglutinin conjugated to KLH
myc (home made)	1:500 in $TBST_{0,1\%}$	3% BSA in $TBST_{0,1\%}$	2.5µg	mouse monoclonal, prepared by Christina Sieber (Freie Universität Berin) according to standard protocols	recognizes aa 410-419 of human c-myc (EQKLISEEDL)
pSmad1/5 8 (Cell Signaling Technology)	1:500 in $TBST_{0,1\%}$, 3% milk	5% milk in$TBST_{0,1\%}$	-	rabbit polyclonal	peptide within the Cterminus of human pSmad5, conjugated to KLH, reacts also with pSmad1 and 8
RGS-His (Qiagen)	1:1000 in $TBST_{0,1\%}$ + 5% BSA	3% BSA in $TBST_{0,1\%}$	1µg	mouse monoclonal, IgG_1	detects 6xHis-tagged proteins
Ror2 (R&D Systems)	1:1000 in $TBST_{0,1\%}$	5% milk in $TBST_{0,1\%}$	-	human monoclonal, goat IgG	NS0-derived rhROR2 extracellular domain
Ror2 323/324 (purification 240/241)	1:300 in $TBST_{0,1\%}$	5% milk in $TBST_{0,1\%}$	2.5µg	rabbit polyclonal	described in [194]
pTyr, PY99 (sc-7020)	1:200 in $PBST_{0,5\%}$ + 1% BSA	$PBST_{0,5\%}$	-	mouse monoclonal, IgG_{2b}, affinity purified	raised against phosphotyrosine conjugated to keyhole limpet hemocyanin
Ubiquitin (Cell Signaling)	1:1000 in $TBST_{0,1\%}$ + 5% BSA	5% milk in $TBST_{0,1\%}$	n.a.	mouse monoclonal	P4D1, detects ubiquitin, polyubiquitin and ubiquitinated proteins
β-actin (Sigma-Aldrich)	1:10,000 in $TBST_{0,1\%}$	5% milk in $TBST_{0,1\%}$	-	mouse monoclonal, IgG_1	slightly modified β-cytoplasmic actin N-terminal peptide, Ac-Asp-Asp-Asp-Ile-Ala-Ala-Leu-Val-Ile-Asp-Asn-Gly-Ser-Gly-Lys, conjugated to KLH.

Table 2.12 Primary antibodies

2.12.1 Production of anti-Ror2 323/324 antibody

Polyclonal anti-Ror2 antibodies were produced in cooperation with Eurogentec (Brussels) [194]. Briefly, two KLH-coupled peptides were selected for rabbit immunization. Peptide 323 (DTLGQPDGPDSPLPT) corresponds to amino acids 42-56 and lies just N-terminal of the Ror2 Ig domain. Peptide 324 (RLGPTHSPNHNFQ) corresponds to amino acides 153-165 and sits within the Ror2 Ig domain. Antibody was purified from serum by Eurogentec

(Brussels). For studies presented here, antibodies from the second round of purification were used (sera 323 and 324 corresponding to antibody purifications 240 and 241, respectively).

2.13 Secondary Antibodies

Secondary Antibody	Western blot	Type / Origin	Epitope / Recognition
goat α-mouse-HRP (Dianova)	1:10,000 in $TBST_{0,1\%}$	goat	heavy and light chains of mouse IgGs
goat α-rabbit-HRP (Dianova)	1:10,000 in $TBST_{0,1\%}$	goat	heavy and light chains of mouse IgGs
R-phycoerythrin (Invitrogen)	1:1,000 in PBS, 1%BSA	goat	heavy and light chains of mouse IgGs

Table 2.13 Secondary antibodies

3 Methods

3.1 Microbiological

3.1.1 Sterilization and Disinfection

name	principle
heat sterilization	Heat-stable and non-volatile solutions, media and materials were made sterile by autoclaving at 1.1bar for 20 minutes. Under these conditions the boiling temperature of water increases to 121°C. Glassware was sterilized using dry heat at 180°C for 3 hours.
sterile filtration	Non-heat-stable and volatile media and solutions are made sterile by filtration. Filters with a pore size of 0.2 to 0.4µm (Schleicher & Schuell) were used.
disinfection	70% denatured EtOH and Mycoplasma-Off (Minerva Biolabs) were used to wipe and sterilize plain surfaces as well as pipets, racks and other tools.

Table 3.1 Sterilization and disinfection techniques

3.1.2 Bacterial Media

name	ingredients & preparation
Luria Bertani (LB) medium	10g/l trypton, 5g/l yeast extract, 10g/l NaCl Ingredients were dissolved in ddH_20 and autoclaved.
LB agar plates	LB medium was supplemented with 15g/l agar and autoclaved. After the medium temperature had cooled down to approximately 40°C it was supplemented with antibiotic(s) and poured onto LB agar plates where it cooled down to room termperature. Plates were stored at 4°C.
SOB medium	20g/l trypton, 5g/l yeast extract, 0.5g/l NaCl, 0.83g/l KCl Ingredients were dissolved in ddH_20, the pH was adjusted to pH7.0 with NaOH and the medium was autoclaved.
SOC medium	sterile SOB medium was supplemented with 10mM $MgCl_2$,10mM $MgSO_4$ and 40% v/v glucose. SOC medium was prepared fresh.
TB Buffer	10mM Pipes, 15mM $CaCl_2$, 250mM KCl Ingredients were dissolved in ddH_20, the pH was adjusted to pH6.7 using KOH. To this solution 55mM $MnCl_2$ were added and the medium was autoclaved.

Table 3.2 Bacterial media

3.1.3 Cultivation and Conservation of E.coli Strains

Bacteria were grown in LB medium and on LB agar plates supplemented with appropriate antibiotics to select for resistant strains carrying the plasmid of interest. Generally, cultures were gorwn at 37°C under permanent shaking. For cryo-storage of bacteria, 500µl of a fresh culture with an $OD_{550nM} > 0.6$ were mixed with 500µl of sterile 86% glycerol, transferred into a cryo vial and stored at -80°C.

antibiotic name	details
Ampicillin	stock solution 100mg/ml dissolved in ddH_20 aliquots stored at -20°C; working aliquots stored at 4°C, stable for 4 weeks
Kanamycin	stock solution 100mg/ml dissolved in ddH_20 aliquots stored at -20°C; working aliquots stored at 4°C, stable for 4 weeks
Tetracycline	stock solution 7.5mg/ml dissolved in ddH_20 aliquots stored at -20°C; working aliquots stored at 4°C, light protected stable for 4 weeks

Table 3.3 Antibiotics

3.1.4 Preparation of Heat Competent *E. coli* strains

Heat competent bacterial cells are able to take up plasmid DNA when treated with a Heat Shock. To gain heat competent cells, *E. coli* bacteria were treated the following way:
Bacteria were plated on an agar plate and incubated at 37°C over night. Fresh clones were transferred to 250ml SOC medium and cultivated at 37°C for to an OD_{550nM} of 0.6 for approximately 6 hours. Cells were incubated on ice for 10 minutes, pelleted (4,000rpm, 10min, 4°C) and resuspended in 10ml ice dold and sterile TB buffer. Resuspended cells from two centrifugation tubes were pooled in a reaction tube and the volume was filled up to 40ml with ice cold TB buffer. Cells were incubated on ice for 10 minutes and centrifuged (3,500rpm, 10min, 4°C). The resulting pellets were carefully resuspended in 5ml ice cold TB buffer, two resuspended volumes were pooled and 8.5ml ice cold TB buffer was added. Finally, 1.5ml dimethylsulfoxide (DMSO) was slowly added to the cell suspension while pivoting the flask on ice. Cells were incubated on ice for 10 minutes. Aliquots à 200µl were transferred into pre-cooled cryo vials, frozen in liquid nitrogen and stored at -80°C.

3.1.5 Transformatin of Heat Competent *E. coli* strains

Heat competent bacteria (see 3.1.4) were thawed on ice. 100µl of cells were supplemented with 1-500ng of plasmid DNA and incubated on ice for 30 minutes. The cell-DNA mixture was then heat-shocked at 42°C for 90 seconds, followed by incubation on ice for 1 minute. The mixtue was supplemented with 1ml pre-warmed SOC-medium and cultivated at 37°C for 30-60 minutes. Cells were centrifuged at 3,000rpm for 10 minutes, resuspended in 100µl LB medium, plated on agar plate supplemented with the respective antibiotic(s) and incubated at 37°C over night to select for transformed and hence antibiotic-resistant cells. The next day single clones were picked, cultured in 2ml LB medium supplemented with the respective antibiotic(s) for 5-8 hours. 1.5ml were used to extract plasmid DNA for sequencing (see Table 3.4), and 0.5ml were used to create a cryo stock of the plasmid-carrying bacteria (see 3.1.3).

3.2 Molecular Biological

method	details
amplificaton and isolation of plasmid DNA from transformed bacterial	To amplify plasmid carrying bacteria, bacteria were grown as described (see 3.1.3). Plasmid DNA was isolated using various kits, according to manufacturer's instructions. Kits used included Mini, Midi and Maxi Plasmid Kits from Qiagen. Plasmid DNA was dissolved in ddH_2O and stored at -20°C.
determination of nucleic acid concentrations	DNA concentration was measured at 260nm, using a Nanodrop ND-1000 (Thermo Fisher Scientific).
DNA sequencing	Plasmid DNA was sequenced by GATC Biotech. DNA was provided as required by the company.

Table 3.4 List of molecular biological methods.

3.3 Cell Biological

3.3.1 Cultivation and Cryo Conservation of Cells

cell line	growth medium	incubation
Cos7	DMEM, low glucose, 10% FCS, 1% penicillin/strptomycine and 2mM L-glutamine.	5% CO_2 37°C 95% atmospheric humidity
C2C12	DMEM, low glucose, 10% FCS, 1% penicillin/strptomycine and 2mM L-glutamine.	10% CO_2 37°C 95% atmospheric humidity
C2C12-BRIb	DMEM, low glucose, 10% FCS, 1% penicillin/strptomycine and 2mM L-glutamine. For every other passage, growth medium was supplemented with G418 to a final concentration of 0.5mg/ml to select for stably transfected cells.	10% CO_2 37°C 95% atmospheric humidity

Table 3.5 List of cell types and culture conditions.

Medium was "refreshed" by a repeated supplementation with 2mM L-glutamine when the medium was older than 6 weeks.

To detach and passage adherent cells, they were treated with 2x trypsin for 2-5 minutes at 37°C. Enzymatic activity was stopped by adding growth medium containing FCS. Cells were grown to a density of roughly 70%, which required passaging every 2-3 days. C2C12 cells were generally splitted 1:10 – 1:15, while Cos7 cells required a splitting of 1:15 – 1:25.

For cryo conservation, cells were harvested, centrifuged at 1,200rpm for 3 mintues and resuspended in cooled growth medium containing 10% DMSO. Aliquots of 1ml per cryo vial were prepared, vials stored on ice for 5 minutes, then stored at -80°C for 1-2 days. For long-term conservation cryo vials were stored in tanks containing liquid nitrogen at -150°C.

3.3.2 Determination of Cell Number

To count living cells, 50µl of cells were suspended with 50µl of trypan blue and a drop was added to a Neubauer chamber (Hartenstein Laborbedarf) for cell counting under the microscope. Living cells appeared white, while blueish cells represented damaged, dying and/or dead cells and were not counted. The number of cells per ml was calculated like this: (number of cells : number of quadrants) x dilution factor x chamber factor (10^4)

3.3.3 Transfection of Eukaryotic Cells

3.3.3.1 Transient transfection of C2C12 and C2C12-BRIb cells using Lipofectamine2000™

The day before transfection, C2C12 or C2C12-BRIb cells were seeded into cell culture dishes and cultivated over night. Lipofectamine2000™ transfection was carried out according to manufacturer's instructions. For reportergene assays the respective reporters (BRE-luc or SBE-luc and RL-TK) were transfected in addition to the total amount of DNA and the amount of Lipofectamine2000™ was adjusted accordingly (see Table 3.6, highlighted fields). Following supplementation with transfection medium, cells were cultivated over night in the cell incubator. The next day transfection efficiency was controlled (see 3.3.3.3) and cells were subjected to various assays.

	24-well		6-well	
number of cells	$2*10^4$		$1.3*10^5$	
amount of DNA	0.5µg		2µg	
firefly reporter	0.2µg		1µg	
renilla reporter	0.06µg		0.3µg	
Lipofectamine2000™	1.5µl	2µl	8µl	10µl
premix	100µl		500µl	

Table 3.6 Lipofectamine2000™ transfection scheme for C2C12 and C2C12-BRIb cells

3.3.3.2 Transient transfection of C2C12 and Cos7 cells using polyethylenimine (PEI)

For transfection, cells were seeded and cultivated in growth medium over night. The following day they were transfected using PEI (Sigma-Aldrich). For each well or plate DNA was pipetted into a reaction tube of sufficient size. Then a premix of DMEM medium and PEI was created and added to the DNA. The DMEM-PEI-DNA premix was vortexed and incubated at room temperature for 30 minutes. The premix was filled up to a sufficient volume with DMEM, wells or plates were cleared from growth medium and the transfection mix was added. Transfection was allowed to proceed for 5 hours in the cell incubator. The transfection was stopped by replacing the transfection medium with growth medium. Cells were allowed to grow over night in the cell incubator. The next day transfection efficiency was controlled (see 3.3.3.3) and cells were subjected to various assays.

	6-well and 3cm plate	6cm plate	10cm plate	15cm plate
number of C2C12 cells	$1.3*10^5$	$3*10^5$	-	$2\text{-}3*10^6$
number of Cos7 cells	-	-	$1*10^6$	$2\text{-}3*10^6$
amount of DNA	2µg	5µg	10µg	20µg
amount of PEI (Roth)	2µg	5µg	10µg	20µg
premix	200µl	500µl	1ml	2ml
final volume	1ml	3ml	10ml	15ml

Table 3.7 PEI transfection scheme for C2C12 and Cos7 cells

3.3.3.3 Determination of transfection efficiency

Transfection efficiency was measured using GFP as a reference. Cells transfected with GFP emitt light at a wavelength of 509nm when excicated with light of 488nm wavelength. The amount of green fluorescent cells was analyzed using a fluorescence microscope.

3.3.4 Treatment of Cells with Growth Factors and Inhibitors

To study the effects of downstream signaling, cells were starved with DMEM containing 0.5% FCS. Starvation leads to a synchronization of the cell cycle and sensitizes cells for stimulation with growth factors. Following starvation, cells were treated with growth factors (BMP2 or GDF5 variants) or inhibitors for varying amounts of times (30 minutes to 20 hours).

C2C12 and C2C12-BRIb cells	reporter gene assay	pSmad	FACS
starvation	3hrs	3-5hrs	3hrs
stimulation time	20hrs	30min and up to 20hrs	30min and up to 20hrs
stimulation concentration	500fM - 10nM	1nM	1nM

Table 3.8 Starvation and stimulation times for C2C12 and C2C12-BRIb cells

Cos7 cells	MG132	Chlorpromazine	Chloroquine	MβCD
starvation	2-5hrs	5hrs	5hrs	5hrs
treatment time	1-2hrs	2hrs	2-3hrs	1-2hrs
treatment concentration	10-25µM	10-50µM	50µM	10mM

Table 3.9 Starvation and treatment times for Cos7 cells

Reporter gene assays were carried out using the Dual-Luciferase® Reporter Assay kit (Promega) and cells were harvested according to the manufacturer's instructions.

For all other assays, cells were transfected (see 3.3.3.2) and harvested using a TNE lysis buffer, supplemented with detergent as well as protease and phosphatase inhibitors (see 3.4.1).

3.4 Protein Biochemical

3.4.1 Preparing Cells for FACS Measurements

For fluorescence activated cell sorting (FACS) C2C12 or C2C12-BRIb cells were seeded in 6cm dishes. Depending on the assay cells were starved and treated with growth factors as described above. Further, cells were washed with ice cold PBS and detached from the culture plate by incubation with 1ml Accutase (PAA) for 5 minutes. The enzyme activity was stopped by applying 5ml of growth medium. Cells that still attached to the plate were removed and by pipetting individualized by pipetting. Resulting cell suspensions were transferred into 15ml reaction tubes and centrifuged at 1,200rpm for 3 minutes. The supernatant was discarded and cell pellets were resolved in ice cold PBS. In all washing steps, PBS was supplemented with 1% BSA. The cell suspension was transferred to 1.5ml reaction tubes and washed with PBS 2 times by centrifuging at 250g at 4°C for 3 minutes. After the final washing step the cell pellet was carefully resolved in 50µl PBS and a 50µl solution of the primary antibody (1µg per 10^6 cells) was added. The cell-antibody suspension was incubated on ice for 30-45minutes. To remove excess antibody, cells were washed 3 times with ice cold PBS as described above. The cell pellet was again resolved in 50µl PBS and 50µl of a 1:1,000 solution of the secondary antibody carrying the fluorescent dye R-phycoerythrin (Invitrogen) was added to the cells, followed by a second incubation step on ice for 30-45 minutes. Following staining with the secondary antibody, cells were washed 3 times with ice cold PBS, resolved in 1ml of ice cold PBS (without BSA) and finally subjected to FACS analysis.
FACS measurements were carried out by Daniel Horbelt, AG Knaus.

3.4.2 Preparation of Cell Lysates

Before harvesting, cells were washed with ice cold PBS, lysed, scraped off the plate suing a cell scraper (Hartenstein Laborbedarf), incubated on ice for 10 minutes and centrifuged (12,000rpm, 4°C, 10min) to remove insoluble cell debris. The pellet was discarded and the supernatant was subjected to further analysis. Lysates were supplemented with 6x protein sample buffer, boiled at 95°C for 3 minutes and stored at -20°C.

name	ingredients / details
TNE lysis buffer	20mM Tris/HCl pH7.5 150mM NaCl 1mM EDTA 1x protease inhibitor mix (PI) 1mM PMSF (protease inhibitor) 10mM NaF (phosphatase inhibitor) 2mM NaP_2O_7 (phosphatase inhibitor) dissolved in ddH_2O
standard detergent alternative detergent (used for assay to separate detergent-resistant microdomains)	1% Triton X-100 (v/v) 20mM CHAPS
Complete EDTA free (Roche Diagnostics)	25x stock solution dissolved in ddH_2O aliquots stored at -20°C
phenylmethylsulfonylfluoride (PMSF)	100mM stock solution dissolved in isopropanol at 4°C stored in aliquots at -20°C
NaF	1M stock solution dissolved in ddH_2O stored at room temperature
NaP_2O_7	200mM stock solution dissolved in ddH_2O stored at room temperature
Na_3VO_4	200mM stock solution dissolved in ddH_2O pH adjusted to pH10 activated according to [224] stored at -80°C

Table 3.10 Lysis buffer and supplements for lysis of C2C12, C2C12-BRIb and Cos7 cells

name	recipe
6x protein sample buffer (new)	125mM Tris HCl pH6.8 6% SDS 20% glycerol 10% β-mercaptoethanol pinch of bromphenol blue dissolved in ddH_2O stored in aliquots at -20°C
6x prtotein sample buffer (Würzburg)	30mM Tris HCl pH6.8 12mM EDTA 12%SDS 60% glycerol 864mM β-mercaptoethanol pinch of bromphenol blue dissolved in ddH_2O stored in aliquots at -20°C
6x protein sample buffer (DTT, Anke)	125mM Tris HCl pH6.8 10% SDS 30% glycerol 600mM DTT pinch of bromphenol blue dissolved in ddH_2O stored in aliquots at -20°C

Table 3.11 Protein sample buffer recipes

3.4.3 Determination of Protein Content Using BCA Assay (Redinbaugh)

To determine the amount of protein in cell lysates, the bichinonic acid (BCA) method according to Redinbaugh was applied. As two molecules of BCA and one Cu^{2+} ion form a

chelate, a purple product emerges, which indicates the amount of protein present in the sample and is measured at 550nm in a microplate reader (Sunrise, Tecan).

Cell lysates are diluted 1:10 in ddH_2O and 20µl of each diluted sample was pipetted in duplicates on a 96-well plate. Likewise the standards were transferred to the place as a reference. BCA solutions A and B were mixed 49:1 and 200µl of each mixture added to each well. The plate was incubated at 60°C for 30-60 minutes and measured when a light purple staining was visible in all samples. Protein concentrations were calculated based on the calibration curve of the BSA standards.

name	ingredients & preparation
BSA standard	25µg/ml - 50µg/ml - 75µg/ml - 100µg/ml - 150µg/ml - 200µg/ml - 250µg/ml
BCA solution A	1.35% $NaHCO_3$ (w/v) 0.58% NaOH (w/v) 1% bichinonic acid (w/v) 0.57% $KNaC_4H_4O_6*4\ H_2O$ (w/v) dissolved in ddH_2O stored in aliquots at -20°C
BCA solution B	2.3% $CuSO_4$ (w/v) dissolved in ddH_2O

Table 3.12 Ingredients for BCA assay

3.4.4 Separation of Detergent-Resistant Microdomains

Transiently transfected Cos7 cells were lysed with TNE lysis buffer containing 20mM of the detergent CHAPS and homogenized using three strokes of a potter apparatus (Sartorius AG) at 1,000rpm and 4°C. The lysate was adjusted to an OptiPrep® (Sigma-Aldrich) concentration of 40%. The lysate was placed at the bottom of a centrifugation tube (Beckmann) and a discontinous OptiPrep® gradient from 30% to 5% was formed above the lysate. The centrifugation tubes were transferred into free swinging buckets of a centrifuge rotor. The gradient was ultracentrifuged at 39,000g and 4°C for 20 hours. After ultracentrifugation, the gradient was fractioned on ice from top to bottom by pipetting 11 fractions à 1ml. The remaining volume of around 1.5 – 2ml was very viscous and required vortexing to remove the final 12^{th} fraction. See Figure 3.1 for a model.

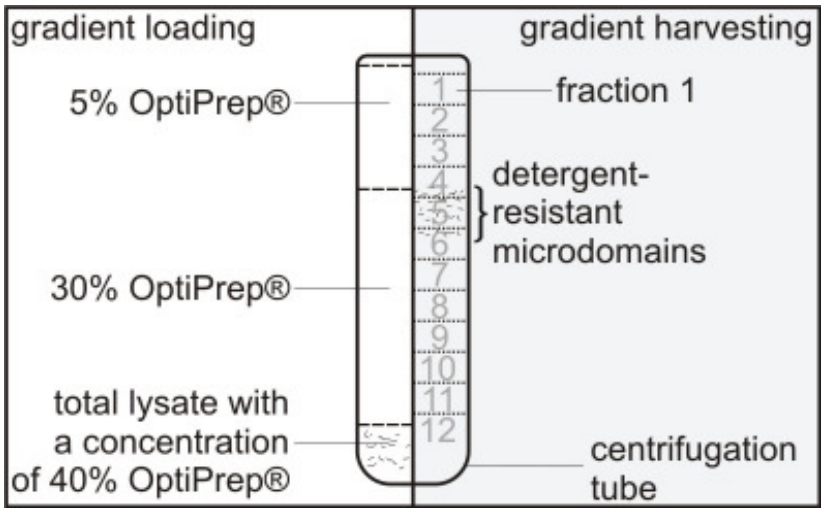

Figure 3.1 Model for separation of detergent-resistant microdomains

The left shows how the gradient is loaded. The lysate with a concentration of 40% OptiPrep® is placed at the bottom of the centrifugation tube and covered with 30% and 5% OptiPrep®.
The right shows how the gradient is harvested. After ultracentrifugation 1ml fractions are removed from top to bottom. Detergent-resistant microdomains are expected to float at the border of 30% to 5% OptiPrep®.

Fractions were analyzed using SDS-PAGE, Western blotting and antibody staining as described below.

material	type	manufacturer
potter	Potter S	Sartorius AG (Göttingen, Germany)
iodixanol (60% solution in water; further diluted in TNE lysis buffer w/o detergent and protease or phosphatase inhibitors)	OptiPrep®	Sigma-Aldrich GmbH (Hannover, Germany)
ultracentrifugation tubes	Ultra-Clear™ tubes	Beckman (Palo Alto, CA, USA)
ultracentrifuge rotor	SW41	Beckman (Palo Alto, CA, USA)
ultracentrifuge	L-60	Beckman (Palo Alto, CA, USA)

Table 3.13 Materials and devices used to separate deterteng-resistant microdomains

3.4.5 Co-immunoprecipitation

For co-immunoprecipitation and cells were transfected with plasmid DNA of interested and lysed as described above. Lysates were supplemented with 0.5 – 5µg of an antibody to specifically immunoprecipitate one protein of interest, and 50µl of protein A sepharose beads (from *Staphylococcus aureus*; Sigma-Aldrich) that specifically binds to the andibody's F_c part. The suspension was adjusted to a volume of 1ml with TNE lysis buffer. Samples were incubated at 4°C on a reaction tube rotator over night. The next day the sepharose beads were washed 3 times with ice cold TNE lysis buffer. After the final washing step remaining buffer was removed using a Hamilton pipet and 20µl of fresh TNE lysis buffer were added immediately. Finally, 10µl of 6x protein sample buffer were added and samples were boiled at 95°C for 5 minutes.

3.4.6 SDS Polyacrylamide Gelelectrophoresis

Proteins were separated by their molecular weight using SDS (sodiumdodecylsulfate) polyacrylamide gelelectrophoresis (SDS-PAGE) according to Laemmli et al. [225].

name	ingredients & preparation
acrylamide/bis-acrylamide	30% acrylamide (w/v) 1% bis-acrylamide (w/v) dissolved in ddH_2O
lower tris (4x stock)	1.5M Tris 0.4% SDS (w/v) dissolved in ddH_2O pH adjusted to pH8.8
upper tris (4x stock)	0.5M Tris 0.4% SDS (w/v) dissolved in ddH_2O pH adjusted to pH6.8
ammoniumpersulfate (APS) (Roth)	40% APS (w/v) dissolved in ddH_2O stored in aliquots at -20°C working aliquots sotred at 4°C
TEMED (N,N,N'N'-tetramethylethylendiamine) (Roth)	
SDS running buffer	25mM Tris 190mM glycine 0.1% SDS (w/v) dissolved in ddH_2O

Table 3.14 Solutions required for SDS-PAGE

	7.5%	10%	12.5%	stacking gel
AA/Bis-AA (30 : 0.8)	2.5ml	4ml	5ml	500µl
ddH_2O	5ml	5ml	4ml	2.5ml
lower tris (4x stock)	2.5ml	3ml	3ml	-
upper tris (4x stock)	-	-	-	1ml
40% APS	20µl	20µl	20µl	8µl
TEMED	20µl	20µl	20µl	8µl

Table 3.15 Recipe suited for one mini gel of the Mini Protean gelelectrophoresis system

3.4.7 Coomassie-G Staining of Proteins

Following SDS-PAGE the gel was washed with dH_2O and prefixed with gel fixation solution for 10-15 minutes. This step was proceeded by Coomassie-G staining for 30 – 60 minutes. The gel was destained in gel destaining solution over night and stored in dH_2O.

name	ingredients & preparation
Coomasse-G staining	0.006% Coomassie-G-250 (v/v) (Roth) 10% acidic acid (v/v) dissolved in ddH_2O
gel fixation and destaining	25% isopropanol (v/v) 10% acidic acid (v/v) dissolved in ddH_2O

Table 3.16 Solutions required for Coomassie-G staining

3.4.8 Western Blot

To detect proteins with the help of antibodies, they were transferred from the gel onto a nitrocellulose membrane. Finally, the peroxidase-coupled second antibody was detected using enhanced chemiluminescence (ECL) [226].

Protein transfer was achieved using the wetblot method (Mini-V 8.10 system, Bio-Rad). Transfer was carried out at 90V for 90 minutes in WB transfer buffer, passively cooled with a block of ice. Successful protein transfer and equal loading were controlled by reversible Ponceau S staining. The membrane was destained using dH2O or TBS-$T_{0.1\%}$.

To preoccupy the membrane with protein and avoid unspecific binding of the primary or secondary antibodies, the blot was saturated with milk or bovine serum albumine (BSA) in a concentration of 3-4% in TBS-$T_{0.1\%}$ shaking at room termperature (RT), typically for 1 hour, alternatively at 4°C over night. Next the blot was incubated with the primary antibody, typically at 4°C over night or at RT for 1 hour. The primary antibody was washed off extensively with TBS-$T_{0.1\%}$ and the membrane was incubated with a species-specific secondary antibody conjugated to horseradish peroxidase (HRP) at RT for 1 hour on a shaker. To remove residual antibody, the blot was washed thoroughly with TBS-$T_{0.1\%}$ and finally subjected to ECL.

name	ingredients & preparation
WB transfer buffer	25mM Tris 190mM glycine 20% methanol (v/v) dissolved in ddH_2O
Ponceau S staining solution	0.5% Ponceau S (w/v) 3% TCA (v/v) dissolved in ddH_2O
WB washing buffer	50mM Tris HCl pH8 150mM NaCl 0.1% Tween (w/v) dissolved in ddH_2O

Table 3.17 Solutions required for Western blot

3.4.9 Detection of Proteins Using Enhanced Chemiluminescence

To visualize antibody-labelled proteins, 1ml per blot of each Solution A and solution B were prepared separately. The two solutions were mixed and added to the blot for incubation of 45-60 seconds. To ensure equal distribution, the blot was covered with a plasic foil after the solution was added and the solution was swept out before an x-ray film was exposed to the blot for 10 seconds to 30 minutes, depending on the (expected) signal intensity.

To remove the primary and secondary antibodies, the blot was washed with TBS-$T_{0.1\%}$ and then stripped with WB stripping buffer at 60°C for 30-45 minutes. To remove excess SDS

and β-mercaptoethanol, the blot was washed thoroughly with PBS until no foaming could be observed.

name	ingredients & preparation
ECL solution A	1ml luminol solution 4.4µl para-coumaric acid
ECL solution B	1ml 0.1M Tris HCl pH8.5 1µl H_2O_2
Luminol solution	2.2mM 3-aminophtal-hydrazide (Marck) dissolved in DMSO 0.1M Tris HCL pH8.5 dissolved in ddH_2O
para-coumaric acid	90mM para-coumuaric acid dissolved in DMSO stored in aliquots at -20°C working aliquots stored at 4°C
H_2O_2	30% stock solution (v/v)
WB stripping buffer	62.5mM Tris HCl pH6.5 10% SDS (w/v) 0.7% β-mercaptoethanol dissolved in ddH_2O

Table 3.18 Solutions required for protein detection via ECL

3.4.10 Well Binding Assay

To study direct protein-protein interaction in a cell-free in vitro system, a well binding assay was carried out. For this procedure, PCR-generated fragments of the extracellular domains of Ror2 (ecRor2) and Ror2 ΔCRD (ecRor2 ΔCRD), generated from the respective plasmid DNA templates, were in vitro translated and labeled with [^{35}S]methionine using the TnT® Quick Coupled Translation System (Promega Corporation), according to the manufacturer's instructions. To remove excess [^{35}S]methionine the probes were cleared using Zeba™ desalt spin columns (Pierce).

For the assay, a 96-well microtiter plate (Immulon 4HBX Flat Bottom; Thermo Fisher Scientific) was coated with 500ng of ecBRIb [227] in 100µl PBS, gently rocking at 4°C over night. Similarly control wells were coated with 30mg/ml BSA in PBS. To prevent unspecific protein binding, the target protein was removed and wells were blocked with 300µl BSA solution for 4-6 hours at room temperature. The blocking solution was removed and 100µl of radiolabeled protein in PBS were added to the wells. The probes were incubated with gentle shaking at room temperature for 1-2 hours. To remove unbound protein, wells were washed five times with 200µl of PBS. To elute proteins, 50µl of 5% SDS dissolved in water was added to each well. The elution was transferred to scintillation vials containing 1ml of scintillation fluid and counted using a scintillation counter (PerkinElmer).

3.4.11 MALDI-TOF Mass Spectrometry

To analyze immunoprecipitated protein using mass spectrometry, Cos7 cells were seeded, transfected, lysed, co-immunoprecipitated, sepatarted via SDS-PAGE and stained with Coomassie-G as described above.

The following steps were carried out by Christoph Weise of AG Multhaup. Briefly, potential protein bands were excised from the Coomassie-G-stained gel, carbamidomethylated and cleaved in situ with sequencing-grade trypsin (Roche) as described previously [228].

For mass-spectrometric analysis samples of the digest supernatant were prepared using the dried droplet crystallization technique with α-cyano-4-hydroxycinnamic acid (HCCA) as matrix: 0.5 µl of supernatant was mixed 1:1 with a saturated HCCA solution (20 mg/ml in 33% acetonitrile/0.1% trifluoroacetic acid in water) and applied onto a polished steel target.

Samples were then analyzed via MALDI-TOF mass spectrometry using an Ultraflex-II TOF/TOF mass spectrometer (Bruker Daltonics) in the reflector mode. Spectra were externally calibrated using a peptide standard.

Database searches using the recorded peptide masses were performed with the Mascot search engine (Matrix Science Ltd.) at http://www.matrixscience.com (search parameters: mono-isotopic masses M+H, mass tolerance ± 50 ppm, maximum one missed cleavage site).

In order to validate the assignment obtained from the mass fingerprint, high-energy MALDI-TOF/TOF spectra from selected peptides were additionally recorded on the same instrument.

4 Prelude

Reams of failed approaches and discarded experiments pave the way to each and every scientific publication. In this chapter I will briefly introduce and discuss three side projects that led the way to the main results part of my thesis.

4.1 Characterization of Ror2 interaction with Tak1

Background & aim of this project:

In 2004 we published that Ror2 inhibits Smad signaling [165]. Early on in the following year Hoffmann et al. could show that Tak1 interacts with R-Smads 1-5, interfering with nuclear shutteling but not phosphorylation of R-Smads [229]. In regard to Ror2 inhibiting Smad signaling, this was in line with observations that Ror2 has no effect on Smad phosphorylation, as will be described further down (Figure 4.9). Thus it was speculated that Ror2 may sequester Smads in the cytoplasm through an interaction with Tak1.

4.1.1 Tak1 interacts with full length Ror2

Cos7 cells were transfected with the indicated constructs. Cells were harvested in TNE lysis buffer. Since both Ror2 and the Tak1 constructs are Flag-tagged, an immunoprecipitation (IP) against Ror2 using anti-Ror2 323/324 antibody [194] was performed. Precipitates and total lysates were separated with SDS-PAGE, proteins were transferred to a nitrocellulose membrane and visualized with anti-Flag antibody.

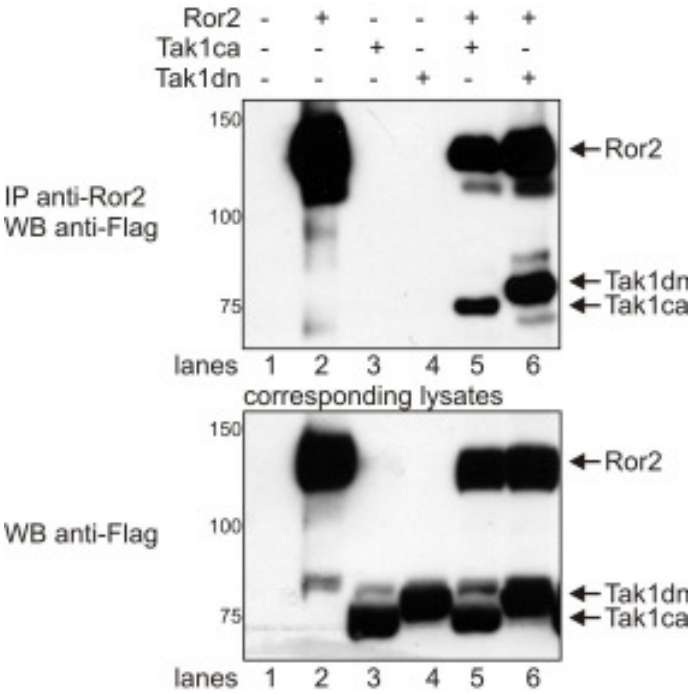

Figure 4.1 Ror2 interacts with constitutive active and dominant negative Tak1

Flag-tagged Ror2 and Tak1 constructs were transiently expressed in Cos7 cells. Ror2 was immunoprecipitated (IP) with anti-Ror2 antibodies. Precipitates (upper panel) and lysates (lower panel) were analyzed by Western blotting (WB) using anti-Flag antibody.

Figure 4.1 shows specific interaction of Ror2 with constitutive active (ca; lane 5) and dominant negative (dn; lane 6) Tak1. The corresponding lysates show that all proteins are well expressed. The constitutive active variant of Tak1 lacks 22 N-terminal amino acids [131]. This is why it migrates slightly faster than the dominant negative Tak1, which only carries a single amino acid exchange from Lysine to Tryptophan at position 63 [229].

It should be mentioned that in some experiments the controls, i.e. Tak1ca or Tak1dn expressed alone followed by an IP anti-Ror2, were not negative for both the dominant negative and the constitutive active Tak1. This is clearly due to interaction of Tak1 with endogenous Ror2. As will be shown in the main results part, the Ror2 antibody precipitates endogenous Ror2 from Cos7 cells (not shown).

4.1.2 Tak1 interacts with truncated Ror2

In the following experiments, several truncation mutants of Ror2 were tested for interaction with either Tak1ca (Figure 4.2) or Tak1dn (Figure 4.3).

Cos7 cells were transiently transfected with the indicated constructs and lysates were subjected to an IP anti-Ror2. To test for successful precipitation of Flag-tagged Ror2 and co-immunoprecipitation of Flag-tagged Tak1, the Western blot was stained with anti-Flag antibody.

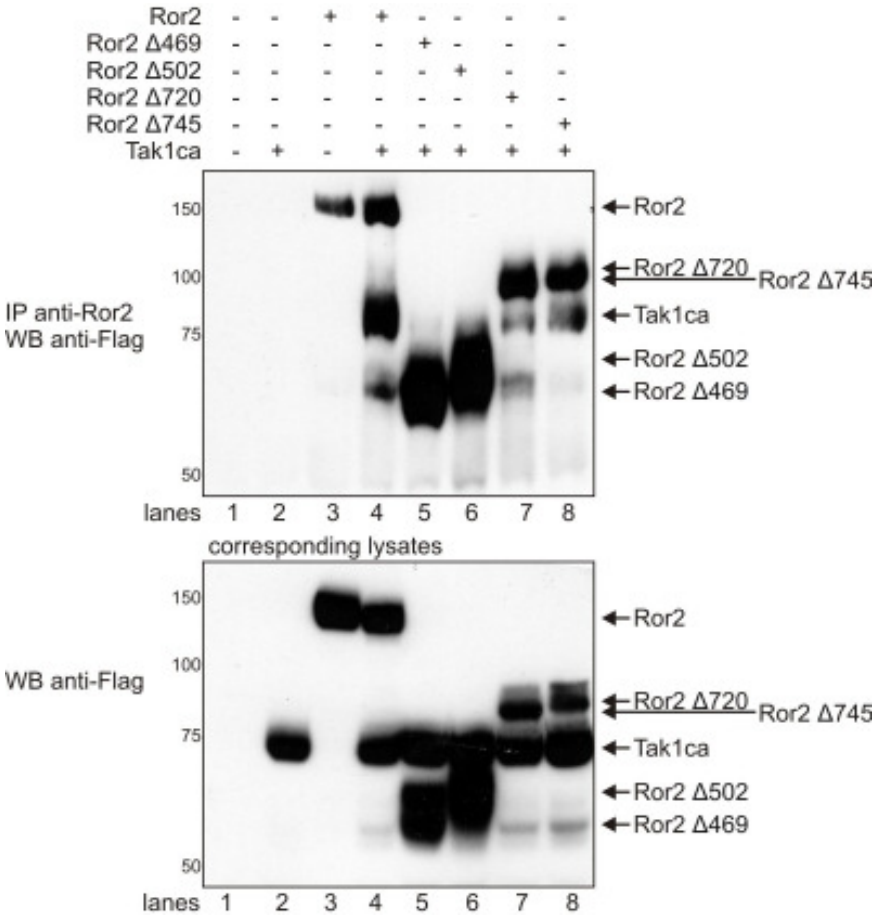

Figure 4.2 Ror2 interacts with Tak1ca up to truncation Δ469

Flag-tagged Tak1ca, wildtype Ror2 and Ror2 truncation mutants were transiently expressed in Cos7 cells. Ror2 was immunoprecipitated (IP) using anti-Ror2 antibodies. Precipitates (upper panel) and lysates (lower panel) were analyzed by Western blotting (WB) with anti-Flag antibody.

For Figure 4.2, interaction of the Ror2 truncation mutants Δ469, Δ502, Δ720, and Δ745 with Tak1ca was tested. A clear interaction is visible for the positive control Ror2 (lane 4), additionally Tak1 appears to interact with both Δ720 (lane 7) and Δ745 (lane 8). A very faint band can be seen for the truncation mutants lacking either all or large parts of the Ror2 kinase domain, Δ469 (lane 5) and Δ502 (lane 6) respectively. However, as mentioned before this band could result from Tak1 interacting with endogenous Ror2, even so the negative control does not show a band for Tak1 (lane 2).

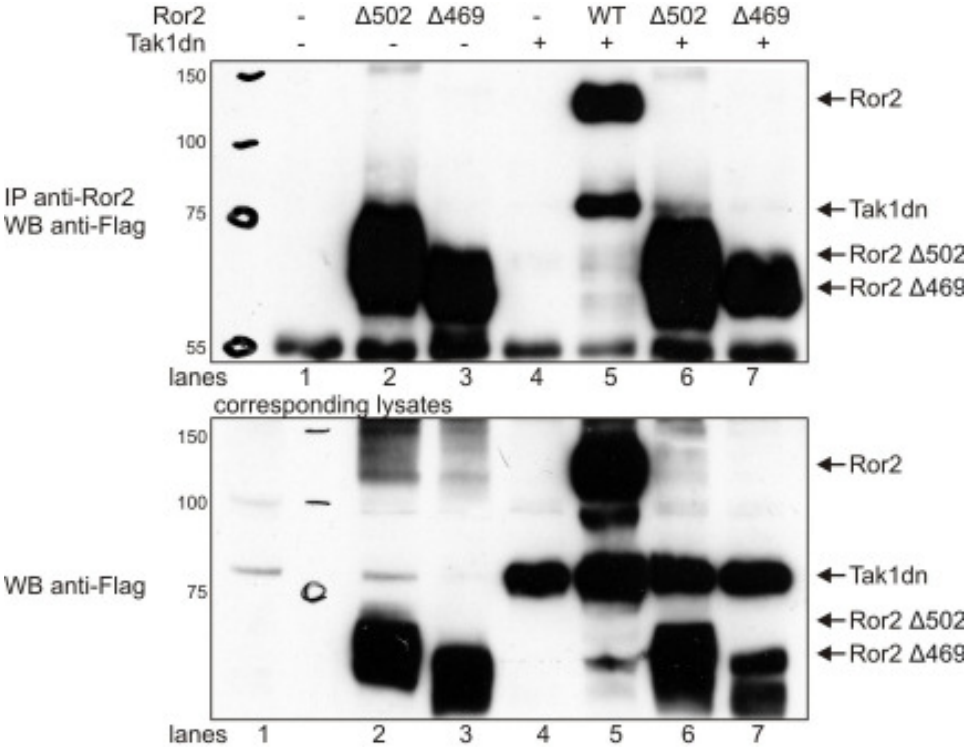

Figure 4.3 Ror2 interacts with Tak1dn up to truncation Δ469

Flag-tagged Tak1dn, wildtype Ror2 and Ror2 truncation mutants were transiently expressed in Cos7 cells. Ror2 was immunoprecipitated (IP) using anti-Ror2 antibodies. Precipitates (upper panel) and lysates (lower panel) were analyzed by Western blotting (WB) with anti-Flag antibody.

Figure 4.3 confirms interaction of Ror2 with Tak1dn (lane 5). Furthermore, the truncation mutants Ror2 Δ502 and Δ469 were tested with matching negative controls. Again the Tak1 negative control in the IP anti-Ror2 does not display unspecific bands, while both Ror2 Δ502 (lane 6) and Δ469 (lane 7) show a co-immunoprecipitation of Tak1dn. This appears to be much stronger for Ror2 Δ502 (lane 6) and only a very faint Tak1dn band is visible with Ror2 Δ469 (lane 7).

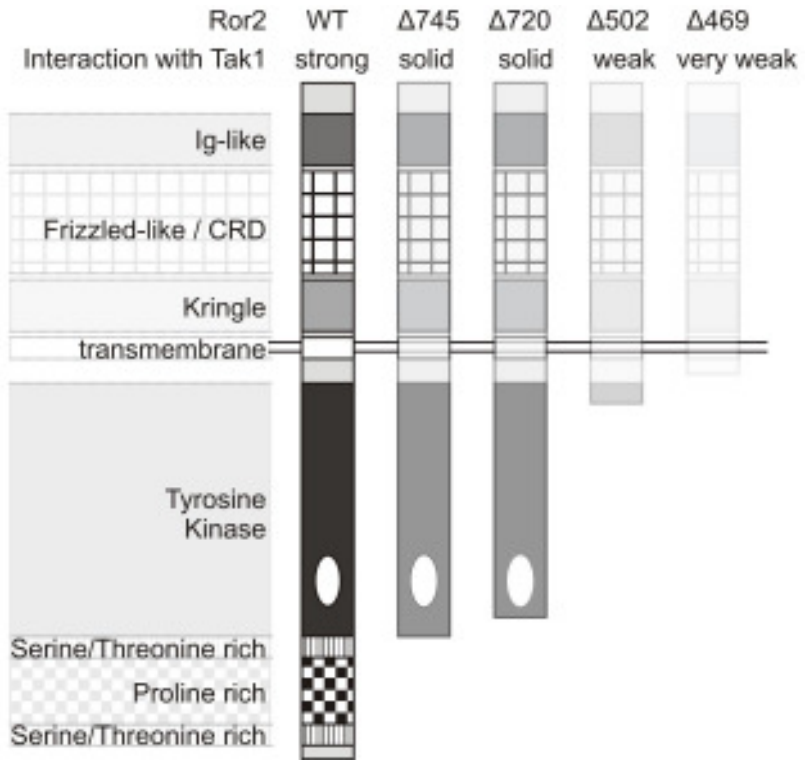

Figure 4.4 Ror2 – Tak1 interaction scheme

Tak1 dn and Tak1 ca where shown to interact strongly with wildtype Ror2 (WT). Also the Ror2 mutants resulting in a membrane distal truncation (Ror2 Δ720 and Ror2 Δ745) displayed a solid interaction with Ror2. The interaction of Tak1 with the membrane proximal truncation Ror2 Δ502 and Ror2 Δ69 appeared weak and very weak, respectively.

Figure 4.4 sumarizes the above described findings. A strong interaction was found with Ror2 WT for both constitutive active and dominant negative Tak1 (Figure 4.1). The Ror2 truncations lacking the cytoplasmic Ror2 tail (Ror2 Δ720 and Ror2 Δ745) showed a solid interaction with bothTak1 ca (Figure 4.2) and Tak1 dn (not shown). Interaction of Tak1 ca and Tak1 dn with the truncations lacking most (Ror2 Δ502) or all (Ror2 Δ469) of the kinase domain, exhibited a weak or very weak interaction, respectively (Figure 4.2 and Figure 4.3).

These data are contradictory to the observations communicated to us by Andreas Winkel in 2005 and published by Winkel et al. in 2008. They claim that Tak1 interacts with the C-terminal tail region of Ror2, which is lacking in all of the truncation mutants tested above. Furthermore, they show that Tak1dn does not interact with Ror2 [171]. It should be noted that we received the Flag-tagged Tak1 constructs described above from this lab. However, for their 2008 publication all co-immunoprecipitation studies with Ror2 were perfomed using HA-tagged Tak1, most probably due to lack of a commercial Ror2 antibody suited for IP. The group used the standard cell line HEK 293T for co-IP experiments.

It is debatable, whether or not Tak1 interacts with the truncation mutants Ror2 Δ502 (Figure 4.2, lane 6 and Figure 4.3 lane 6) or Ror2 Δ469 (Figure 4.2, lane 5 and Figure 4.3, lane 7). The weak interaction that could be observed with these membrane proximal truncations may

be mediated through endogenous proteins. As will be shown in the main results part, Ror2 forms homodimers independent of ligand stimulation and the dimerzation appears to depend on the C-terminal tail region of Ror2. However, dimerization can also be induced through binding of a ligand, such as endogenous Wnt5a. Whether or not ligand-induced Ror2 dimerization depends on intracellular receptor domains has not been shown to date. To demonstrate Wnt5a-induced homodimerization of Ror2, Liu et al. used full length Ror2 and a chimeric receptor that carried the extracellular domains of Ror2 and the intracellular domains of TrkB [183]. It can thus be speculated whether the interaction seen between Tak1 and the membrane proximal Ror2 truncations is due to interaction of Tak1 with wildtype endogenous Ror2, that in turn formed dimers with the overexpressed mutant Ror2 receptor in response to presence of endogenous Wnt5a.

Nevertheless, there is no doubt that dominant negative Tak1 does co-immunoprecipitate with full length Ror2 (Figure 4.1, lane 6). Moreover, it is obvious, that constitutive active Tak1 interacts with Ror2 Δ745 (Figure 4.2, lane 8), a truncation mutant lacking the entire C-terminal tail region of the receptor, and also with Ror2 Δ720 (Figure 4.2, lane 7), an even shorter truncation that also lacks parts of the kinase domain.

Taken together we show that in Cos7 cells Ror2 interacts with constitutive active and dominant negative Tak1. This interaction is probably mediated through the kinase domain of Ror2, but definitely not through its C-terminal domain, as described in a recent publication [171].

4.2 Characterization of the Ror2/BRIb interaction

Background & aim of this project:

As we have described previously, Ror2 interacts with BRIb and thereby inhibits GDF5/BRIb-mediated Smad signaling in reporter gene assays. Furthermore, Ror2 is hyperphosphorylated in the presence of BRIb [165]. In a recent publication we show that this phosphorylation is independent of Ror2 kinase activity, but depends on BRIb kinase activity. Furthermore, the transphosphorylation of Ror2 seen with BRIb is specific, as it was not observed with either BRIa or BRII. We also show that the interaction of Ror2 with BRIb is independent of disulfide bonds, although Ror2 and BRIb were shown to interact through the cysteine-rich domain (CRD) of Ror2 [165]. Furthermore, the interaction is independent of N-linked carbohydrates, but we confirm that Ror2 is glycosylated. Moreover, the complex is very stable in the presence of NaCl, but appeared sensitive to SDS [194].

However, in the scope of these publications it was not revealed how the inhibititory effect of Ror2 on the Smad-dependent pathway is achieved. To gain further insight into the possible mechanism, the Ror2-BRIb complex and potential downstream effects of this interaction were examined.

4.2.1 Interaction of Ror2 with BRIb is direct

For the following experiment the recombinant ectodomain of BRIb (ecBRIb), as well as the extracellular parts of wildtype Ror2 (ecRor2) and Ror2 ΔCRD (ecRor2 ΔCRD) were applied. Both Ror2 proteins were in vitro translated and labelled with ^{35}S-Methionine in a rabbit reticulocyte lysate kit from Ambion. The recombinant ecBRIb was a kind gift from AG Sebald, Würzburg.

A microtiter plate was coated with the ecBRIb or BSA as a control. The multiwell plate was blocked with BSA to prevent unspecific binding of protein. Next, all wells were incubated with radiolabeled Ror2 for two hours. Unbound radiolabeled protein was removed and wells were washed extensively with PBS. Finally, remaining protein was eluted off the plate and the amount of radiolabeled protein in the resulting probes was determined with a scintillation counter (Perkin-Elmer).

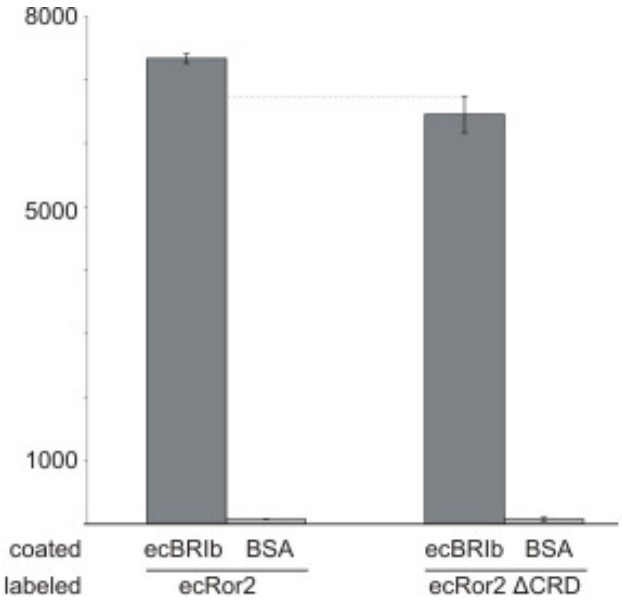

Figure 4.5 Ror2 and BRIb interact directly

A microtiter plate coated with ecBRIb or BSA was incubated with radiolabeled ecRor2 or ecRor2 ΔCRD. Unbound radiolabeled protein was washed off, remaining protein was eluted from the plate and the amount of radiolabeled protein that had bound was determined using a scintillation counter.

In standard co-immunoprecipitation assays Ror2 ΔCRD does not interact with BRIb [165]. Thus we intended to use Ror2 ΔCRD as a negative control in this experiment. However, Figure 4.5 clearly shows that both ecRor2 and ecRor2 ΔCRD directly bind to ecBRIb. The BSA control is negative for both proteins, indicating that both Ror2 and Ror2 ΔCRD show no unspecific binding.

The binding seen for both Ror2 proteins must be due to a direct interaction with BRIb as the cell-free system can only translate protein from the provided mRNA, which excludes the possibility of a third protein mediating the interaction.

Nevertheless, this result was not expected for the ecRor2 ΔCRD, but was seen consistently in three different experiments. It cannot be ruled out that ecBRIb is very sticky in this experimental setup. However, the same protein is also used for Biacore measurements and no unspecific binding or otherwise unexpected behavior was reported in these assays. Even though unspecific binding of BRIb cannot be excluded, it seems highly unlikely. Therefore, we have to speculate why ecRor2 ΔCRD can bind to ecBRIb under these conditions.

The expression system used to synthesize ecRor2 and ecRor2 ΔCRD is a cell-free rabbit reticulocyte lysate [230], provided in a kit from Ambion. It contains all components required for protein translation and was treated with nuclease to remove endogenous globin mRNA. The reticulocyte lysate theoretically provides chaperones for proper protein folding. However, according to the Ambion FAQ for its in vitro translation kits, problems have been observed in

regard to folding of certain membrane proteins. To overcome these difficulties, Ambion recommends supplementing the lysate with canine pancreatic microsomes. Moreover, the FAQ states that glycosylation has not been characterized well for this translation system. Meanwhile several studies conclude that posttranslational modifications are carried out reliably in the presence of the previously mentioned microsomal membranes [231, 232].

Since Ror2 is a large transmembrane protein, a decoy variant of the receptor lacking the transmembrane and the entire intracellular domain was applied as a template to produce the mRNA used for in vitro translation. This may be an additional source for alternative protein folding or improper posttranslational modification.

Taken together, it appears that Ror2 and BRIb interact directly, despite unexpected binding of ecRor2 ΔCRD to ecBRIb. However, the in vitro translation system used to generate ecRor2 and ecRor2 ΔCRD is highly artificial, possibly yielding incorrectly folded protein, which additionally may lack proper posttranslational modifications. Under these conditions, it may well be that the so fabricated ecRor2 ΔCRD exposes amino acid sequences and protein folds that are not accessible for interaction under physiological conditions.

For future studies it is recommendable to supplement the kit with microsomal membranes, which may reconstitute more physiological protein folding and posttranslational modification.

4.2.2 Ror2 and BRIb co-fractionate in DRMs

To characterize the distribution of Ror2 across membrane microdomains and to examine whether its presence has an influence on localization of BRIb in detergent-resistant microdomains (DRMs), detergent-insoluble membrane domains were separated and analyzed.

Native C2C12 cells or C2C12 cells stably expressing BRIb were transiently transfected with Ror2. As a positive control, the stable C2C12 cell line was left untransfected. A day post transfection cells were harvested and homogenized in TNE lysis buffer containing the detergent CHAPS. The lysate was loaded on a discontinuous OptiPrep gradient and subjected to ultracentrifugation. The gradient was fractioned on ice by removing 11 fractions of 1ml each from top to bottom. The remaining 1.5 – 2.5ml of the gradient usually contained a very viscous gel-like bottom that was vortexed to yield a semi-viscous mixture representing the 12th fraction.

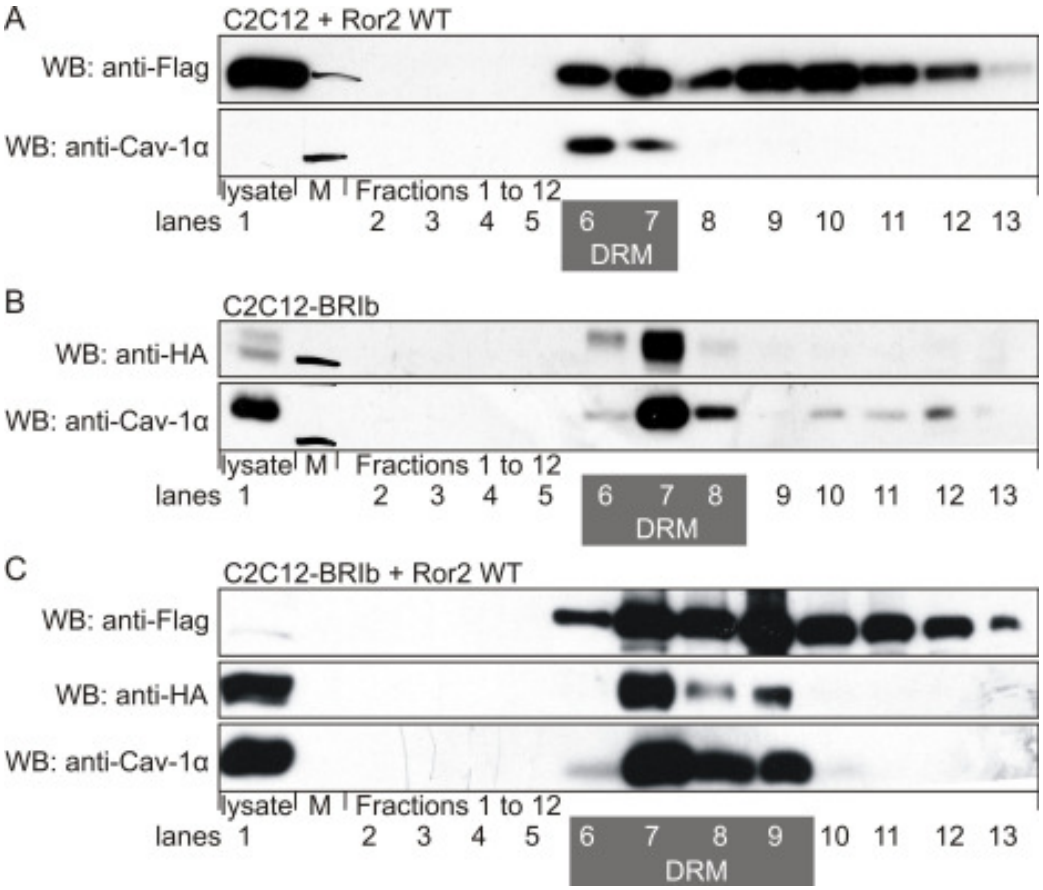

Figure 4.6 Ror2 co-localizes with BRIb in detergent resistant microdomains

C2C12 or C2C12-BRIb cells were transiently transfected Ror2. Lysates were homogenized, adjusted to 40% iodixanol concentration and transferred into ultracentrifugation tubes. Above the lystate, a discontinuous gradient from 30% to 5% iodixanol diluted in lysis buffer was formed. The probes underwent ultracentrifugation at 39,000g and 4℃ for 20h. The resulting gradient was harvested in 1ml fractions, proteins were separated using SDS-PAGE, transferred to a nitrocellulose membrane in a Western blot, and detected using the indicated antibodies.

Figure 4.6 shows a comparison of the results from three different assays. In (A) we see that Ror2 co-fractionates with caveolin (lanes 6 and 7), but is also present in all other fractions. This closely resembles the distribution also seen for BRII [73]. The panels in (B) illustrate that BRIb is exclusively localized in the major caveolin-positive fractions (lanes 6 and 7), although residual caveolin is seen throughout all following fractions. The blots seen in (C) indicate that presence of Ror2 has no influence on the localization of BRIb in DRMs and vice versa BRIb has no influence on distribution of Ror2 across all protein fractions.

BRIb is a protein that resides predominantly in DRMs on the plasma membrane. BRII on the other hand can shuttle between caveolin-positive and –negative membrane fractions. Furthermore, Smad-signaling requires internalization of the receptor complex via clathrin-coated pits (CCPs) [73]. Recently, the interaction of BRII with caveolin was shown to be responsible for its location within DRMs [74]. Thus it appears as though signaling for both the Smad-independent and the Smad-dependent pathway may be initiated within DRMs.

These results show that Ror2 co-localizes in caveolin-positive membrane fractions, where it may interact with BRIb. Presence of either protein does not alter the distribution of the respective other protein across membrane fractions. However, as Ror2 inhibits Smad signaling and as Smad signaling may be initiated at DRM sites, it can be speculated whether Ror2 traps BRIb in DRMs and thus prevents its translocation to CCPs and downstream Smad-dependent signaling. Ror2 may also compete with BRII for binding of BRIb, which would abrogate both Smad-dependent and –independent signaling. Whether or not Ror2 inhibits Smad-independent signaling has not been shown.

In future studies it should be examined whether the presence of Ror2 prevents BRIb from undergoing clathrin-dependent endocytosis, which is required for Smad-dependent signaling.

4.2.3 Ror2 potentially disturbs the BRIb/BRII signaling complex

To further scrutinize speculations whether Ror2 may interfere with the BRIb/BRII preformed signaling complex, the effect of Ror2 on a constitutive active variant of BRIb (c.a.BRIb) was examined.

C2C12 cells were transiently transfected with equal amounts of the indicated constructs, as well as the BMP response element (BRE) [121] and RL-TK (renilla) to control transfection efficiency and calculate relative luciferase activity. The following day cells were staved for 5 hours and stimulated for 20 hours. After stimulation cells were lysed and measured as described. Each probe represents a triplicate.

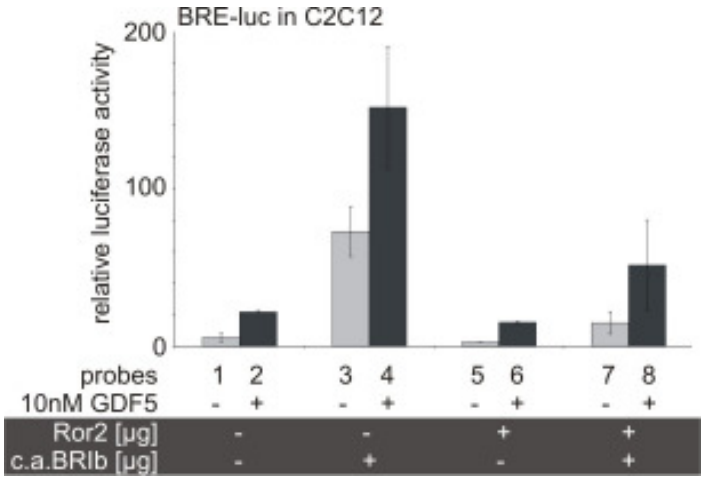

Figure 4.7 Ror2 inhibits Smad signaling independent of ligand

C2C12 cells were transiently transfected with Ror2, c.a.BRIB, the firefly luciferase reporter BRE and renilla luciferase to quantify transfection efficiency and calculate relative luciferase activity. The next day cells were starved for 5 hours and stimulated for 20 hours with 10nM GDF5. Cells were harvested and measured using the Dual-Luciferase™ Reporter Assay kit (Promega Incorporation) according to the manufacturer's instructions.

Figure 4.7 shows that c.a.BRIb can stimulate reporter gene expression independent of ligand stimulation (compare probes 1 and 2 with probe 3). However, stimulation with GDF5 leads to a significant increase compared to the unstimulated probe (compare probes 3 and 4). Although the receptor is constitutive active and does not require an activating phosphorylation by BRII, it may still be required to form preformed complexes (PFCs) with endogenous BRII for further signaling. Binding of the ligand to PFCs may stimulate conformational changes that enhance activity of c.a.BRIb and so increase subsequent Smad phosphorylation and BRE reporter gene activity.

Ror2 on the other hand does not initiate Smad reporter gene expression, neither for the TGFβ/BMP Smad reporter SBE (see Figure 4.13), nor for the BMP Smad-specific reporter BRE (probes 5 and 6). As will be shown also for SBE in Figure 4.13, Ror2 even represses endogenous reporter gene activity as seen in mock-transfected cells (compare probes 1 and 2 with probes 5 and 6). Furthermore, Ror2 efficiently inhibits unstimulated downstream signaling of c.a.BRIb, which confirms that this event is independent of ligand interaction. Ror2 also represses reporter gene activity upon stimulation of c.a.BRIb with GDF5.

To sum up, these data confirm that Ror2 inhibits Smad signaling independent of interaction with the ligand GDF5. However, this experiment does not reveal whether or not Ror2 interferes with binding of BRIb to BRII, as it is not known whether endogenous BRII is required for efficient signaling of c.a.BRIb in this experimental setup. However, as Smad-dependent signaling requires endocytosis via clathrin-coated pits (CCPs) and since BRIb is predominantly located in caveolin-positive membrane fractions [73], BRII is most probably required to form a PFC with c.a.BRIb which is then guided into CCPs for endocytosis and downstream signaling.

To gain further insight into the matter, the effect of Ror2 on BRIb and BRIILF in a reporter gene assay was tested in a preliminary experiment.

C2C12 cells were transiently transfected with the indicated amounts of Ror2, BRIb, BRIILF or empty vector (pcDNA3), as well as 1µg of the Smad Binding Element (SBE) reporter gene and 0.3µg RL-TK per probe. One day post transfection cells were staved for 5 hours and stimulated with 10nM GDF5. After 20 hours of stimulation cells were harvested and lysates were measured as described.

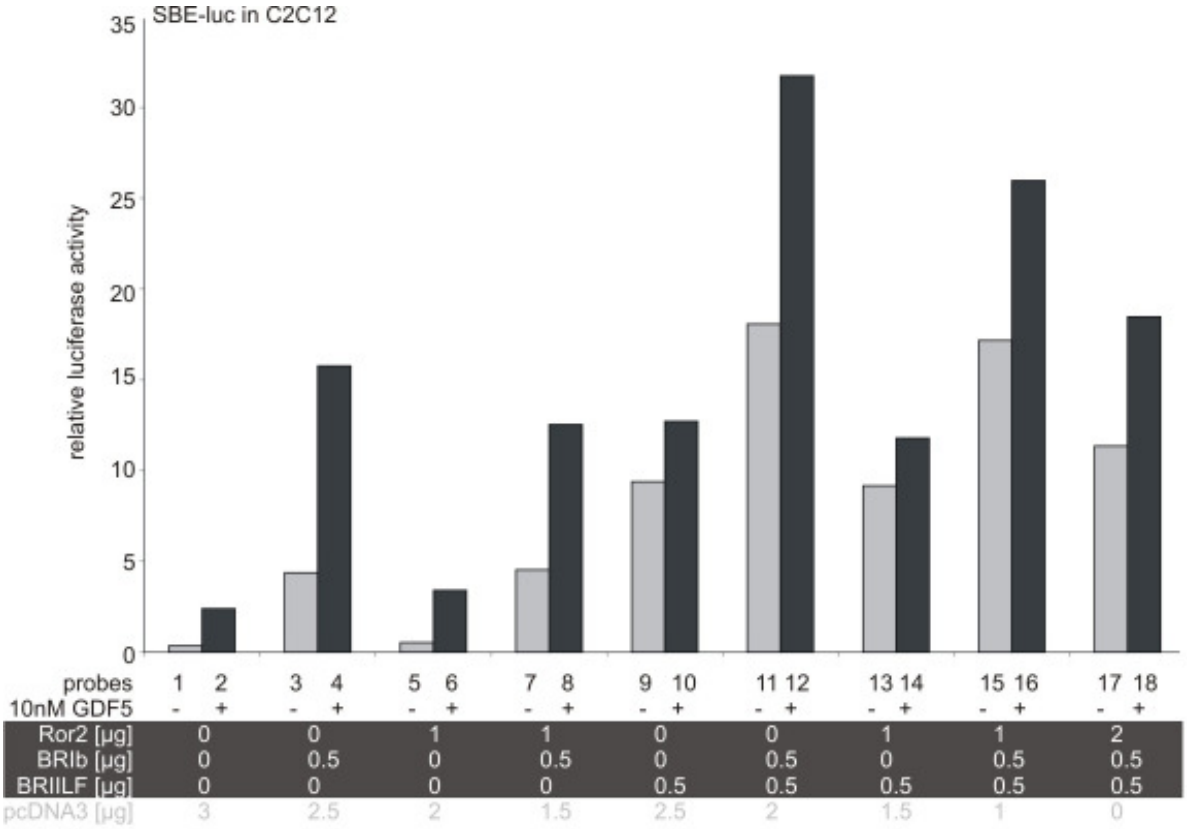

Figure 4.8 Ror2 may interfere with BRIb-BRIILF complex formation

C2C12 cells were transiently transfected with Ror2, c.a.BRIB, the firefly luciferase reporter SBE and the renilla luciferase to calculate relative luciferase activity. The next day cells were starved for 5 hours and stimulated with 10nM GDF5 for 20 hours. Cells were harvested and measured using the Dual-Luciferase™ Reporter Assay kit (Promega Incorporation) according to the manufacturer's instructions.

Since Figure 4.8 displays a preliminary experiment, it is lacking duplicates or triplicates. Nevertheless, a trend is visible. BRIb shows a nice induction upon stimulation with GDF5 (probes 3 and 4), while Ror2 does not initiate reporter gene activity, resembling the mock control (compare probes 1 and 2 with probes 5 and 6). The inhibitory effect of Ror2 on BRIb is not very well pronounced in this experiment (compare probes 3 and 4 with probes 7 and 8), even though Ror2 was transfected in twice the amount as BRIb. While BRIILF usually gives a much stronger signal than seen in this experiment (probes 9 and 10), the co-

expression of BRIILF with BRIb appears normal (probes 11 and 12). Interestingly, co-expression of Ror2 with BRIILF does not have an effect (compare probes 9 and 10 with probes 13 and 14). However, when all three constructs are co-expressed the signal is clearly repressed (compare probes 11 and 12 with probes 15 and 16) and also a dose-dependent effect of Ror2 can be observed (probes 17 and 18).

These data support the previous speculations that Ror2 may compete with BRII for binding to BRIb or otherwise interfere with the BRIb/BRII preformed complex (PFC) or downstream signaling.

Future experiments should further examine effects of Ror2 on the BRIb/BRII complex, for example its membrane distribution and internalization upon ligand stimulation in the presence of Ror2.

4.2.4 Ror2 has no effect on immediate Smad phosphorylation

Previous experiments only examined the long-term effect of Ror2 on downstream Smad signaling, i.e. activation of reporter genes or impact on differentiation events. The following experiment was set out to test the obvious, i.e. the effect of Ror2 on immediate Smad phosphorylation.

C2C12-BRIb cells were transiently transfected with Ror2 or equal amounts of β-Gal using Lipofectamine 2000. The following day cells were starved in DMEM containing 0.5% FCS for 3 hours and stimulated with 1nM GDF5 in starvation medium for 5 to 60 minutes. Cells were harvested in TNE lysis buffer containing protease and phosphatase inhibitors, subjected to SDS-PAGE, Western blotting and the proteins were subsequently stained using the indicated antibodies.

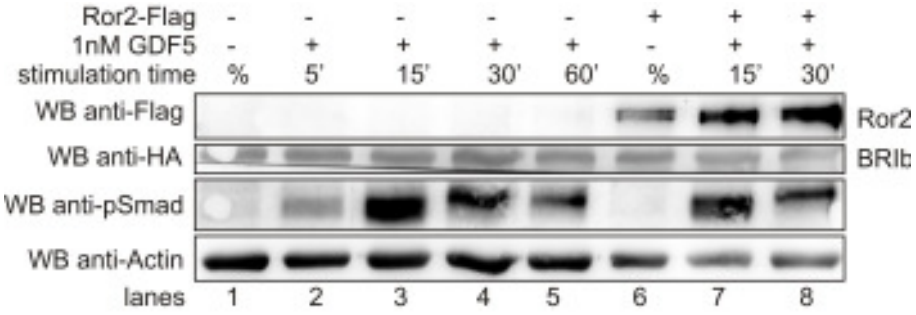

Figure 4.9 Effect of Ror2 on Smad phosphorylation in C2C12-BRIb cells

C2C12-BRIb cells were transiently transfected with Ror2 or β-Gal. The following day cells were starved for 3 hours in DMEM containing 0.5% FCS and stimulated with 1nM GDF5 dissolved in starvation medium for the indicated amounts of time. Cells were lysed, protein was separated with SDS-PAGE, followed by Western blotting to a nitrocellulose membrane on which proteins were detected and visualized using the indicated antibodies.

Figure 4.9 demonstrates that in C2C12-BRIb cells Smad phosphorylation can be clearly detected after as little as 5 minutes and persists for at least one hour (WB anti-pSmad, lanes 2 to 5). When taking the actin bands into account, it has to be concluded that Ror2 does not affect Smad phosphorylation (WB anti-pSmad, compare lane 3 with lane 15 and lane 4 with lane 8). Ror2 is well expressed (WB anti-Flag, lanes 6 to 8) and has no impact on expression of stably transfected BRIb (WB anti-HA, compare lanes 1 to 5 with lanes 6 to 8).

The WB anti-pSmad further reveals stepwise phosphorylation of Smads as a molecular weight shift can be observed between the 5 minutes and 30 minutes stimulation time, while a double band is observed at the 15 minutes stimulation time point. This molecular weight shift most likely represents Smad linker phosphorylation through the MAPK pathway followed by phosphorylation through GSK3 as described in chapter 1.1.6.2.4. Both MAPK- and GSK3-mediated linker phosphorylation enhance interaction of Smad1 with Smurf1, which in turn promotes ubiquitination, proteasome-dependent degradation of Smad and subsequent abrogation of downstream Smad signaling [87, 109].

We speculated that Ror2 might either inhibit Smad C-terminal phosphorylation or enhance Smad linker phosphorylation to promote its degradation. However, the Smad phosphorylation pattern does not appear different in the presence of Ror2 and the molecular weight shift also appears between 15 and 30 minutes, rather than at an earlier time point (WB anti-pSmad, compare lanes 3 and 4 with lanes 7 and 8).

Taken together these results indicate that Ror2 has no inhibiting effect on immediate Smad C-terminal phosphorylation. This finding also disproves previous speculations that Ror2 may disturb the formation of the preformed signaling complex required for Smad-dependent signaling. Furthermore, Ror2 does not promote Smad linker phosphorylation.

4.2.5 Decreased BRIb protein levels during co-expression with Ror2

While studying the interaction of Ror2 with BRIb, BRIb would regularly show reduced expression levels when co-expressed with Ror2. This was independent of DNA preparations or transfection methods, as a former Post Doc in the lab (Sammar) had made similar observations. Thus the effect was studied in more detail to see whether the inhibitory effect of Ror2 on downstream Smad-signaling is achieved through BRIb degradation.

Cos7 cells were transfected with 5µg BRIb and 2 to 5µg amounts of Ror2 as indicated. Total DNA was adjusted to 10µg per probe using β-Gal plasmid DNA. One day after transfection,

the cells were starved for 2 hours and stimulated with 5nM GDF5 for 30 minutes. Cells were harvested in TNE lysis buffer, separated by SDS-PAGE, transferred onto a nitrocellulose membrane, blocked with milk and stained with the indicated antibodies.

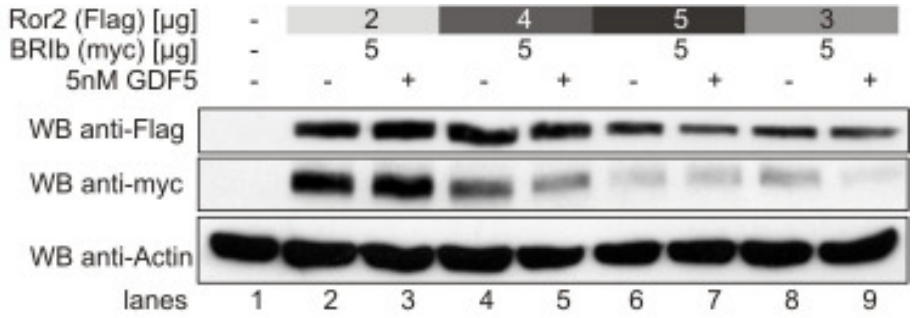

Figure 4.10 Co-expression of Ror2 and BRIb leads to reduced BRIb protein levels

Cos7 cells were co-transfected with the indicated amounts of Ror2 and BRIb, total DNA was adjusted to the same volume in all probes using β-Gal. Cells were lysed, protein was separated with SDS-PAGE, followed by Western blotting to a nitrocellulose membrane on which proteins were detected and visualized using the indicated antibodies.

As seen in Figure 4.10, co-expression of BRIb with Ror2 in Cos7 cells led to reduced BRIb protein levels when cells were transfected with more than 2µg of Ror2 DNA (WB anti-myc, compare lanes 2, 4, 6, and 8). But also Ror2 expression levels decreased in four of the samples, which is not always observed (WB anti-Flag, lanes 6 to 9). GDF5 appeared to have no major impact on this phenomenon (compare lanes 2 and 3, 4 and 5, 6 and 7, 8 and 9).

To examine whether loss of BRIb protein could be ascribed to protein degradation, proteasomal and lysosomal degradation pathways were inhibited. Cos7 cells were transiently transfected with the indicated constructs. Following transfection, cells were treated with the lysosome inhibitor Chloroquine or the proteasome inhibitor MG132 for 2 hours. Cells appeared fine after treatment for 2 hours. They were harvested and lysates were processed as described (not shown).

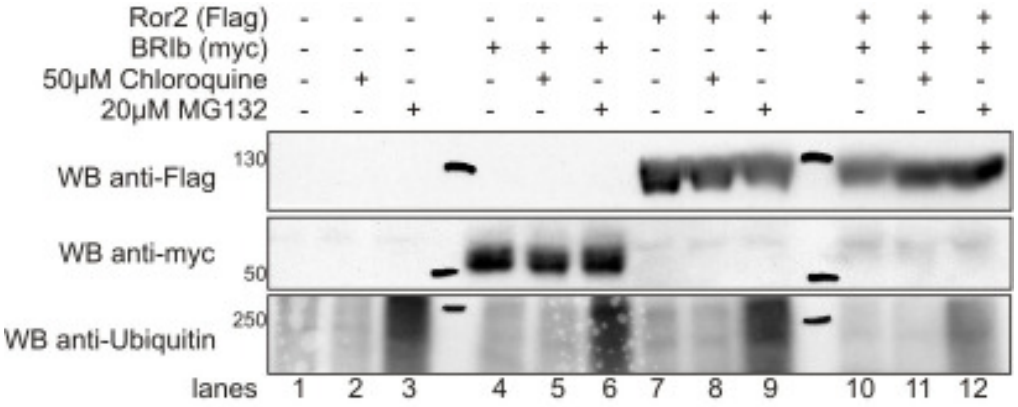

Figure 4.11 Inhibition of proteasome or lysosome has no impact on BRIb protein levels

Cos7 cells were co-transfected with Ror2 and BRIb. The following day cells were treated with 20µM MG132 or 50µM Chloroquine in DMEM supplemented with 0.5% FCS for 2 hours. Cells were then lysed, protein was separated with SDS-PAGE, followed by Western blotting to a nitrocellulose membrane on which proteins were detected and visualized using the indicated antibodies.

Figure 4.11 shows that proteasome inhibition was effective as indicated by the stronger ubiquitin ladder seen in the WB anti-Ubiquitin (lanes 3, 6, 9, and 12). Nevertheless, BRIb protein was not rescued (WB anti-myc, compare lanes 4 and 5 with lanes 10 and 12). Also inhibition of lysosomal degradation had no effect (WB anti-myc, compare lanes 4 and 5 with lanes 10 and 11). Ror2 displayed equal amounts in all samples (WB anti-Flag, lanes 7 to 12).

This experiment was repeated with 30µM of the proteasome inhibitor MG132 and treatment was extended to 4 hours. The inhibitor did not have a visually destructive impact on Cos7 cells, although the cells did look slightly stressed after treatment for 4 hours (not shown).

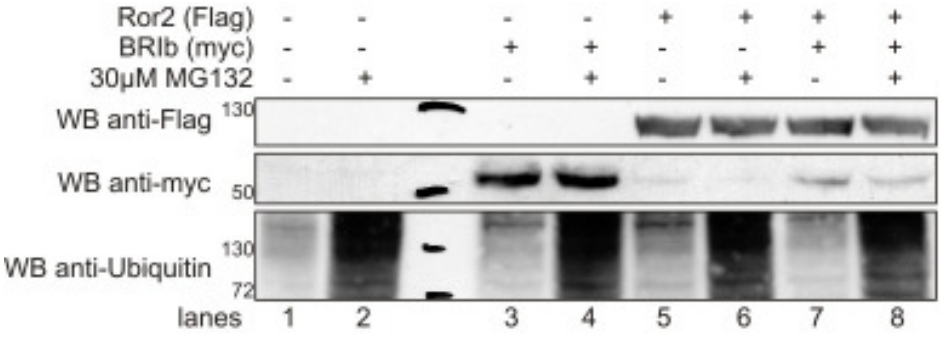

Figure 4.12 Extended proteasome inhibition has no effect on BRIb protein levels

Cos7 cells were co-transfected with Ror2 and BRIb. The next day cells were treated with 30µM MG132 in medium containing 0.5% FCS for 4 hours. Post treatment cells were lysed, protein was separated with SDS-PAGE, followed by Western blotting to a nitrocellulose membrane on which proteins were detected and visualized using the indicated antibodies.

Figure 4.12 confirms the pattern seen in Figure 4.11. The more intense ubiquitin ladder seen with MG132 treatment indicates that the inhibitor was efficient (WB anti-Ubiquitin, lanes 2, 4, 6, and 8). However, this had no effect on BRIb protein levels (Wb anti-myc, compare lanes 3

and 4 with lanes 7 and 8). Ror2 displayed equal amounts in all samples (WB anti-Flag, lanes 5 to 8).

As neither proteasomal, nor lysosomal degradation appear to be responsible for the loss of BRIb protein, it was speculated whether protein translation rather than degradation was to be accounted for the reduced BRIb protein levels.

To test whether this was the case and to circumvent co-transfection, Ror2 was transiently expressed in C2C12 cells stably expressing BRIb. Lysates were subsequently tested for Ror2 and BRIb expression. Although well expressed, Ror2 had not effect on the expression of BRIb in the stable cell line (not shown).

These data strongly suggested that what had been observed in transiently transfected Cos7 cells was an artefact.

To examine potential artefacts of transient transfection, several control experiments were carried out. For this purpose, different receptors were co-expressed with Ror2 in Cos7 cells (not shown). Additionally, constructs in different DNA plasmids were co-expressed, to see the effects independent of Ror2 (not shown). These experiments suggested that the effects described in the previous Figures are indeed most likely due to reduced translation.

The finding that the reduced BRIb protein levels were indeed an artefact of transient transfection immediately challenged the concept of Ror2 inhibiting Smad signaling [165], as the functional data supporting this statement were yielded from transiently transfected ATDC5 or C2C12 cells.

To scrutinize the reliability of the published data, the effect of Ror2 on Smad signaling was tested in C2C12 cells stably expressing BRIb (C2C12-BRIb).

C2C12-BRIb cells were transiently transfected with increasing amounts of Ror2 to yield a dose-effect curve, as well as the reporter genes SBE and RL-TK. One day post transfection cells were starved for 5 hours and then stimulated with 10nM GDF5. The next day after approximately 20 hours of stimulation, cells were harvested and measured as described.

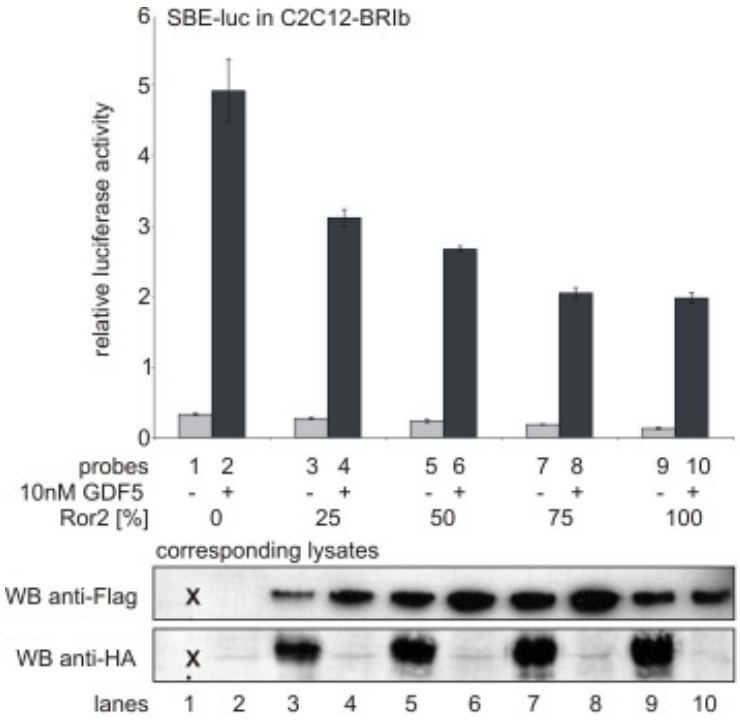

Figure 4.13 Ror2 inhibits reporter gene activation in C2C12-BRIb cells

C2C12-BRIb cells were transfected with increasing amounts of Ror2 as well as the reporter genes SBE and RL-TK. A day post transfection cells were starved for 5 hours and stimulated with 10nM GDF5 for 20 hours. Cells were harvested and measured as described. Additionally, probes were separated using SDS-PAGE and analyzed in a Western blot using the indicated antibodies.

As seen in Figure 4.13, increasing amounts of Ror2 inhibit BRIb-mediated downstream Smad signaling upon GDF5 stimulation in a dose-dependent manner (compare probe 2 with probes 4, 6, 8, and 10). Even in unstimulated cells Ror2 has a repressing effect on the background signal seen in the mock control (compare probe 1 with probes 3, 5, 7, and 9).
As described previously, transient expression of Ror2 in C2C12-BRIb cells (see WB anti-Flag, lanes 3 to 10) has no effect on the stable expression of BRIb in these cells (see WB anti-HA, lanes 3, 5, 7, and 9).

However, it is quite apparent that BRIb protein disappears upon stimulation with GDF5 (see WB anti-HA, lanes 2, 4, 6, 8, and 10). Unfortunately, the lysate in lane 1 which shows unstimulated cells in the absence of Ror2 was lost. Nevertheless, as will be shown further down, this event is independent of Ror2 and does not explain the inhibitory effect of Ror2 on Smad signaling, although the unstimulated control in lane 1 is missing.

From this experiment it can be concluded that Ror2 indeed inhibits downstream Smad signaling and that this is not merely an artefact of transient transfection. Furthermore, it appears that extended stimulation of C2C12-BRIb cells with GDF5 leads to degradation of BRIb protein, which is the subject of the next paragraph.

4.3 Characterization of BRIb protein loss in stable C2C12 cells

Background & aim of this project:

As has been shown in Figure 4.13 in the previous paragraph and as seen in Figure 4.14 below, long-term stimulation of C2C12-BRIb cells leads to a loss of BRIb protein (see WB anti-HA, lanes 2, 4, 6, 8, and 10). Since the transiently transfected protein Ror2 is well expressed in all probes (WB anti-Flag, lanes 3 to 10), this must be a specific event and not a general abrogation of transcription or protein translation. Thus the aim of this project was to unravel the mechanism behind this phenomenon.

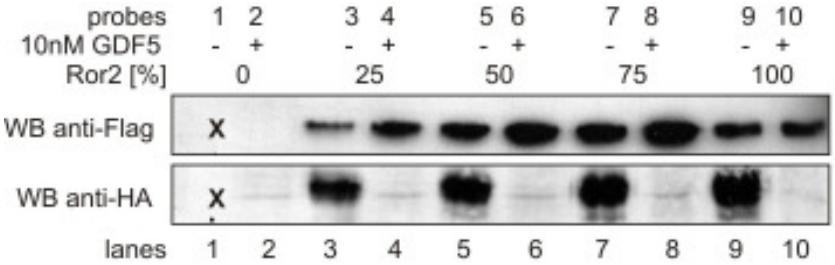

Figure 4.14 Lysates from SBE reporter gene assay in C2C12-BRIb cells

This is an excerpt from Figure 4.13. Probes from the reporter gene assay described in chapter 4.2.5 were separated using SDS-PAGE and analyzed in a Western blot using the indicated antibodies.

4.3.1 C2C12-BRIb cells lose surface expression of BRIb and show reduced GFP levels upon stimulation with BMP2 or GDF5

C2C12 cells stably transfected with BRIb (C2C12-BRIb) express both BRIb and GFP. Both genes were introduced with a single retroviral vector. The site of insertion of the viral DNA into the native C2C12 cell DNA is unknown. Translation of GFP is initiated at an internal ribosomal entry site (IRES). It is thus independent of BRIb translation for as long as the single mRNA strand for translation of both proteins remains stable.

Repeatedly, the expression of GFP appeared to be lower in wells that were stimulated with GDF5 or BMP2 over night. To examine whether a reduction in GFP expression correlated with reduced BRIb protein levels and to quantify both events, C2C12- BRIb cells were analyzed using fluorescence activated cell sorting (FACS).

For the FACS assay, C2C12-BRIb cells were starved or stimulated over night with 1nM GDF5 or 1nM BMP2. The following day cells were washed with PBS and treated with Accutase to detach them from culture plates. Detached cells were immediately transferred into complete medium to inactivate Accutase enzyme activity, followed by two wash cycles with ice cold PBS. To detect stably expressed BRIb which carries a HA tag, cells were incubated with the primary antibody (anti-HA) in PBS on ice for 45 minutes. To remove the

primary antibody, cells were washed three times with ice cold PBS. Cells were then incubated with the secondary antibody (Invitrogen) carrying the fluorescent dye in PBS on ice for 30 minutes. Finally, cells were washed three times with ice cold PBS, resuspended in 1ml PBS and subjected to FACS analysis.

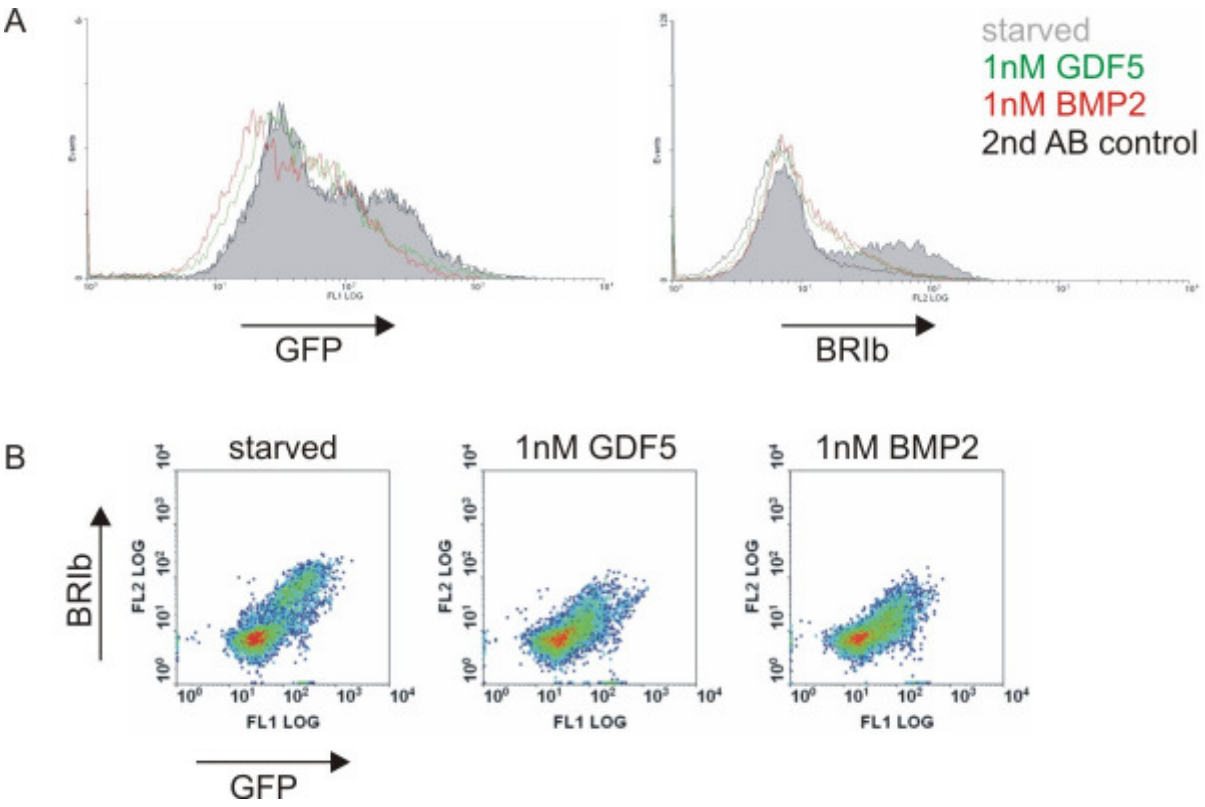

Figure 4.15 Stimulation with GDF5 leads to reduction BRIb at the plasma membrane and GFP

C2C12-BRIb cells were starved or stimulated with 1nM GDF5 or 1nM BMP2 in starvation medium over night. The next day cells were detached, washed thoroughly with ice cold PBS and stained with anti-HA antibody for 45 minutes. To remove unbound primary antibody cells were washed three times with ice cold PBS. Primary antibody was stained with a fluorescent secondary antibody for 45 minutes and removed by extensive washing with ice cold PBS. The antibody-labeled cells were resuspended in 1ml of ice cold PBS and subjected to FACS analysis.
FACS measurements and visual data presentation were carried out by Daniel Horbelt, AG Knaus.

The mountains highlighted in grey in Figure 4.15 A represent starved cells. The peaks in the GFP graph show cells with a strong GFP fluorescence (rightmost peak) and cells with a medium fluorescent GFP signal (middle peak). In the BRIb graph the rightmost peak indicates cells that were stained for BRIb surface expression. The leftmost peak in both graphs depicts low fluorescent cells. The colored lines show the situation in stimulated cells (green for GDF5 and red for BMP2). The black line in the BRIb graph represents unspecific binding of the fluorescent secondary antibody. It confirms that the secondary antibody does not stain cells unspecifically, as in the absence of the primary antibody the signal of the secondary antibody is very low for the BRIb-specific peak on the far right.
When cells are stimulated with either GDF5 or BMP2, the rightmost peak almost disappears in both the GFP and BRIb graphs. For GFP the peaks shift to the left and the middle peak

increases (left graph). These data suggest that less GFP is expressed in stimulated cells. For BRIb the low fluorescent peak is extended and increases (right graph). As the cells were not permeabilized, the graph for BRIb merely shows that cell surface expression of BRIb upon stimulation with GDF5 or BMP is dramatically reduced and no statement can be made regarding cytosolic protein.

Looking at the graphs in Figure 4.15 B confirms the observations made in Figure 4.15 B. In starved cells (leftmost graph) a distinct population positive for both GFP and BRIb is detectable in the upper right. Upon stimulation with GDF5 (middle graph) or BMP2 (rightmost graph) this distinct population almost disappears as it merges with the lower left population of low fluorescent cells.

Taken together the FACS data confirm that upon long term ligand stimulation, cell surface expression of BRIb as well as total GFP is reduced in C2C12-BRIb cells. These observations indicate that the single mRNA transcript from which both proteins are translated must be affected by long term ligand stimulation. Otherwise the reduction in GFP fluorescence can hardly be explained.

4.3.2 BRIb protein levels decrease after stimulation with GDF5

To evaluate how fast the protein escapes detection in Western blot and whether the event may indeed be due to a feedback mechanism regulating transcription, mRNA stability or translation, the rate at which the protein vanishes was determined in a Western blot.

C2C12-BRIb cells were starved for 3 hours and stimulated or starved further for the indicated amounts of time. Cells were harvested with TNE lysis buffer, equal amounts of lysate were separated using SDS-PAGE, protein was blotted onto a nitrocellulose membrane and visualized using anti-HA antibody produced as described.

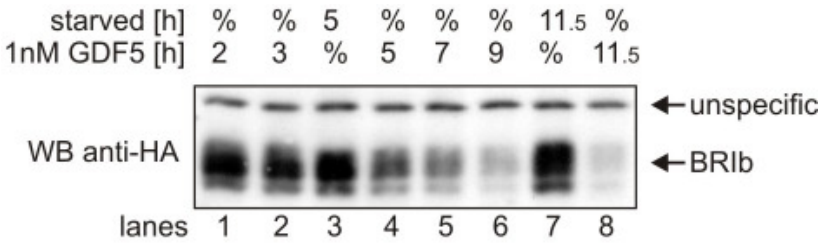

Figure 4.16 BRIb protein levels decrease after extended stimulation with GDF5

C2C12-BRIb cells were starved for 3 hours and stimulated with 1nM GDF5 for the indicated amounts of time. Cells were lysed and proteins were separated with SDS-PAGE and visualized using Western blotting and staining of the nitrocellulose membrane with anti-HA antibody.

As seen in Figure 4.16, cells that were starved for 5 or 11.5 hours exhibit steady expression of BRIb (lanes 3 and 7). Stimulation with GDF5 for 2 hours or less has no effect (lane 1 and not shown). After 3 hours the amount of protein detectable in Western blot appears slightly decreased (lane 2). During the period between 5 and 7 hours detection of BRIb protein is dramatically reduced (lanes 4 and 5). After stimulation with GDF5 for 9 and 11.5 hours the protein has almost vanished.
With total lysates, the indicated unspecific band is always seen in Western blots anti-HA and indirectly confirms that equal amounts of total protein were loaded onto the gel.

These observations indicate that BRIb protein starts to disappear from the Western blot after 3 to 4 hours and almost vanishes after around 9 hours of ligand stimulation, while starvation for the same amount of time has no effect.

It would be interesting to see, whether short stimulation with GDF5 is sufficient to trigger internalization and steady reduction of BRIb protein levels via a negative feedback loop. For this purpose, an experiment should be carried out in which C2C12-BRIb cells are probed for BRIb expression over time after stimulation with GDF5 for 30 minutes. Furthermore it should be investigated, how fast BRIb protein levels recover and whether recovery can be induced by starvation or other treatment.

To detect immediate Smad phosphorylation, cells are usually stimulated for 30 minutes. However, Smad phosphorylation is detectable in a Western blot after as little as 1 to 2 minutes of stimulation. Recently, it was communicated at a conference that phosphorylated Smads appear in the nucleus only a few minutes after stimulation, meaning they must rapidly translocate into the nucleus (unpublished data).
We have shown that phosphorylation of Smads occurs at the plasma membrane, but that transfer of the receptor complex into clathrin-coated pits and subsequent internalization into early endosomes is required for Smads to detach from the type I receptor and translocate into the nucleus [73].
It seems that these events occur within a very short time frame. Nevertheless, it takes several hours until protein detectable in a Western blot vanishes. Interestingly, it has been observed in our lab that reporter gene activity, as measured in the dual luciferase reporter gene assay, achieves full capacity after around 6 hours (not shown). These observations indicate that this is the time frame within which phosphorylated Smads activate the expression of target genes. Thus, the loss of BRIb protein we are seeing in the Western blot may be a combination of receptor internalization and degradation, and a negative feedback mechanism abrogating BRIb expression in order to shut down subsequent activation of target genes.

In summary, these data suggest that BRIb may not just be degraded after phosphorylated Smads detach and translocate into the nucleus. Its expression may also be shut down in a negative feedback response to long term stimulation of cells and subsequent constituent activation of Smad target genes.

4.3.3 Loss of BRIb protein is a specific event upon initiation of the Smad-dependent signaling pathway

To investigate the specificity of the observed loss of BRIb protein, different ligands of the TGFβ/BMP family were tested for their effect on BRIb protein expression and their ability to initiate downstream Smad signaling. For this purpose a BRE reporter gene assay in C2C12-BRIb cells was carried out.

C2C12-BRIb cells were transfected with the reporter genes BRE and RL-TK. The following day cells were starved for 5 hours and stimulated with the indicated ligands and ligand concentrations (conc.) for 17 hours.

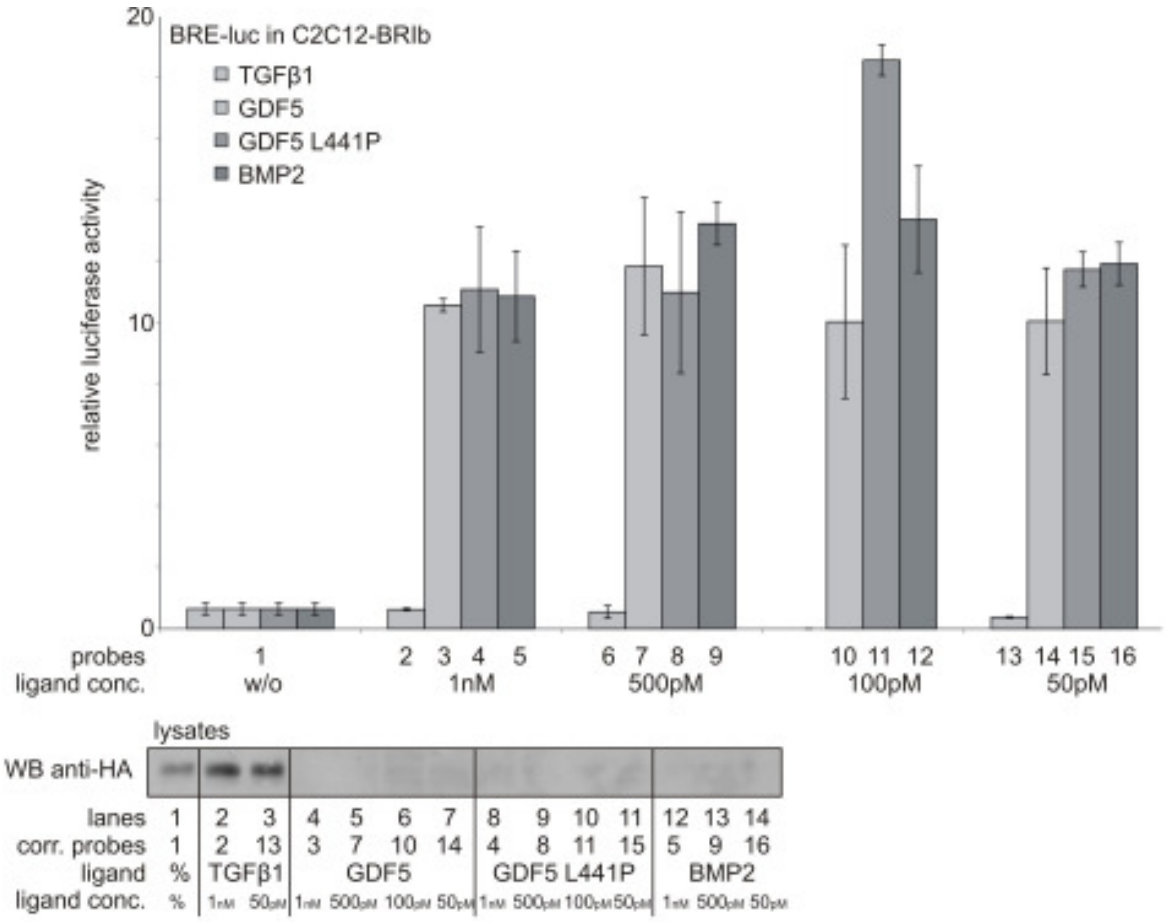

Figure 4.17 C2C12-BRIb cells respond to 50pM of BMP family ligands in BRE reporter gene assay, and only BMP family ligands cause reduction in BRIb protein level, not TGFβ1

C2C12-BRIb cells were transiently transfected with the reporter genes BRE and RL-TK. A day post transfection cells were starved for 5 hours and stimulated with the indicated concentrations of the ligands TGFβ1, GDF5, GDF5 L441P and BMP2 for 20 hours. Cells were harvested and measured as described. Additionally, pools of the triplicates were separated using SDS-PAGE and analyzed in a Western blot staining protein with anti-HA antibody.

Figure 4.17 demonstrates that only ligands of the BMP family are able to induce reporter gene activity via BRIb (probes 3 to 5, 7 to 8, 10 to 12, and 14 to 16), while TGFβ1 remains at the level of unstimulated cells (compare probe 1 with probes 2, 6 and 13). Furthermore, a ligand concentration (conc.) of as little as 50pM is sufficient to induce reporter gene activity equal to stimulation with 1nM. Even a ligand concentration of 500fM yielded respectable and comparable amounts of BRE reporter gene activity in C2C12-BRIb cells (not shown).

Interestingly, the GDF5 mutant L441P, which has lost its affinity to the BRIb receptor, is still able to induce reporter gene activity (probes 4, 8, 11, and 15), supporting the concept that the Smad-dependent pathway is initiated by binding of the ligand to preformed complexes (PFCs) [219].

The lysates from this assay reveal that all ligands able to initiate downstream reporter gene activity also cause the protein to disappear in the Western blot (lanes 4 to 14). Untreated cells (lane 1) and cells treated with TGFβ1 (lanes 2 and 3) steadily express BRIb. The

corresponding (corr.) probes from the reporter gene assay are listed below each lane of the Western blot.

These data confirm that stably expressed BRIb disappears in response to activation of the Smad-dependent signaling pathway. Consistently, binding of the ligand to BRIb is not required to cause loss of the protein. The Smad-dependent pathway is initiated through binding of the ligand to PFCs [219]. Hence, the affinity to BRII alone is sufficient to induce Smad phosphorylation and subsequent signaling. TGFβ1 served as a control and had no effect.

A preliminary quantitative Real Time PCR (qRT-PCR) approach indicated that BRIb mRNA levels are not reduced after stimulation of the cells for 20 hours. If this result could be confirmed it would strongly suggest that protein translation is abrogated independent of mRNA degradation.
Furthermore, the qRT-PCR in combination with the FACS data suggests that the mRNA is locked down and no longer accessible to translation. This is possibly achieved through miRNA-mediated silencing and storage of the mRNA in P bodies, from where the mRNA can either be recovered for translation or processed to degradation [233].

Future qRT-PCR and Western blot experiments are required to examine whether a loss of protein expression upon extended ligand stimulation can also be observed for other proteins of the BMP pathway such as BRII or BRIa. These experiments can be carried out either in cell lines stably expressing these proteins or on the endogenous level. It should also be determined, whether the event occurs in transiently transfected cells. As the cause may lie within miRNA-mediated storage of the respective mRNA in P bodies, immunofluorescence experiments could reveal an increase of cytoplasmic P bodies after long term stimulation. P bodies can be visualized through marker proteins like GW182 [234].

4.3.4 Functional consequences of BRIb protein loss

To evaluate the consequence of reduced BRIb protein levels on Smad phosphorylation in C2C12-BRIb cells, different starvation and stimulation procedures were examined.

C2C12-BRIb cells were treated as indicated in Figure 4.18. Cells were harvested in groups, meaning each group was harvested at the same time point after its procedure was completed. Group 1 was harvested on day 1, while all other groups were harvested on day 2. Cells were lysed in TNE lysis buffer, equal amounts of total lysate were loaded on a SDS-PA

gel, protein was transferred to a nitrocellulose membrane and detected using the indicated antibodies.

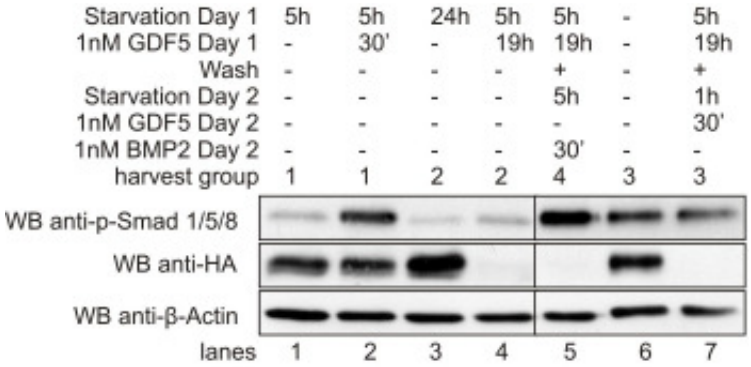

Figure 4.18 C2C12-BRIb retain or quickly regain responsiveness to BMP2 after loss of BRIb protein due to long term GDF5 stimulation

C2C12-BRIb cells were seeded collectively and starved in DMEM containing 0.5% FCS for the indicated amounts of time on day 1 post seeding. Cells remained in starvation medium or were stimulated with 1nM GDF5 for the indicated amounts of time. Harvest group 1 was harvested on day 1 directly after stimulation (lanes 1 and 2). Cells from harvest group 2 were lysed the following day after stimulation for 19 hours was completed (lanes 3 and 4). Cells of harvest group 4 were partly washed on day 2 (lanes 5 and 7) and underwent additional treatment, namely a second starvation and stimulation step as indicated. Cells were lysed and proteins were separated with SDS-PAGE and visualized using Western blotting and staining of the nitrocellulose membrane with the indicated antibodies.

Lanes 1 and 2 of Figure 4.18 depict the standard phospho-Smad assay. Cells were starved for 5 hours and the probe in lane 2 was stimulated with 1nM GDF5 for 30 minutes. Starved cells possess low levels of phosphorylated Smads 1/5/8 (WB anti-p-Smad, lane 1), while a nice induction of phospho-Smad 1/5/8 can be observed in the stimulated cells (WB anti-p-Smad, lane 2). In both cases BRIb is nicely expressed (WB anti-HA, lanes 1 and 2).
When cells are starved for 24 hours, the level of phosphorylated Smads 1/5/8 is even lower than after starvation for 5 hours (WB anti-p-Smad, compare lanes 1 and 3). Furthermore, the induction of Smad 1/5/8 phosphorylation seems very weak after stimulation of the cells for 19 hours (WB anti-p-Smad, compare lanes 2 and 4). As shown previously, BRIb can no longer be detected in the Western blot after stimulation for 19 hours (WB anti-HA, lane 4), while its expression appears much stronger after starvation for 24 hours (WB anti-HA, compare lanes 1 and 3).

To examine the matter even further, cells were stimulated with GDF5 for 19 hours, washed extensively the next day, starved for an additional 1 (lane 7) or 5 hours (lane 5) and stimulated with 1nM GDF5 (lane 8) or 1nM BMP2 (lane 5) for 30 minutes. Only cells treated with BMP2 after an additional 5 hours of starvation show a nice induction of phospho-Smad 1/5/8 (WB anti-p-Smad 1/5/8, lane 5). Interestingly, this occurs in the absence of BRIb (WB anti-HA, lane 5). Only a weak induction can be observed for stimulation with GDF5 (WB anti-

p-Smad 1/5/8, compare lane 5 with lane 7), however this is not comparable with the BMP2-treated cells since these probes were starved for 5 hours on day 2. Unfortunately, the matching controls for the BMP2-treated cells, i.e. cells stimulated over night, starved for 5 hours on day 2 and stimulated with GDF5 for 30 minutes, failed and were thus removed from Figure 4.18.
Lane 6 displays the situation of cells kept in complete medium for the whole procedure.

Nevertheless, these results indicate that other endogenously expressed type I receptors such as BRIa may be able to compensate for the loss of BRIb. Alternatively, the cell may be able to recover during the additional starvation time and express sufficient amounts of BRIb to achieve a significant induction of phospho-Smad 1/5/8. This latter view is supported by the observation, that GDF5 stimulation over night, followed by a recovery time of only 1 hour starvation on day 2 as seen in lane 7, yields at least a mild induction of phopho-Smad 1/5/8 upon afresh stimulation with GDF5 for 30 minutes.

In summary these data show that C2C12-BRIb cells stimulated for an extended period of time lose the expression of BRIb and no longer exhibit high levels of phosphorylated Smads 1/5/8 when compared to cells stimulated for only 30 minutes. However, the cell can either compensate for the loss of one type I receptor or rapidly recover once the ligand stimulation is lifted. On the other hand it is not known whether ligand is at all present in the stimulation medium after 19 hours, as it may be consumed by the cells within a shorter time frame.

It is a hypothesis that expression of BRIb is repressed through miRNA and that the respective mRNA is not degraded but stored in P bodies. If this was the case, a rapid recovery of receptor expression would be possible once the negative feedback mechanism was released due to removal of constituent ligand stimulation. However, this model is highly speculative. Future studies are required to reveal the detailed mechanisms that underlie the observations described above.

Several miRNAs potentially bind mouse BRIb and could account for the inhibition of receptor expression in C2C12-BRIb cells. The potential miRNAs are depicted in Table 4.1 below. The data were kindly collected by Mohammad Belverdi using the listed programs.

miRNA	program	source
mmu-miR-301a mmu-miR-409-5p mmu-let-7d*	miRBase Targets Version 5	http://microrna.sanger.ac.uk/targets/v5/
mmu-miR-301b mmu-miR-130a mmu-miR-721 mmu-miR-130b	TargetScan Release 4.2	http://www.targetscan.org/
mmu-miR-301 mmu-miR-301b mmu-miR-302 mmu-miR-302b mmu-miR-302c mmu-miR-33 mmu-miR-346 mmu-miR-369-3p mmu-miR-376a mmu-miR-703 mmu-miR-744	miRGen	http://www.diana.pcbi.upenn.edu/cgi-bin/miRGen/v3/Targets.cgi#Results

Table 4.1 Potential miRNAs targeting BRIb in mouse cells

5 Results

5.1 Characterization of the Ror2 receptor tyrosine kinase

Ror2 was the first tyrosine kinase receptor described to interact with a serine/threonine kinase receptor [165]. Neither a dedicated ligand nor a dedicated downstream pathway have been characterized for Ror2. But this receptor appears to adopt a critical position in several different pathways and contexts, i.e. cartilage and bone development, as well as cell proliferation and migration (see 1.2.4 and 1.2.5). However, until recently little was published about its most basic protein biochemical characteristics as a tyrosine kinase receptor.

5.1.1 Ror2 homodimerizes independent of ligand

Ror2 was described as tyrosine kinase due to sequence similarities to well known tyrosine kinases [158]. Tyrosine kinases are known to homodimerize and autophosphorylate in response to ligand stimulation [235]. Ror2 was shown to dimerize and phosphorylate target proteins in response to stimulation with Wnt5a [183].
Our cooperation partners from the AG Mundlos at the MPI for Molecular Genetics found a mutation in the BMP antagonist *noggin* that causes Brachydactyly Type B (BDB) [36]. BDB was previously described to be cuased by mutations in *ror2* [196]. Subsequent studies revealed that Noggin interacts with Ror2 via the Ror2 CRD domain (unpublished data, oral communication with Florian Witte, AG Mundlos, MPI).

To test whether the potential Ror2 ligand Noggin has in impact on Ror2 dimerization, Cos7 cells were co-transfected with HA- and Flag-tagged Ror2. Cells were starved for 3 hours in DMEM containing 0.5% FCS and stimulated for 30 minutes with 5nM Noggin in starvation medium. Ror2-Flag was immunoprecipitated using anti-Flag antibody and co-precipitated Ror2-HA was detected in a Western blot anti-HA.

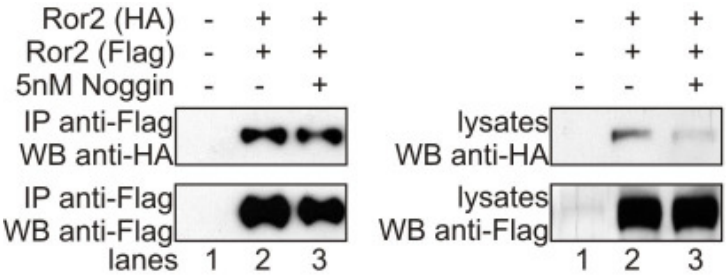

Figure 5.1 Ror2 homodimerizes independent of ligand stimulation

Cos7 cells were transiently co-transfected with HA- and Flag-tagged Ror2. The follwing day cells were starved for 3 hours and treated with 5nM Noggin for 30 minutes. Cells were harvested and lysates were subjected to co-immunoprecipitation (IP) with anti-Flag antibody. Precipitates (IP, lanes 1-3) and lysates (lysates, lanes 1-3) were analyzed by Western blotting (WB) with the indicated antibodies. This result is representative for three independent experiments.

Figure 5.1 shows Ror2-HA co-immunoprecipitated with Ror2-Flag (IP anti-Flag, WB anti-HA, lanes 2 and 3). Ror2 dimerization occurs in a ligand-independent fashion (IP anti-Flag, WB anti-HA, lane 2) and stimulation with Noggin does not seem to promote dimerization of Ror2 (IP anti-Flag, WB anti-HA, lane 3).

Although less Ror2-HA appears to be co-precipitated in cells stimulated with Noggin (IP anti-Flag, WB anti-HA, lane 3), this is only due to less Ror2-Flag being precipitated in the IP anti-Flag (IP anti-Flag, WB anti-Flag, lane 3). Equal amounts of Ror2-Flag were expressed (lysates, WB anti-Flag, lanes 2 and 3). Expression of Ror2-HA appears reduced in cells stimulated with Noggin (lysates, WB anti-HA, lane 3).

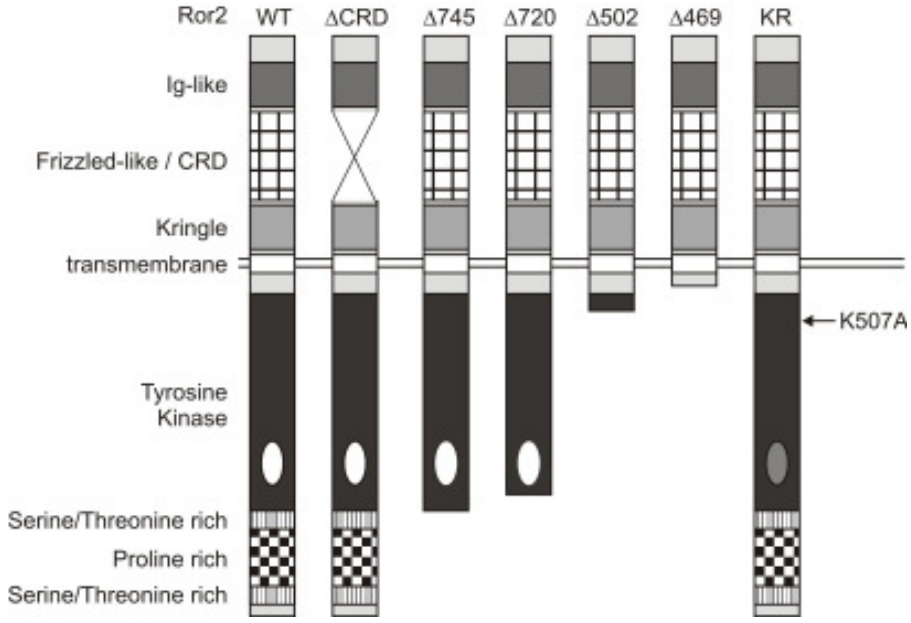

Figure 5.2 Domain structures of wildtype and mutant Ror2 constructs used in this study

Overview of the protein domain structure of Ror2 constructs. WT = wildtype / full length Ror2; Ror2 ΔCRD lacks the extracellular cysteine-rich domain; Ror2 Δ745 is a membrane distal truncation lacking the entire C-terminal tail region; Ror2 Δ720 is a distal truncation lacking small parts of the kinase domain and the C-terminal tail region; Ror2 Δ502 is a membrane proximal truncation containing only a small portion of the kinase domain, Ror2 Δ469 is a proximal truncation that is truncated just before the kinase domain; KR = kinase reduced, Ror2 KR carries a mutation of lysine 507 to alanine and shows reduced autophosphorylation on tyrosine residues.

Figure 5.2 gives a structural overview of the Ror2 point, deletion and truncation mutants used in the following experiments. For more details about the domains present in Ror2, please see Figure 1.8 and chapter 1.2.1.

To specify the dimerzation domain of Ror2, Cos7 cells were co-transfected with full length Ror2-HA and mutant Ror2-Flag constructs (see Figure 5.2 for details). Lysates were subjected to an IP anti-HA, followed by a Western blot with anti-Flag antibody, to detect co-immunoprecipitated receptors.

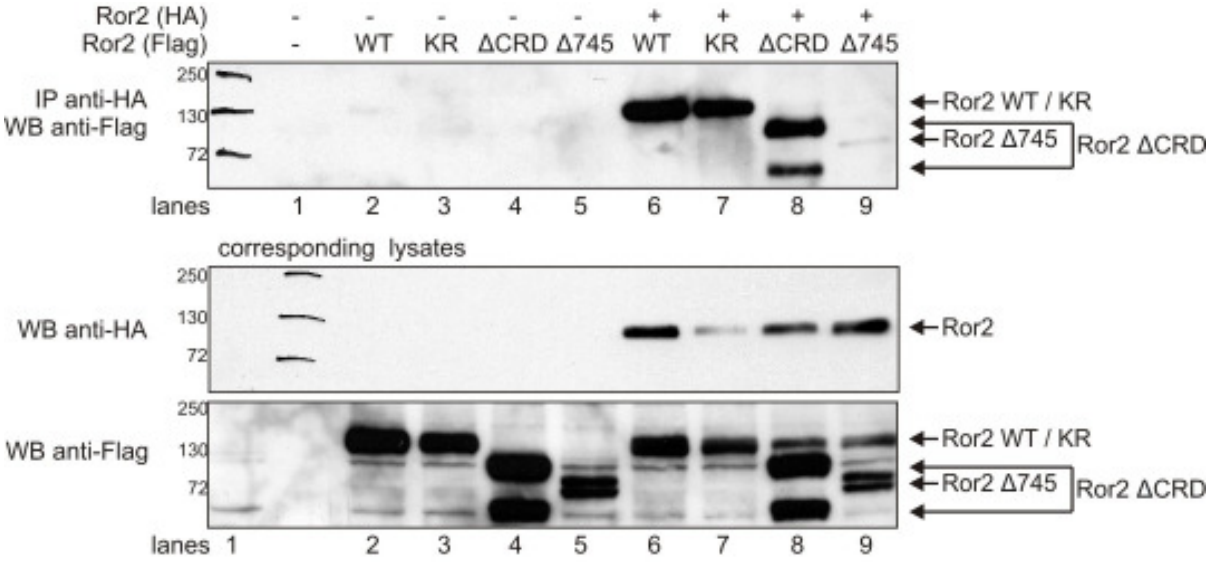

Figure 5.3 Ror2 homodimerizes within its C-terminal tail region

Cos7 cells were transiently co-transfected with HA-tagged full length Ror2 and Flag-tagged deletion mutants or truncations of Ror2. Lysates were subjected to co-immunoprecipitation (IP) using anti-HA agarose beads. Precipitates (upper panel) and lysates (lower panels) were analyzed by Western blotting (WB) with the indicated antibodies.

In Figure 5.3 we see that Ror2 wildtype (WT), Ror2 kinase reduced (KR) and the extracellular deletion mutant Ror2 ΔCRD clearly co-immunoprecipitated with HA-tagged Ror2 (IP anti-HA, WB anti-Flag, lanes 6, 7 and 8, respectively). The intracellular truncation mutant Ror2 Δ745, which is lacking the tail region C-terminal of the tyrosine kinase domain, shows only a very faint band (IP anti-HA, WB anti-Flag, lane 9), suggesting that it has lost the ability to efficiently dimerize with full length Ror2-HA.

5.1.2 Ror2 phosphorylation is increased in the presence of vanadate

Vanadate is a potent tyrosine phosphatase inhibitor, which leads to accumulation of tyrosine phosphorylated protein. This in turn leads to a steady activation of kinases that are usually retained in an inactive state by dephosphorylation. To gain more insight into the tyrosine phosphorylation of Ror2, Cos7 cells transiently expressing Ror2 were treated with vanadate

for up to 30 minutes. Ror2 was immunoprecipitated using anti-Flag antibodies and phosphotyrosine was visualized in a Western blot.

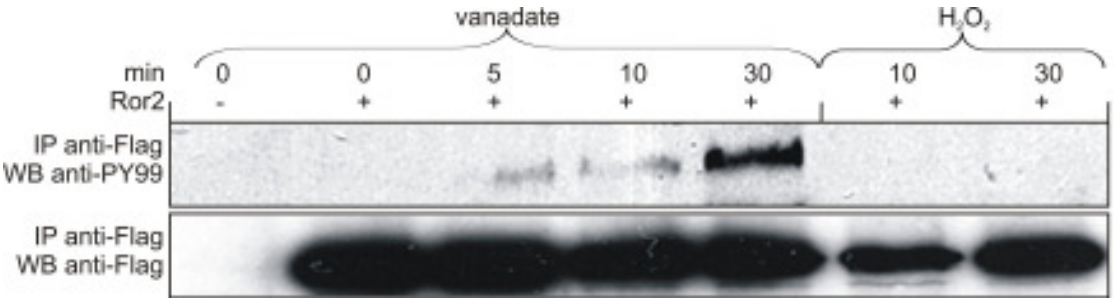

Figure 5.4 Tyrosine phosphorylated Ror2 is sequestered upon treatment with vanadate

Cos7 cells were transiently transfected with Flag-tagged Ror2. Cells were treated with 200µM vanadate for the indicated amounts of time and corresponding amounts of H_2O_2 as a control. Cell lysates were subjected to immunoprecipitation (IP) with anti-Flag antibody. Precipitates were analyzed by Western blotting (WB) with the indicated antibodies.
These data were obtained by Dr. Marei Sammer who kindly provided the figure for discussion.

Figure 5.4 demonstrates that treatment with vanadate for 5 minutes leads to visible amounts of tyrosine phosphorylated Ror2, which increases considerably after 30 minutes. Treatment with H_2O_2 on the other hand has no effect.

Taken together, these experiments demonstrate that Ror2 shows characteristics of a classic tyrosine kinase in that it is capable of homodimerization and autophosphorylation on tyrosine residues. Both events depend on its tail region.

5.2 Ror2 ubiquitination

We could previously show that co-expression of Ror2 and BRIb leads to inhibition of GDF5-dependent Smad signaling [165]. How this inhibition is achieved remains poorly understood. As outlined in the previous chapter, Ror2 does not affect initial Smad phosphorylation (Figure 4.9). Also, interaction of Ror2 with Tak1 (Figure 4.1) has no impact on p38 phosphorylation and thus can not be held responsible for the effect on downstream Smad signaling [171].
While trying to further understand the interaction between Ror2 and BRIb, several observations suggested that degradation may be involved. BRIb was previously shown to be ubiquitinated via Smurf1 and degraded through the proteasome-dependent pathway [86]. Furthermore, we found that BRIb is almost exclusively found in detergent-resistant microdomains (DRMs) [73]. Moreover, experiments carried out within this thesis revealed that Ror2 and BRIb co-localize in DRMs (Figure 4.6) [194]. Taken together, these findings led to speculations whether proteasome-dependent degradation may be responsible for Ror2-mediated inhibition of GDF5-dependent Smad signaling [165].

5.2.1 Ror2 is ubiquitinated

To test whether Ror2 and the BMP receptors are ubiquitinated, Cos7 cells were transiently transfected with Ror2 (Flag), BRIb (myc), BRIILF (HA), and ubiquitin (RGS-His), and the receptors were immunoprecipitated with anti-Flag, anti-myc or anti-HA antibodies, as indicated.

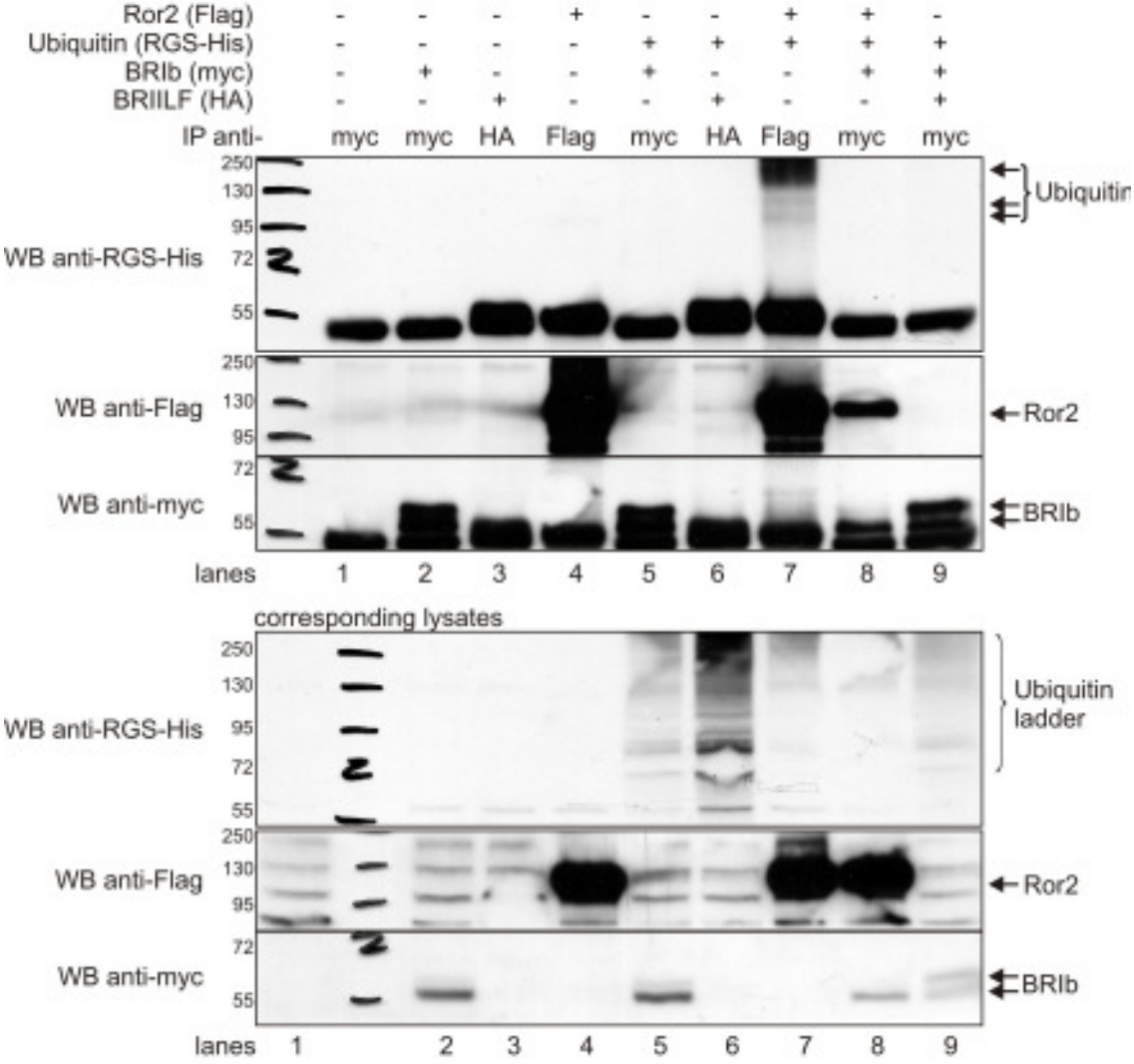

Figure 5.5 Ror2 is ubiquitinated

Cos7 cells were transiently co-transfected with the indicated constructs. Lysates were subjected to co-immunoprecipitation (IP) with the indicated antibodies. Precipitates (upper panels) and lysates (lower panels) were analyzed on a Western blot (WB) using the indicated antibodies.

Figure 5.5 shows that co-expression of Ror2 (Flag) with ubiquitin (RGS-His), followed by an immunoprecipitation of Ror2 with anti-Flag and a Western blot against the RGS-His tag of ubiquitin yielded a clear RGS-His signal (IP, WB anti-RGS-His, lane 7). No signal was detected in any other lane, suggesting that neither BRIb (IP, WB anti-RGS-His, lane 5), nor BRIILF (IP, WB anti-RGS-His, lane 6) or Ror2 precipitated with BRIb (IP, WB anti-RGS-His, lane 8) were ubiquitinated. Although BRIILF was well expressed (not shown), the co-

immunoprecipitation with BRIb in the presence of ubiquitin (lane 9) was very weak (not shown).

Another interesting observation made in Figure 5.5 is the changing pattern of BRIb protein bands. The BRIb double band appears both in immunoprecipitates (IP, WB anti-myc, lanes 2, 5, 8 and 9) and in the corresponding lysates (WB anti-myc, lanes 2, 5, 8, and 9). At this point it is unknown what type of receptor modification the upper band represents. As shown by Sammar et al. it is not N-Glycosylation [194]. Based on this result the upper band could represent phosporylated BRIb, since it appears much stronger in the presence of BRIILF, while the lower band is much weaker (lysate, WB anti-myc, lane 9). Interestingly, the upper band was clearly lacking in the co-immunoprecipitation with Ror2 (IP and lysates, WB anti-myc, lane 8), suggesting that BRIb is not accessible to be phosphorylated by endogenous BRII in the presence of Ror2. Alternatively, the upper band could represent glycosylated or otherwise posttranslationally modified receptor, suggesting that Ror2 preferentially interacts with unmodified BRIb or BRIb that is located within the endoplasmatic reticulum (IP, WB anti-myc, lane 8). However, I could show in my diploma thesis that Ror2 and BRIb co-localize at the plasma membrane.
Since the pattern of the BRIb double band is not consistent throughout all experiments and since the upper band sometimes does appear in immunoprecipitations with Ror2, it is impossible to draw a conclusion regarding its nature at this point. For this purpose, further studies must be carried out.

5.2.2 Ubiquitination confirmed with HA-tagged Ror2

To confirm ubiquitination of Ror2 independent of the lysine-containing Flag tag, an experiment using HA-tagged Ror2 was carried out. Cos7 cells were transiently transfected with Ror2 (HA) and ubiquitin (RGS-His) as indicated. Co-immunoprecipitation of RGS-His-tagged ubiquitin with HA-tagged Ror2 was performed using anti-HA agarose beads.

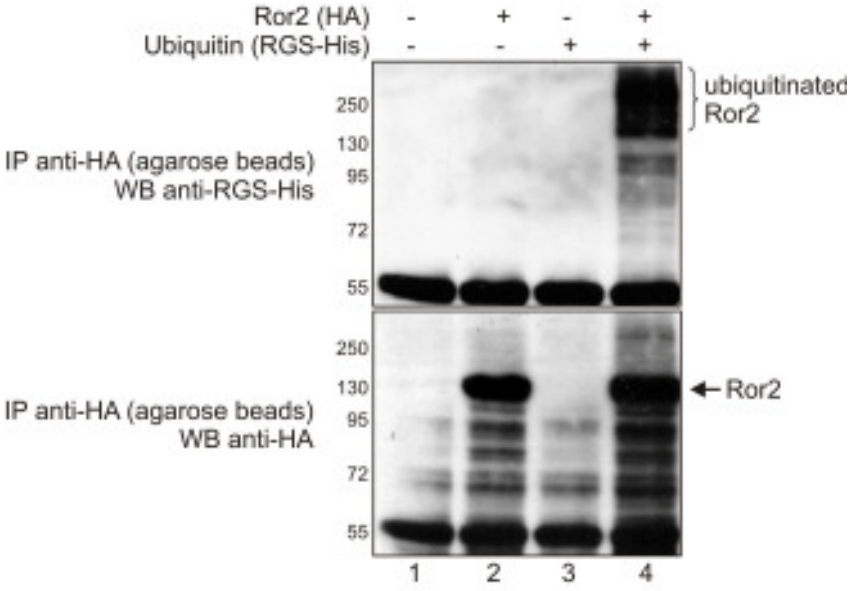

Figure 5.6 Ubiquitination of Ror2 confirmed with HA-tagged Ror2

Cos7 cells were transiently co-transfected with HA-tagged Ror2 and RGS-His-tagged ubiquitin. Lysates were subjected to co-immunoprecipitation (IP) using anti-HA agarose beads. Precipitates were analyzed by Western blotting (WB) with the indicated antibodies.

As depicted in Figure 5.6, co-expression of Ror2 (HA) with ubiquitin (RGS-His) resulted in a strong signal (IP anti-HA, WB anti-RGS-His, lane 4), while the control lanes (IP anti-HA, WB anti-RGS-His, lanes 1 through 3) remained clear. Ror2 was precipitated in equal amounts (IP anti-HA, WB anti-HA, lanes 2 and 4), and both Ror2 (HA) and ubiquitin (RGS-His) were well expressed (not shown).

5.2.3 Ubiquitination of Ror2 shown with endogenous ubiquitin

To further refine the evidence for Ror2 ubiquitination, a “semi-endogenous” approach was carried out. Cos7 cells were transiently transfected with empty vector, Ror2 or Ror2 ΔCRD (both Flag-tagged). Lysates were subjected to an IP anti-Flag and the Western blot was stained with anti-Ubiquitin to determine ubiquitination, followed by anti-Flag to detect precipitated protein.

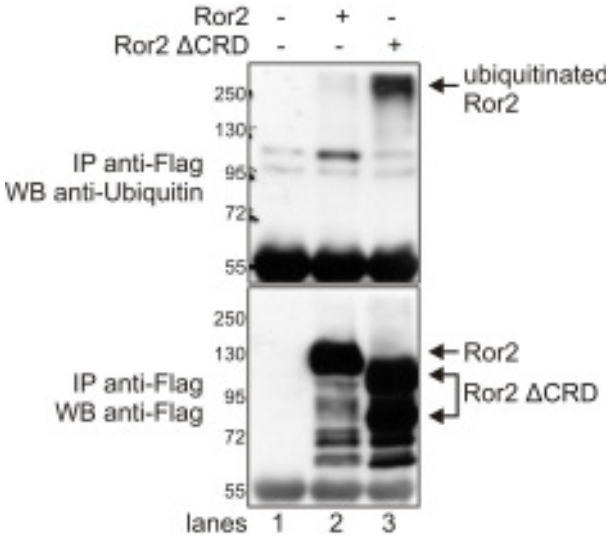

Figure 5.7 Ror2 shows ubiquitination with endogenous ubiquitin

Cos7 cells were transiently co-transfected with Flag-tagged wildtypic Ror2 and Ror2 ΔCRD. Lysates were subjected to co-immunoprecipitation (IP) using anti-Flag antibody. Precipitates were separated through SDS-PAGE and analyzed by Western blotting (WB) with the indicated antibodies.

Figure 5.7 shows an immunoprecipitation of overexpressed wildtype Ror2 and Ror2 ΔCRD. In the Western blot anti-Ubiquitin a very weak ubiquitin signal is visible in lane 2, which indicates ubiquitination of Ror2. In contrast, lane 3 shows a much stronger smear, suggesting that Ror2 ΔCRD is highly ubiquitinated. The Western Blot anti-Flag confirms that both proteins were precipitated (lanes 2 and 3, respectively).

A vice versa approach, overexpressing ubiquitin and precipitating either overexpressed ubiquitin or endogenous Ror2 failed (data not shown). Likewise, a fully endogenous approach failed, but will be presented in Figure 5.8 to demonstrate efficiency of our own anti-Ror2 323/324 (purification 240/241, see 2.12.1) and commercial anti-Ror2 antibodies.

C2C12 and Cos7 cells were seeded in 15cm dishes and harvested as described. Endogenous Ror2 was immunoprecipitated using a anti-Ror2 323/324 antibody [194] or a commercial Ror2 antibody (R&D Systems). Endogenous ubiquitin was precipitated using an anti-Ubiquitin antibody (Cell Signaling). The resulting probes were separated with SDS-PAGE, Western blotted onto a nitrocellulose membrane and stained with the indicated antibodies.

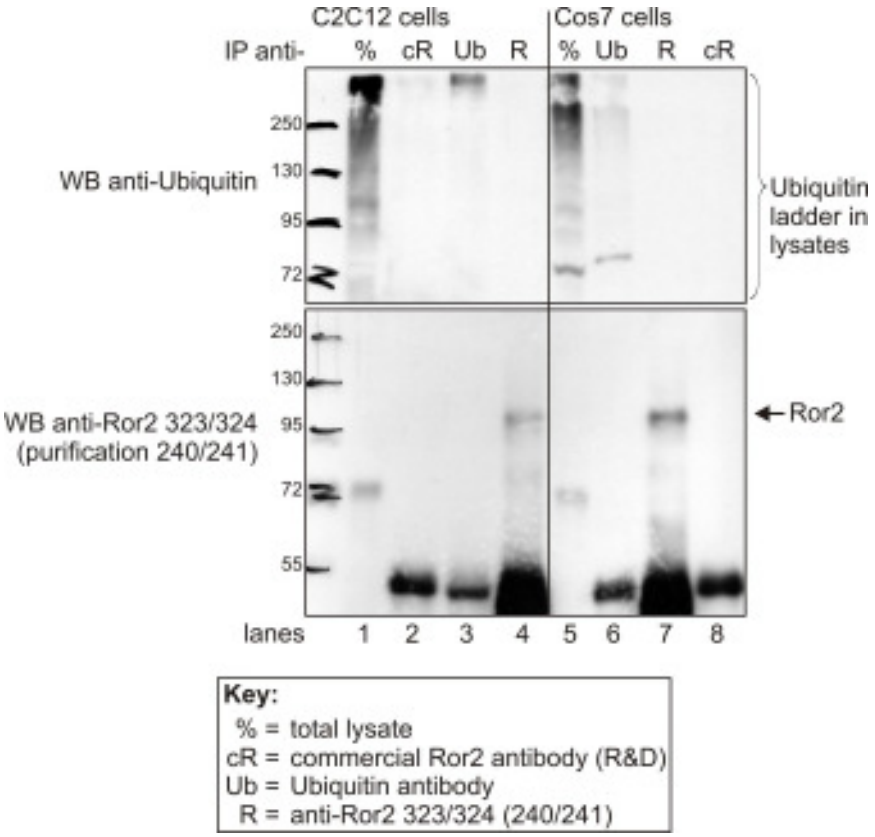

Figure 5.8 Ubiquitination of endogenous Ror2 can not be confirmed

Lysates from C2C12 (lanes 1 - 4) and Cos7 cells (lanes 5 - 8) were subjected to an immunoprecipitation (IP) using a commercial Ror2 antibody (lanes 2 and 8), our anti-Ror2 323/324 antibody (lanes 4 and 7) or an anti-Ubiquitin antibody (lanes 3 and 6). Precipitates (lanes 2 - 4 and 6 – 8) and lysates (lane 1 and 5) were analyzed by Western blotting (WB) using the indicated antibodies.

Figure 5.8 shows an exemplary result of an endogenous approach. The lysate presents a nice endogenous ubiquitin ladder for both cell lines, but endogenous Ror2 is not detectable in the lysate (WB anti-Ror2, C2C12: lane 1, Cos7: lane 5). The immunoprecipitation (IP) using the commercial Ror2 antibody was not successful, no Ror2 could be detected in either cell line (WB anti-Ror2, C2C12: lane 2, Cos7: lane 8). In contrast to that, our anti-Ror2 323/324 antibody precipitated endogenous Ror2 from both cell lines (WB anti-Ror2 323/324, C2C12: lane 4, Cos7: lane 7). However, no ubiquitin signal could be detected (WB anti-Ubiquitin, lanes 4 and 7) and no Ror2 was detected in the IP against endogenous ubiquitin (WB anti-Ror2 323/324, lanes 3 and 6).

Although endogenous ubiquitination of Ror2 can not be observed, this experiment demonstrates the potency of the anti-Ror2 323/324 antibod. This antibody immunoprecipitates endogenous Ror2 from Cos7 and C2C12 cells, while the commercial antibody fails to do so under these conditions.

5.2.4 Verification of ubiquitinated Ror2 using MALDI TOF mass spectrometry

In co-immunoprecipitations of ubiquitin with Ror2 the Western blot anti-RGS-His or anti-Ubiquitin revealed bands of high molecular weight, presumably representing ubiquitinated Ror2. However, in the Western blot anti-Flag or anti-Ror2 usually only a single band for Ror2 was detected. To verify whether or not the high molecular bands detected in Western blots anti-RGS-His or anti-Ubiquitin represented ubiquitinated Ror2, analyzation of the respective bands using MALDI mass spectrometry (MALDI-MS) was attempted.

Ror2 (Flag) and ubiquitin (RGS-His) were co-expressed in Cos7 cells and an IP anti-Flag was carried out as described. Lysates and immunoprecipitates were loaded onto a SDS PA gel and separated by electrophoresis. The gel was stained with Coomassie-G. Based on its size and its presence in both lane 3 and 4 a band migrating at just below 130kDa (Figure 5.9 A, band 1) was identified as Ror2. Merely one unique band (Figure 5.9 A, band 2) could only be detected in the presence of ubiquitin. This band was identified as potentially ubiquitinated Ror2. Both bands were excised, subjected to trypsin in-gel digestion and the resulting probes were analyzed using MALDI-MS by Dr. Christoph Weise.

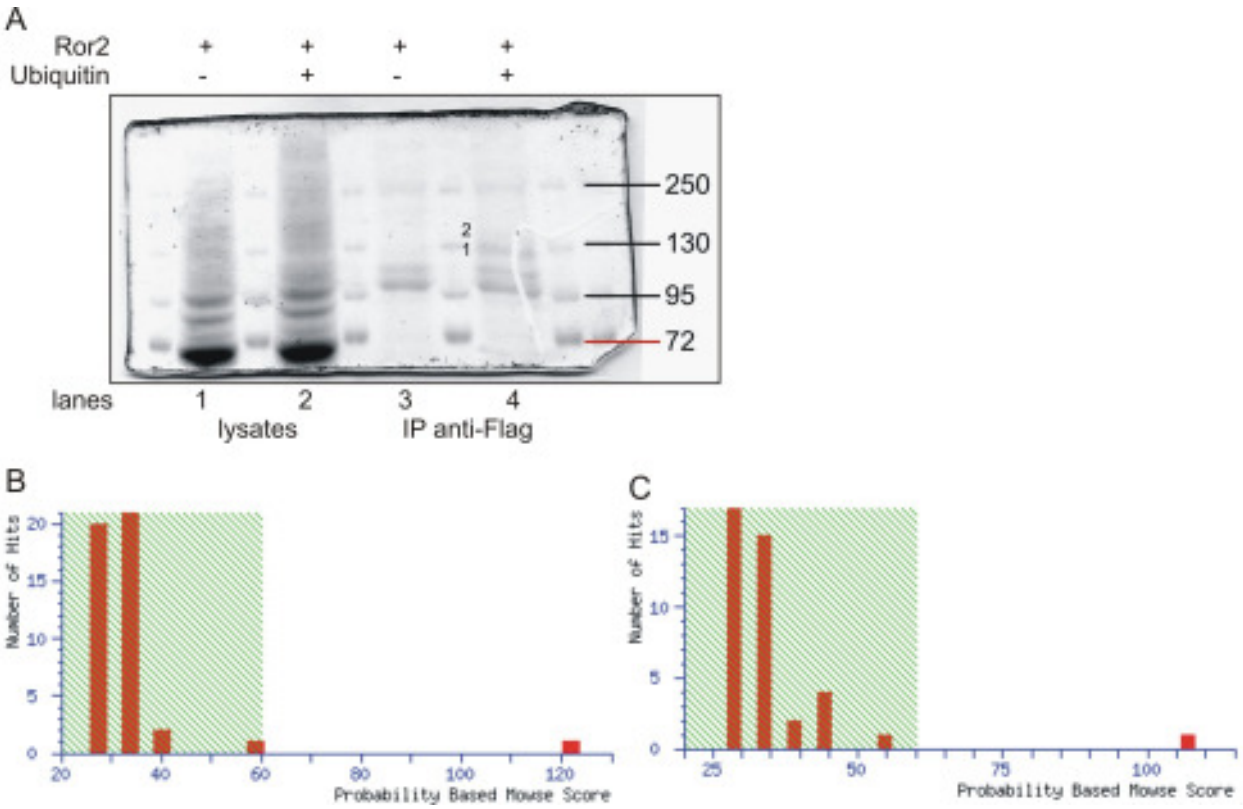

Figure 5.9 Identification of ubiquitinated Ror2 through mass spectrometry

(A) Cos7 cells were transiently transfected with Flag-tagged Ror2 and ubiquitin. Lysates were subjected to an IP anti-Flag. Precipitates and lysates were separated using SDS-PAGE. The resulting gel was stained with Coomassie-G and two bands (1 and 2) were excised. The probes corresponding to bands 1 and 2 were trypsin-digested in-gel and analyzed using MALDI mass spectrometry.
(B) and (C) The mass spectrometry data were analyzed and visualized using the Mascot search engine.
Excision of bands, trypsin in-gel digestion and peptide analysis was carried out by Dr. Christoph Weise, who also provided the statistical data and images for this figure.

Figure 5.9 (A) shows the gel of which bands 1 and 2 were excised from lane 4. Band 1 corresponds to the expected and previously seen molecular weight of Flag-tagged Ror2, which runs just below the 130kDa marker band. Unfortunately, it can barely be seen in the absence of ubiquitin (lane 3). Band 2 on the other hand presents a slightly higher molecular weight of just above 130kDa and is not visible in lane 3. Compared with each other, the lysates (lanes 1 and 2) do not reveal a strikingly different band profiles and no distinct band for overexpressed Ror2 can be detected (lane 2).

In Figure 5.9 (B) and (C) we see the results from the Mascot search for the mass spectrometry data acquired from bands 1 and 2, respectively. In these graphs, probability-based mowse scores greater than 60 are significant. For the probe extracted from band 1 (A) the highest score is 122 with an expectation value of $3.9e^{-08}$ for 22 queries matched. For the second probe (B) the highest score is 107 with an expectation value of $1.2e^{-06}$ for 18 queries matched. Both of these results are highly significant and were reported as tyrosine-protein kinase transmembrane receptor ROR2 precursor from Mus musculus (mouse). To gain additional confirmation, a Ror2-derived peptide that had one of the largest signals in both

samples 1 and 2 was sequenced and identified as Ror2 (data not shown). The type of modification that constituted for the difference of molecular weight between probe 1 and 2 was not detected.

5.2.5 Ror2 is ubiquitinated up to truncation Δ469

Since Ror2 contains over 20 lysines in its intracellular part, potential sites for ubiquitination were narrowed down by testing several truncated forms of Ror2. Cos7 cells were transiently transfected with the indicated Flag-tagged Ror2 constructs in the presence or absence of RGS-His-tagged ubiquitin. Lysates were subjected to an immunoprecipitation using anti-Flag antibody, and the Western blot was probed with anti-RGS-His and anti-Flag antibodies.
For an overview of the domain structure of the mutant Ror2 contructs, please see Figure 5.2.

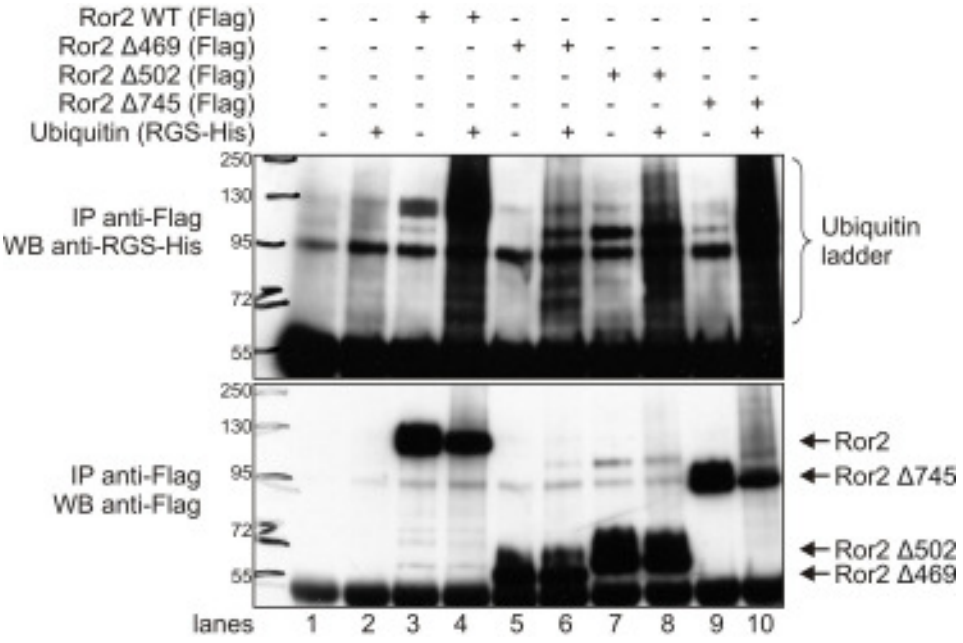

Figure 5.10 Ror2 shows ubiquitination up to truncation Δ469

The indicated Ror2 constructs were transiently transfected into Cos7 cells in the presence or absence of ubiquitin. Ror2 was immunoprecipitated (IP) with anti-Flag antibody. Precipitates were separated using SDS-PAGE and analyzed after Western blotting (WB) with the indicated antibodies.

Ubiquitination of full length Ror2 is confirmed in Figure 5.10 (IP anti-Flag, WB anti-RGS-His, lane 4). Additionally, all truncations of Ror2 show a clear ubiquitin ladder in the presence of ubiquitin (IP anti-Flag, WB anti-RGS-His, lanes 6, 8 and 10). This ladder is not detected in the absence of Ror2 (IP anti-Flag, WB anti-RGS-His, lane 2). This indicates that all tested Ror2 truncations are ubiquitinated.

In the Western blot against RGS-His, a strong band appears at around 130kDa in lane 3 of Figure 5.10, although no RGS-His-tagged ubiquitin is present in this lane. The band corresponds to full length Ror2 in height and most likely originates from occasional unspecific

binding of the RGS-His antibody to Flag-tagged Ror2, which was seen several times. Note that the equivalent probe in Figure 5.5 (IP, WB anti-RGS-His, lane 4) shows no such unspecific binding.

5.2.6 Ror2 is multiubiquitinated

Polyubiquitination is achieved by stepwise attachment of ubiquitin moieties to form a chain that anchors on a single lysine on the polyubiquitinated protein. To test whether Ror2 might be polyubiquitinated, a Flag-tagged ubiquitin construct, carrying lysine to arginine mutations on all of its seven lysines (Ubiquitin K7) was tested. This K7 mutant can still be attached to ubiquitin target sites of a given protein. However, it can no longer form polyubiquitin chains since it is lacking all lysines.

Cos7 cells were transiently transfected with HA-tagged Ror2 and Flag-tagged Ubiquitin K7. Lysates were subjected to an immunoprecipitation (IP) with anti-HA agarose beads to precipitate Ror2. To detect ubiquitinated protein, the Western blot was stained with anti-Flag antibody, followed by anti-HA antibody to visualize precipitated Ror2.

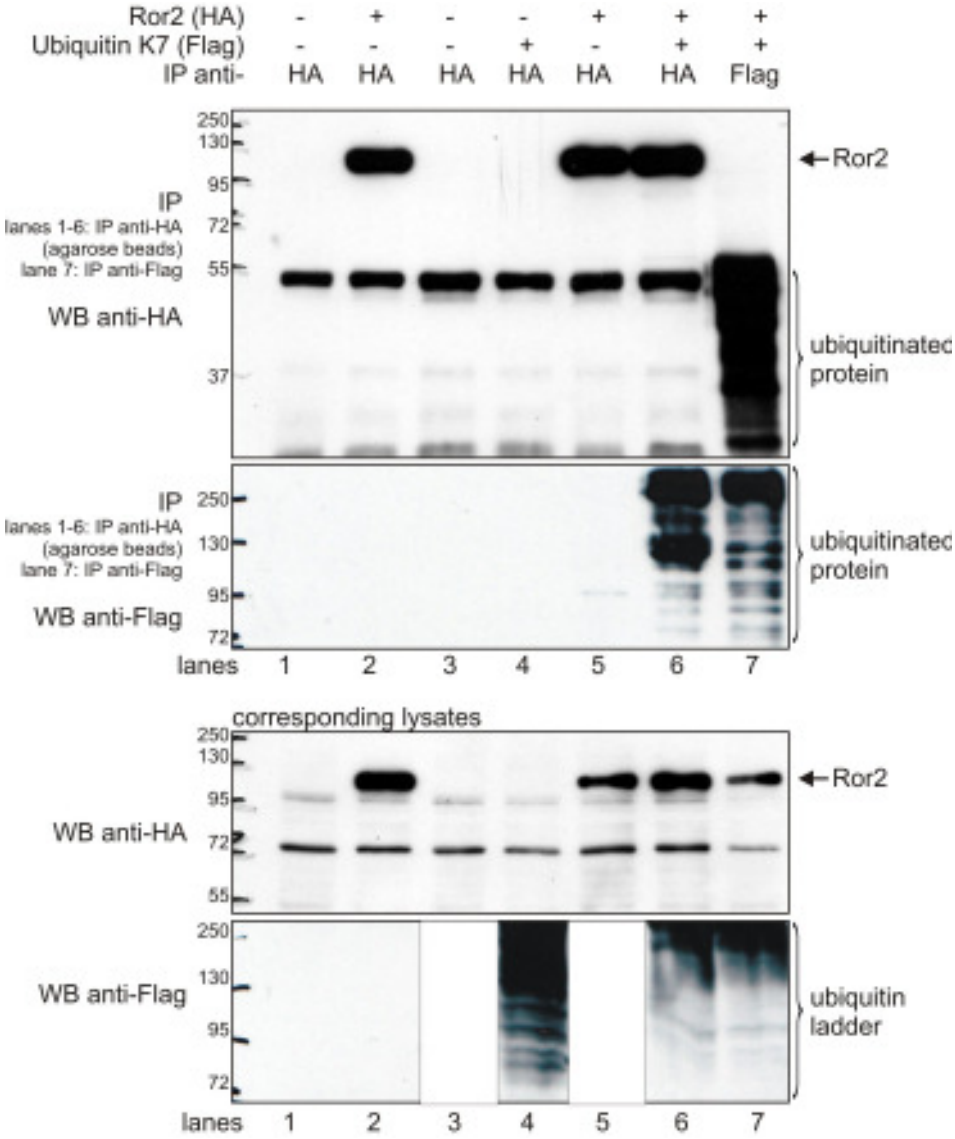

Figure 5.11 Ror2 shows multiubiquitination and degradation

HA-tagged Ror2 and Flag-tagged Ubiquitin K7 were co-expressed in Cos7 cells. Lysates were subjected to an immunorprecipitation (IP) anti-HA (agarose beads, lanes 1-6) or anti-Flag (lane 7). One third and two thirds of the precipitates as well as equal amounts of the lysates were separated via SDS-PAGE. Proteins from all gels were transferred to a nitrocellulose membrane each using Western Blot. Two gels (IP 2/3 and lysates) were stained with anti-Flag antibody, the remaining two (IP 1/3 and lysates) were stained with anti-HA antibody. This procedure was selected after stripping of anti-Flag antibodies from the first set of membranes failed.
The probes in lanes 3 and 5 were unrelated to this experiment and were thus hidden in the image showing the anti-Flag Western blot of the corresponding lysates.

Figure 5.11 shows ubiquitination of immunoprecipitated Ror2 co-expressed with Ubiquitin K7 (IP anti-HA, WB anti-Flag, lane 6; and IP anti-Flag, WB anti-Flag, lane 7). The controls of Ror2 and Ubiquitin K7 expressed alone are negative (IP anti-HA, WB anti-Flag, lanes 2 and 4, respectively). Since the Ubiquitin K7 mutant is only capable of monoubiquitination, what is visible in lanes 6 and 7 most likely represents multiubiquitinated Ror2, i.e. monoubiquitination of Ror2 on several lysines.

Interestingly, in the IP anti-Flag and WB anti-HA a ubiquitin ladder of ubiquitinated protein can be seen below 55kDa. These bands must represent degraded HA-tagged Ror2, however, they have not been observed previously with Flag-tagged Ror2. Just like the Flag tag, the HA tag is situated on the C-terminus of Ror2, which suggests cleaving and degradation of the receptor from its N- to its C-terminal end. Only light bands are seen for the full length Ror2. This hypothesis could be tested by comparing N-terminally tagged with C-terminally tagged protein.

5.2.7 Ubiquitinated Ror2 accumulates upon proteasome inhibition

The observation that Ror2 appears to be multiubiquitinated suggested that it could be internalized via clathrin-coated pits and targeted to early endosomes, rather than to proteasome-dependent degradation via caveolae. Subsequently, the effect of different inhibitors on Ror2 ubiquitination was examined.

Cos7 cells were transiently transfected with Flag-tagged Ror2 and RGS-His-tagged ubiquitin. A day post transfection cells were starved with DMEM containing 0.5% FCS for 5 hours. Following starvation, cells were treated with the proteasome inhibitor MG132 or with Chlorpromazine, which inhibits clathrin-dependent internalization, for 2 hours. The inhibitors were dissolved in starvation medium. Next, cells were lysed and an immunoprecipitation using anti-Flag antibody was carried out. The resulting probes were separated using SDS-PAGE and Western blotted onto a nitrocellulose membrane on which proteins were stained using the indicated antibodies.

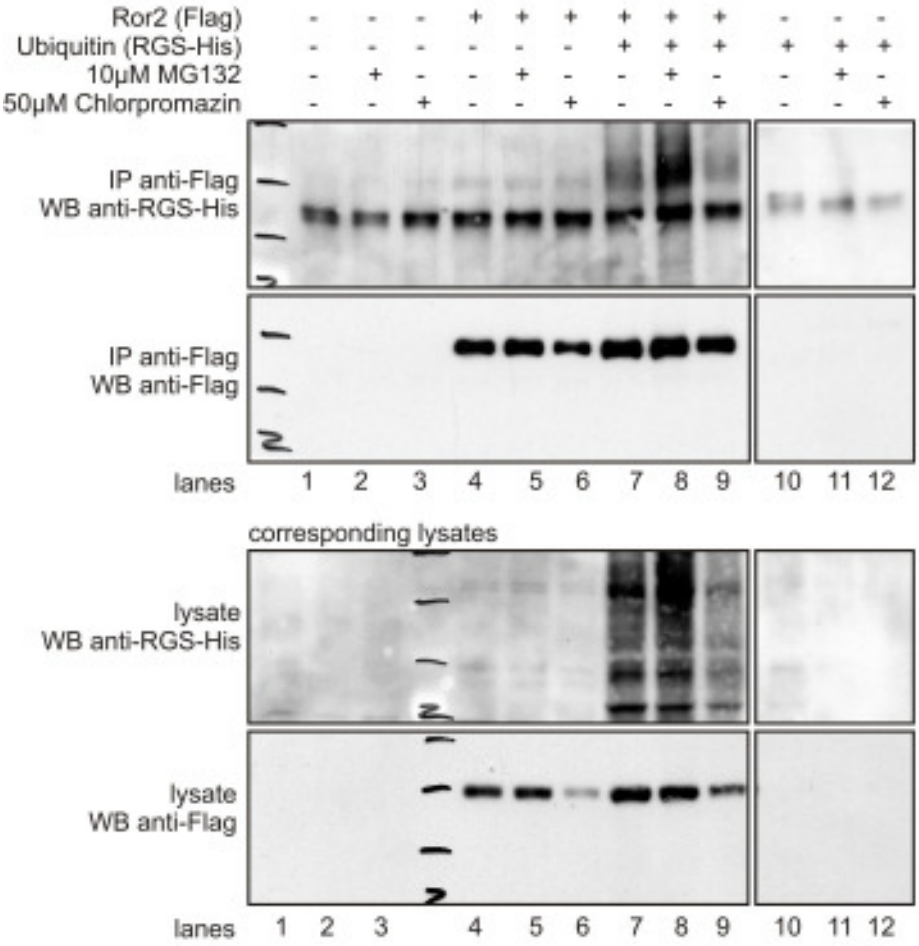

Figure 5.12 Ror2 ubiquitination accumulates upon proteasome inhibition

Ror2 and ubiquitin were transiently expressed in Cos7 cells. The day post transfection cells were starved for 5 hours in DMEM containing 0.5% FCS and treated with 10µM MG132 or 50µM Chlorpromazine for 2 hours. Cells were lysed and subjected to an immunoprecipitation (IP) againt anti-Flag antibody. Lysates and precipitates were separated using SDS-PAGE and visualized using Western blotting (WB) and antibody staining as indicated.
Images shown above originate from a single membrane for each the IP and the lysates. For each antibody staining, the scan images of a single x-ray film were cut to remove two lanes that probed ubiquitination of Ror2 ΔCRD, which however was not expressed.

Despite indications that Ror2 is multiubiquitinated, Figure 5.12 reveals that only the proteasome inhibitor MG132 caused an accumulation of ubiquitinated Ror2 compared to untreated cells (IP anti-Flag, WB anti-RGS-His, compare lanes 7 and 8), while Chlorpromazine had no such effect (IP anti-Flag, WB anti-RGS-His, compare lanes 7 and 9). The amount of Ror2 expressed in untreated and MG132-treated cells is comparable (lysate, WB anti-Flag, compare lanes 7 and 8), as well as the amount of precipitated Ror2 from these cells (IP anti-Flag, WB anti-Flag, compare lanes 7 and 8). However, the amount of Ror2 seen in Chlorpromazine-treated cells is considerably lower than that of untreated and MG132-treated cells (lysate, WB anti-Flag, compare lanes 7 and 8 with lane 9). Subsequently, also the amount of precipitated Ror2 was slightly lower (IP anti-Flag, WB anti-Flag, compare lanes 7 and 8 with lane 9). This can be explained by the high amount of Chlorpromazine used in this experiment, which exposed the cells to a great amount of stress. Nevertheless,

even with lower amounts of Chlorpromazine (30µM and 10µM) no accumulation of ubiquitinated Ror2 could be observed (not shown).

Similarly, treatment with the lysosome inhibitor Chloroquine had no effect on Ror2 ubiquitination (not shown). Experiments using the cholesterol sequesting substance MβCD which inhibits formation of detergent-resistant microdomains (DRMs) were not conclusive (not shown) and need to be repeated.

Interestingly, even though immunoprecipitated ubiquitinated protein, that presumably represents ubiquitinated Ror2, accumulates upon treatment with MG132, no significant change of Ror2 protein levels is seen in the IP or lysate. This was observed in three different experiments.

5.2.8 Ubiquitinated protein localizes to DRM fractions in presence of Ror2

Previous experiments revealed that Ror2 is present in detergent-resistant microdomains (DRMs), as well as in other membrane fractions (Figure 4.6). To study the distribution of ubiquitinated Ror2 in membrane fractions, Cos7 cells were transiently transfected with RGS-His-tagged ubiquitin alone and co-transfected with Flag-tagged Ror2 or Ror2 ΔCRD with ubiquitin. For this assay, cells were lysed using 20mM of the detergent CHAPS rather than 1% Triton. The lysates were homogenized, adjusted to an iodixanol (OptiPrep, Sigma-Aldrich) concentration of 40% and subjected to ultracentrifuge-mediated separation of DRM from non-DRM fractions within a discontinuous OptiPrep gradient from 30% to 5% above the lysate.

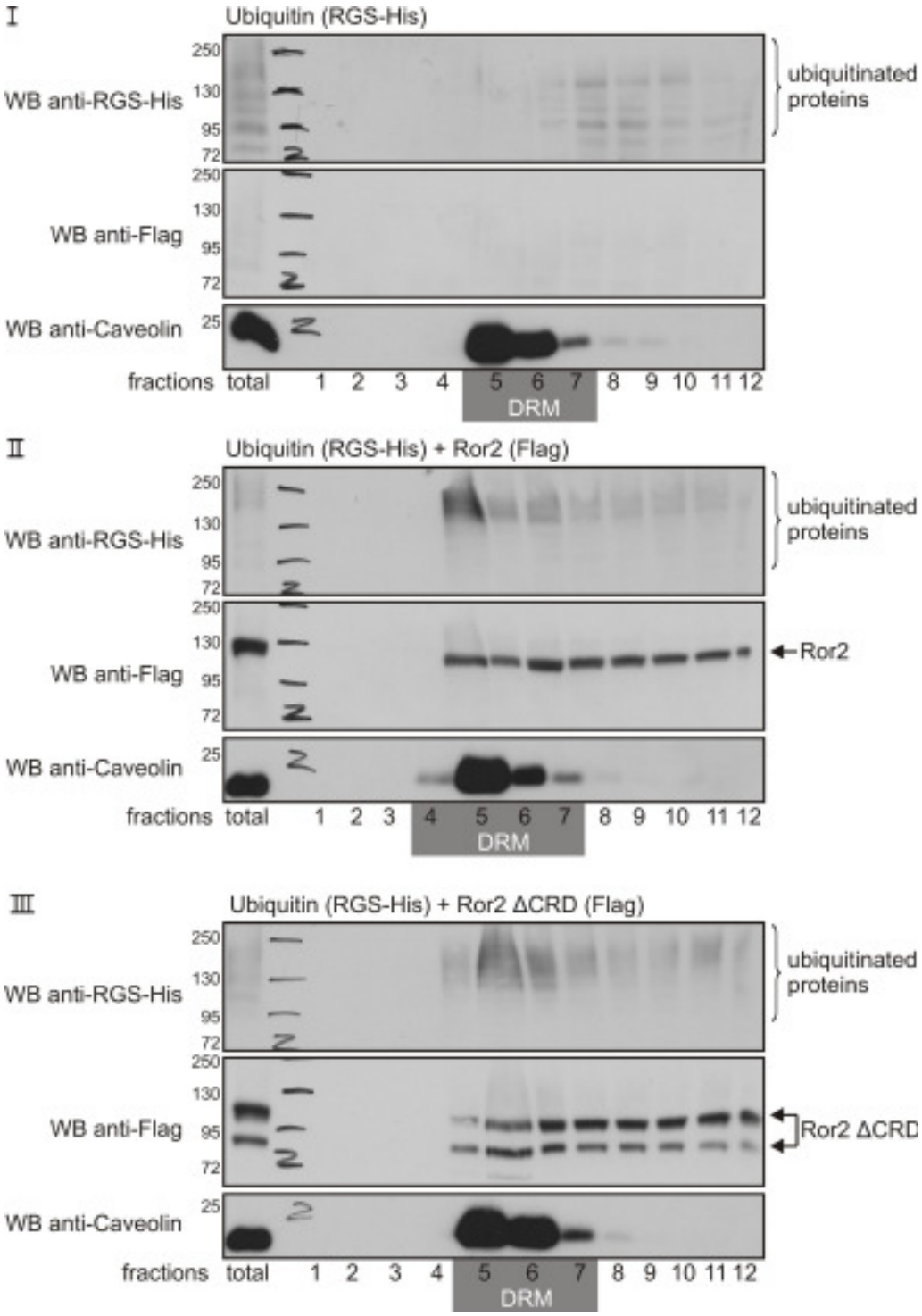

Figure 5.13 Ubiquitinated protein accumulates in DRMs in presence of Ror2

Cos7 cells were transiently transfected with the indicated constructs. Lysates were homogenized, adjusted to 40% iodixanol concentration and transferred into ultracentrifugation tubes. Above the lystate, a discontinuous gradient from 30% to 5% iodixanol diluted in lysis buffer was formed. The probes underwent ultracentrifugation at 39,000g and 4℃ for 20h. The resulting gradient was harvested in 1ml fractions, proteins were separated using SDS-PAGE, transferred to a nitrocellulose membrane in a Western blot, and detected using the indicated antibodies.

Figure 5.13 shows separation of detergent-resistant microdomains (DRMs) in Cos7 cells transfected with ubiquitin (I), ubiquitin and Ror2 (II) and ubiquitin and Ror2 ΔCRD (III).

When ubiquitin was transfected alone, ubiquitinated protein was detected in all protein-containing fractions (I, WB anti-RGS-His, fractions 5 to 12), however it was predominantly located in non-DRM fractions 8 to 12. DRM fractions are characterized by the presence of caveolin.

Both Ror2 (II) and Ror2 ΔCRD (III) are evenly distributed throughout all protein-containing fractions (II and III, WB anti-Flag). In the presence of Ror2, ubiquitinated protein appeared to accumulate in caveolin-positive DRM fractions (compare I, II and III, WB anti-RGS-His and WB anti-Caveolin, fractions 5 to 7, 4 to 7 and 5 to 7, respectively).

An immunoprecipitation anti-Flag from pooled DRM versus pooled non-DRM fractios likely failed due to the high concentrations of iodixanol in these probes. To elucidate whether ubiquitinated Ror2 displays a preferential membrane distribution, the immunoprecipitation must be repeated following isolation of the protein from the respective fractions.

5.2.9 Ror2 interacts with ubiquitin E3 ligase Smurf1

To test whether Ror2 interacts with Smurf1 Cos7 cells were co-transfected with Ror2, wildtype Smurf1 (Smurf1 WT), and dominant negative Smurf1 (Smurf1 DN). Since all constructs used in this experiment were Flag-tagged, the lysates were subjected to an IP using anti-Ror2 antibody and proteins were visualized on a Western Blot using anti-Flag antibody.

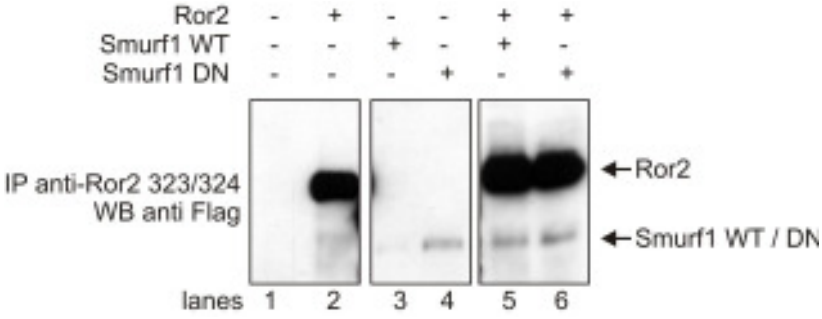

Figure 5.14 Ror2 may interact with Smurf1

Cos7 cells were transiently transfected with Flag-tagged Ror2 and Smurf1 constructs as indicated. Ror2 was immunoprecipitated (IP) from the cell lysates using anti-Ror2 323/324 antibodies. Proteins were separated using SDS-PAGE, transferred to a nitrocellulose membrane in a Western blot, and Flag-tagged Ror2 and Smurf1 proteins were detected on the blot using anti-Flag antibody.
The lanes displayed above were cut from a film's scan image showing a single blot in order to omit additional data including co-IP of Ror2 ΔCRD with Smurf1 WT and DN.

Figure 5.14 shows that Flag-tagged Ror2 was nicely precipitated with anti-Ror2 323/324 antibodies (IP anti-Ror2 323/324, WB anti-Flag, lanes 2, 5 and 6). Both Smurf1 WT and Smurf1 DN appear to co-immunoprecipitate with Ror2 (IP anti-Ror2 323/324, WB anti-Flag, lanes 5 and 6, respectively). However, slightly weaker bands for Smurf1 WT and DN are also visible in the controls where no Ror2 was co-expressed (IP anti-Ror2 323/324, WB anti-Flag,

lanes 3 and 4, respectively). The weak band appearing at around the same height as Smurf1 WT and DN when Ror2 is expressed alone (IP anti-Ror2 323/324, WB anti-Flag, lane 2) is slightly higher than the Smurfs and also appears in all other lanes showing immunoprecipitated Ror2.

Evidently, a sepharose control without antibody is lacking in this experiment to prove that Smurfs do not stick to the sepharaose but were specifically co-immunoprecipitated with overexpressed or endogenous Ror2. We have previously seen that the anti-Ror2 antibody precipitates endogenous Ror2 from Cos7 cells (see Figure 5.8), so it is reasonable to speculate that Smurf1 WT and DN were co-immunoprecipitated with endogenous Ror2.

To confirm specific interaction of Ror2 with Smurf1, two differentially tagged proteins were co-expressed in Cos7 cells. Smurf1 DN was used since it exhibited better expression than the wildtype. Ror2-HA was immunoprecipitated (IP) using anti-HA agarose beads. Lysates and IP probes were separated using SDS-PAGE, Western blotted onto a nitrocellulose membrane, and the membrane was stained with anti-Flag antibody to detect co-expressed and potentially co-IPed Smurf1 DN. Subsequently the blot was stripped to remove anti-Flag antibody and incubated with anti-HA antibody to detect Ror2.

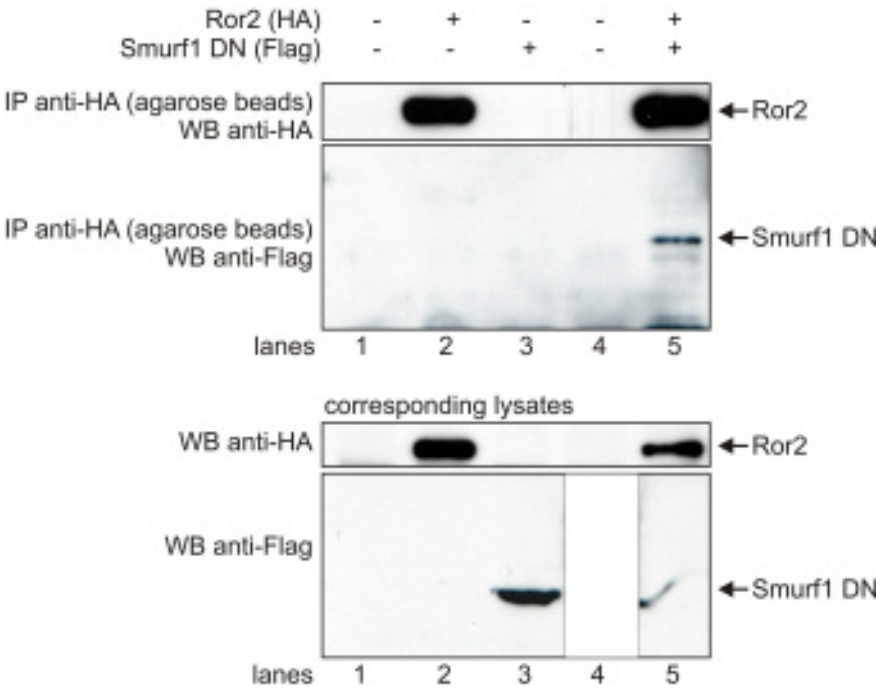

Figure 5.15 Smurf1 co-immunoprecipitates with Ror2

HA-tagged Ror2 and Flag-tagged Smurf1 were co-expressed in Cos7 cells. Lysates were subjected to an IP anti-HA (agarose beads) and probes were separated via SDS-PAGE. Proteins were transferred to a nitrocellulose membrane using Western Blot and stained with anti-Flag antibody. Next, the anti-Flag antibody was stripped from the blots and they were incubated with anti-HA antibody.
The probe in lane 4 was unrelated to this experiment and was thus hidden in the image showing the corresponding lysates.

Figure 5.15 shows specific co-IP of Smurf1 DN with Ror2 (IP anti-HA, WB anti-Flag, lane 5). No unspecific signal is seen in the control where Smurf1 DN is expressed alone (IP anti-HA, WB anti-Flag, lane 3). Expectedly, Ror2 was nicely precipitated (IP anti-HA, WB anti-HA, lanes 2 and 5). Both Ror2 (lysates, WB anti-HA, lanes 2 and 5) and Smurf1 DN are well expressed (lysates, WB anti-Flag, lanes 3 and 5), although a disturbance in the gel caused a deformation of the Smurf1 DN band (lysates, WB anti-Flag, lane 5). The probe in lane 4 is unrelated.

6 Discussion

Receptor tyrosine kinases are involved in a number of crucial physiological processes, including tissue development, cell proliferation, cell differentiation and apoptosis [235]. In general the most revealing insights into the distinct and critical roles of proteins emerge from cases where the tightly regulated signaling networks they are involved in are disturbed. In the case of receptor tyrosine kinases there are many mutations known to cause human diseases, the most studied one being the onset and progression of different forms of cancer.

Based on specific sequence or structural characteristics, receptor tyrosine kinases (RTKs) are grouped into several different classes. Thanks to their flagships, the EGF and Insulin receptors, RTKs are probably the most well characterized transmembrane proteins to date. In comparison, little specific information was available about the RTK class XII, representing the Ror receptor family, around the time when work for this thesis began.

The Regeneron orphan receptor 2 (Ror2) was first described in 1992 and classified as a receptor tyrosine kinase (RTK) based on sequence similarities to other RTKs [158]. Meanwhile a growing body of evidene suggests a role for Ror2 in Wnt signaling, proposing that Wnt proteins act as ligands for Ror2 [160]. We have shown that Ror2 is also involved in the inhibition of BMP signaling, an event that depends on the interaction of Ror2 with the BMP receptor type Ib (BRIb) [165]. Furthermore, we could characterize the Ror2/BRIb receptor complex [194]. The mechanism by which Ror2 achieves inhibition of GDF5-mediated Smad signaling however remains to be elucidated.

6.1 Ror2 is an almost typical receptor tyrosine kinase

Typically, RTKs homodimerize and undergo tyrosine phosphorylation in response to binding of the ligand [235]. The insulin receptor and the insulin-like growth factor-I (IGF-I) receptor are exceptions as they form disulfide-linked covalent dimers. All other RTKs described so far require binding of the ligand to form noncovalent dimers or oligomers [236]. Serine/threonine receptors on the other hand can form homo- and heterodimers or –oligomers independent of ligand, nevertheless depending on binding of the ligand for full activation and initiation of downstream signaling events [71, 237, 238]. For Ror2 it was described more recently, that the receptor homodimerizes and is autophosphorylated on tyrosine residues in response to treatment with Wnt5a [173, 183].

This study shows that Ror2 homodimerizes independent of external ligand stimulation in starved Cos7 cells (Figure 5.1). Moreover, data obtained in the lab of Prof. Dr. Yoav Henis

(Tel Aviv, Israel), examining distribution of differentially tagged Ror2 contructs on the surface of Cos7 cells using receptor co-patching immunofluorescence (described in [7]), imply that more than 50% of Ror2 is engaged in homodimers in the absence of ligand stimulation (oral communication with Yoav Henis, data not shown). A receptor lacking the Wnt binding site, the CRD domain, can still form homodimers with the wildtype receptor (Figure 5.3, IP anti-HA, WB anti-Flag, lane 8), challenging the notion that Ror2 homodimerization is mediated exclusively through Wnt proteins. Furthermore, it is shown here that homodimerization of Ror2 depends on its tail region (Figure 5.3, IP anti-HA, WB anti-Flag, lane 9). These experiments were done in Cos7 cells and it can also not be exluded that intrinsic dimerization of Ror2 in these cells is induced by endogenous secretion of Ror2 ligands, although the cells were starved prior to analyzing Ror2 dimerization.

In line with these findings that a great portion of Ror2 protein situated at the plasma membrane is homodimerized, we found that Ror2 is autophosphorylated on tyrosine residues, an event that also occurs independent of ligand stimulation (Figure 5.4). The autophosphorylation seen in this experiment depends on the C-terminal tail region of Ror2, but not on the presence of its extracellular CRD domain, which serves as interaction site for Wnt proteins (unpublished data of Marei Sammar).

These data indicate that Wnt stimulation is not required for basal activation levels of Ror2 as the receptor is readily homodimerized and autophosphorylated in starved cells, even when the Wnt binding site is deleted.

Figure 6.1 demonstrates the hypothetic distribution models of monomeric and dimeric Ror2 at the plasma membrane.

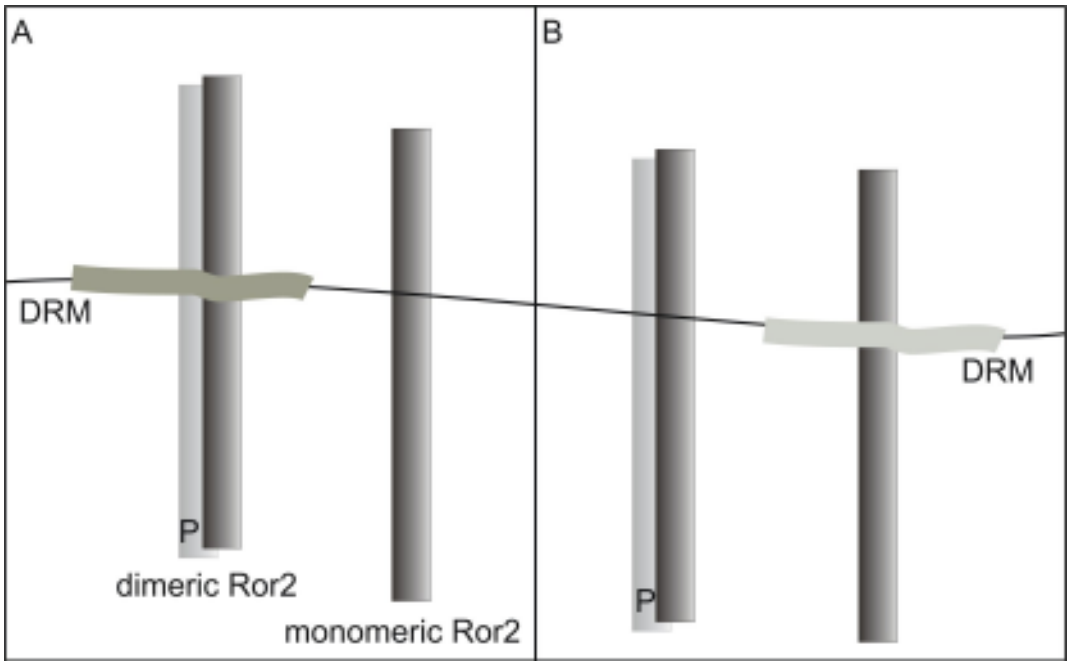

Figure 6.1 Potential plasma membrane distribution of monomeric and dimeric Ror2

Ror2 is found in all membrane regions, including detergent resistant microdomains (DRMs) and Ror2 is found to homodimerize and autophosphorylate in the absence of ligand.
A: Homodimers of Ror2 that are potentially autophosphorylated may form within DRMs, which may be similar to serine/threonine kinase receptors, while monomeric Ror2 may be found in non-DRM regions.
B: Based on data published for the EGF receptor, inactive receptor tyrosine kinases (RTKs) reside in DRMs and homodimerize and autophosphorylate upon ligand activation. Thus monomeric Ror2 may be located in DRMs and transfer to non-DRM membrane regions upon dimerization and autophosphorylation.

6.2 Evidence for ubiquitination of Ror2

In 2003 Murakami et al. published that BRIb interacts with Smurf1 via inhibitory Smads (I-Smads) 6 and 7, leading to ubiquitination of BRIb through Smurf1. BRIb is subsequently targeted for proteasome-dependent degradation which abrogates BMP signaling [86].

We speculated whether Ror2 might mediate inhibition of Smad signaling through induction of receptor degradation, thus ubiquitination of BMP receptors and Ror2 was examined. Figure 5.5 demonstrates ubiquitination of Ror2 (IP, WB anti-RGS-His, lane 7). However, no ubiquitination is seen for BRIb (IP, WB anti-RGS-His, lane 5). Although unexpected, these data indicate that Ror2 must be either highly ubiquitinated or less-rapidly degraded compared to BRIb. To detect ubiquitinated BRIb, Murakami et al. treated transiently transfected 293T cells with the proteasome inhibitor lactacystin for 24h prior to cell lysis and immunoprecipitation [86]. None such treatment is required to show ubiquitinated Ror2 in Cos7 cells.

What is even more striking is that ubiquitination of Ror2 can not be detected when the receptor is co-immunoprecipitated with BRIb (IP, WB anti-RGS-His, lane 8). Although considerably more protein is present when Ror2 is precipitated directly (IP, WB anti-Flag, compare lanes 7 and 8), the observed signal for Ror2 ubiquitination appears strong enough to expect at least a slight signal when Ror2 is co-immunoprecipitated with BRIb.

Several attempts to show interaction of BRIb with ubiquitinated Ror2 failed, while directly immunoprecipitated Ror2 always displayed solid ubiquitination, even in C2C12 cells stably expressing BRIb (data not shown). Ror2 interacting with BRIb may be protected from ubiquitination or ubiquitinated Ror2 does not interact with BRIb, possibly because it is situated in different membrane regions. Alternatively, the amount of ubiquitinated Ror2 interacting with BRIb may be too small to be detected in a Western blot.

The notion that BRIb may protect Ror2 from ubiquitination came from observations of Ror2 ΔCRD displaying much stronger ubiquitination signals than the wildtype receptor (Figure 5.7 and further data not shown). Ror2 ΔCRD does not immunoprecipitate with BRIb [165].

However, these data must be treated cautiously as there are other possible explanations. For example the receptor complex of ubiquitinated Ror2 with BRIb could be rapidly degraded. Moreover, Ror2 ΔCRD represents an artificial mutant in which a great portion of the extracellular domain is lacking. It may thus be susceptible to malfolding and frequently fail the quality control within the endoplasmatic reticulum. Subsequently it may undergo ubiquitination and endoplasmatic reticulum associated degradation, which would explain its stronger ubiquitination compared to the wildtype.

Among BRIb [165], there are several other proteins interacting with Ror2 through its CRD domain, such as Wnt1 [186], Wnt3 [186], Frizzled2 receptor and Wnt5a [164]. The impact of these proteins on Ror2 ubiquitination remains to be examined.

The Ror2 construct used in the initial experiment showing Ror2 ubiquitination carries a C-terminal Flag tag. The Flag tag contains two lysine residues and it is an acidic tag. Ubiquitination occurs almost exclusively on lysine residues, where an isopeptide bond is created between a lysine on the target protein and the C-terminal glycine of ubiquitin. Previous studies have shown that in many plasma membrane proteins, acidic stretches are necessary for ubiquitination [239]. Another study suggests that the acidic stretch in the NF-κB1 precursor p105 may serve as binding site for its E3 ligase [240]. However, Flag-tagged proteins, especially Flag-tagged ubiquitin, are routinely used for these types of experiments. Although, Flag has not been reported to yield unspecific ubiquitination or give an unspecific RGS-His signal, the experiment was repeated using a Ror2 construct containing a C-terminal HA tag, as well as a ubiquitin construct containing a RGS-His tag (Figure 5.6). In this assay, HA-tagged Ror2 displayed the same ubiquitin bands as seen with Flag-tagged Ror2, which confirms that Ror2 ubiquitination is independent of its intracellular tag.

Overexpression of proteins is often criticized for yielding highly artificial results. Especially overexpression of ubiquitin may cause unwanted side effects, such as nonsense promotion of protein degradation [241]. Thus, experiments on endogenous proteins were carried out to show ubiquitination of Ror2.

In a “semi-endogenous” approach Ror2 and Ror2 ΔCRD were overexpressed and tested for ubiquitination with endogenous ubiquitin (Figure 5.7). Both the wildtype (IP anti-Flag, WB anti-Ubiquitin, lane 2) and the deletion mutant (IP anti-Flag, WB anti-Ubiquitin, lane 3) appeared to be ubiquitinated. Interestingly and as mentioned before, Ror2 ΔCRD displayed a much stronger signal than the wildtype receptor.
A vice versa approach in which endogenous Ror2 was precipitated in the presence of transiently overexpressed ubiquitin failed, as well as the approach based on endogenous protein alone (Figure 5.8). In both cases detection of ubiquitinated protein likely failed due to insufficient amounts of immunoprecipitated Ror2 protein.
As seen in Figure 5.8, our anti-Ror2 323/324 antibody precipitated detectable amounts of Ror2 from both C2C12 (WB anti-Ror2, lane 4) and Cos7 (WB anti-Ror2, lane 7) cells. However, even though several million cells were pooled for the lysate, the band remained rather faint. Consequently, an even fainter ubiquitin band than that seen in Figure 5.7 with the overexpressed receptor (WB anti-Ubiquitin, lane 2) may simply escape the detection capacity of a Western blot.
It must thus be concluded that the anti-Ror323/324 antibody does not immunoprecipitate sufficient amounts of the endogenous Ror2 to detect ubiquitination.

On the other hand, overexpression of a large and complex protein like Ror2 alone may trigger its ubiquitination, for example due to increased incidents of malfolded protein or intrinsic cellular feedback mechanisms that control expression levels of proteins. These rather potential scenarios highlight the artificial side effects of transient overexpression.
However, even if overexpression of Ror2 dramatically pushed its ubiquitination, it would still appear to be an event specific for Ror2, since no ubiquitination was seen for other overexpressed receptors. Under the same experimental conditions, neither BRIb nor BRII (Figure 5.5, IP, WB anti-RGS-His, lanes 5 and 6, respectively), not even in co-expression with Ror2 (IP, WB anti-RGS-His, lane 8) or when BRIb and BRII were co-expressed (IP, WB anti-RGS-His, lane 9), showed any signs of ubiquitination. Besides, protein degradation does not appear to be the motif for Ror2 ubiquitination since protein levels in the lysates never indicated receptor degradation upon co-expression of ubiquitin (Figure 5.5, lysate, WB anti-Flag, compare lanes 4, 7 and 8). Hence, ubiquitination of Ror2 does not appear to serve as a cellular mechanism to rapidly reject overexpressed protein. In any case, these data suggest that specific mechanisms are in place to ubiquitinate Ror2. Nevertheless, these mechanisms may be pronounced in response to overexpression of Ror2, in combination with its high homodimerization and subsequent autophosphorylation capacity.

When examining ubiquitination of Ror2, co-expression of Ror2 with ubiquitin yielded very strong high molecular weight bands in the Western blot detecting ubiquitinated protein (anti-

Ubiquitin or anti-RGS-His). However, the Western blot detecting Ror2 (anti-Flag or anti-HA) usually only yielded a single band representing the tagged receptor. The tag antibody did never recognize the high molecular weight bands that represented ubiquitinated protein (e.g. Figure 5.10, Figure 5.11 and Figure 5.12). Although a smear of lower molecular weight bands below the band representing the receptor could be seen in some experiments, it was usually present to a similar extend also in the absence of overexpressed ubiquitin and to a lesser extend in the absence of Ror2 and ubiquitin alltogether, which suggests the presence of unspecific bands or routinely degraded forms of the receptor (e.g. Figure 5.6 and Figure 5.7). Besides, Ror2 expression levels in the lysates remained largely unimpressed by ubiquitin co-expression in all experiments, even though the receptor appeared highly ubiquitinated (e.g. Figure 5.5 and Figure 5.12). These observations raised several questions.

To verify whether the ubiquitinated protein seen in the Western blots anti-RGS-His or anti-ubiquitin was indeed Ror2, immunoprecipitates were separated on a SDS gel and the gel was stained with Coomassie-G to visualize the high molecular ubiquitin bands seen with immunoprecipitated Ror2 in the Western blot anti-RGS-His. These bands appeared very prominent in the Western blot, yet it turned out to be very difficult to detect them in the Coomassie-G-stained gel, although up to four times the amount of material was pooled for this purpose. What could be detected was merely a single clearly visible band that appeared only in the presence of ubiquitin. This band and another band migrating at the expected molecular weight of Ror2 were identified as Ror2 using MALDI mass spectrometry. However, the nature of the modification of the upper band could not be revealed. It is well appreciated that Ror2 is constitutively N-glycosylated [194, 197] and the upper band seen in the Coomassie gel could represent a further glycosylated or otherwise modified Ror2, but not necessarily ubiquitinated Ror2. Hence the findings of this experiment remain vague.
Coomassie-G staining was recommended by Christoph Weise, who performed the mass spectrometry. Apparently silver staining complicates the procedure, while not yielding a considerably improved staining result. Nevertheless, the experiment must be repeated with a more sensitive staining method, for example using a more sensitive Coomassie or applying silver staining after all. Furthermore, future experiments must include the control of ubiquitin immunoprecipitated with anti-Flag antibody in the absence of Ror2 to exclude unspecific bands. Under these circumstances it might be possible to detect the high molecular weight bands and to specifically identify the ubiquitinated protein. These experiments are ongoing.

In the event that ubiquitination of Ror2 led to degradation of the receptor, it would have been expected to see a smear of the ubiquitinated protein compared to a distinct band of the non-ubiquitinated protein. However, no smear of Flag- or HA-tagged protein was ever detected specifically in the presence of overexpressed ubiquitin. This of course may be due to the

nature of the HA- or Flag-tag Ror2 is carrying. In both cases the tag is situated at the C-terminal end of the receptor. Degradation of the receptor may be initated at its C-terminus, immediately digesting the tag and thus withdrawing the receptor from anti-tag antibody detection. However, partly digested receptor should still be detectable using the anti-Ror2 antibody, which has never been tried but should be considered in the future. As mentioned previously, it never seemed as if ubiquitination had a primary impact on Ror2 degradation because overexpression of ubiquitin never caused a significant decrease in Ror2 expression levels. On the other hand, there may only be a small portion of Ror2 that is degraded in response to ubiquitination. Additionally, Western blots were never done in a quantitative manner and hence these potential and possibly marginal differences escape a proper recognition.

6.3 Nature of Ror2 ubiquitination

Ror2 contains over 20 lysines in its intracellular part. To narrow down potential sites for ubiquitination, several Ror2 truncations were probed for potential ubiquitination. Figure 5.10 demonstrates that all applied truncations appear to be ubiquitinated. The shortest truncation, Ror2 Δ469, contains five intracellular lysines, i.e. five potential sites for ubiquitination. The ubiquitin ladder seen for Ror2 Δ469 in Figure 5.10 shows a specific signal up to around 85kDa. Although there are further bands above that, these are also seen in other lanes and in the absence of ubiquitin. Ror2 Δ469 has a molecular weight of around 60kDa. The molecular mass of ubiquitin is around 8.5kDa. Hence a difference of 30-40kDa could be attributed to either short polyubiquitin chains or monoubiquitination of the receptor on several lysines, i.e. multiubiquitination. A polyubiquitin chain of as little as four Ubiquitins is sufficient for recognition and targeting to proteasom-dependent degradation [242] and rapid degradation of freshly ubiquitinated Ror2 could prevent the formation of longer polyubiquitin chains. Thus no conclusion as to whether Ror2 is poly- or multiubiquitinated can be drawn from this experiment. However, at least one of the five membrane-proximal lysines appears to be ubiquitinated and this finding will be followed up by creating Ror2 mutants lacking these lysines. The location of lysines within the intracellular region of full length Ror2 is demonstrated in Figure 6.2.

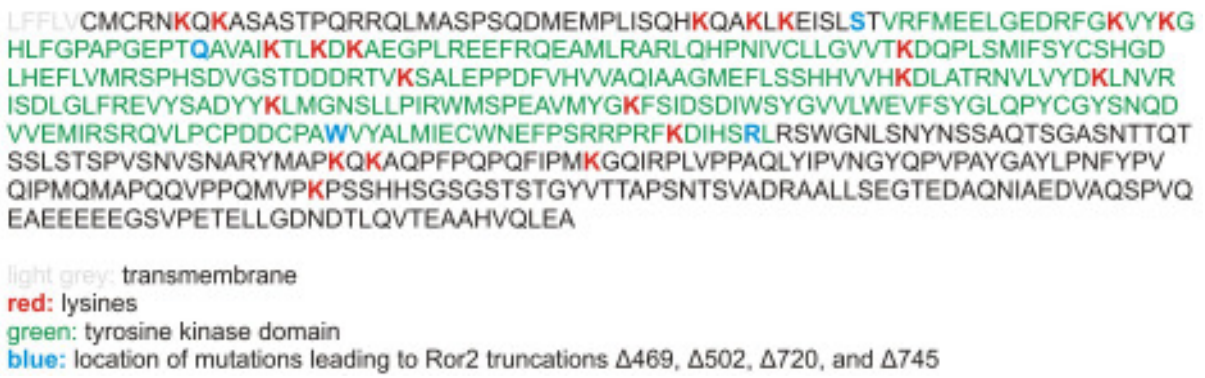

Figure 6.2 Amino acid sequence of intracellular portions of Ror2

Ror2 contains 21 intracellular lysine residues, marked in red. Five are located prior to the tyrosine kinase domain, marked in green and truncated in Ror2 Δ469. Two lysines follow within the next 20 amino acids and are present in the Ror2 truncation Δ502. There are nine more lysines in the truncation mutant Ror2 Δ720 and one additional lysine in Δ745. The C-termain tail region contains four lysine residues. Amino acids mutated in the Ror2 truncation mutants are marked in blue.
The sequence for mouse Ror2 was obtained from NCBI (NP_038874).

To reveal whether Ror2 is poly- or multiubiquitinated, an experiment was carried out using a mutant form of ubiquitin only capable of monoubiquitination. In this ubiquitin mutant all seven lysines were mutated to arginine (Ubiquitin K7). Figure 5.11 shows that Ror2 must be multiubiquitinated as the high molecular weight bands detected in all other experiments persist upon co-expression of Ubiquitin K7 (IP anti-HA and IP anti-Flag, WB anti-Flag, lanes 6 and 7, respectively).
Interestingly, the IP anti-Flag, i.e. precipitating Flag-tagged ubiquitin, shows very prominent bands below 55kDa in the Western Blot anti-HA, i.e. detecting HA-tagged Ror2. Only very weak bands can be seen for the full length receptor (IP anti-Flag, WB anti-HA, lane 7). This suggests degradation of ubiquitin-associated Ror2. While the amount of precipitated Ror2 appears equal (IP anti-HA, WB anti-HA, lanes 2 and 6), the expression levels seen in the lysates may be slightly reduced (lysates, WB anti-HA, lanes 2, 6 and 7). The degradation bands were never seen for co-expression with RGS-His tagged wildtype Ubiquitin and the Flag-tagged Ror2 (not shown), and were also not observed when the receptor, rather than Ubiquitin, was immunoprecipitated directly (IP anti-HA, WB anti-HA, lane 6). These data further suggest that the majority of Ror2 is not degraded, but that a small portion of the receptor is heavily multiubiquitinated and subsequently degraded very rapidly.

In many cases receptor internalization is required for the initiation of downstream signaling events. Mono- or multiubiquitination typically leads to internalization via clathrin-coated pits and usually has a critical role in progression of downstream signaling events, rather than merely leading to protein degradation. Receptors internalized via clathrin-coated pits progress into early and late endosomes from where they may be recycled back to the plasma membrane or degraded in a lysosome-dependent manner within multivesicular bodies [243]. The prototype receptor tyrosine kinase, the EGF receptor, undergoes ligand-induced mono-

or multiubiquitinated by the ubiquitin E3 ligase Cbl. The EGF receptor is subsequently internalized via clathrin-coated pits and takes the recycling or degradation route described above [244]. Several other RTKs are ubiquitinated and internalized via the same mechanisms as has been shown for the hepatocyte growth factor receptor (c-Met), platelet-derived growth ractor receptor and c-kit [245, 246]. Hence this route appears to be typical for receptor tyrosine kinases.

For this study, several approaches were undertaken to reveal the internalization mode of ubiquitinated Ror2. Figure 5.12 demonstrates that ubiquitinated Ror2 accumulates upon inhibition of the proteasome using the inhibitor MG132 (IP anti-Flag, WB anti-RGS-His, lane 8). Chlorpromazin on the other hand, an inhibitor of clathrin-coated pit formation, had no effect (IP anti-Flag, WB anti-RGS-His, lane 9) as seen in three different experiments. Likewise, inhibition of the lysosome with Chloroquine treatment had no effect on Ror2 ubiquitination or protein levels (not shown). Experiments in which cholesterol was depeleted to inhibit formation of detergent-resistant microdomains using MβCD were not conclusive (not shown) and must be repeated. Interestingly, proteasome inhibition does not lead to accumulation of total Ror2 protein, as protein levels appear to remain stable regardless of an inhibition. As discussed previously however, this may be due to the non quantitative manner in which these experiments were carried out on the one hand, and on the potentially small fraction of Ror2 protein undergoing degradation on the other.
Based on these findings Ror2 appears to take a different route from most other receptor tyrosine kinases. It should be kept in mind though that the proteasome inhibitor MG132 also inhibits lysosomal degradation which could be shown in the case of the EGF receptor [247]. Although the specific lysosome inhibitor Chloroquine had no effect, the compound used for this study didn't result in an accumulation of ubiquitinated protein visible as ubiquitin ladder in a Western blot anti-Ubiquitin. In contrast, a nice ubiquitin ladder could be observed upon treatment of Cos7 cells with MG132 (Figure 4.11, WB anti-Ubiquitin, compare lanes 1 to 3, lanes 4 to 6, lanes 7 to 9, and lanes 10 to 12). Possibly the compound was not used in sufficient amounts or it degenerated and needs to be replaced.

Based on the observation that Ror2 exhibits an even distribution across the plasma membrane independent of BRIb, which is predominantly found in detergent resistant microdomains (DRMs; Figure 4.6), the distribution of ubiquitinated Ror2 across the plasma membrane was examined. Figure 5.13 confirms Ror2 membrane distribution and shows that Ror2 ΔCRD which no longer interacts with BRIb exhibits the same membrane distribution as the wildtype. Interestingly, it appears that ubiquitinated protein accumulates in DRMs in the presence of both wildtypic Ror2 and Ror2 ΔCRD. Since in this assay total cell lysates are examined no conclusion can be drawn as to whether the ubiquitinated protein seen in the

DRM fraction represents ubiquitinated Ror2. Nevertheless, the observation that overexpression of Ror2 leads to a significant increase of ubiquitinated protein in DRMs is intriguing. Unfortunately, an attempt to immunoprecipitate ubiquitinated Ror2 from either caveolin-positive DRM or caveolin-negative membrane fractions failed due to the nature of the lysates containing high amounts of iodixanol. Nevertheless, an immunoprecipitation should be repeated following removal of iodixanol.

Besides studying the ubiquitination and internalization mode of Ror2, it was attempted to identify the E3 ubiquitin ligase responsible for the ubiquitination of Ror2. We considered Smurf1 a prime candidate since it promotes degradation of both R-Smads and BRIb, which would be in line with the inhibitory effect Ror2 has on BRIb-mediated Smad signaling [80, 86, 90, 165].

For this study Flag-tagged wildtype and dominant negative Smurf1 were obtained and an immunoprecipitation anti-Ror2 revealed co-immunoprecipitation of both Smurf1 WT and Smurf1 DN with Ror2 (Figure 5.14, IP anti-Ror2, Wb anti-Flag, lanes 5 and 6). However, both Smurf1 variants were also co-immunoprecipitated in probes where Ror2 was not overexpressed (Figure 5.14, IP anti-Ror2, WN anti-Flag, lanes 3 and 4). As outlined previously the anti-Ror2 323/324 antibody is capable of precipitating endogenous protein and thus may have co-precipitated Smurf1. Unfortunately, the sepharose control confirming specific, antibody-dependent interaction of Smurf1 with endogenous Ror2 was lacking.

Hence it was attempted to confirm the interaction in a second approach using differentially tagged proteins, i.e. Flag-tagged Smurf1 DN and HA-tagged Ror2. Figure 5.15 demonstrates specific interaction of Smurf1 DN with Ror2 (IP anti-HA, WB anti-Flag, lane 5). Interaction with Smurf1 WT could not be confirmed at this point as the construct yields very weak expression levels.

The interaction with Smurf1 does not prove that Smurf1 ubiquitinates Ror2. With Ror2 being involved in so many signal cascades, there may be other ubiquitin E3 ligases and several mechanisms through which Ror2 is ubiquitinated for various purposes. At this point no studies have been published examining the role of ubiquitination in regards to Ror2 signaling. Ror2 exhibits ubiquitination on membrane-proximal lysines in truncations lacking the tyrosine kinase domain and the C-terminal microdomains. Nevertheless, full length Ror2 may attract E3 ligases via SH2 or SH3 containing adaptor proteins when it is phosphorylated. This was shown for the EGF receptor, where Grb2 binds to phosphorylated tyrosine residues and mediates ubiquitination of the EGF receptor through the E3 ligase Cbl [212]. However, in regards to Ror2 these notions are highly speculative and lack experimental evidence.

Future research will be required to show whether Smurf1 ubiquitinates Ror2. This could be achieved by inhibiting Smurf1-mediated ubiquitination, by knocking down endogenous

Smurf1 or by competing for endogenous Smurf1 with overexpressed dominant negative Smurf1 (Smurf1 DN).

6.4 Potential impact of Ror2 interaction with Smurf1 on BMP signaling

The data outlined in this thesis may provide an interesting loop back to the initial findings that Ror2 inhibits BRIb-mediated Smad signaling. In fact they may shed a whole new light onto the inhibitory effect of Ror2 on Smad signaling. Although Ror2 directly interacts with BRIb [194], it has no effect on immediate Smad1/5/8 (subsequently termed Smad) phosphorylation, observed after short-term stimulation of C2C12-BRIb cells with ligand (Figure 4.9). Consequences of Ror2 inhibition only become evident after several hours, when downstream events such as the expression of Smad target genes (e.g. reporter genes) fail to appear. Thus it seems that immediate phosphorylation of Smads is not affected by Ror2, but the mid and long-term fate of phosphorylated Smads in the presence of Ror2 was never studied. It remains to be seen whether Smads can translocate into the nucleus under the inhibitory influence of Ror2. Another scenario could be that Ror2 serves as a shuttle, directing Smurf1 to BRIb, resulting in ubiquitination and degradation of a great portion of phosphorylated Smads. Furthermore, Ror2 may inhibit receptor internalization into early endosomes, which is required for phosphorylated Smads to dissociate from the receptor and subsequently translocate into the nucleus [73]. In this event mono- or multiubiquitination of Ror2 may be required to guide it into the right membrane regions. Furthermore we could show that interaction of Ror2 with BRIb most likely depends on DRMs as the receptor complex is susceptible to treatment with SDS, a detergent that is capable of dissolving DRMs [194]. Another study shows that the BMP type II receptor (BRII) which is required in the signaling ligand-receptor complex for activation of BRIb, is delivered to the plasma membrane in a caveolin1-dependent manner and that this event is required for the onset of BMP-dependent Smad signaling [74]. Like Ror2, BRII shows an even distribution across the plasma membrane [73], but Ror2 was never shown to directly interact with BRII [194]. In any case, the receptor complex of BRIb and BRII may be assembled in the same membrane regions where Ror2 and BRIb form a complex, hence offering the possibility that Ror2 is assembled into the preformed complex of BRI and BRII through its interaction with BRI.

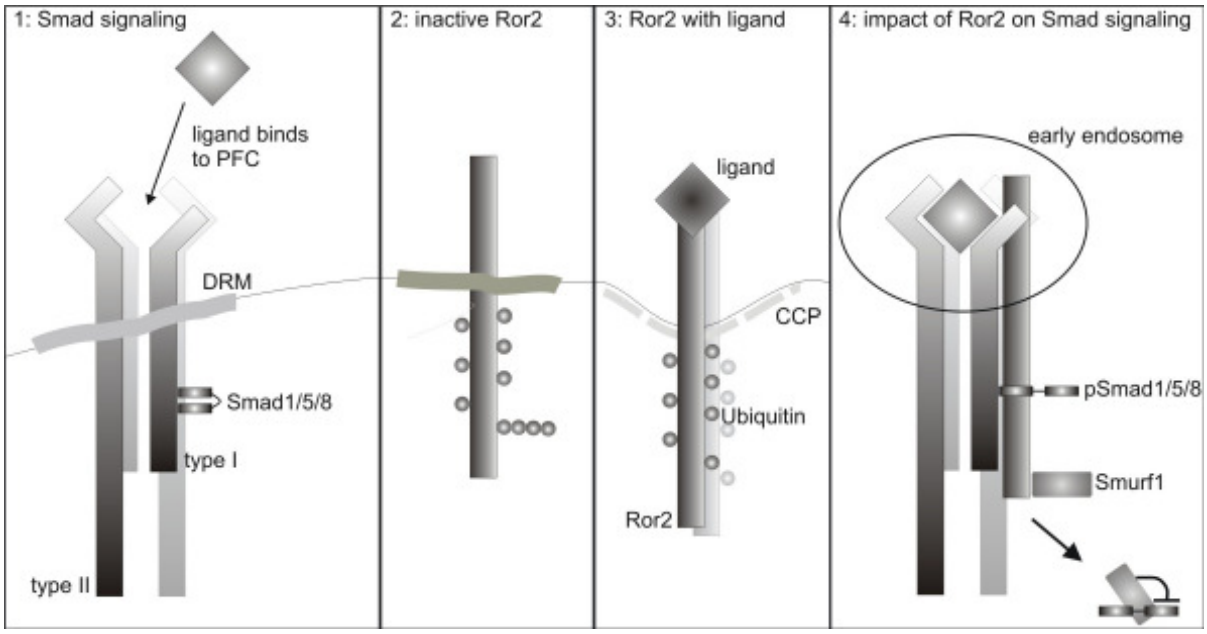

Figure 6.3 Impact of Ror2 on Smad signaling

1: The type I receptor (BRIb) is predominantly located within detergent-resistant microdomains (DRMs). The type II receptor (BRII) is delivered to the membrane in a caveolin-dependent manner. Nonphosphorylated Smads are attached to the type I receptor. This hypothesis assumes that the preformed complex (PFC) of BRI and BRII forms within DRMs. Binding of the ligand (BMP2 or GDF5) to the PFC initiates Smad signaling.
2: For this hypothesis we assume that inactive, monomeric Ror2 sits in DRMs, where it is possibly ubiquitinated and degraded via the proteasome-dependent pathway. It may also interact with Smurf1.
3: Upon ligand (Wnt5a) stimulation Ror2 dimerizes and this model proposes that it translocates into clathrin-coated pits (CCP) from where further downstream signaling is initiated, possibly depending on Ror2 mono- or multiubiquitination.
4: The hypothesis of this model is that the Ror2/BRIb complex forms in DRMs, inhibiting downstream Ror2 signaling. However, this interaction does not disturb formation of the PFC as Ror2 does not inhibit immediate Smad phosphorylation. The model further proposes that Ror2 is drawn to early endosomes along with the ligand-activated PFC. Further down this route, phosphorylated Smad1 may receive an inhibitory linker phosphorylation via the MAPK pathway, which enables interaction of Smurf1 with Smad1. Ror2 may act as an adaptor, guiding Smurf1 to phosphorylated Smads in the respective cellular compartments, an act that may protect itself from ubiquitination. On the other hand the receptors may be degraded following internalization to early endosomes, as has been shown in this thesis for stably expressed BRIb in response to GDF5 stimulation.

What this model lacks is the notion that BRIb protects Ror2 from ubiquitination. This idea was based on data showing that ubiquitinated Ror2 could never be co-precipitated with BRIb, which was attempted to be shown several times in different cell lines. Also co-expression of Ror2 with BRIb in stable C2C12-BRIb cells never resulted in decreased BRIb protein expression levels, and vice versa co-expression of BRIb with Ror2 in C2C12 or Cos7 cells had no impact on expression levels of Ror2 (not shown). As has been mentioned several times earlier on, there may only be a small fraction of ubiquitinated Ror2 that undergoes degradation, and in the overexpression system this amount may escape quantitative detection. Besides, Ror2 does not have an absolute inhibitory effect on Smad signaling, since the most we could show was an inhibition of 50% (Figure 4.13), which is in line with observations that a great portion of cell surface expressed Ror2 is engaged in homodimers and may thus not be available for interaction with BRIb. Hence, it may be suspected that

Ror2 and BRIb undergo ligand-induced degradation and that BRIb does not protect Ror2 from ubiquitination, but rather leads to its subsequent degradation. In my Diploma thesis I could show that Ror2 and BRIb co-localize at the plasma membrane and are internalized more rapidly in the presence of a GDF5 stimulus (unpublished data). Furthermore, several scenarios can be imagined in which Ror2-mediated signaling events are shut down, for example degradation of Ror2 or Ror2 being captured in a complex with BRI and BRII or Ror2 being guided into certain membrane compartments. Co-expression of Ror2 and BRIb inhibits chondrogenic differentiation in ATDC5 cells, which could be shown in our lab [165].

7 Summary

The Regeneron orphan receptor 2 (Ror2) is a receptor tyrosine kinase (RTK). Since it was first described in 1992, Ror2 was found to adopt a critical role in many processes during embryogenesis and in the adult organism, including skeletal and neuronal development, cell polarity, and cell movement. In recent years Ror2 has emerged as a key player in Wnt signaling, but it was also described to have an impact on bone morphogenetic protein (BMP) signaling.

The BMP family of growth factors signals through two types of transmembrane serine/threonine kinase receptors, the BMP type I receptor (BRI, i.e. BRIa or BRIb) and the BMP type II receptor (BRII). Binding of the ligand to heteromeric preformed complexes (PFC) of BRI and BRII activates Smad signaling, while binding of the ligand to its high affinity type I receptor, followed by recruitment of the type II receptor (BMP-induced signaling complex, BISC) activates MAPK pathways. The high affinity ligand for BRIb is growth and differentiation factor 5 (GDF5).

Ror2 interacts with BRIb and inhibits GDF5-mediated Smad signaling. How this inhibition is achieved remains poorly understood. However, the Ror2/BRIb receptor complex is susceptible to treatment with SDS and Ror2 co-localizes with BRIb in detergent-resistant microdomains (DRMs), indicating that the complex may form in these membrane regions.

RTKs such as the epidermal growth factor (EGF) receptor have been shown to dimerize and autophosphorylate upon ligand stimulation. In the inactive state the EGF receptor sits in DRMs. Upon activation through binding of the ligand the receptor transfers into clathrin-coated pits. Progression of signaling depends on receptor internalization to early endosomes. The internalization step may require ubiquitination.

Ubiquitination is a post-translational modification mediated through specific ubiquitin ligases. E3 ligases are required for substrate-specific ubiquitination. The E3 ligase Smad ubiquitin regulated factor 1 (Smurf1) was described to inhibit BMP Smad signaling by ubiquitinating Smad1 and thereby targeting it for proteasome-dependent degradation.

This thesis demonstrates that Ror2 is constitutively homodimerized to a large extent in the absence of external ligand stimulation and that Ror2 dimerization depends on its C-terminal tail region. Furthermore, Ror2 exhibits high tyrosine autophosphorylation capacity. These data confirm that Ror2 has characteristics of classic tyrosine kinases. Moreover, Ror2 is ubiquitinated on multiple lysines, including one or more of its five membrane-proximal lysines. Ror2 is evenly distributed across the plasma membrane and is also found in DRMs. In the presence of Ror2 an accumulation of ubiquitinated protein in DRMs could be observed, suggesting that DRM-associated Ror2 may be ubiquitinated. Data introduced in the present thesis demonstrate that the E3 ligase Smurf1 interacts with Ror2. Since immediate Smad phosphorylation is not altered in the presence of Ror2, the interaction of Ror2 with Smurf1 may possibly account for the inhibitory effect of Ror2 on Smad signaling. Future studies must reveal whether Ror2 is ubiquitinated by Smurf1 and whether the interaction of Ror2 with Smurf1 mediates ubiquitination and degradation of Smads through Smurf1, and based on which mechanisms this effect is achieved.

8 Zusammenfassung

Der Regeneron orphan receptor 2 (Ror2) ist eine Rezeptor Tyrosin Kinase (RTK). Seit Ror2 im Jahr 1992 zum ersten Mal beschrieben wurde, ist klar geworden, welch zentrale Rolle Ror2 in vielen Prozessen während der Embryogenese und im adulten Organismus einnimmt. Dazu gehören seketale und neuronale Entwicklung, Zellpolarität und Zellbewegung. Zuletzt hat sich Ror2 als Schlüsselfigur in der Wnt Signalgebung herausgestellt, aber Ror2 hat auch einen Einfluss auf den bone morphogenetic protein (BMP) Signalweg.

Die BMP Familie von Wachstumsfaktoren leitet Signale über zwei Typen von transmembranen Serin/Threonin Kinasen weiter, den BMP Typ I Rezeptor (BRI, d.h. BRIa oder BRIb) und den BMP Typ II Rezeptor (BRII). Bindet der Ligand einen heteromeren präformierten Komplex (PFC) von BRI und BRII, so wird die Smad Signalkaskade aktiviert, während Binden an den hoch affinen BRI, gefolgt von Rekrutieren des BRII zur Aktivierung von MAPK Signalwegen führt. Der hoch affine Ligand für BRIb ist growth and differentiation factor 5 (GDF5).

Ror2 interagiert mit BRIb und inhibiert GDF5-vermittelte Smad Signalgebung. Wie diese Inhibierung erreicht wird ist weiterhin unklar. Der Ror/BRIb Rezeptorkomplex ist jedoch empfindlich gegenüber Behandlung mit SDS und Ror2 co-lokalisiert mit BRIb in Detergenz-resistenten Mikrodomänen (DRMs). Diese Daten deuten an, dass der Rezeptorkomplex möglicherweise in diesen Membranregionen gebildet wird.

Für RTKs, wie zum Beispiel den epidermal growth factor (EGF) Rezeptor, ist bekannt, dass sie nach Bindung des Liganden dimerisieren und autophosphorylieren. Im inaktiven Zustand verweilt der EGF Rezeptor in DRMs. Nach Stimulation mit dem Liganden wandert der Rezeptor in clathrin-coated pits. Der weitere Verlauf des Signalwegs hängt von der Internalisierung des Rezeptors in frühe Endosomen ab. Dieser Schritt beruht möglicherweise auf Ubiquitinierung des Rezeptors.

Ubiquitinierung ist eine post-translationale Modifikation, welche durch spezifische Ubiquitin.igasen vermittelt wird. E3 Ligasen werden für die Substraterkennung und spezifische Ubiquitinierung benötigt. Die E3 Ligase Smad ubiquitin regulated factor 1 (Smurf1) inhibiert den BMP Smad Signalweg, indem sie Smad1 ubiquitiniert und es somit der Proteasom-abhängigen Degradation zuführt.

Die vorliegende Arbeit zeigt, dass ein Großteil von Ror2 in konstitutiv dimerisierter Form vorliegt und zwar unabhängig von externer Ligandenstimulation. Weiterhin wird für die Dimerisierung die C-terminale Schwanzregion von Ror2 benötigt. Diese Daten bestätigen, dass Ror2 Merkmale von klassischen Tyrosin Kinasen besitzt. Zudem ist Ror2 an mehreren Lysinen ubiquitiniert, einschließlich einem oder mehrerer seiner fünf membranproximalen Lysine. Ror2 weist eine gleichmäßige Verteilung über die Plasmamembran auf, wobei es auch in DRMs vorliegt. In Anwesenheit von Ror2 wurde eine Akkumulierung von ubiquitiniertem Protein in DRMs beobachtet, was darauf hinweist, dass DRM-assoziiertes Ror2 ubiquitiniert sein könnte. Weitere Daten aus dieser Arbeit zeigen, das Ror2 mit Smurf1 interagiert. Da die direkte Phosohorylierung von Smads im Beisein von Ror2 nicht gestört ist, besteht die Möglichkeit, dass die Interaktion von Ror2 mit Smurf1 für die inhibierende Wirkung von Ror2 auf die Smad Signalkaskade verantwortlich ist. Weitere Studien müssen aufdecken, ob Ror2 durch Smurf1 ubiquitiniert wird und ob die Interaktion von Ror2 mit Smurf1 die Ubiquitinierung von Smads via Smurf1 vermittelt und wie genau dieser Mechanismus abläuft.

9 Side project

9.1 Monomeric and dimeric GDF-5 show equal type I receptor binding and oligomerization capability and have the same biological activity [7]

Growth and differentiation factor 5 (GDF-5) is a homodimeric protein stabilized by a single disulfide bridge between cysteine 465 in the respective monomers, as well as by three intramolecular cysteine bridges within each subunit. A mature recombinant human GDF-5 variant with cysteine 465 replaced by alanine (rhGDF-5 C465A) was expressed in E. coli, purified to homogeneity, and chemically renatured. Biochemical analysis showed that this procedure eliminated the sole interchain disulfide bond. Surprisingly, the monomeric variant of rhGDF-5 is as potent in vitro as the dimeric form. This could be confirmed by alkaline phosphatase assays and Smad reporter gene activation. Furthermore, dimeric and monomeric rhGDF-5 show comparable binding to their specific type I receptor BRIb. Studies on living cells showed that both the dimeric and monomeric rhGDF-5 induce homomeric BRIb and heteromeric BRIb/BRII oligomers. Our results suggest that rhGDF-5 C465A has the same biological activity as rhGDF-5 with respect to binding to, oligomerization of and signaling through the BMP receptor type Ib.

10 References

[1] S. Shimasaki, R.K. Moore, F. Otsuka, and G.F. Erickson, The bone morphogenetic protein system in mammalian reproduction, Endocr Rev 25 (2004) 72-101.

[2] S.S. Molloy, P.A. Bresnahan, S.H. Leppla, K.R. Klimpel, and G. Thomas, Human furin is a calcium-dependent serine endoprotease that recognizes the sequence Arg-X-X-Arg and efficiently cleaves anthrax toxin protective antigen, J Biol Chem 267 (1992) 16396-402.

[3] M.P. SchluneggerM.G. Grutter, An unusual feature revealed by the crystal structure at 2.2 A resolution of human transforming growth factor-beta 2, Nature 358 (1992) 430-4.

[4] D.M. Kingsley, The TGF-beta superfamily: new members, new receptors, and new genetic tests of function in different organisms, Genes Dev 8 (1994) 133-46.

[5] A.C. McPherronS.J. Lee, GDF-3 and GDF-9: two new members of the transforming growth factor-beta superfamily containing a novel pattern of cysteines, J Biol Chem 268 (1993) 3444-9.

[6] W.X. Liao, R.K. Moore, F. Otsuka, and S. Shimasaki, Effect of intracellular interactions on the processing and secretion of bone morphogenetic protein-15 (BMP-15) and growth and differentiation factor-9. Implication of the aberrant ovarian phenotype of BMP-15 mutant sheep, J Biol Chem 278 (2003) 3713-9.

[7] C. Sieber, F. Ploger, R. Schwappacher, R. Bechtold, M. Hanke, S. Kawai, Y. Muraki, M. Katsuura, M. Kimura, M.M. Rechtman, Y.I. Henis, J. Pohl, and P. Knaus, Monomeric and dimeric GDF-5 show equal type I receptor binding and oligomerization capability and have the same biological activity, Biol Chem 387 (2006) 451-60.

[8] D.I. Israel, J. Nove, K.M. Kerns, R.J. Kaufman, V. Rosen, K.A. Cox, and J.M. Wozney, Heterodimeric bone morphogenetic proteins show enhanced activity in vitro and in vivo, Growth Factors 13 (1996) 291-300.

[9] C. Scheufler, W. Sebald, and M. Hulsmeyer, Crystal structure of human bone morphogenetic protein-2 at 2.7 A resolution, J Mol Biol 287 (1999) 103-15.

[10] D.L. Griffith, P.C. Keck, T.K. Sampath, D.C. Rueger, and W.D. Carlson, Three-dimensional structure of recombinant human osteogenic protein 1: structural paradigm for the transforming growth factor beta superfamily, Proc Natl Acad Sci U S A 93 (1996) 878-83.

[11] J. Greenwald, J. Groppe, P. Gray, E. Wiater, W. Kwiatkowski, W. Vale, and S. Choe, The BMP7/ActRII extracellular domain complex provides new insights into the cooperative nature of receptor assembly, Mol Cell 11 (2003) 605-17.

[12] M.A. Brown, Q. Zhao, K.A. Baker, C. Naik, C. Chen, L. Pukac, M. Singh, T. Tsareva, Y. Parice, A. Mahoney, V. Roschke, I. Sanyal, and S. Choe, Crystal structure of BMP-9 and functional interactions with pro-region and receptors, J Biol Chem 280 (2005) 25111-8.

[13] H. Schreuder, A. Liesum, J. Pohl, M. Kruse, and M. Koyama, Crystal structure of recombinant human growth and differentiation factor 5: evidence for interaction of the type I and type II receptor-binding sites, Biochem Biophys Res Commun 329 (2005) 1076-86.

[14] S.J. Lin, T.F. Lerch, R.W. Cook, T.S. Jardetzky, and T.K. Woodruff, The structural basis of TGF-beta, bone morphogenetic protein, and activin ligand binding, Reproduction 132 (2006) 179-90.

[15] K. Lehmann, P. Seemann, J. Boergermann, G. Morin, S. Reif, P. Knaus, and S. Mundlos, A novel R486Q mutation in BMPR1B resulting in either a brachydactyly type C/symphalangism-like phenotype or brachydactyly type A2, Eur J Hum Genet 14 (2006) 1248-1254.

[16] K.W. Kjaer, H. Eiberg, L. Hansen, C.B. van der Hagen, K. Rosendahl, N. Tommerup, and S. Mundlos, A mutation in the receptor binding site of GDF5 causes Mohr-Wriedt brachydactyly type A2, J Med Genet 43 (2006) 225-31.

[17] K. Lehmann, P. Seemann, S. Stricker, M. Sammar, B. Meyer, K. Suring, F. Majewski, S. Tinschert, K.H. Grzeschik, D. Muller, P. Knaus, P. Nurnberg, and S. Mundlos, Mutations in bone morphogenetic protein receptor 1B cause brachydactyly type A2, Proc Natl Acad Sci U S A 100 (2003) 12277-82.

[18] P. Seemann, R. Schwappacher, K.W. Kjaer, D. Krakow, K. Lehmann, K. Dawson, S. Stricker, J. Pohl, F. Ploger, E. Staub, J. Nickel, W. Sebald, P. Knaus, and S. Mundlos, Activating and deactivating mutations in the receptor interaction site of GDF5 cause symphalangism or brachydactyly type A2, J Clin Invest 115 (2005) 2373-81.

[19] H. ZhangA. Bradley, Mice deficient for BMP2 are nonviable and have defects in amnion/chorion and cardiac development, Development 122 (1996) 2977-86.

[20] G. Winnier, M. Blessing, P.A. Labosky, and B.L. Hogan, Bone morphogenetic protein-4 is required for mesoderm formation and patterning in the mouse, Genes Dev 9 (1995) 2105-16.

[21] G. Luo, C. Hofmann, A.L. Bronckers, M. Sohocki, A. Bradley, and G. Karsenty, BMP-7 is an inducer of nephrogenesis, and is also required for eye development and skeletal patterning, Genes Dev 9 (1995) 2808-20.

[22] A.T. Dudley, K.M. Lyons, and E.J. Robertson, A requirement for bone morphogenetic protein-7 during development of the mammalian kidney and eye, Genes Dev 9 (1995) 2795-807.

[23] U.A. Vitt, S.Y. Hsu, and A.J. Hsueh, Evolution and classification of cystine knot-containing hormones and related extracellular signaling molecules, Mol Endocrinol 15 (2001) 681-94.

[24] O. Avsian-KretchmerA.J. Hsueh, Comparative genomic analysis of the eight-membered ring cystine knot-containing bone morphogenetic protein antagonists, Mol Endocrinol 18 (2004) 1-12.

[25] L.B. Zimmerman, J.M. De Jesus-Escobar, and R.M. Harland, The Spemann organizer signal noggin binds and inactivates bone morphogenetic protein 4, Cell 86 (1996) 599-606.

[26] J. Groppe, J. Greenwald, E. Wiater, J. Rodriguez-Leon, A.N. Economides, W. Kwiatkowski, M. Affolter, W.W. Vale, J.C. Belmonte, and S. Choe, Structural basis of BMP signalling inhibition by the cystine knot protein Noggin, Nature 420 (2002) 636-42.

[27] C. Sieber, G.K. Schwaerzer, and P. Knaus, *Bone Morphogenetic Proteins: From Local to Systemic Therapeutics; article: BMP signaling is fine tuned on multiple levels*. hardcover ed. Progress in Inflammation Research, ed. S.S. Vukicevic, Kuber T. Vol. XI. 2008: Birkhäuser. 343.

[28] R.M. Anderson, A.R. Lawrence, R.W. Stottmann, D. Bachiller, and J. Klingensmith, Chordin and noggin promote organizing centers of forebrain development in the mouse, Development 129 (2002) 4975-87.

[29] W.C. SmithR.M. Harland, Expression cloning of noggin, a new dorsalizing factor localized to the Spemann organizer in Xenopus embryos, Cell 70 (1992) 829-40.

[30] M.S. Dionne, L.J. Brunet, P.M. Eimon, and R.M. Harland, Noggin is required for correct guidance of dorsal root ganglion axons, Dev Biol 251 (2002) 283-93.

[31] P. Aspenberg, C. Jeppsson, and A.N. Economides, The bone morphogenetic proteins antagonist Noggin inhibits membranous ossification, J Bone Miner Res 16 (2001) 497-500.

[32] D.C. Wan, J.H. Pomerantz, L.J. Brunet, J.B. Kim, Y.F. Chou, B.M. Wu, R. Harland, H.M. Blau, and M.T. Longaker, Noggin suppression enhances in vitro osteogenesis and accelerates in vivo bone formation, J Biol Chem (2007)

[33] L.J. Brunet, J.A. McMahon, A.P. McMahon, and R.M. Harland, Noggin, cartilage morphogenesis, and joint formation in the mammalian skeleton, Science 280 (1998) 1455-7.

[34] Y. Gong, D. Krakow, J. Marcelino, D. Wilkin, D. Chitayat, R. Babul-Hirji, L. Hudgins, C.W. Cremers, F.P. Cremers, H.G. Brunner, K. Reinker, D.L. Rimoin, D.H. Cohn, F.R. Goodman, W. Reardon, M. Patton, C.A. Francomano, and M.L. Warman, Heterozygous mutations in the gene encoding noggin affect human joint morphogenesis, Nat Genet 21 (1999) 302-4.

[35] J. Marcelino, C.M. Sciortino, M.F. Romero, L.M. Ulatowski, R.T. Ballock, A.N. Economides, P.M. Eimon, R.M. Harland, and M.L. Warman, Human disease-causing NOG missense mutations: effects on noggin secretion, dimer formation, and bone morphogenetic protein binding, Proc Natl Acad Sci U S A 98 (2001) 11353-8.

[36] K. Lehmann, P. Seemann, F. Silan, T.O. Goecke, S. Irgang, K.W. Kjaer, S. Kjaergaard, M.J. Mahoney, S. Morlot, C. Reissner, B. Kerr, A.O. Wilkie, and S. Mundlos, A New Subtype of Brachydactyly Type B Caused by Point Mutations in the Bone Morphogenetic Protein Antagonist NOGGIN, Am J Hum Genet 81 (2007) 388-96.

[37] M. Oldridge, A.M. Fortuna, M. Maringa, P. Propping, S. Mansour, C. Pollitt, T.M. DeChiara, R.B. Kimble, D.M. Valenzuela, G.D. Yancopoulos, and A.O. Wilkie, Dominant mutations in ROR2, encoding an orphan receptor tyrosine kinase, cause brachydactyly type B, Nat Genet 24 (2000) 275-8.

[38] J.A. McMahon, S. Takada, L.B. Zimmerman, C.M. Fan, R.M. Harland, and A.P. McMahon, Noggin-mediated antagonism of BMP signaling is required for growth and patterning of the neural tube and somite, Genes Dev 12 (1998) 1438-52.

[39] R.D. Devlin, Z. Du, R.C. Pereira, R.B. Kimble, A.N. Economides, V. Jorgetti, and E. Canalis, Skeletal overexpression of noggin results in osteopenia and reduced bone formation, Endocrinology 144 (2003) 1972-8.

[40] Y.G. Chen, A. Hata, R.S. Lo, D. Wotton, Y. Shi, N. Pavletich, and J. Massague, Determinants of specificity in TGF-beta signal transduction, Genes Dev 12 (1998) 2144-52.

[41] R.S. Lo, Y.G. Chen, Y. Shi, N.P. Pavletich, and J. Massague, The L3 loop: a structural motif determining specific interactions between SMAD proteins and TGF-beta receptors, Embo J 17 (1998) 996-1005.

[42] P. ten Dijke, H. Ichijo, P. Franzen, P. Schulz, J. Saras, H. Toyoshima, C.H. Heldin, and K. Miyazono, Activin receptor-like kinases: a novel subclass of cell-surface receptors with predicted serine/threonine kinase activity, Oncogene 8 (1993) 2879-87.

[43] P. ten Dijke, H. Yamashita, T.K. Sampath, A.H. Reddi, M. Estevez, D.L. Riddle, H. Ichijo, C.H. Heldin, and K. Miyazono, Identification of type I receptors for osteogenic protein-1 and bone morphogenetic protein-4, J Biol Chem 269 (1994) 16985-8.

[44] C.M. ZimmermanL.S. Mathews, Activin receptors: cellular signalling by receptor serine kinases, Biochem Soc Symp 62 (1996) 25-38.

[45] M. Kawabata, A. Chytil, and H.L. Moses, Cloning of a novel type II serine/threonine kinase receptor through interaction with the type I transforming growth factor-beta receptor, J Biol Chem 270 (1995) 5625-30.

[46] B.L. Rosenzweig, T. Imamura, T. Okadome, G.N. Cox, H. Yamashita, P. ten Dijke, C.H. Heldin, and K. Miyazono, Cloning and characterization of a human type II receptor for bone morphogenetic proteins, Proc Natl Acad Sci U S A 92 (1995) 7632-6.

[47] F. Liu, F. Ventura, J. Doody, and J. Massague, Human type II receptor for bone morphogenic proteins (BMPs): extension of the two-kinase receptor model to the BMPs, Mol Cell Biol 15 (1995) 3479-86.

[48] T. Nohno, T. Ishikawa, T. Saito, K. Hosokawa, S. Noji, D.H. Wolsing, and J.S. Rosenbaum, Identification of a human type II receptor for bone morphogenetic protein-4 that forms differential heteromeric complexes with bone morphogenetic protein type I receptors, J Biol Chem 270 (1995) 22522-6.

[49] S. Hassel, A. Eichner, M. Yakymovych, U. Hellman, P. Knaus, and S. Souchelnytskyi, Proteins associated with type II bone morphogenetic protein receptor (BMPR-II) and identified by two-dimensional gel electrophoresis and mass spectrometry, Proteomics 4 (2004) 1346-58.

[50] H. Zou, R. Wieser, J. Massague, and L. Niswander, Distinct roles of type I bone morphogenetic protein receptors in the formation and differentiation of cartilage, Genes Dev 11 (1997) 2191-203.

[51] J.R. Howe, J.L. Bair, M.G. Sayed, M.E. Anderson, F.A. Mitros, G.M. Petersen, V.E. Velculescu, G. Traverso, and B. Vogelstein, Germline mutations of the gene encoding bone morphogenetic protein receptor 1A in juvenile polyposis, Nat Genet 28 (2001) 184-7.

[52] A. Kotzsch, J. Nickel, A. Seher, K. Heinecke, L. van Geersdaele, T. Herrmann, W. Sebald, and T.D. Mueller, Structure analysis of bone morphogenetic protein-2 type I receptor complexes reveals a mechanism of receptor inactivation in juvenile polyposis syndrome, J Biol Chem 283 (2008) 5876-87.

[53] M.G. Sayed, A.F. Ahmed, J.R. Ringold, M.E. Anderson, J.L. Bair, F.A. Mitros, H.T. Lynch, S.T. Tinley, G.M. Petersen, F.M. Giardiello, B. Vogelstein, and J.R. Howe, Germline SMAD4 or BMPR1A mutations and phenotype of juvenile polyposis, Ann Surg Oncol 9 (2002) 901-6.

[54] A.S. Virdi, E.M. Shore, R.O. Oreffo, M. Li, J.M. Connor, R. Smith, F.S. Kaplan, and J.T. Triffitt, Phenotypic and molecular heterogeneity in fibrodysplasia ossificans progressiva, Calcif Tissue Int 65 (1999) 250-5.

[55] E.M. Shore, M. Xu, G.J. Feldman, D.A. Fenstermacher, T.J. Cho, I.H. Choi, J.M. Connor, P. Delai, D.L. Glaser, M. LeMerrer, R. Morhart, J.G. Rogers, R. Smith, J.T. Triffitt, J.A. Urtizberea, M. Zasloff, M.A. Brown, and F.S. Kaplan, A recurrent mutation in the BMP type I receptor ACVR1 causes inherited and sporadic fibrodysplasia ossificans progressiva, Nat Genet 38 (2006) 525-7.

[56] F.S. Kaplan, M. Xu, P. Seemann, J.M. Connor, D.L. Glaser, L. Carroll, P. Delai, E. Fastnacht-Urban, S.J. Forman, G. Gillessen-Kaesbach, J. Hoover-Fong, B. Koster, R.M. Pauli, W. Reardon, S.A. Zaidi, M. Zasloff, R. Morhart, S. Mundlos, J. Groppe, and E.M. Shore, Classic and atypical fibrodysplasia ossificans progressiva (FOP) phenotypes are caused by mutations in the bone morphogenetic protein (BMP) type I receptor ACVR1, Hum Mutat (2008)

[57] N.W. Morrell, Pulmonary hypertension due to BMPR2 mutation: a new paradigm for tissue remodeling? Proc Am Thorac Soc 3 (2006) 680-6.

[58] J. Yang, R.J. Davies, M. Southwood, L. Long, X. Yang, A. Sobolewski, P.D. Upton, R.C. Trembath, and N.W. Morrell, Mutations in bone morphogenetic protein type II receptor cause dysregulation of Id gene expression in pulmonary artery smooth muscle cells: implications for familial pulmonary arterial hypertension, Circ Res 102 (2008) 1212-21.

[59] V.C. Foletta, M.A. Lim, J. Soosairajah, A.P. Kelly, E.G. Stanley, M. Shannon, W. He, S. Das, J. Massague, and O. Bernard, Direct signaling by the BMP type II receptor via the cytoskeletal regulator LIMK1, J Cell Biol 162 (2003) 1089-98.

[60] D. Liu, J. Wang, B. Kinzel, M. Mueller, X. Mao, R. Valdez, Y. Liu, and E. Li, Dosage-dependent requirement of BMP type II receptor for maintenance of vascular integrity, Blood (2007)

[61] A. Zakrzewicz, M. Hecker, L.M. Marsh, G. Kwapiszewska, B. Nejman, L. Long, W. Seeger, R.T. Schermuly, N.W. Morrell, R.E. Morty, and O. Eickelberg, Receptor for activated C-kinase 1, a novel interaction partner of type II bone morphogenetic protein receptor, regulates smooth muscle cell proliferation in pulmonary arterial hypertension, Circulation 115 (2007) 2957-68.

[62] T. Kirsch, W. Sebald, and M.K. Dreyer, Crystal structure of the BMP-2-BRIA ectodomain complex, Nat Struct Biol 7 (2000) 492-6.

[63] T. Kirsch, J. Nickel, and W. Sebald, Isolation of recombinant BMP receptor IA ectodomain and its 2:1 complex with BMP-2, FEBS Lett 468 (2000) 215-9.

[64] G.P. Allendorph, W.W. Vale, and S. Choe, Structure of the ternary signaling complex of a TGF-beta superfamily member, Proc Natl Acad Sci U S A 103 (2006) 7643-8.

[65] D. Weber, A. Kotzsch, J. Nickel, S. Harth, A. Seher, U. Mueller, W. Sebald, and T.D. Mueller, A silent H-bond can be mutationally activated for high-affinity interaction of BMP-2 and activin type IIB receptor, BMC Struct Biol 7 (2007) 6.

[66] P.C. Gray, J. Greenwald, A.L. Blount, K.S. Kunitake, C.J. Donaldson, S. Choe, and W. Vale, Identification of a binding site on the type II activin receptor for activin and inhibin, J Biol Chem 275 (2000) 3206-12.

[67] J. Klages, A. Kotzsch, M. Coles, W. Sebald, J. Nickel, T. Muller, and H. Kessler, The solution structure of BMPR-IA reveals a local disorder-to-order transition upon BMP-2 binding, Biochemistry 47 (2008) 11930-9.

[68] P. KnausW. Sebald, Cooperativity of binding epitopes and receptor chains in the BMP/TGFbeta superfamily, Biol Chem 382 (2001) 1189-95.

[69] H. Mitchell, A. Choudhury, R.E. Pagano, and E.B. Leof, Ligand-dependent and -independent transforming growth factor-beta receptor recycling regulated by clathrin-mediated endocytosis and Rab11, Mol Biol Cell 15 (2004) 4166-78.

[70] G.M. Di Guglielmo, C. Le Roy, A.F. Goodfellow, and J.L. Wrana, Distinct endocytic pathways regulate TGF-beta receptor signalling and turnover, Nat Cell Biol 5 (2003) 410-21.

[71] L. Gilboa, A. Nohe, T. Geissendorfer, W. Sebald, Y.I. Henis, and P. Knaus, Bone morphogenetic protein receptor complexes on the surface of live cells: a new oligomerization mode for serine/threonine kinase receptors, Mol Biol Cell 11 (2000) 1023-35.

[72] A. Nohe, E. Keating, P. Knaus, and N.O. Petersen, Signal transduction of bone morphogenetic protein receptors, Cell Signal 16 (2004) 291-9.

[73] A. Hartung, K. Bitton-Worms, M.M. Rechtman, V. Wenzel, J.H. Boergermann, S. Hassel, Y.I. Henis, and P. Knaus, Different routes of bone morphogenic protein (BMP) receptor endocytosis influence BMP signaling, Mol Cell Biol 26 (2006) 7791-805.

[74] J.W. WertzP.M. Bauer, Caveolin-1 regulates BMPRII localization and signaling in vascular smooth muscle cells, Biochem Biophys Res Commun 375 (2008) 557-61.

[75] K. Miyazono, S. Maeda, and T. Imamura, BMP receptor signaling: transcriptional targets, regulation of signals, and signaling cross-talk, Cytokine Growth Factor Rev 16 (2005) 251-63.

[76] Y. ShiJ. Massague, Mechanisms of TGF-beta signaling from cell membrane to the nucleus, Cell 113 (2003) 685-700.

[77] W. Shi, C. Chang, S. Nie, S. Xie, M. Wan, and X. Cao, Endofin acts as a Smad anchor for receptor activation in BMP signaling, J Cell Sci 120 (2007) 1216-24.
[78] Y.G. Chen, Z. Wang, J. Ma, L. Zhang, and Z. Lu, Endofin, a FYVE domain protein, interacts with Smad4 and facilitates transforming growth factor-beta signaling, J Biol Chem 282 (2007) 9688-95.
[79] C. Murphy, Endo-fin-ally a SARA for BMP receptors, J Cell Sci 120 (2007) 1153-5.
[80] H. Zhu, P. Kavsak, S. Abdollah, J.L. Wrana, and G.H. Thomsen, A SMAD ubiquitin ligase targets the BMP pathway and affects embryonic pattern formation, Nature 400 (1999) 687-93.
[81] S. Sangadala, S.D. Boden, R.P. Metpally, and B.V. Reddy, Modeling and analysis of molecularinteraction between Smurf1-WW2 domain and various isoforms of LIM mineralization protein, Proteins 68 (2007) 690-701.
[82] Y. Zhang, C. Chang, D.J. Gehling, A. Hemmati-Brivanlou, and R. Derynck, Regulation of Smad degradation and activity by Smurf2, an E3 ubiquitin ligase, Proc Natl Acad Sci U S A 98 (2001) 974-9.
[83] P. Kavsak, R.K. Rasmussen, C.G. Causing, S. Bonni, H. Zhu, G.H. Thomsen, and J.L. Wrana, Smad7 binds to Smurf2 to form an E3 ubiquitin ligase that targets the TGF beta receptor for degradation, Mol Cell 6 (2000) 1365-75.
[84] T. Ebisawa, M. Fukuchi, G. Murakami, T. Chiba, K. Tanaka, T. Imamura, and K. Miyazono, Smurf1 interacts with transforming growth factor-beta type I receptor through Smad7 and induces receptor degradation, J Biol Chem 276 (2001) 12477-80.
[85] C. Suzuki, G. Murakami, M. Fukuchi, T. Shimanuki, Y. Shikauchi, T. Imamura, and K. Miyazono, Smurf1 regulates the inhibitory activity of Smad7 by targeting Smad7 to the plasma membrane, J Biol Chem 277 (2002) 39919-25.
[86] G. Murakami, T. Watabe, K. Takaoka, K. Miyazono, and T. Imamura, Cooperative inhibition of bone morphogenetic protein signaling by Smurf1 and inhibitory Smads, Mol Biol Cell 14 (2003) 2809-17.
[87] G. Sapkota, C. Alarcon, F.M. Spagnoli, A.H. Brivanlou, and J. Massague, Balancing BMP signaling through integrated inputs into the Smad1 linker, Mol Cell 25 (2007) 441-54.
[88] S.X. Ying, Z.J. Hussain, and Y.E. Zhang, Smurf1 facilitates myogenic differentiation and antagonizes the bone morphogenetic protein-2-induced osteoblast conversion by targeting Smad5 for degradation, J Biol Chem 278 (2003) 39029-36.
[89] M. Zhao, M. Qiao, B.O. Oyajobi, G.R. Mundy, and D. Chen, E3 ubiquitin ligase Smurf1 mediates core-binding factor alpha1/Runx2 degradation and plays a specific role in osteoblast differentiation, J Biol Chem 278 (2003) 27939-44.
[90] M. Zhao, M. Qiao, S.E. Harris, B.O. Oyajobi, G.R. Mundy, and D. Chen, Smurf1 inhibits osteoblast differentiation and bone formation in vitro and in vivo, J Biol Chem 279 (2004) 12854-9.
[91] R. Shen, M. Chen, Y.J. Wang, H. Kaneki, L. Xing, J. O'Keefe R, and D. Chen, Smad6 interacts with Runx2 and mediates Smad ubiquitin regulatory factor 1-induced Runx2 degradation, J Biol Chem 281 (2006) 3569-76.
[92] M. Yamashita, S.X. Ying, G.M. Zhang, C. Li, S.Y. Cheng, C.X. Deng, and Y.E. Zhang, Ubiquitin ligase Smurf1 controls osteoblast activity and bone homeostasis by targeting MEKK2 for degradation, Cell 121 (2005) 101-13.
[93] R. Guo, M. Yamashita, Q. Zhang, Q. Zhou, D. Chen, D.G. Reynolds, H.A. Awad, L. Yanoso, L. Zhao, E.M. Schwarz, Y.E. Zhang, B.F. Boyce, and L. Xing, Ubiquitin ligase Smurf1 mediates tumor necrosis factor-induced systemic bone loss by promoting proteasomal degradation of bone morphogenetic signaling proteins, J Biol Chem 283 (2008) 23084-92.
[94] M. Horiki, T. Imamura, M. Okamoto, M. Hayashi, J. Murai, A. Myoui, T. Ochi, K. Miyazono, H. Yoshikawa, and N. Tsumaki, Smad6/Smurf1 overexpression in cartilage delays chondrocyte hypertrophy and causes dwarfism with osteopenia, J Cell Biol 165 (2004) 433-45.
[95] H.R. Wang, Y. Zhang, B. Ozdamar, A.A. Ogunjimi, E. Alexandrova, G.H. Thomsen, and J.L. Wrana, Regulation of cell polarity and protrusion formation by targeting RhoA for degradation, Science 302 (2003) 1775-9.
[96] Y. Zhang, H.R. Wang, and J.L. Wrana, Smurf1: a link between cell polarity and ubiquitination, Cell Cycle 3 (2004) 391-2.
[97] A. Moren, T. Imamura, K. Miyazono, C.H. Heldin, and A. Moustakas, Degradation of the tumor suppressor Smad4 by WW and HECT domain ubiquitin ligases, J Biol Chem 280 (2005) 22115-23.
[98] M.C. Chan, P.H. Nguyen, B.N. Davis, N. Ohoka, H. Hayashi, K. Du, G. Lagna, and A. Hata, A novel regulatory mechanism of the Bone Morphogenetic Protein (BMP) signaling pathway involving the carboxyl-terminal tail domain of BMP type II receptor, Mol Cell Biol (2007)
[99] M. Wan, X. Cao, Y. Wu, S. Bai, L. Wu, X. Shi, N. Wang, and X. Cao, Jab1 antagonizes TGF-beta signaling by inducing Smad4 degradation, EMBO Rep 3 (2002) 171-6.
[100] J. HaagT. Aigner, Jun activation domain-binding protein 1 binds Smad5 and inhibits bone morphogenetic protein signaling, Arthritis Rheum 54 (2006) 3878-84.
[101] L. Li, H. Xin, X. Xu, M. Huang, X. Zhang, Y. Chen, S. Zhang, X.Y. Fu, and Z. Chang, CHIP mediates degradation of Smad proteins and potentially regulates Smad-induced transcription, Mol Cell Biol 24 (2004) 856-64.
[102] M. Wan, Y. Tang, E.M. Tytler, C. Lu, B. Jin, S.M. Vickers, L. Yang, X. Shi, and X. Cao, Smad4 protein stability is regulated by ubiquitin ligase SCF beta-TrCP1, J Biol Chem 279 (2004) 14484-7.
[103] X. Lin, M. Liang, Y.Y. Liang, F.C. Brunicardi, and X.H. Feng, SUMO-1/Ubc9 promotes nuclear accumulation and metabolic stability of tumor suppressor Smad4, J Biol Chem 278 (2003) 31043-8.
[104] A. Komuro, T. Imamura, M. Saitoh, Y. Yoshida, T. Yamori, K. Miyazono, and K. Miyazawa, Negative regulation of transforming growth factor-beta (TGF-beta) signaling by WW domain-containing protein 1 (WWP1), Oncogene 23 (2004) 6914-23.

[105] B.Y. Qin, B.M. Chacko, S.S. Lam, M.P. de Caestecker, J.J. Correia, and K. Lin, Structural basis of Smad1 activation by receptor kinase phosphorylation, Mol Cell 8 (2001) 1303-12.

[106] M. Kretzschmar, J. Doody, and J. Massague, Opposing BMP and EGF signalling pathways converge on the TGF-beta family mediator Smad1, Nature 389 (1997) 618-22.

[107] E.M. Pera, A. Ikeda, E. Eivers, and E.M. De Robertis, Integration of IGF, FGF, and anti-BMP signals via Smad1 phosphorylation in neural induction, Genes Dev 17 (2003) 3023-8.

[108] K. Nakayama, Y. Tamura, M. Suzawa, S. Harada, S. Fukumoto, M. Kato, K. Miyazono, G.A. Rodan, Y. Takeuchi, and T. Fujita, Receptor tyrosine kinases inhibit bone morphogenetic protein-Smad responsive promoter activity and differentiation of murine MC3T3-E1 osteoblast-like cells, J Bone Miner Res 18 (2003) 827-35.

[109] L.C. Fuentealba, E. Eivers, A. Ikeda, C. Hurtado, H. Kuroda, E.M. Pera, and E.M. De Robertis, Integrating patterning signals: Wnt/GSK3 regulates the duration of the BMP/Smad1 signal, Cell 131 (2007) 980-93.

[110] H.B. Chen, J. Shen, Y.T. Ip, and L. Xu, Identification of phosphatases for Smad in the BMP/DPP pathway, Genes Dev 20 (2006) 648-53.

[111] X. Duan, Y.Y. Liang, X.H. Feng, and X. Lin, Protein serine/threonine phosphatase PPM1A dephosphorylates Smad1 in the bone morphogenetic protein signaling pathway, J Biol Chem 281 (2006) 36526-32.

[112] M. Knockaert, G. Sapkota, C. Alarcon, J. Massague, and A.H. Brivanlou, Unique players in the BMP pathway: small C-terminal domain phosphatases dephosphorylate Smad1 to attenuate BMP signaling, Proc Natl Acad Sci U S A 103 (2006) 11940-5.

[113] G. Sapkota, M. Knockaert, C. Alarcon, E. Montalvo, A.H. Brivanlou, and J. Massague, Dephosphorylation of the linker regions of Smad1 and Smad2/3 by small C-terminal domain phosphatases has distinct outcomes for bone morphogenetic protein and transforming growth factor-beta pathways, J Biol Chem 281 (2006) 40412-9.

[114] L. Bengtsson, R. Schwappacher, M. Roth, J. Boergermann, S. Hassel, and P. Knaus, PP2A regulates BMP signaling by interacting with BMP receptor complexes and by dephosphorylating both the C-terminus and the linker region of Smad1, J Cell Sci ahead of print (2009 (accepted))

[115] F.J. Nicolas, K. De Bosscher, B. Schmierer, and C.S. Hill, Analysis of Smad nucleocytoplasmic shuttling in living cells, J Cell Sci 117 (2004) 4113-25.

[116] B. SchmiererC.S. Hill, Kinetic analysis of Smad nucleocytoplasmic shuttling reveals a mechanism for transforming growth factor beta-dependent nuclear accumulation of Smads, Mol Cell Biol 25 (2005) 9845-58.

[117] M. Watanabe, N. Masuyama, M. Fukuda, and E. Nishida, Regulation of intracellular dynamics of Smad4 by its leucine-rich nuclear export signal, EMBO Rep 1 (2000) 176-82.

[118] Y. Shi, Y.F. Wang, L. Jayaraman, H. Yang, J. Massague, and N.P. Pavletich, Crystal structure of a Smad MH1 domain bound to DNA: insights on DNA binding in TGF-beta signaling, Cell 94 (1998) 585-94.

[119] L.J. Jonk, S. Itoh, C.H. Heldin, P. ten Dijke, and W. Kruijer, Identification and functional characterization of a Smad binding element (SBE) in the JunB promoter that acts as a transforming growth factor-beta, activin, and bone morphogenetic protein-inducible enhancer, J Biol Chem 273 (1998) 21145-52.

[120] E. Chalaux, T. Lopez-Rovira, J.L. Rosa, R. Bartrons, and F. Ventura, JunB is involved in the inhibition of myogenic differentiation by bone morphogenetic protein-2, J Biol Chem 273 (1998) 537-43.

[121] O. KorchynskyiP. ten Dijke, Identification and functional characterization of distinct critically important bone morphogenetic protein-specific response elements in the Id1 promoter, J Biol Chem 277 (2002) 4883-91.

[122] K.S. Lee, H.J. Kim, Q.L. Li, X.Z. Chi, C. Ueta, T. Komori, J.M. Wozney, E.G. Kim, J.Y. Choi, H.M. Ryoo, and S.C. Bae, Runx2 is a common target of transforming growth factor beta1 and bone morphogenetic protein 2, and cooperation between Runx2 and Smad5 induces osteoblast-specific gene expression in the pluripotent mesenchymal precursor cell line C2C12, Mol Cell Biol 20 (2000) 8783-92.

[123] S.C. Bae, K.S. Lee, Y.W. Zhang, and Y. Ito, Intimate relationship between TGF-beta/BMP signaling and runt domain transcription factor, PEBP2/CBF, J Bone Joint Surg Am 83-A Suppl 1 (2001) S48-55.

[124] K.L. Pearson, T. Hunter, and R. Janknecht, Activation of Smad1-mediated transcription by p300/CBP, Biochim Biophys Acta 1489 (1999) 354-64.

[125] E.J. Jeon, K.Y. Lee, N.S. Choi, M.H. Lee, H.N. Kim, Y.H. Jin, H.M. Ryoo, J.Y. Choi, M. Yoshida, N. Nishino, B.C. Oh, K.S. Lee, Y.H. Lee, and S.C. Bae, Bone morphogenetic protein-2 stimulates Runx2 acetylation, J Biol Chem 281 (2006) 16502-11.

[126] Y.H. Jin, E.J. Jeon, Q.L. Li, Y.H. Lee, J.K. Choi, W.J. Kim, K.Y. Lee, and S.C. Bae, Transforming growth factor-beta stimulates p300-dependent RUNX3 acetylation, which inhibits ubiquitination-mediated degradation, J Biol Chem 279 (2004) 29409-17.

[127] X. Liu, Y. Sun, R.A. Weinberg, and H.F. Lodish, Ski/Sno and TGF-beta signaling, Cytokine Growth Factor Rev 12 (2001) 1-8.

[128] W. Wang, F.V. Mariani, R.M. Harland, and K. Luo, Ski represses bone morphogenic protein signaling in Xenopus and mammalian cells, Proc Natl Acad Sci U S A 97 (2000) 14394-9.

[129] M. Takeda, M. Mizuide, M. Oka, T. Watabe, H. Inoue, H. Suzuki, T. Fujita, T. Imamura, K. Miyazono, and K. Miyazawa, Interaction with Smad4 is indispensable for suppression of BMP signaling by c-Ski, Mol Biol Cell 15 (2004) 963-72.

[130] K. Yamaguchi, S. Nagai, J. Ninomiya-Tsuji, M. Nishita, K. Tamai, K. Irie, N. Ueno, E. Nishida, H. Shibuya, and K. Matsumoto, XIAP, a cellular member of the inhibitor of apoptosis protein family, links the receptors to TAB1-TAK1 in the BMP signaling pathway, Embo J 18 (1999) 179-87.

[131] K. Yamaguchi, K. Shirakabe, H. Shibuya, K. Irie, I. Oishi, N. Ueno, T. Taniguchi, E. Nishida, and K. Matsumoto, Identification of a member of the MAPKKK family as a potential mediator of TGF-beta signal transduction, Science 270 (1995) 2008-11.

[132] T. Moriguchi, N. Kuroyanagi, K. Yamaguchi, Y. Gotoh, K. Irie, T. Kano, K. Shirakabe, Y. Muro, H. Shibuya, K. Matsumoto, E. Nishida, and M. Hagiwara, A novel kinase cascade mediated by mitogen-activated protein kinase kinase 6 and MKK3, J Biol Chem 271 (1996) 13675-9.

[133] K. Shirakabe, K. Yamaguchi, H. Shibuya, K. Irie, S. Matsuda, T. Moriguchi, Y. Gotoh, K. Matsumoto, and E. Nishida, TAK1 mediates the ceramide signaling to stress-activated protein kinase/c-Jun N-terminal kinase, J Biol Chem 272 (1997) 8141-4.

[134] Y. Sano, J. Harada, S. Tashiro, R. Gotoh-Mandeville, T. Maekawa, and S. Ishii, ATF-2 is a common nuclear target of Smad and TAK1 pathways in transforming growth factor-beta signaling, J Biol Chem 274 (1999) 8949-57.

[135] C.F. LaiS.L. Cheng, Signal transductions induced by bone morphogenetic protein-2 and transforming growth factor-beta in normal human osteoblastic cells, J Biol Chem 277 (2002) 15514-22.

[136] N. Kimura, R. Matsuo, H. Shibuya, K. Nakashima, and T. Taga, BMP2-induced apoptosis is mediated by activation of the TAK1-p38 kinase pathway that is negatively regulated by Smad6, J Biol Chem 275 (2000) 17647-52.

[137] S. Edlund, S. Bu, N. Schuster, P. Aspenstrom, R. Heuchel, N.E. Heldin, P. ten Dijke, C.H. Heldin, and M. Landstrom, Transforming growth factor-beta1 (TGF-beta)-induced apoptosis of prostate cancer cells involves Smad7-dependent activation of p38 by TGF-beta-activated kinase 1 and mitogen-activated protein kinase kinase 3, Mol Biol Cell 14 (2003) 529-44.

[138] R.H. Xu, Z. Dong, M. Maeno, J. Kim, A. Suzuki, N. Ueno, D. Sredni, N.H. Colburn, and H.F. Kung, Involvement of Ras/Raf/AP-1 in BMP-4 signaling during Xenopus embryonic development, Proc Natl Acad Sci U S A 93 (1996) 834-8.

[139] W. Kolch, Meaningful relationships: the regulation of the Ras/Raf/MEK/ERK pathway by protein interactions, Biochem J 351 Pt 2 (2000) 289-305.

[140] S. Gallea, F. Lallemand, A. Atfi, G. Rawadi, V. Ramez, S. Spinella-Jaegle, S. Kawai, C. Faucheu, L. Huet, R. Baron, and S. Roman-Roman, Activation of mitogen-activated protein kinase cascades is involved in regulation of bone morphogenetic protein-2-induced osteoblast differentiation in pluripotent C2C12 cells, Bone 28 (2001) 491-8.

[141] J. Yue, R.S. Frey, and K.M. Mulder, Cross-talk between the Smad1 and Ras/MEK signaling pathways for TGFbeta, Oncogene 18 (1999) 2033-7.

[142] K. Miyazono, TGF-beta receptors and signal transduction, Int J Hematol 65 (1997) 97-104.

[143] D. Onichtchouk, Y.G. Chen, R. Dosch, V. Gawantka, H. Delius, J. Massague, and C. Niehrs, Silencing of TGF-beta signalling by the pseudoreceptor BAMBI, Nature 401 (1999) 480-5.

[144] T.A. Samad, A. Rebbapragada, E. Bell, Y. Zhang, Y. Sidis, S.J. Jeong, J.A. Campagna, S. Perusini, D.A. Fabrizio, A.L. Schneyer, H.Y. Lin, A.H. Brivanlou, L. Attisano, and C.J. Woolf, DRAGON, a bone morphogenetic protein co-receptor, J Biol Chem 280 (2005) 14122-9.

[145] T.A. Samad, A. Srinivasan, L.A. Karchewski, S.J. Jeong, J.A. Campagna, R.R. Ji, D.A. Fabrizio, Y. Zhang, H.Y. Lin, E. Bell, and C.J. Woolf, DRAGON: a member of the repulsive guidance molecule-related family of neuronal- and muscle-expressed membrane proteins is regulated by DRG11 and has neuronal adhesive properties, J Neurosci 24 (2004) 2027-36.

[146] E. Matsunaga, H. Nakamura, and A. Chedotal, Repulsive guidance molecule plays multiple roles in neuronal differentiation and axon guidance, J Neurosci 26 (2006) 6082-8.

[147] J.L. Babitt, Y. Zhang, T.A. Samad, Y. Xia, J. Tang, J.A. Campagna, A.L. Schneyer, C.J. Woolf, and H.Y. Lin, Repulsive guidance molecule (RGMa), a DRAGON homologue, is a bone morphogenetic protein co-receptor, J Biol Chem 280 (2005) 29820-7.

[148] J.L. Babitt, F.W. Huang, D.M. Wrighting, Y. Xia, Y. Sidis, T.A. Samad, J.A. Campagna, R.T. Chung, A.L. Schneyer, C.J. Woolf, N.C. Andrews, and H.Y. Lin, Bone morphogenetic protein signaling by hemojuvelin regulates hepcidin expression, Nat Genet 38 (2006) 531-9.

[149] J.L. Babitt, F.W. Huang, Y. Xia, Y. Sidis, N.C. Andrews, and H.Y. Lin, Modulation of bone morphogenetic protein signaling in vivo regulates systemic iron balance, J Clin Invest 117 (2007) 1933-9.

[150] P.J. Halbrooks, R. Ding, J.M. Wozney, and G. Bain, Role of RGM coreceptors in bone morphogenetic protein signaling, J Mol Signal 2 (2007) 4.

[151] V.C. Broudy, Stem cell factor and hematopoiesis, Blood 90 (1997) 1345-64.

[152] G. Bilbe, E. Roberts, M. Birch, and D.B. Evans, PCR phenotyping of cytokines, growth factors and their receptors and bone matrix proteins in human osteoblast-like cell lines, Bone 19 (1996) 437-45.

[153] L. Palmqvist, C.H. Glover, L. Hsu, M. Lu, B. Bossen, J.M. Piret, R.K. Humphries, and C.D. Helgason, Correlation of murine embryonic stem cell gene expression profiles with functional measures of pluripotency, Stem Cells 23 (2005) 663-80.

[154] M. SattlerR. Salgia, Targeting c-Kit mutations: basic science to novel therapies, Leuk Res 28 Suppl 1 (2004) S11-20.

[155] R. Roskoski, Jr., Structure and regulation of Kit protein-tyrosine kinase--the stem cell factor receptor, Biochem Biophys Res Commun 338 (2005) 1307-15.

[156] S. Hassel, M. Yakymovych, U. Hellman, L. Ronnstrand, P. Knaus, and S. Souchelnytskyi, Interaction and functional cooperation between the serine/threonine kinase bone morphogenetic protein type II receptor with the tyrosine kinase stem cell factor receptor, J Cell Physiol 206 (2006) 457-67.

[157] A. Hartung, C. Sieber, and P. Knaus, Yin and Yang in BMP signaling: Impact on the pathology of diseases and potential for tissue regeneration, Signal Transduction 6 (2006) 314-328.

[158] P. MasiakowskiR.D. Carroll, A novel family of cell surface receptors with tyrosine kinase-like domain, J Biol Chem 267 (1992) 26181-90.
[159] S. Takeuchi, K. Takeda, I. Oishi, M. Nomi, M. Ikeya, K. Itoh, S. Tamura, T. Ueda, T. Hatta, H. Otani, T. Terashima, S. Takada, H. Yamamura, S. Akira, and Y. Minami, Mouse Ror2 receptor tyrosine kinase is required for the heart development and limb formation, Genes Cells 5 (2000) 71-8.
[160] J.L. Green, S.G. Kuntz, and P.W. Sternberg, Ror receptor tyrosine kinases: orphans no more, Trends Cell Biol 18 (2008) 536-44.
[161] Q. Wang, B. Zhang, Y.E. Wang, W.C. Xiong, and L. Mei, The Ig1/2 domain of MuSK binds to muscle surface and is involved in acetylcholine receptor clustering, Neurosignals 16 (2008) 246-53.
[162] C. Carron, A. Pascal, A. Djiane, J.C. Boucaut, D.L. Shi, and M. Umbhauer, Frizzled receptor dimerization is sufficient to activate the Wnt/beta-catenin pathway, J Cell Sci 116 (2003) 2541-50.
[163] M.P. YavropoulouJ.G. Yovos, The role of the Wnt signaling pathway in osteoblast commitment and differentiation, Hormones (Athens) 6 (2007) 279-94.
[164] I. Oishi, H. Suzuki, N. Onishi, R. Takada, S. Kani, B. Ohkawara, I. Koshida, K. Suzuki, G. Yamada, G.C. Schwabe, S. Mundlos, H. Shibuya, S. Takada, and Y. Minami, The receptor tyrosine kinase Ror2 is involved in non-canonical Wnt5a/JNK signalling pathway, Genes Cells 8 (2003) 645-54.
[165] M. Sammar, S. Stricker, G.C. Schwabe, C. Sieber, A. Hartung, M. Hanke, I. Oishi, J. Pohl, Y. Minami, W. Sebald, S. Mundlos, and P. Knaus, Modulation of GDF5/BRI-b signalling through interaction with the tyrosine kinase receptor Ror2, Genes Cells 9 (2004) 1227-38.
[166] A.R. Afzal, A. Rajab, C.D. Fenske, M. Oldridge, N. Elanko, E. Ternes-Pereira, B. Tuysuz, V.A. Murday, M.A. Patton, A.O. Wilkie, and S. Jeffery, Recessive Robinow syndrome, allelic to dominant brachydactyly type B, is caused by mutation of ROR2, Nat Genet 25 (2000) 419-22.
[167] H. van Bokhoven, J. Celli, H. Kayserili, E. van Beusekom, S. Balci, W. Brussel, F. Skovby, B. Kerr, E.F. Percin, N. Akarsu, and H.G. Brunner, Mutation of the gene encoding the ROR2 tyrosine kinase causes autosomal recessive Robinow syndrome, Nat Genet 25 (2000) 423-6.
[168] Y. Cao, R. Cao, and N. Veitonmaki, Kringle structures and antiangiogenesis, Curr Med Chem Anticancer Agents 2 (2002) 667-81.
[169] C. Wilson, D.C. Goberdhan, and H. Steller, Dror, a potential neurotrophic receptor gene, encodes a Drosophila homolog of the vertebrate Ror family of Trk-related receptor tyrosine kinases, Proc Natl Acad Sci U S A 90 (1993) 7109-13.
[170] T. Matsuda, H. Suzuki, I. Oishi, S. Kani, Y. Kuroda, T. Komori, A. Sasaki, K. Watanabe, and Y. Minami, The receptor tyrosine kinase Ror2 associates with the MAGE-family protein Dlxin-1 and regulates its intracellular distribution, J Biol Chem 16 (2003) 16.
[171] A. Winkel, S. Stricker, P. Tylzanowski, V. Seiffart, S. Mundlos, G. Gross, and A. Hoffmann, Wnt-ligand-dependent interaction of TAK1 (TGF-beta-activated kinase-1) with the receptor tyrosine kinase Ror2 modulates canonical Wnt-signalling, Cell Signal 20 (2008) 2134-44.
[172] I. Oishi, S. Takeuchi, R. Hashimoto, A. Nagabukuro, T. Ueda, Z.J. Liu, T. Hatta, S. Akira, Y. Matsuda, H. Yamamura, H. Otani, and Y. Minami, Spatio-temporally regulated expression of receptor tyrosine kinases, mRor1, mRor2, during mouse development: implications in development and function of the nervous system, Genes Cells 4 (1999) 41-56.
[173] S. Akbarzadeh, L.M. Wheldon, S.M. Sweet, S. Talma, F.K. Mardakheh, and J.K. Heath, The deleted in brachydactyly B domain of ROR2 is required for receptor activation by recruitment of Src, PLoS ONE 3 (2008) e1873.
[174] I. Oishi, S. Sugiyama, Z.J. Liu, H. Yamamura, Y. Nishida, and Y. Minami, A novel Drosophila receptor tyrosine kinase expressed specifically in the nervous system. Unique structural features and implication in developmental signaling, J Biol Chem 272 (1997) 11916-23.
[175] T.M. DeChiara, R.B. Kimble, W.T. Poueymirou, J. Rojas, P. Masiakowski, D.M. Valenzuela, and G.D. Yancopoulos, Ror2, encoding a receptor-like tyrosine kinase, is required for cartilage and growth plate development, Nat Genet 24 (2000) 271-4.
[176] M. Nomi, I. Oishi, S. Kani, H. Suzuki, T. Matsuda, A. Yoda, M. Kitamura, K. Itoh, S. Takeuchi, K. Takeda, S. Akira, M. Ikeya, S. Takada, and Y. Minami, Loss of mRor1 enhances the heart and skeletal abnormalities in mRor2- deficient mice: redundant and pleiotropic functions of mRor1 and mRor2 receptor tyrosine kinases, Mol Cell Biol 21 (2001) 8329-35.
[177] C. Fuerer, R. Nusse, and D. Ten Berge, Wnt signalling in development and disease. Max Delbruck Center for Molecular Medicine meeting on Wnt signaling in Development and Disease, EMBO Rep 9 (2008) 134-8.
[178] M. Kuhl, L.C. Sheldahl, M. Park, J.R. Miller, and R.T. Moon, The Wnt/Ca2+ pathway: a new vertebrate Wnt signaling pathway takes shape, Trends Genet 16 (2000) 279-83.
[179] C.R. WestonR.J. Davis, The JNK signal transduction pathway, Curr Opin Genet Dev 12 (2002) 14-21.
[180] M. Montcouquiol, E.B. Crenshaw, 3rd, and M.W. Kelley, Noncanonical Wnt signaling and neural polarity, Annu Rev Neurosci 29 (2006) 363-86.
[181] Y. Liu, R.A. Bhat, L.M. Seestaller-Wehr, S. Fukayama, A. Mangine, R.A. Moran, B.S. Komm, P.V. Bodine, and J. Billiard, The orphan receptor tyrosine kinase Ror2 promotes osteoblast differentiation and enhances ex vivo bone formation, Mol Endocrinol 21 (2007) 376-87.
[182] Y. Liu, J.F. Ross, P.V. Bodine, and J. Billiard, Homodimerization of Ror2 tyrosine kinase receptor induces 14-3-3(beta) phosphorylation and promotes osteoblast differentiation and bone formation, Mol Endocrinol 21 (2007) 3050-61.
[183] Y. Liu, B. Rubin, P.V. Bodine, and J. Billiard, Wnt5a induces homodimerization and activation of Ror2 receptor tyrosine kinase, J Cell Biochem (2008)
[184] M.A. PattonA.R. Afzal, Robinow syndrome, J Med Genet 39 (2002) 305-10.

[185] S. Kani, I. Oishi, H. Yamamoto, A. Yoda, H. Suzuki, A. Nomachi, K. Iozumi, M. Nishita, A. Kikuchi, T. Takumi, and Y. Minami, The receptor tyrosine kinase Ror2 associates with and is activated by casein kinase Iepsilon, J Biol Chem 279 (2004) 50102-9.

[186] J. Billiard, D.S. Way, L.M. Seestaller-Wehr, R.A. Moran, A. Mangine, and P.V. Bodine, The orphan receptor tyrosine kinase Ror2 modulates canonical Wnt signaling in osteoblastic cells, Mol Endocrinol 19 (2005) 90-101.

[187] C. Li, H. Chen, L. Hu, Y. Xing, T. Sasaki, M.F. Villosis, J. Li, M. Nishita, Y. Minami, and P. Minoo, Ror2 modulates the canonical Wnt signaling in lung epithelial cells through cooperation with Fzd2, BMC Mol Biol 9 (2008) 11.

[188] H. Yamamoto, S.K. Yoo, M. Nishita, A. Kikuchi, and Y. Minami, Wnt5a modulates glycogen synthase kinase 3 to induce phosphorylation of receptor tyrosine kinase Ror2, Genes Cells 12 (2007) 1215-23.

[189] M. Nishita, S.K. Yoo, A. Nomachi, S. Kani, N. Sougawa, Y. Ohta, S. Takada, A. Kikuchi, and Y. Minami, Filopodia formation mediated by receptor tyrosine kinase Ror2 is required for Wnt5a-induced cell migration, J Cell Biol 175 (2006) 555-62.

[190] F. He, W. Xiong, X. Yu, R. Espinoza-Lewis, C. Liu, S. Gu, M. Nishita, K. Suzuki, G. Yamada, Y. Minami, and Y. Chen, Wnt5a regulates directional cell migration and cell proliferation via Ror2-mediated noncanonical pathway in mammalian palate development, Development 135 (2008) 3871-9.

[191] A. Nomachi, M. Nishita, D. Inaba, M. Enomoto, M. Hamasaki, and Y. Minami, Receptor tyrosine kinase Ror2 mediates Wnt5a-induced polarized cell migration by activating c-Jun N-terminal kinase via actin-binding protein filamin A, J Biol Chem 283 (2008) 27973-81.

[192] A. SchambonyD. Wedlich, Wnt-5A/Ror2 regulate expression of XPAPC through an alternative noncanonical signaling pathway, Dev Cell 12 (2007) 779-92.

[193] A.J. MikelsR. Nusse, Purified Wnt5a protein activates or inhibits beta-catenin-TCF signaling depending on receptor context, PLoS Biol 4 (2006) e115.

[194] M. Sammar, C. Sieber, and P. Knaus, Biochemical and functional characterization of the Ror2/BRIb receptor complex, Biochem Biophys Res Commun (2009)

[195] S.A. TemtamyM.S. Aglan, Brachydactyly, Orphanet J Rare Dis 3 (2008) 15.

[196] G.C. Schwabe, S. Tinschert, C. Buschow, P. Meinecke, G. Wolff, G. Gillessen-Kaesbach, M. Oldridge, A.O. Wilkie, R. Komec, and S. Mundlos, Distinct mutations in the receptor tyrosine kinase gene ROR2 cause brachydactyly type B, Am J Hum Genet 67 (2000) 822-31.

[197] Y. Chen, W.P. Bellamy, M.C. Seabra, M.C. Field, and B.R. Ali, ER-associated protein degradation is a common mechanism underpinning numerous monogenic diseases including Robinow syndrome, Hum Mol Genet 14 (2005) 2559-69.

[198] A.L. SchwartzA. Ciechanover, Targeting Proteins for Destruction by the Ubiquitin System: Implications for Human Pathobiology, Annu Rev Pharmacol Toxicol (2008)

[199] S. Oddo, The ubiquitin-proteasome system in Alzheimer's disease, J Cell Mol Med 12 (2008) 363-73.

[200] D. MukhopadhyayH. Riezman, Proteasome-independent functions of ubiquitin in endocytosis and signaling, Science 315 (2007) 201-5.

[201] T. RavidM. Hochstrasser, Diversity of degradation signals in the ubiquitin-proteasome system, Nat Rev Mol Cell Biol 9 (2008) 679-90.

[202] Y. Saeki, T. Kudo, T. Sone, Y. Kikuchi, H. Yokosawa, E.A. Toh, and K. Tanaka, Lysine 63-linked polyubiquitin chain may serve as a targeting signal for the 26S proteasome, Embo J (2009)

[203] R.M. Vabulas, Proteasome function and protein biosynthesis, Curr Opin Clin Nutr Metab Care 10 (2007) 24-31.

[204] C. Le RoyJ.L. Wrana, Clathrin- and non-clathrin-mediated endocytic regulation of cell signalling, Nat Rev Mol Cell Biol 6 (2005) 112-26.

[205] G. Asher, N. Reuven, and Y. Shaul, 20S proteasomes and protein degradation "by default", Bioessays 28 (2006) 844-9.

[206] Y. InoueT. Imamura, Regulation of TGF-beta family signaling by E3 ubiquitin ligases, Cancer Sci 99 (2008) 2107-12.

[207] S.S. VembarJ.L. Brodsky, One step at a time: endoplasmic reticulum-associated degradation, Nat Rev Mol Cell Biol 9 (2008) 944-57.

[208] C. Mineo, G.N. Gill, and R.G. Anderson, Regulated migration of epidermal growth factor receptor from caveolae, J Biol Chem 274 (1999) 30636-43.

[209] S. Sigismund, T. Woelk, C. Puri, E. Maspero, C. Tacchetti, P. Transidico, P.P. Di Fiore, and S. Polo, Clathrin-independent endocytosis of ubiquitinated cargos, Proc Natl Acad Sci U S A 102 (2005) 2760-5.

[210] C. Puri, D. Tosoni, R. Comai, A. Rabellino, D. Segat, F. Caneva, P. Luzzi, P.P. Di Fiore, and C. Tacchetti, Relationships between EGFR signaling-competent and endocytosis-competent membrane microdomains, Mol Biol Cell 16 (2005) 2704-18.

[211] M. Kazazic, K. Roepstorff, L.E. Johannessen, N.M. Pedersen, B. van Deurs, E. Stang, and I.H. Madshus, EGF-induced activation of the EGF receptor does not trigger mobilization of caveolae, Traffic 7 (2006) 1518-27.

[212] A. SorkinL.K. Goh, Endocytosis and intracellular trafficking of ErbBs, Exp Cell Res 314 (2008) 3093-106.

[213] A.H. Kesarwala, M.M. Samrakandi, and D. Piwnica-Worms, Proteasome inhibition blocks ligand-induced dynamic processing and internalization of epidermal growth factor receptor via altered receptor ubiquitination and phosphorylation, Cancer Res 69 (2009) 976-83.

[214] D.B. Everman, C.F. Bartels, Y. Yang, N. Yanamandra, F.R. Goodman, J.R. Mendoza-Londono, R. Savarirayan, S.M. White, J.M. Graham, Jr., R.P. Gale, E. Svarch, W.G. Newman, A.R. Kleckers, C.A. Francomano, V. Govindaiah, L.

Singh, S. Morrison, J.T. Thomas, and M.L. Warman, The mutational spectrum of brachydactyly type C, Am J Med Genet 112 (2002) 291-6.
[215] H. Hikasa, M. Shibata, I. Hiratani, and M. Taira, The Xenopus receptor tyrosine kinase Xror2 modulates morphogenetic movements of the axial mesoderm and neuroectoderm via Wnt signaling, Development 129 (2002) 5227-39.
[216] Y. Liu, P.V. Bodine, and J. Billiard, Ror2, a novel modulator of osteogenesis, J Musculoskelet Neuronal Interact 7 (2007) 323-4.
[217] H. Niwa, K. Yamamura, and J. Miyazaki, Efficient selection for high-expression transfectants with a novel eukaryotic vector, Gene 108 (1991) 193-9.
[218] S. Andersson, D.L. Davis, H. Dahlback, H. Jornvall, and D.W. Russell, Cloning, structure, and expression of the mitochondrial cytochrome P-450 sterol 26-hydroxylase, a bile acid biosynthetic enzyme, J Biol Chem 264 (1989) 8222-9.
[219] A. Nohe, S. Hassel, M. Ehrlich, F. Neubauer, W. Sebald, Y.I. Henis, and P. Knaus, The mode of bone morphogenetic protein (BMP) receptor oligomerization determines different BMP-2 signaling pathways, J Biol Chem 277 (2002) 5330-8.
[220] D. Hanahan, Studies on transformation of Escherichia coli with plasmids, J Mol Biol 166 (1983) 557-80.
[221] K.A. Young, C. Ivester, J. West, M. Carr, and D.M. Rodman, BMP signaling controls PASMC KV channel expression in vitro and in vivo, Am J Physiol Lung Cell Mol Physiol 290 (2006) L841-8.
[222] F.W. StudierB.A. Moffatt, Use of bacteriophage T7 RNA polymerase to direct selective high-level expression of cloned genes, J Mol Biol 189 (1986) 113-30.
[223] S. Hassel, S. Schmitt, A. Hartung, M. Roth, A. Nohe, N. Petersen, M. Ehrlich, Y.I. Henis, W. Sebald, and P. Knaus, Initiation of Smad-dependent and Smad-independent signaling via distinct BMP-receptor complexes, J Bone Joint Surg Am 85-A Suppl 3 (2003) 44-51.
[224] J.A. Gordon, Use of vanadate as protein-phosphotyrosine phosphatase inhibitor, Methods Enzymol 201 (1991) 477-82.
[225] U.K. Laemmli, Cleavage of structural proteins during the assembly of the head of bacteriophage T4, Nature 227 (1970) 680-5.
[226] W.N. Burnette, "Western blotting": electrophoretic transfer of proteins from sodium dodecyl sulfate--polyacrylamide gels to unmodified nitrocellulose and radiographic detection with antibody and radioiodinated protein A, Anal Biochem 112 (1981) 195-203.
[227] J. Nickel, A. Kotzsch, W. Sebald, and T.D. Mueller, A single residue of GDF-5 defines binding specificity to BMP receptor IB, J Mol Biol 349 (2005) 933-47.
[228] A. Shevchenko, M. Wilm, O. Vorm, and M. Mann, Mass spectrometric sequencing of proteins silver-stained polyacrylamide gels, Anal Chem 68 (1996) 850-8.
[229] A. Hoffmann, O. Preobrazhenska, C. Wodarczyk, Y. Medler, A. Winkel, S. Shahab, D. Huylebroeck, G. Gross, and K. Verschueren, Transforming growth factor-beta-activated kinase-1 (TAK1), a MAP3K, interacts with Smad proteins and interferes with osteogenesis in murine mesenchymal progenitors, J Biol Chem 280 (2005) 27271-83.
[230] H.R. PelhamR.J. Jackson, An efficient mRNA-dependent translation system from reticulocyte lysates, Eur J Biochem 67 (1976) 247-56.
[231] G. Scheele, Methods for the study of protein translocation across the RER membrane using the reticulocyte lysate translation system and canine pancreatic microsomal membranes, Methods Enzymol 96 (1983) 94-111.
[232] E. Carlson, N. Bays, L. David, and W.R. Skach, Reticulocyte lysate as a model system to study endoplasmic reticulum membrane protein degradation, Methods Mol Biol 301 (2005) 185-205.
[233] M.P. PerronP. Provost, Protein interactions and complexes in human microRNA biogenesis and function, Front Biosci 13 (2008) 2537-47.
[234] L. DingM. Han, GW182 family proteins are crucial for microRNA-mediated gene silencing, Trends Cell Biol 17 (2007) 411-6.
[235] S.R. HubbardJ.H. Till, Protein tyrosine kinase structure and function, Annu Rev Biochem 69 (2000) 373-98.
[236] P. De Meyts, The insulin receptor: a prototype for dimeric, allosteric membrane receptors? Trends Biochem Sci 33 (2008) 376-84.
[237] Y.I. Henis, A. Moustakas, H.Y. Lin, and H.F. Lodish, The types II and III transforming growth factor-beta receptors form homo-oligomers, J Cell Biol 126 (1994) 139-54.
[238] L. Gilboa, R.G. Wells, H.F. Lodish, and Y.I. Henis, Oligomeric structure of type I and type II transforming growth factor beta receptors: homodimers form in the ER and persist at the plasma membrane, J Cell Biol 140 (1998) 767-77.
[239] S. Dupre, D. Urban-Grimal, and R. Haguenauer-Tsapis, Ubiquitin and endocytic internalization in yeast and animal cells, Biochim Biophys Acta 1695 (2004) 89-111.
[240] A. Ciechanover, H. Gonen, B. Bercovich, S. Cohen, I. Fajerman, A. Israel, F. Mercurio, C. Kahana, A.L. Schwartz, K. Iwai, and A. Orian, Mechanisms of ubiquitin-mediated, limited processing of the NF-kappaB1 precursor protein p105, Biochimie 83 (2001) 341-9.
[241] R. Crinelli, M. Bianchi, M. Menotta, E. Carloni, E. Giacomini, M. Pennati, and M. Magnani, Ubiquitin over-expression promotes E6AP autodegradation and reactivation of the p53/MDM2 pathway in HeLa cells, Mol Cell Biochem 318 (2008) 129-45.
[242] C.M. Pickart, Mechanisms underlying ubiquitination, Annu Rev Biochem 70 (2001) 503-33.

[243] R.C. PiperJ.P. Luzio, Ubiquitin-dependent sorting of integral membrane proteins for degradation in lysosomes, Curr Opin Cell Biol 19 (2007) 459-65.
[244] I. Dikic, Mechanisms controlling EGF receptor endocytosis and degradation, Biochem Soc Trans 31 (2003) 1178-81.
[245] I. Szymkiewicz, K. Kowanetz, P. Soubeyran, A. Dinarina, S. Lipkowitz, and I. Dikic, CIN85 participates in Cbl-b-mediated down-regulation of receptor tyrosine kinases, J Biol Chem 277 (2002) 39666-72.
[246] A. Petrelli, G.F. Gilestro, S. Lanzardo, P.M. Comoglio, N. Migone, and S. Giordano, The endophilin-CIN85-Cbl complex mediates ligand-dependent downregulation of c-Met, Nature 416 (2002) 187-90.
[247] M.S. Melikova, A.A. Aksenov, N.N. Nikol'skii, and E.S. Kornilova, [Effect of synthetic proteasomal inhibitor MG132 on dynamics of EGF-receptor complexes endocytosis in A431 cells], Tsitologiia 46 (2004) 601-8.

Acknowledgment / Danksagung

Es gibt wenige Dinge die ein Mensch gänzlich alleine schaffen kann, denn jeder Mensch ist in nahzu allem was er tut abhängig von anderen Menschen. Ich möchte an dieser Stelle eben jenen Menschen danken, welche zum Gelingen dieser Arbeit beigetragen haben.

An erster Stelle möchte ich mich besonders herzlich bei meiner Doktormutter **Prof. Dr. Petra Knaus** bedanken. Ihr gilt mein Dank für das Anvertrauen des Themas, die Bereitstellung der Resourcen und nicht zuletzt für ihre wissenschaftliche Unterstützung und stete Motivation.

Bei **Prof. Dr. Stefan Mundlos** möchte ich mich sehr für die Übernahme des Zweitgutachtens bedanken. Des Weiteren danke ich dem gesamten Ror2 Team der AG Mundlos am MPI, insbesondere **Dr. Sigmar Stricker** und **Florian Witte**, für viele wissenschaftliche Diskussionen und die zur Verfügung Stellung von Konstrukten und anderen Materialien.

Prof. Dr. Walter Sebald gilt mein Dank für die gute Zeit am Institut für Physiologische Chemie II an der Julius-Maximilians-Universität Würzburg. An dieser Stelle möchte ich mich auch bei allen nicht weiter benannten ehemaligen Kollegen der PCII für ihre Unterstützung, Diskussionen und Ratschläge bedanken.
I would like to express my gratitude to **Dr. Marei Sammar** who laid the foundation for the Ror2 project. I thank Sammar for helpful discussions and providing me with the right spirit. Quote: *The person saying it cannot be done should not interrupt the person doing it.*

Dr. Sylke Haßel und **Dr. Raphaela Schwappacher** waren mir im Laboralltag beeindruckende Vorbilder, und ich möchte beiden sehr für ihre immerwährende Hilfsbereitschaft und Geduld danken. Bei Raphaela möchte ich mich außerdem für ihre Geradlinigkeit, ihren wissenschaftlichen Rat und viele offene Worte bedanken.
Ein weiteres Vorbild war mir **Dr. Luiza Bengtsson**, deren wissenschaftliche Geradlinigkeit, Sprach- und Organisationstalent mich immer wieder in Staunen versetzt haben. Ich danke ihr für die kritische Auseinandersetzung mit meinem Thema und ihren Rat.
Gerburg Schwärzer sei gedankt für ihre Art mit der sie mir immer wieder den Laboralltag erheitern konnte, ihre Geduld und Gutmütigkeit mir gegenüber wenn ich selbige gerade nicht aufbringen konnte, für die lebhafen Diskussionen über Wissenschaftliches und Privates, für die Grundversorgung mit Schokolade und natürlich für ihre Freundschaft.

Neil Meshraqi möchte ich für seinen unermüdlichen Einsatz danken mit dem er die IT Situation der Arbeitsgruppe extrem verbessert und mir sehr viel Arbeit abgenommen hat. Außerdem danke ich ihm für viele lustige und ernsthafte Gespräche, die eine wunderbare Abwechslung im Laboralltag waren.

Der **Dahlem Research School** danke ich für das Stipendium, mit Hilfe dessen ich meine Promotion beenden konnte. Ebenso danke ich der **Frauenförderung** der Freien Universität, die es mir ermöglicht hat an Kongressen teilzunehmen.

Bei **Prof. Dr. Hucho**, **Prof. Dr. Yoav Henis**, **Dr. Christoph Weise**, **Dr. Henning Otto**, **Katharina Hoffmann**, **Giampiero Bandini**, **Gisela Wendel**, **Daniel Horbelt**, **Jan Börgermann**, **Veronika Wiese**, **Uli Rockenbauch** und **Mohammad Belverdi** bedanke ich mich für praktische und theoretische Unterstützung, sowie Diskussionen die mich weitergebracht haben.
Des Weiteren möchte ich mich bei allen nicht benannten aktuellen und ehemaligen Kollegen der AG Knaus und des Instituts für die gute Zeit bedanken. It would not have been the same without you!

Meinen Freunden **Miriam (Miri) Kniele**, **Christiane (Tina) Scheffel**, **Bianca (Binc) Thaci**, **Bianca Kesselring**, **Angela (Angi) Grieß**, **Akin Özgür**, **Dr. Sabrina Scholz**, **Sérgio Pinto**, sowie **Mark O'Neill** und den Autoren von **MUO** und meinen **Couch Surfing** Gästen und Gastgebern möchte ich einfach nur so danken. Thank you guys, you have been great!

Meiner **Famile** schulde ich natürlich den allergrößten Dank. Meinen Eltern **Silvia** und **Hartmut Sieber** danke ich dafür, dass sie mich immer unterstützt, gefördert und an mich geglaubt haben. Meine Geschwister **Lisa** und **Dirk Sieber** sind großartige Menschen, die ich nicht missen möchte. Ein ebenso wunderbarer Mensch war **Marco Sieber**, der mich rückblickend viele Lektionen gelehrt hat.

Publications

Sammar M*, **Sieber C***, Knaus P.
Biochemical and functional characterization of the Ror2/BRIb receptor complex
Biochem Biophys Res Commun. 2009 Jan 8. [Epub ahead of print]
*equal contribution

Christina Sieber, Gerburg K. Schwaerzer and Petra Knaus
Book: Bone Morphogenetic Proteins: From Local to Systemic Therapeutics
Chapter: BMP signaling is fine tuned on multiple levels
Progress in Inflammation Research 2008
ISBN 978-3-7643-8551-4 (Print) 978-3-7643-8552-1

Hartung A, **Sieber C**, Knaus P.
Yin and Yang in BMP signaling: Impact on the pathology of diseases and potential for tissue regeneration.
Signal Transduction 2006 Sep;6(5):297-99.

Sieber C*, Ploeger F*, Schwappacher R, Bechthold R, Hanke M, Kawai S, Muraki Y, Katsuura M, Kimura M, Mouler Rechtman M, Henis YI, Pohl J, Knaus P.
Monomeric and dimeric GDF-5 show same type I receptor binding and oligomerization capability and same biological activity
Biol. Chem. 2006 Apr;387(4):451-60.
*equal contribution

Marei Sammar, Sigmar Stricker, Georg C. Schwabe, **Christina Sieber**, Anke Hartung, Michael Hanke, Isao Oishi, Jens Pohl, Yasuhiro Minami, Walter Sebald, Stefan Mundlos and Petra Knaus
Modulation of GDF5/BRI-b signalling through interaction with the tyrosine kinase receptor Ror2
Genes to Cells 2004 Dec;9(12):1227-38.

Abbreviations

Terms

ab	antibody
abs	absorption
AChR	acetylcholine receptor
ActRI	Activin receptor I
ActRII	Activin receptor II
AD	Alzheimer's disease
ADP	adenosine di-phosphate
ALK	Activin-like kinase
ALP	alkaline phosphatase
ARF	ADP ribosylation factor
ATP	adenosintriphosphate
BAMBI	BMP and activin membrane-bound inhibitor
BISC	BMP-induced signaling complex
BMP	bone morphogenetic protein
BRE	BMP response element
BRI	BMP receptor I
BRIb	BMP receptor type Ib
BRII	BMP receptor II
c	cytoplasm
C. elegans	*Caenorhabditis elegans*
ca	constitutively active
Cav1	caveolin1
cbl	Casitas B-lineage lymphoma
CBP	CREB binding protein
CCP	clathin-coated pits
Cdc48	cell-division cycle-48
Co-Smad	common mediator Smad
CRD	cysteine-rich domain
CRE	cAMP response element
CREB	CRE brinding protein
D. melanogaster	*Drosophila melanogaster*
dn	dominant negative
DNA	2-deoxyribonucleic acid
Dnrk	*Drosophila* neurospecific receptor kinase
DPP	decapentaplegic
DRM	detergent-resistant microdomains
ds	double strand
Dvl	dishevelled
E	embryonic
E. coli	*Escherichia coli*
ECM	extracellular matrix
EGF	epidermal growth factor
ER	endoplasmatic reticulum
ERAD	ER-associated degradation
Erk	extracellular signal-regulated kinase
ES cell	embryonic stel cell
FGF	fibroblast growth factor
FOP	fibrodysplasia ossificans progressiva
Fzd	frizzled
GDF	growth and differentiation factor
GFP	green fluorescent protein
GGA3	golgi-associated, gamma adaptin ear containing, ARF binding protein 3
Grb2	growth factor receptor-bound protein 2
GS-hox	glycine/serine-richt box
GSK3	glycogen synthase kinase 3
GST	glutathione S transferase
HA	haemagglutinin
HECT	homologous to E6-AP C-terminus
Id1	inhibitor of differentiation 1
Ig	immunoglobulin-like
IGF	insulin-like growth factor
I-Smad	inhibitory Smad
JNK	c-jun N-terminal kinase
JPS	juvenile polyposis syndrome
K	lysine
Kg	kringle
LF	long form
LIMK1	LIM domain kinase 1
LRP	low density lipoprotein receptor-related protein
MAPK	mitogen-activated protein kinase
MAPKK	MAPK kinase
MAPKKK	MAPKK kinase
MBP	maltose binding protein
MEK	MAP Erk kinase
MH domain	MAD homology domain

miRNA	microRNA
MLC	myosin light chain
MuSK	muscle-specific kinase
MVBs	multivesicular bodies
MW	molecular weight
n	nucleus
NES	nuclear export signal
NFκB	nuclear factor κB
NGF	nerve growth factor
NLS	nuclear localization sequence
PAH	pulmonary arterial hypertension
PDE	phosphodiesterase
PDGF	platelet-derived growth factor
PDP	pyruvate dehydrogenase phosphatase
PFC	preformed complex
PKA	protein kinase A
PKC	protein kinase C
Rack1	receptor for activated C-kinase
rFzd	frizzled receptor
RGM	repulsive guidance molecule
RISC	RNA-induced silencing complex
RNA	ribonucleic acid
Ror2	Regeneron orphan receptor
R-Smad	receptor-associated Smad
RTK	receptor tyrosine kinase
SAD	Smad activation domain
SARA	Smad anchor for receptor activation
SBE	Smad binding element
SCP	small C-terminal domain phosphatase
SF	short form
SH2	src homology 2
SID	Smad interaction domain
SIM	Smad interacting motif
Smurf	Smad ubiquitin regulated factor
ss	single strand
TAB	TAK binding protein
Tak1	TGFβ activated kinase 1
TC	truncation
TGFβ	transforming growth factor β
Trb3	tribbles-like protein 3
Trk	tropomyosin-related kinase
Ub	ubiquitin
Wnt	wingless int
XIAP	X-linked inhibitor of apoptosis
β-gal	β-galactosidase

Chemicals – Materials – Methods

^{32}p	radioactively labelled phosphate
A	adenine
APS	ammoniumperoxdisulfat
ATP	adenosintriphosphate
BCA	bichinoic acid
BSA	bovine serum albumin
C	cytosine
cDNA	copy DNA
CMV	cytomegali virus
co-IP	co-immunoprecipitation
DEPC	Diethylpyrocarbonat
DMEM	Dulbecco's modified Eagle medium
DMS	dimethyl suberimidate
DMSO	dimethylsulfoxide
dNTP	desoxyribonuclotide triphosphate
DTT	dithiotreitol
ECL	enhanced chemiluminescence
EDTA	ethylenediaminetetraacetic acid
EtBr	ethidium bromide
FBS	fetal bovine serum
G	guanine
HEPES	N-2-Hydrosyethylenpiperazin-N-ethansulfonsäure
HRP	horseradish peroxidase
IF	immunofluorescence
IgG	immunoglobuline G
IP	immunoprecipitation
IPTG	isopropyl β-D-1-thiogalactopyranoside
LB	Luira-Bertrani
luc	luciferase
MCS	multiple cloning site
MMLV	Moloney murine leukemia virus
mRNA	messenger RNA
MβCD	methyl-β-cyclodextrin
OD	optical density
PAGE	polyacrylamide gelelectrophoresis
PBS	phosphate-bufferd saline
PCR	polymerase chain reaction
PEI	polyethylenimine
pI	isoelectric point
PI	protease inhibitor
PMSF	phenylmetylsulfonylfluoride
PPI	protein phosphatase inhibitor
SDS	sodium dodecyl sulphate
SOB	super optimal broth
SOC	super optimal broth, catabolit repression
SV40	simian virus 40
T	thymin
TBS	tris-buffered saline
TCA	trichloric acid
v/v	volume per volume
w/v	weight per volume
WB	Western blot

Units

%	percent
℃	degrees Celcius
µCi	microCurie
µg	microgram
A	Ampere
aa	amino acid
bp	base pair
Bq	Bequerel
Ci	Curie
d	day
Da	Dalton
fg	femtogram
g	gram
hr	hour
hr	hour
hrs	hours
kb	kilobase
kD	kiloDalton
kV	kiloVolt
l	liter
M	molar
mg	milligram
min	minute
ml	milliliter
mM	millimolar
msec	millisecond
nM	nanomolar
OD600	optical density at wavelength of 600nM
pM	picomolar
RLU	relative light units
rpm	rounds per minute
RT	room temperature
sec	second
U	unit
V	volt

Erklärung

Berlin, im Februar 2009

Ich erkläre hiermit ehrenwörtlich, dass ich die vorliegende Arbeit in allen Teilen selbständig angefertigt und keine anderen als die von mir angegebenen Quellen und Hilfsmittel verwendet habe.

Ich erkläre weiterhin, dass ich diese Dissertation weder in gleicher noch in ähnlicher Form in einem anderen Prüfungsverfahren vorgelegt habe.

Ich habe ausser den mit dem Zustellungsgesuch urkundlich vorgelegten akademischen Graden keine weiteren akademischen Grade erworben oder zu erwerben versucht.

Christina Sieber